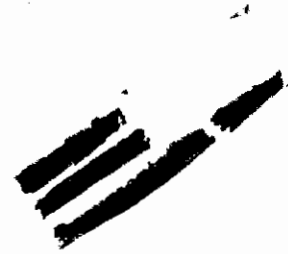


STOL TACTICAL AIRCRAFT INVESTIGATION

Volume II, Part 1

**Aerodynamic Technology: Design Compendium,
Vectored Thrust/Mechanical Flaps**

*William J. Runciman
Gary R. Letsinger
Bernard F. Ray
Fred W. May*



Approved for public release; distribution unlimited

FOREWORD

This report was prepared for the United States Air Force by The Boeing Company, Seattle, Washington in partial fulfillment of Contract F33615-71-C-1757, Project No. 643A. It is one of eight related documents covering the results of investigations of vectored-thrust and jet-flap powered lift technology, under the STOL Tactical Aircraft Investigation (STAI) Program sponsored by the Air Force Flight Dynamics Laboratory, Air Force Systems Command, Wright-Patterson Air Force Base, Ohio. The relation of this report to the others of this series is indicated below:

AFFDL-TR-73-19 STOL TACTICAL AIRCRAFT INVESTIGATION

Vol I Configuration Definition:
Medium STOL Transport with
Vectored Thrust/Mechanical Flaps

Vol II Part I	Aerodynamic Technology: Design Compendium, Vectored Thrust/Mechanical Flaps
------------------	---

THIS
REPORT

Vol II
Part II A Lifting Line Analysis Method
for Jet-Flapped Wings

Vol III Takeoff and Landing Performance
Ground Rules for Powered Lift
STOL Transport Aircraft

Vol IV Analysis of Wind Tunnel Data:
Vectored Thrust/Mechanical
Flaps and Internally Blown
Jet Flaps

Vol V
Part I Flight Control Technology: System
Analysis and Trade Studies for a
Medium STOL Transport with Vectored
Thrust and Mechanical Flaps

Vol V
Part II Flight Control Technology: Piloted
Simulation of a Medium STOL Transport
with Vectored Thrust/Mechanical Flaps

Vol VI Air Cushion Landing System Study

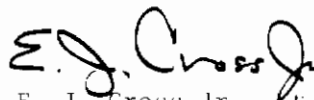
The work reported here was performed in the period June 1971 through December 1972 by the Aero/Propulsion Staff of the Research and Engineering Division, Aerospace Group, The Boeing Company. Mr. Franklyn J. Davenport served as Program Manager.

Contracts

The Air Force Project Engineer for this investigation was Mr. Garland S. Oates, Air Force Flight Dynamics Laboratory, PTA, Wright-Patterson Air Force Base, Ohio.

This report was released within The Boeing Company as Document D180-14409-1, and submitted to the Air Force in December 1972.

This technical report has been reviewed and is approved.



E. J. Cross Jr., Lt. Col., USAF
Chief, Prototype Division
Air Force Flight Dynamics Laboratory

Contrails

ABSTRACT

This report presents methods for predicting the performance-determining aerodynamic characteristics and the stability derivatives of transport-type configurations employing the vectored-thrust/mechanical-flap high-lift concept. These methods are suitable for preliminary design. They have been automated in a FORTRAN IV computer program, for which a users' manual is included in the appendix of this document.

Contrails

Contracts

TABLE OF CONTENTS

<u>Section</u>		<u>Page</u>
I	INTRODUCTION	1
II	LONGITUDINAL CHARACTERISTICS	3
	2.1 Unpowered Aerodynamic Characteristics, Free Air	3
	2.1.1 Lift	3
	2.1.2 Maximum Lift	21
	2.1.3 Drag	30
	2.1.4 Pitching Moment	38
	2.2 Ground Effect	56
	2.2.1 Lift	56
	2.2.2 Drag	57
	2.2.3 Pitching Moment	59
	2.2.4 Downwash	59
	2.3 Vectored Thrust, Free Air	63
	2.3.1 Lift Interference	63
	2.3.2 Drag Interference	65
	2.3.3 Pitching Moment Interference	71
	2.3.4 Downwash Interference	71
	2.4 Vectored Thrust, Ground Effect	77
	2.4.1 Lift Interference	77
	2.4.2 Drag Interference	77
	2.4.3 Pitching Moment Interference	80
	2.4.4 Downwash Interference	80
	2.5 Trim	81
III	STABILITY AND CONTROL DERIVATIVE PREDICTION METHODS	83
	3.1 Stability Derivative Sensitivity Study	83
	3.1.1 Longitudinal	87
	3.1.2 Lateral-Directional	93
	3.2 Stability and Control	96
	3.2.1 Longitudinal Stability and Control	101
	3.2.2 Lateral-Directional Stability Derivatives	116
	3.3 Engine Out	136
APPENDIX	Users Manual for Computer Program	139
References		219

Contrails

LIST OF ILLUSTRATIONS

<u>Figure No.</u>		<u>Page</u>
1	Lift Curve Slope, Test-Estimate Comparison	4
2	2-D Flap Effectiveness, Single Slotted Flap	8
3	2-D Flap Effectiveness, Double Slotted Flap	9
4	3-D Effect on Flap Effectiveness	10
5	Span Loading Factor	11
6	Multi-Element Flap Nomenclature	12
7	Body Lift Carryover	14
8	Flap Lift Increment, Test-Estimate Comparison	15
9	Leading-Edge Flap Effectiveness	19
10	Effect of Leading Edge Device on Maximum Lift	22
11	2-D Maximum Lift Increment	24
12	Trailing-Edge Flap Maximum Lift	26
13	Leading Edge Blowing Boundary Layer Control Effectiveness	29
14	Parasite Drag of Trailing-Edge Flaps	31
15	Part Span Induced Drag Factors (Continuous Flaps with Central Cutout)	33
16	Profile Drag Variation with Lift	34
17	Comparison of Measured and Predicted Power-off Drag Polars	36
18	Nomenclature for ac Location with Inboard Leading-Edge Devices	40
19	Local Aerodynamic Centers Near Middle of Wing	41
20	Load Effectiveness of Part Span Chord Extensions	42

Contrails

LIST OF ILLUSTRATIONS (Continued)

<u>Figure No.</u>		<u>Page</u>
21	Nomenclature for ac Location with Outboard Leading-Edge Devices	44
22	Chordwise Center of Load Due to Flaps	49
23	Spanwise Center of Load Due to Flaps	51
24	Change in Downwash at Horizontal Tail	53
25	Comparison of Measured and Predicted Power-Off Pitching Moment	55
26	Wing-in-Ground Effect	58
27	Ground Effect, Power Off, Test-Estimate Comparison	60
28	Ground Effect, Power Off, Test-Estimate Comparison	61
29	Vectored Thrust, Test-Estimate Comparison	64
30	Vectored Thrust, Lift Interference	66
31	Vectored Thrust, Lift Interference Effect of Nozzle Location	67
32	Vectored Thrust, Drag Interference - Vector Angle 30°	68
33	Vectored Thrust, Drag Interference - Vector Angle 60°	69
34	Vectored Thrust, Drag Interference - Vector Angle 90°	70
35	Vectored Thrust, Pitching Moment Interference - Vector Angle 30°	72
36	Vectored Thrust, Pitching Moment Interference - Vector Angle 60°	73
37	Vectored Thrust, Pitching Moment Interference - Vector Angle 90°	74
38	Vectored Thrust, Downwash Change at Horizontal Tail	75

LIST OF ILLUSTRATIONS (Continued)

<u>Figure No.</u>		<u>Page</u>
39	Vectored Thrust in Ground Effect, Test-Estimate Comparison	78
40	Change in Thrust Interference Effects Due to Ground Effect	79
41	General Arrangement STOL Tactical Transport Model 953-801	84
42	Effect of Angle of Attack Derivative, $C_{m\alpha}$ on Longitudinal Dynamic Stability	89
43	Effect of Angle of Attack Derivatives, $C_{x\alpha}$ and $C_{L\alpha}$ on Longitudinal Dynamic Stability ^α	89
44	Effect of Speed Derivatives on Longitudinal Dynamic Stability	90
45	Effect of Aerodynamic Lag Derivatives on Longitudinal Dynamic Stability	91
46	Effect of Pitch Damping Derivatives on Longitudinal Dynamic Stability	92
47	Effect of Sideslip Derivatives on Dutch Roll Characteristics	94
48	Effect of Sideslip Derivatives on Spiral Mode Stability	95
49	Effect of Roll Rate Derivatives on Dutch Roll Characteristics	97
50	Effect of Roll Rate Derivatives on Spiral Mode Stability	98
51	Effect of Yaw Rate Derivatives on Dutch Roll Characteristics	99
52	Effect of Yaw Rate Derivatives on Spiral Mode Stability	100
53	Effect of Vectored Thrust on Lift Curve Slope	103
54	Effect of Vectored Thrust on Aerodynamic Center	104

Contrails

LIST OF ILLUSTRATIONS (Continued)

<u>Figure No.</u>		<u>Page</u>
55	Effect of Nacelle Spanwise Location on Aerodynamic Center	105
56	Lift Curve Slope Error	108
57	Aerodynamic Center Error	109
58	Effect of Vectored Thrust on Downwash	111
59	Effect of Vectored Thrust on Horizontal Tail Dynamic Pressure	112
60	Vectored Thrust Effect Factors for Sideslip Derivatives, Tail-Off	118
61	Vectored Thrust Effect Factors for Sideslip Derivatives in Ground Effect, Tail-Off	119
62	Sidewash at the Vertical Tail	121
63	Powered Sideslip Derivatives Error	122
64	Thrust Effect on Rudder Power	130
65	Effect of Sideslip on Aileron Power	131
66	Effect of Thrust on Aileron Effectiveness in Free Air and in Ground Effect	132
67	Effect of Aileron Blowing and Engine Thrust on Aileron Effectiveness	133
68	Effect of Thrust on Spoiler Effectiveness	134
69	Spoiler Effectiveness	135
70	Rolling Moment Due to Thrust Loss	137
71	Yawing Moment Due to Thrust Loss	138
72	Nomenclature for Leading Edge Flap	146
73	Nomenclature for Trailing Edge Flap	149
74	Program Deck Stacking	153

Contrails

LIST OF TABLES

<u>Table Number</u>	<u>Title</u>	<u>Page</u>
I	Stability Derivatives, Mass Properties, and Reference Dimensions of Example Airplane	85
II	Stability Derivatives with Important Influence on Airplane Stability	86
III	Test-Prediction Comparison, Angle of Attack Derivatives	106
IV	Test-Prediction Comparison, Sideslip Derivatives	123
V	Input Data Format	155

Contracts

LIST OF ABBREVIATIONS AND SYMBOLS

A	Aspect ratio, $\frac{b^2}{S}$
A_G	Gross aspect ratio, $\frac{b^2}{S_G}$
ac	Aerodynamic center
a_V	Vertical tail lift curve slope, per radian
b	Wing span, ft
b_V	Vortex span, ft
V_e	Equivalent jet velocity ratio
c	Chord length, ft
c'	Extended chord length, ft
\bar{c} or c_{REF}	Mean aerodynamic chord, ft
C_D	Drag coefficient
$\Delta C_{D_{BLC}}$	Drag coefficient due to leading edge boundary layer control
C_{D_i}	Induced drag coefficient
C_{D_p}	Parasite drag coefficient
$C_{D_{RAM}}$	Ram drag coefficient
c_f	Flap chord length, ft
c'_f	Extended flap chord length, ft
cg	Center of gravity
C_J	Thrust coefficient
C_L	Lift coefficient
C_l	Section lift coefficient, or rolling moment coefficient (depends on context)

Contrails

LIST OF ABBREVIATIONS AND SYMBOLS (Continued)

$C_{L\alpha}$	Lift curve slope, per degree
$C_{\ell\alpha}$	Section lift curve slope, per degree
C_n	Yawing moment coefficient
C_m	Pitching moment coefficient
cp	Center of pressure
C_x	Longitudinal force coefficient, stability axis
C_y	Sideforce coefficient, stability axis
C_z	Vertical force coefficient, stability axis
C_μ	Boundary layer control momentum coefficient
h	Height of wing quarter mac above ground plane, ft
I_{xx}	Moment of inertia about the x body reference axis, slug-ft ²
I_{yy}	Moment of inertia about the y body reference axis, slug-ft ²
I_{zz}	Moment of inertia about the z body reference axis, slug-ft ²
I_{xz}	Product of inertia about the x and z body reference axis, slug-ft ²
\mathcal{I}	Imaginary part of a complex number
L	Lift force, lb
ℓ_H	Distance from c.g. to horizontal tail ac, ft
ℓ_V	Distance from c.g. to vertical tail ac, ft
M	Pitching moment, ft-lb
mac	Mean aerodynamic chord, ft
P	Roll rate, radians/sec

Contrails

LIST OF ABBREVIATIONS AND SYMBOLS (Continued)

p	Wing semi-perimeter, or wing tip helix angle, $\frac{Pb}{2V}$, rad (depends on context)
q	Pitch rate angle, $\frac{Qc}{2V}$, rads or dynamic pressure, lbs/ft ² (depends on context)
Q	Pitch rate, rad/sec
\mathcal{R}	Real part of complex number
R	Yaw rate, rad/sec
r	Yaw rate angle, $\frac{Rb}{2V}$, rad
S	Wing area, sq ft
S _G	Wing gross area, sq ft
S _H	Horizontal tail area, sq ft
S _{REF}	Wing reference area, sq ft
S _V	Vertical tail area, sq ft
T _{1/2}	Time to half amplitude, sec
T ₂	Time to double amplitude, sec
u	Perturbation speed normalized by initial speed, $\frac{\Delta U}{V}$
v _i	Induced longitudinal velocity due to image vortex system, ft/sec
v _r	Induced longitudinal velocity due to real vortex system, ft/sec
V	Free stream velocity, ft/sec
W	Weight, lb
w _i	Induced vertical velocity due to image vortex system, ft/sec
w _r	Induced vertical velocity due to real vortex system, ft/sec
x	Longitudinal coordinate, ft from reference station
X _E	Longitudinal distance from nozzle centerline to cg, ft
X _R	Longitudinal distance from centerline of inlet face to cg, ft

Contrails

LIST OF ABBREVIATIONS AND SYMBOLS (Continued)

X_T	Distance from cg to thrust vector in fraction of MAC
Z_T	Distance from c.g. to thrust vector in fraction of MAC, positive down
Z_E	Vertical distance from nozzle centerline to cg, ft
Z_R	Vertical distance from centerline of inlet face to cg, ft
Z_v	Distance from cg down to vertical tail ac, ft
α	Angle of attack, deg
α_δ	Flap effectiveness
β	Angle of sideslip, deg
Γ	Wing circulation, ft ² /sec
γ	Climb angle, deg
Δ	Incremental value
δ_{ALL}	Aileron deflection, deg
δ_E	Elevator deflection, deg
δ_e	Effective flap deflection angle, deg
δ_F	Flap deflection angle, deg
ϵ	Downwash angle, deg
ϵ_e	Effective downwash angle at horizontal tail, deg
η	Ratio of dynamic pressure at the tail to free-stream dynamic pressure, or dimensionless wing semi span (depends on context)
Λ	Sweep angle, deg
λ	Wing loading factor
μ_s	Part span load effectiveness
σ	Thrust deflection angle, side wash angle, deg (depends on context)

LIST OF ABBREVIATIONS AND SYMBOLS (Continued)

Subscripts

AIL	Aileron
avg	Average
B	Body
c/4	1/4 chord
c/2	1/2 chord
c'/2	1/2 extended chord
FA	Free air
GE	Ground effects
H	Horizontal tail
HL	Hinge line
IB	Inboard
INT	Interference
LE	Leading edge
max	Maximum
NET	Indicates data (power on) that has the engine thrust removed
min	Minimum
OB	Outboard
OL	Zero lift
REF	Reference
TE	Trailing edge
TO	Tail-off
trap	Trapezoidal
V	Vertical tail

Contrails

SECTION I

INTRODUCTION

1.1 Background

The U. S. Air Force's need for modernization of its Tactical Airlift capability led to establishment of the Tactical Airlift Technology Advanced Development Program (TAT-ADP). This program was designed to contribute to the technology base for development of an Advanced Medium STOL Transport (AMST).

The AMST must be capable of handling substantial payloads and using airfields considerably shorter than those required by large tactical transports now in the Air Force inventory. If this short field requirement is to be met without unduly compromising aircraft speed, economy, and ride quality, an advanced-technology powered-lift concept will be required.

The STOL Tactical Aircraft Investigation (STAI) is a major part of the TAT-ADP, and comprises studies of the aerodynamics and flight control technology of powered-lift systems under consideration for use on the AMST. Under the STOL-TAI, The Boeing Company was awarded Contract No. F33615-71-C-1757 by the USAF Flight Dynamics Laboratory to conduct investigations of the technology of the vectored-thrust and internally blown jet flap powered-lift concepts. These investigations included:

- o Aerodynamic analysis and wind tunnel testing
- o Configuration studies
- o Control system design, analysis, and simulation

1.2 Objective

The objective of the work reported here was to develop convenient and rapid methods for predicting the performance-determining aerodynamic characteristics and the stability derivatives of configurations using the vectored thrust/mechanical flap powered lift concept. The methods are intended for preliminary design purposes and ease of application has been emphasized.

1.3 State of the Art Prior to the STAI

Early in the STAI, the available literature and test data on vectored thrust was surveyed. It was found that the data base for vectored thrust interference effects on transport-type configurations was almost nonexistent. Consequently, the "State of the Art Design Compendium" compiled from the information then available consisted only of procedures for estimating power-off characteristics and the recommendation to correct for power simply by direct vector addition of the propulsive forces. That is, interference effects were assumed to be zero.

Contrails

To fill the gap in the data base, an extensive program of testing was then carried out in the Boeing V/STOL Wind Tunnel. The results of that program are reported in Volume IV of the present series of documents, and are the basis for the methods presented here.

1.4 Technical Approach

Power effects are described in this report as the sum of forces and moments computed by direct vector addition, plus interference increments. The interference increments were usually found to be best described graphically. That is, no improvement in convenience or understanding was apparent in attempting to reduce the curves to analytical formulae, except for a general dependence of the interference forces on the square root of the thrust coefficient.

1.5 Scope

The scope of this investigation covers vectored thrust/mechanical flap high-lift systems installed on configurations suitable for a STOL tactical transport. These methods are intended to be used in conjunction with the USAF Stability and Control DATCOM (Reference 1).

1.6 Document Organization

Section II presents methods for predicting performance determining aerodynamic characteristics with power off, and for estimating interference effects due to vectored thrust.

Section III presents procedures for computing stability and control derivative corrections due to vectored thrust.

The appendices provide a users' manual and a listing of a FORTRAN IV computer program which automates the procedures given in Section II.

SECTION II

LONGITUDINAL CHARACTERISTICS

Aerodynamic estimation techniques are presented which provide increments of lift, drag, and pitching moment for leading and trailing edge devices. These increments are to be added to the clean airplane values which may be estimated from Datcom or other alternate source.

2.1 Unpowered Aerodynamic Characteristics, Free Air

2.1.1 Lift

Lift estimation below maximum lift has been divided into lift curve slope and flap lift increments. The effects of flap extension (chord extension) which increases the wing area, and flap deflection, which changes the wing camber, are treated separately.

2.1.1.1 Lift Curve Slope

There are a number of theoretical or semi-theoretical formulae which give good agreement between the estimated and experimental lift curve slopes of three-dimensional wings (Refs. 1, 2, 3, 4). One easy-to-use method is that from Jones and Cohen (Ref. 4). See sample problem for additional definition of S_G and p , Page 5.

$$C_{L\alpha} = \frac{2\pi A}{(p/b)(A)+2} \frac{S_G}{S_R} \frac{1}{\text{rad}} \quad (2.1-1)$$

The modern high lift system usually has trailing edge flaps with rearward displacement (chord extension) and may also include a leading edge device with forward displacement. The areas added by these displacements of the leading and trailing edges must be added to the basic planform when estimating flaps down $C_{L\alpha}$. If the inboard edge of the flap is at the side of the body, the added area for flap extension will be based on the assumption that the flap extends to the body centerline.

A comparison of estimated and test $C_{L\alpha}$ are shown in Fig. 1.

Contrails

$\Lambda c/4$	AR	LE	TE	$C_{L\alpha_{Test}}$	$C_{L\alpha_{Est}}$	$\frac{C_{L\alpha_{Est}} - C_{L\alpha_{Test}}}{C_{L\alpha_{Est}}}$
15	6.5	Up	Up	0.0710	0.0713	0.0042
✓	8.0	✓	✓	0.0811	0.0790	-0.0267
✓	10.0	✓	✓	0.0870	0.0860	-0.0116
30	5.36	✓	✓	0.0700	0.0673	-0.0401
✓	6.61	✓	✓	0.0717	0.0735	0.0245
✓	8.26	✓	✓	0.0765	0.0761	-0.0053
0	8.3	✓	✓	0.0790	0.0840	0.0595
30	6.61	Ext	✓	0.0790	0.0779	-0.0141
15	8.0	✓	✓	0.0860	0.0880	0.0227
0	8.3	✓	✓	0.0940	0.0905	-0.0387
15	8.0	Up	Ext	0.0933	0.0970	0.0381
✓	✓	✓	✓	0.0926	0.0970	0.0454
30	6.61	Ext	✓	0.0850	0.0800	-0.0625
15	8.0	Ext	✓	0.0940	0.0988	0.0485
30	6.61	✓	✓	0.0920	0.0846	-0.0875
0	8.3	✓	✓	0.0990	0.1016	0.0256

Data from BVWT 097 (Ref 5)

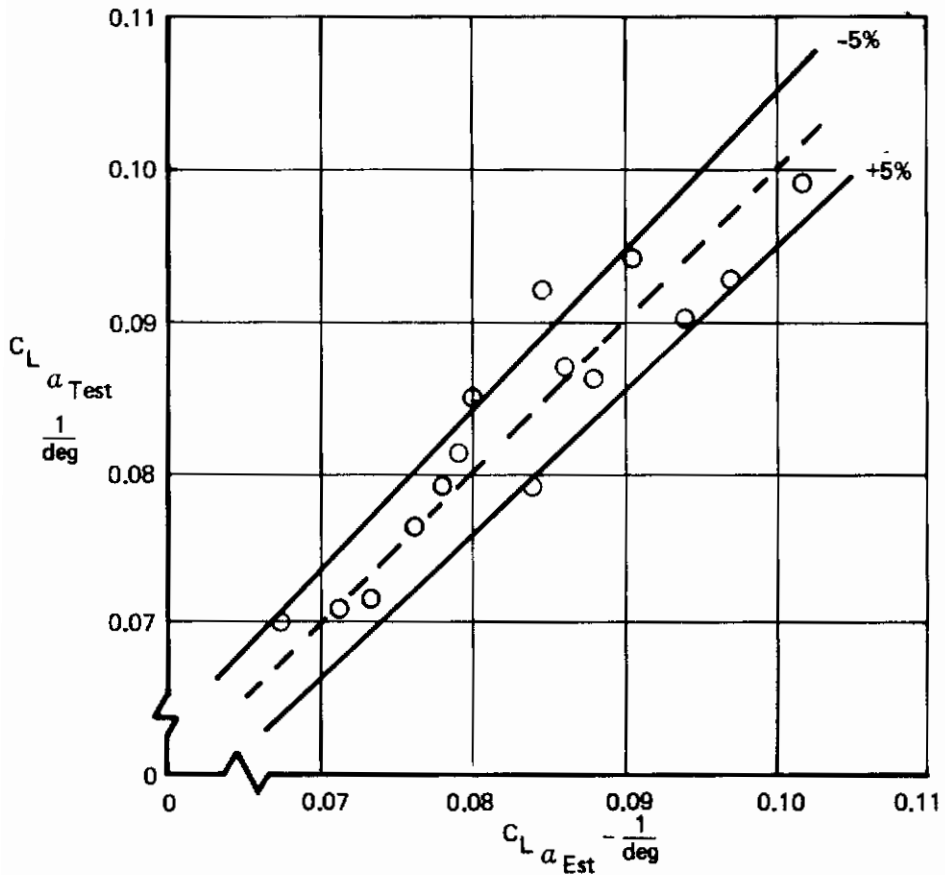
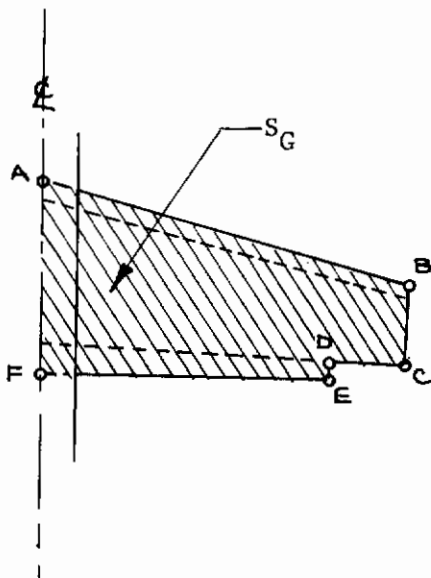


Figure 1: Lift Curve Slope, Test – Estimate Comparison

SAMPLE PROBLEM - LIFT CURVE SLOPE

STAI wind tunnel model LE & TE devices deployed, 15° sweep.



$$S_G = \text{Area ABCDEF} = 8.592 \text{ SF}$$

$$S_{\text{Ref}} = 6.164 \text{ SF}$$

$$b = 84.274 \text{ in.}$$

$$A_{\text{Gross}} = b^2 / S_G = 5.74 \text{ SF}$$

$$P = \text{ABCDEF} = 100.952 \text{ in.}$$

Calculate $C_{L\alpha}$ from Equation 2.1-1.

$$C_{L\alpha} = \left[\frac{(2\pi)(5.74)}{(100.952)(5.74) + 2} \right] \frac{(8.592)}{(6.164)} \frac{1}{57.3}$$

$$C_{L\alpha} = .0988 \text{ deg.}$$

FROM TEST BUWT 097, REF 5

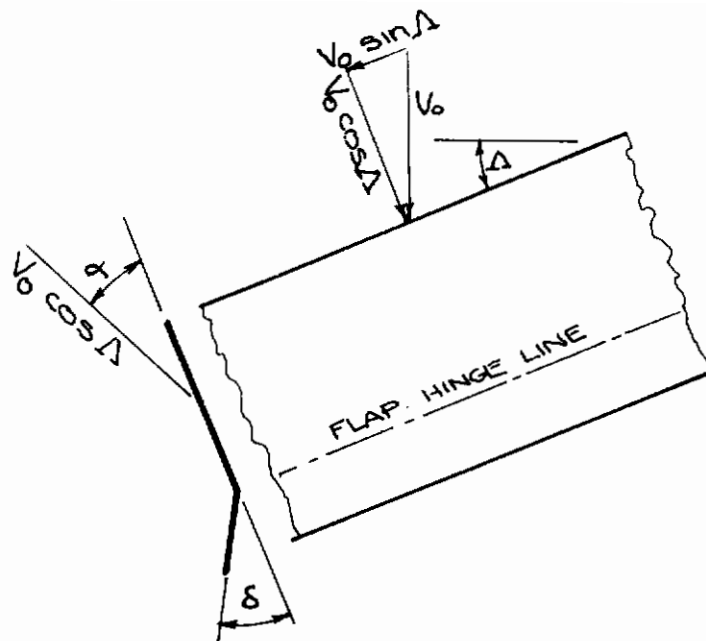
$$C_{L\alpha} = .0940$$

2.1.1.2 Effect of Trailing Edge Flap Deflection

The effect of pure (i.e., no area increase) trailing edge flap deflection is to change the zero-lift angle (α_{0L}) without changing the wing lift curve slope. The approach chosen here to estimate trailing edge zero-lift angle shift is due to Eldridge (Ref. 6 and 7).

Consider an infinite yawed constant-chord wing with trailing edge flap deflection.

Contrails



It can be shown that, referenced to the free stream velocity,

$$C_{l\alpha} = 2\pi \cos \Delta \quad (2.1-2)$$

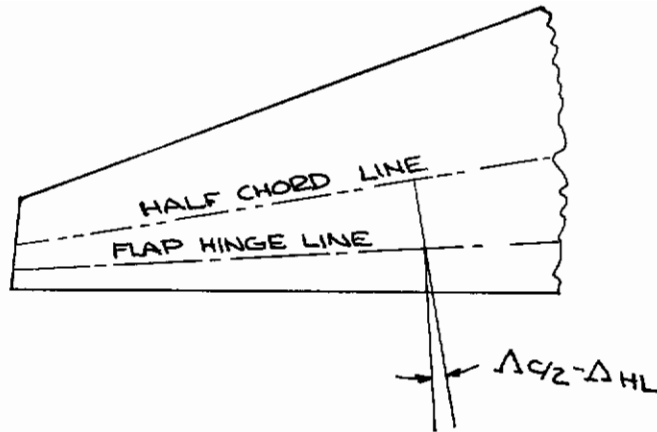
$$C_{l\delta} = 2\pi \alpha_{\delta, \Lambda=0} \cos^2 \Delta \quad (2.1-3)$$

Therefore:

$$\frac{C_{l\delta}}{C_{l\alpha}} = \alpha_{\delta, \Lambda=0} \cos \Delta$$

For flaps on tapered wings, the significant sweep angle is that of the locus of sectional aerodynamic centers for the wing, approximately the quarter chord (used for $C_{l\alpha}$), and the locus of sectional flap centers of pressure, approximately the half chord (used for $C_{l\delta}$). If the flap angle, δ_f , is measured normal to the hingeline, then the effective angle along a chordline normal to the half chordline is

$$\delta_e = \tan^{-1} [\tan \delta_f \cos(\Lambda_{C/2} - \Lambda_{HL})] \quad (2.1-4)$$



$$\Delta\alpha_{OL_{2D}} = [\alpha_{\delta_{2D}}]_{\Lambda=0} \left[\frac{\cos^2 \Lambda c/2}{\cos \Lambda c/4} \right] \tan^{-1} [\tan \delta_f \cos(\Lambda c/2 - \Delta_{HL})] \quad (2.1-6)$$

For a finite aspect ratio wing, lifting surface theory shows that the effective α_{δ} is increased above the two-dimensional value. Therefore, for wings

$$\Delta\alpha_{OL} = [\alpha_{\delta_{2D}}]_{\Lambda=0} \left[\frac{\alpha_{\delta_{3D}}}{\alpha_{\delta_{2D}}} \right] \left[\frac{\cos^2 \Lambda c/2}{\cos \Lambda c/4} \right] \tan^{-1} [\tan \delta_f \cos(\Lambda c/2 - \Delta_{HL})] \Lambda_{TE} \quad (2.1-7)$$

Empirical two-dimensional data has been correlated for single and vane-type double-slotted flaps, Figs. 2 and 3. Lifting surface theory shows that flap effectiveness is affected by aspect ratio. The two-dimensional test value of α_{δ} can be corrected to three-dimensional using the theoretical results of Ref. 8, Fig. 4.

The part span load factor used in Equation 2.1-7 may be found in Figure 5.

For multi-element clamps, contributions of individual elements add algebraically (Fig. 6), so

$$(\Delta\alpha_{OL})_{TE} = (\Delta\alpha_{OL})_1 + (\Delta\alpha_{OL})_2 \quad (2.1-8)$$

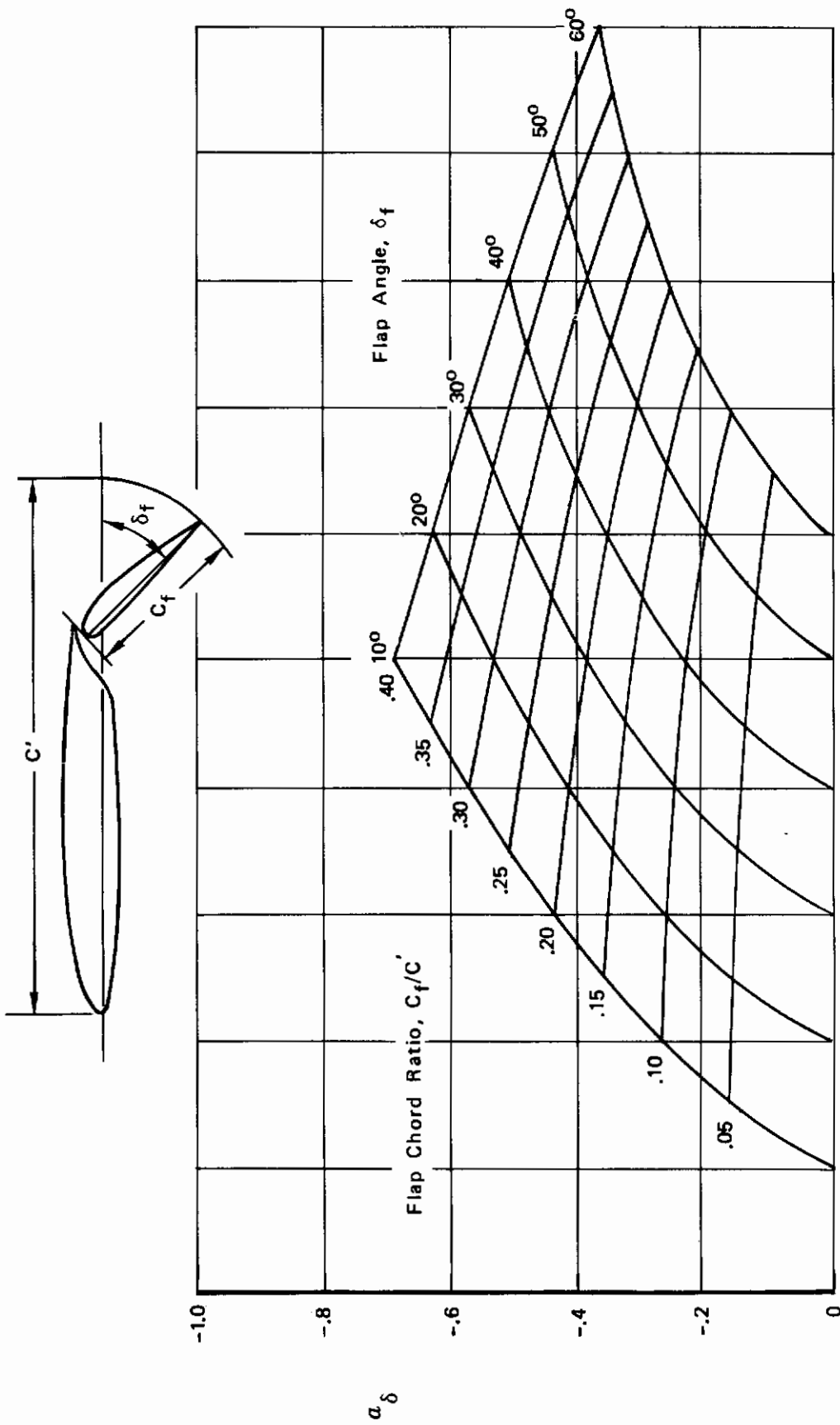


Figure 2: 2-D Flap Effectiveness, Single-Slotted Flap

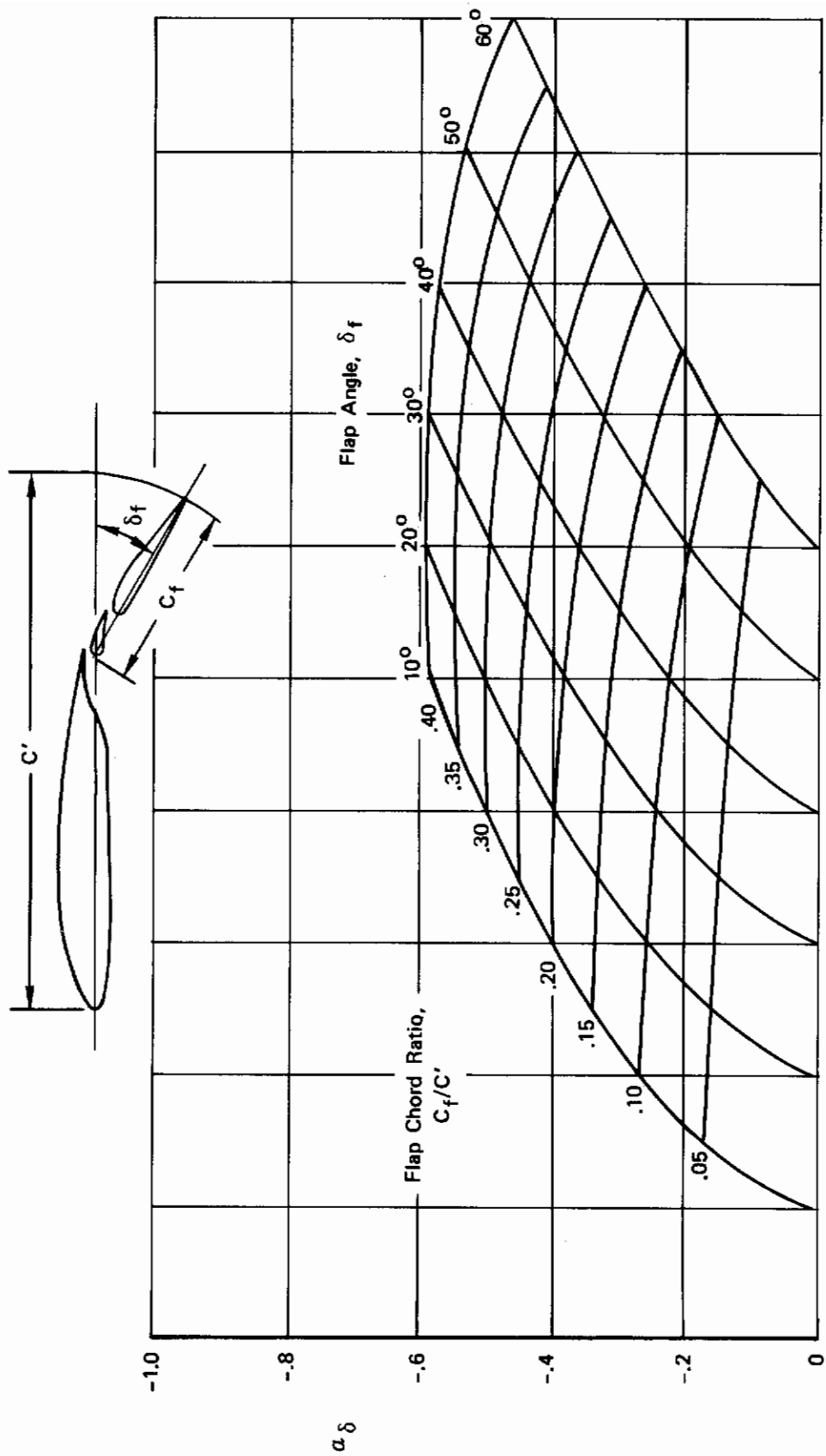


Figure 3: 2-D Flap Effectiveness, Double-Slotted Flap

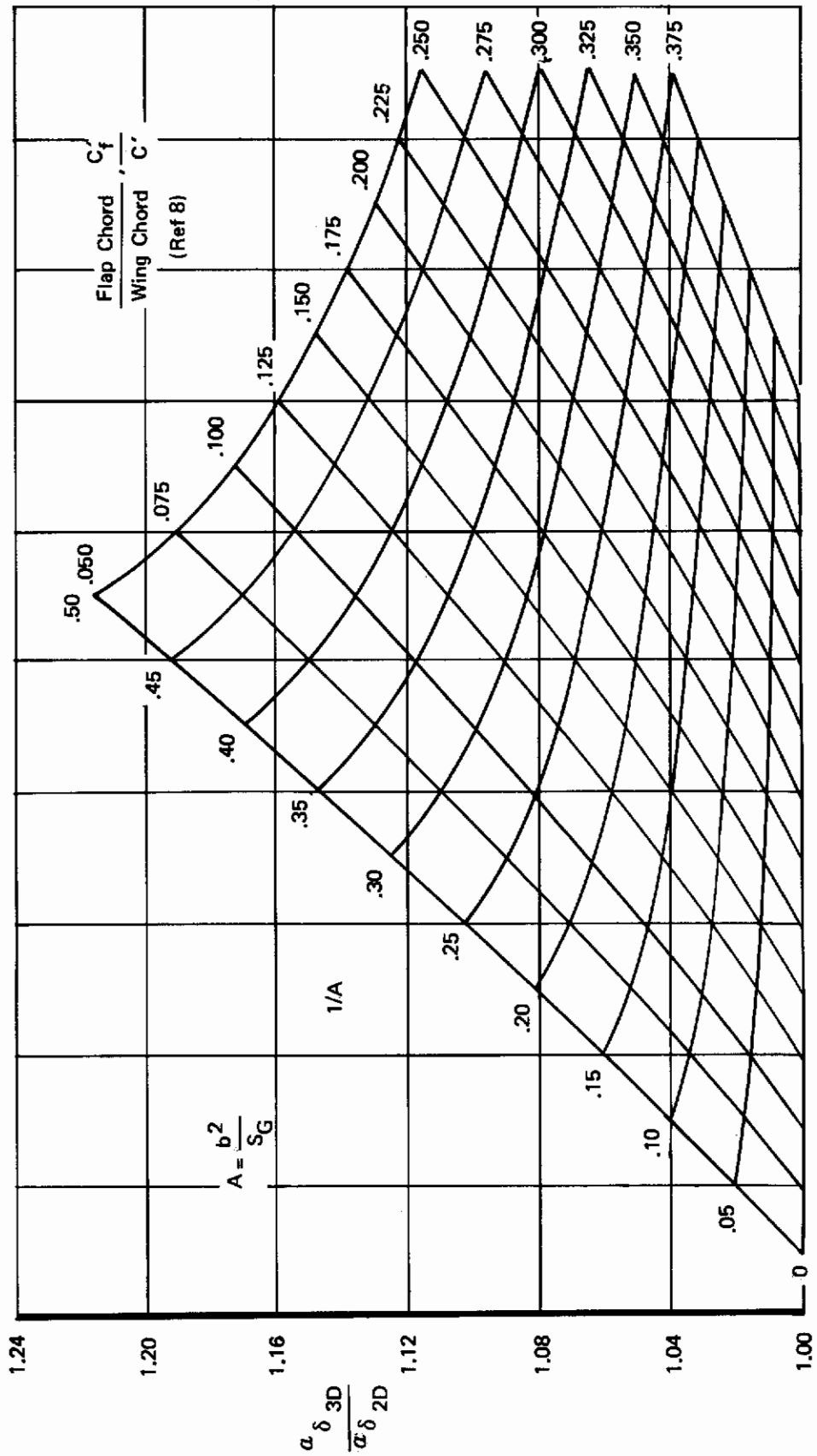


Figure 4: 3-D Effect on Flap Effectiveness

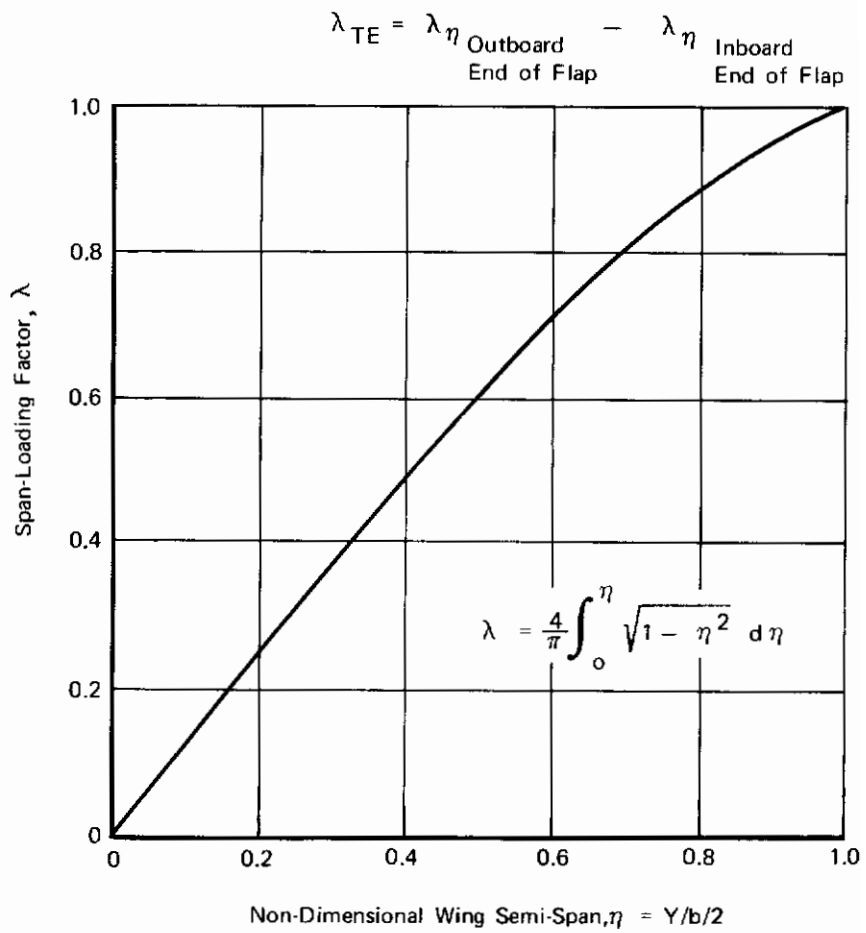
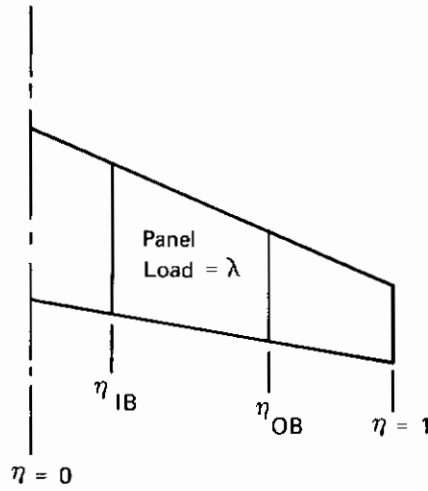


Figure 5: Span-Loading Factor

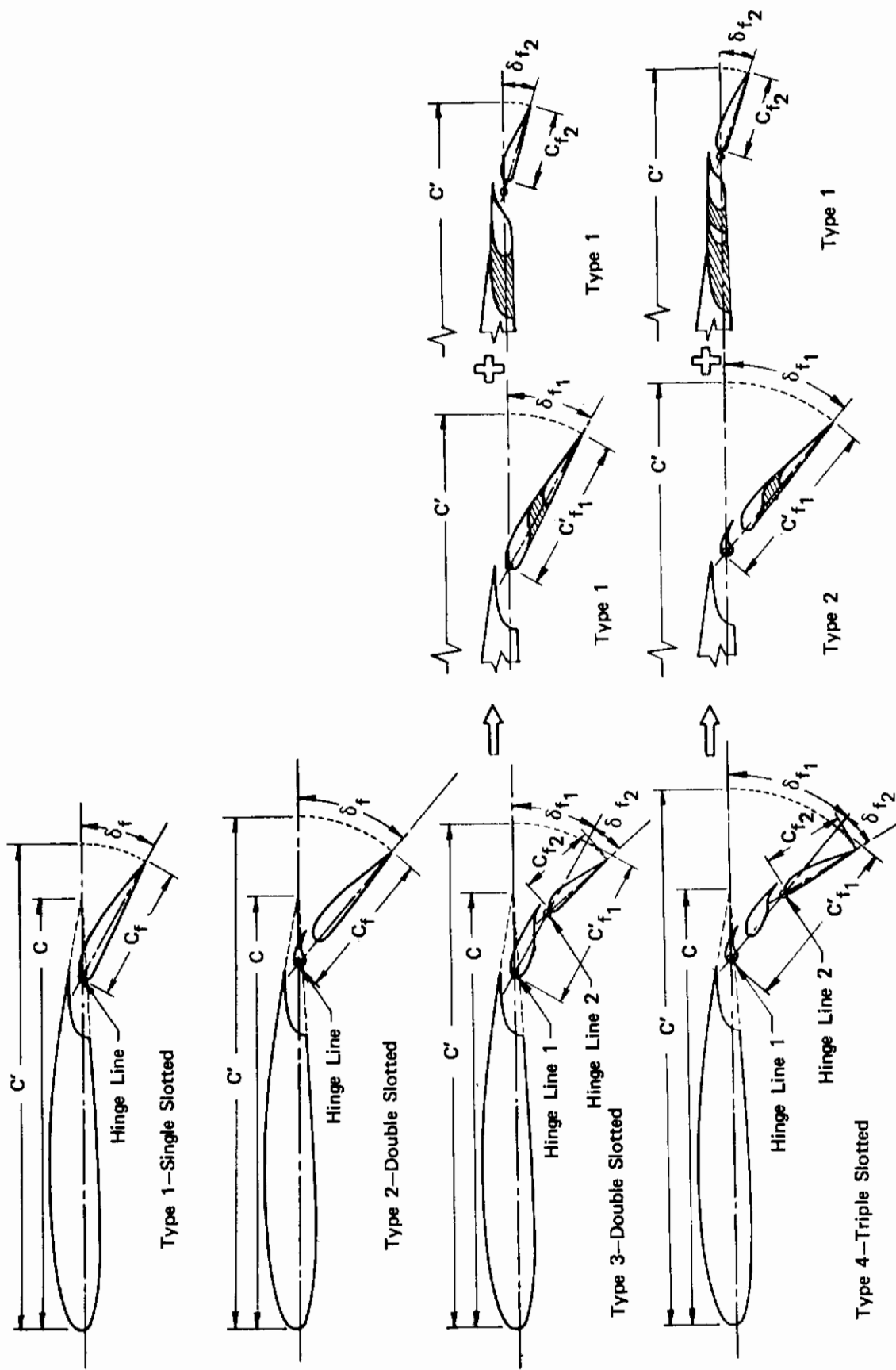


Figure 6: Multi-Element Flap Nomenclature

Contrails

The flap lift increment, measured at the angle for zero lift of the flaps-up wing is

$$\Delta C_{L_{TE_{flap}}} = (C_{L_{\alpha}})(-\Delta\alpha_{OL_{TE_{flap}}}) \quad (2.1-9)$$

Some flap lift will be carried over onto the body. The amount of carry-over will depend on the wing position on the body, the body span to wing span ratio, and the flap lift increment. A limited amount of data for high wing configurations have been correlated as shown in Fig. 7. If it is desired to make the correction for body carry-over, flap lift increments should be calculated assuming the flap ends at the body side and that it extends to the centerline. The difference between these values is then multiplied by the body carry-over factor (k) from Fig. 7 trailing edge flap lift increment with body carry-over is

$$\Delta C_{L_{TE}} = \Delta C_{L_{TE_{flap}}} + (\Delta C_{L_{TE_{flap}}}) \left(\frac{\lambda_{IB}}{\lambda_{OB} - \lambda_{IB}} \right) K \quad (2.1-10)$$

The body carry-over lift increment also results in shifting the angle for zero lift by

$$\Delta\alpha_{OL_B} = -\frac{\Delta C_{L_B}}{C_{L_{\alpha_{flaps\ down}}}} \quad (2.1-11)$$

$$\Delta\alpha_{OL_{TE}} = \Delta\alpha_{OL_{flap}} + \Delta\alpha_{OL_B} \quad (2.1-12)$$

A comparison between test data obtained from STAI wind tunnel testing and calculated data are presented in Fig. 8.

SAMPLE PROBLEM, TRAILING EDGE FLAP LIFT INCREMENT

STAI Wind Tunnel Model LE & LE Devices deployed, T.E. deflection $45^\circ/60^\circ$, $\Lambda_{c/4} = 15^\circ$.

$$S_G = 8.952 \text{ SF}$$

$$S_R = 6.164 \text{ SF}$$

$$b = 84.274 \text{ in.}$$

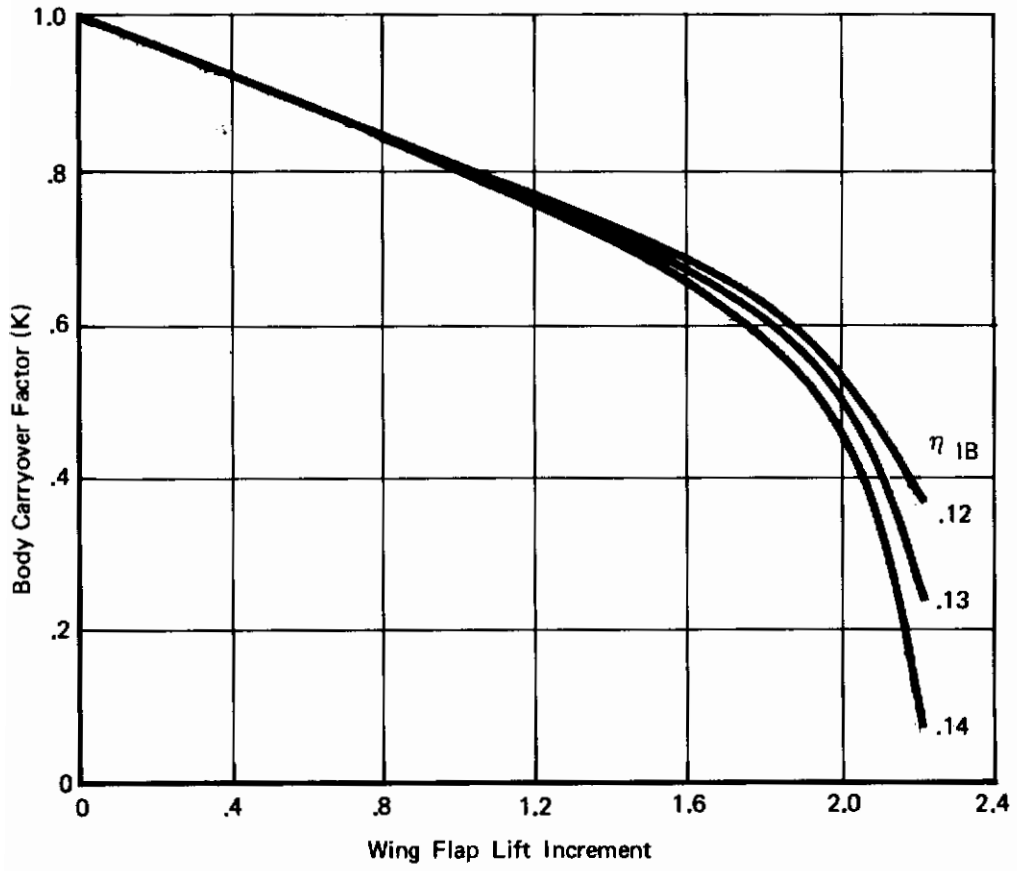


Figure 7: Body Lift Carryover

Contrails

$\Lambda C/4$	AR	Flap Span	δ_F Actual	ΔC_{L_f} test	ΔC_{L_f} Est.	$\frac{\Delta C_{L_f \text{ test}} - \Delta C_{L_f \text{ Est}}}{\Delta C_{L_f \text{ Est}}}$
30	6.61	0.716	30/30	1.03	0.98	-0.051
✓	✓	✓	40/40	1.29	1.26	-0.024
✓	✓	✓	58/40	1.56	1.56	0.090
✓	✓	✓	45/60	1.58	1.59	0.006
✓	✓	0.570	✓	1.26	1.34	0.060
✓	✓	0.848	✓	1.80	1.78	-0.011
✓	✓	1.000	✓	2.01	1.92	-0.047
15	8	0.75	30/30	1.2	1.20	0.0
✓	✓	✓	40/40	1.61	1.55	-0.039
✓	✓	✓	58/60	1.94	1.89	-0.026
✓	✓	✓	45/60	1.91	1.92	0.005
✓	✓	1.0	✓	2.29	2.25	-0.018
✓	6.5	✓	✓	2.15	2.12	-0.014
✓	10.0	✓	✓	2.45	2.31	-0.016
30	5.36	✓	✓	1.65	1.68	0.018
✓	8.26	✓	✓	1.95	2.02	0.035
0	8.30	0.776	30/30	1.36	1.36	0
✓	✓	✓	40/40	1.78	1.72	-0.035
✓	✓	✓	58/60	2.10	2.07	-0.014
✓	✓	✓	45/60	2.17	2.14	-0.014

Data from BVWT 097 (Ref. 5)

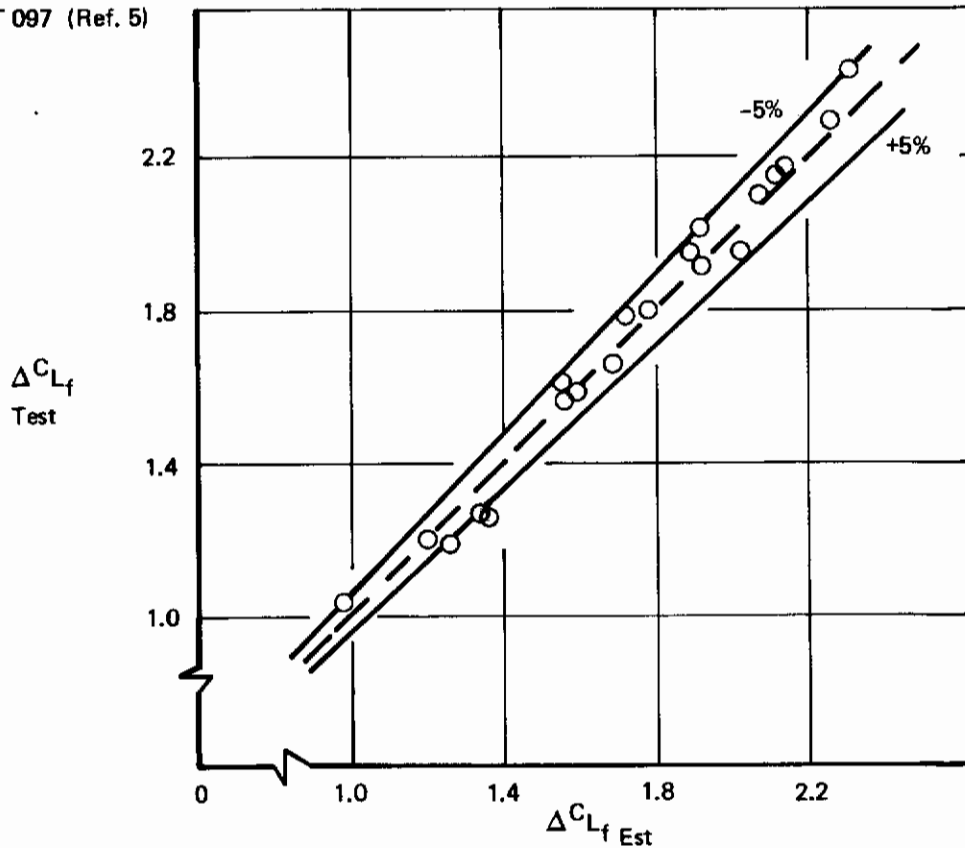


Figure 8: Flap Lift Increment, Test-Estimate Comparison

Contrails

$$A_{\text{Gross}} = 5.74$$

$$p = 100.952 \text{ in.}$$

Flap Type 4, Triple Slotted, see Fig. 6.

$$C'/C = 1.283$$

$$\frac{C_{f1}}{C'} = .323$$

$$C_{f2}/C' = .091$$

$$\delta_{f1} = 45.14$$

$$\delta_{f2} = 15.13$$

$$\eta_{OB} = .145$$

$$\eta_{OB} = .75 \quad \text{Trailing Edge}$$

$$\Lambda C'/4 = 15.401$$

$$\Lambda C'/2 = 11.625^\circ$$

$$\Lambda HL_1 = 7.295^\circ$$

$$\Lambda HL_2 = 3.525^\circ$$

$$C_{L\alpha} = .0988 \quad (\text{calculated by method in Section 2.1.1.1})$$

Calculate flap angles normal to half chord line, Equation 2.1-4.

$$\delta_{e1} = \tan^{-1} [\tan 43.14 \cos (11.625-7.259)] = 45.06^\circ$$

$$\delta_{e2} = \tan^{-1} [\tan 15.13 \cos (11.625-3.525)] = 14.98^\circ$$

For forward flap section using Figure 3, C'_f/C' and δ_{e1} read

$$(\alpha_\delta)_1 = -.485$$

For aft flap section using Fig. 2, C'_{f2}/C' and δ_{e2}

$$(\alpha_\delta)_2 = -.25$$

From Fig. 4, C'_f/C' and A determine

$$\left(\frac{\alpha_\delta 3D}{\alpha_\delta 2D} \right)_1 = 1.03$$

Contrails

From Fig. 4, C_{F_2}/C' and A determine

$$\left(\frac{\alpha_{\delta_{3D}}}{\alpha_{\delta_{2D}}}\right)_2 = 1.057$$

From Fig. 5, η_{1B} and η_{0B}

$$\lambda_{TE} = .849 - .183 = .666$$

Since the flap is the sum of its parts,

$$(\Delta\alpha_{OL})_{TE} = \Delta\alpha_{OL_1} + \Delta\alpha_{OL_2}$$

and α_{OL} from Equation 2.1-7

$$(\Delta\alpha_{OL})_1 = (-.485)(1.03) \left(\frac{\cos^2 11.62}{\cos 15.40}\right) (45.06)(.666) = -14.92$$

$$(\Delta\alpha_{OL})_2 = (-.25)(1.056) \left(\frac{\cos^2 11.62}{\cos 15.40}\right) (14.98)(.666) = -2.62$$

$$\Delta\alpha_{OL_{TE}} = -17.54$$

Then from Equation 2.1-9

$$\Delta C_{L_{TE_{FLAP}}} = -(-17.54)(.0988) = 1.73$$

body carry over factor from Fig. 7, $\Delta C_{L_{TE}}$ and η_{1B} (flaps end at side of body)

$$K = .58$$

with equation 2.1-10

$$\Delta C_{L_{TE}} = 1.73 + (1.73) \left(\frac{.183}{.666}\right) (.58)$$

$$= 1.73 + .28$$

$$\Delta C_{L_{TE}} = 2.01$$

from test

$$C_{L_{TE}} = 1.91$$

Contrails

2.1.1.3 Effect of Leading Edge Flap Deflection

There has been little work done to correlate test data on the effect of leading edge flap deflection on lift below $C_{L_{max}}$. Since this effect is relatively small compared to trailing edge flap deflection, leading edge flap effectiveness is taken to be the potential flow value given in Figure 9.

On a three-dimensional swept wing with a part span leading edge device,

$$\Delta\alpha_{OLLE} = \alpha\delta_{LE} \delta_{LE} \cos\Lambda_{c/4} \lambda_{LE} \quad (2.1-13)$$

$$\Delta C_{LLE} = (C_{L\alpha})(-\Delta\alpha_{LE}) \quad (2.1-14)$$

SAMPLE PROBLEM, LEADING EDGE LIFT INCREMENT

$$C_{LE}/C = .166$$

$$\delta_{LE} = 70^\circ$$

$$\Lambda_{c/4} = 15^\circ$$

$$\eta_{1B} = .145$$

$$\eta_{OB} = 1.0$$

$$C_{L\alpha} = .0988$$

From Fig. 9 and C_{LE}/C read

$$\alpha\delta_{LE} = .028$$

From Fig. 5 and η_{1B} and η_{OB}

$$\lambda_{LE} = 1 - .183 = .817$$

using Equation 2.1-13 and 2.1-16

$$\Delta\alpha_{OL} = (.028)(70)(.966)(.817) = 1.55$$

$$\Delta C_{LLE} = -(.0988)(1.55) = -.15$$

from test

$$\Delta C_{LLE} = -.18$$

Contrails

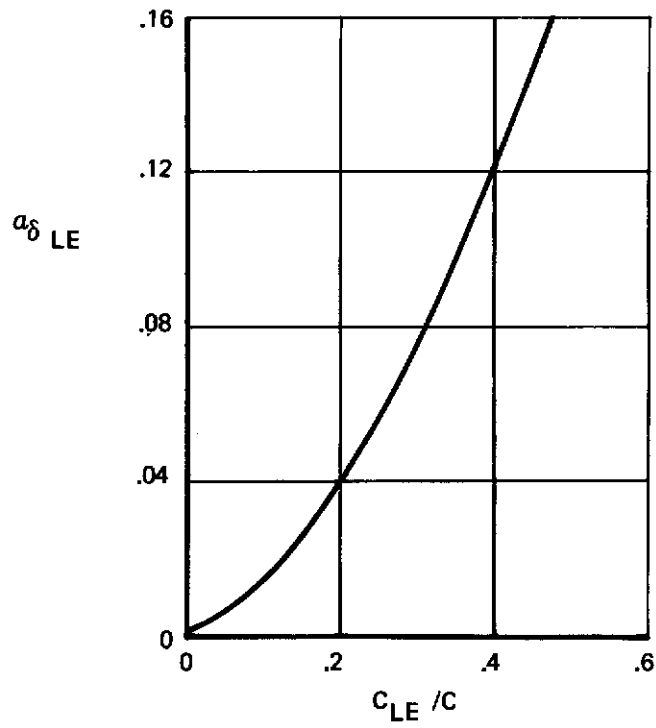
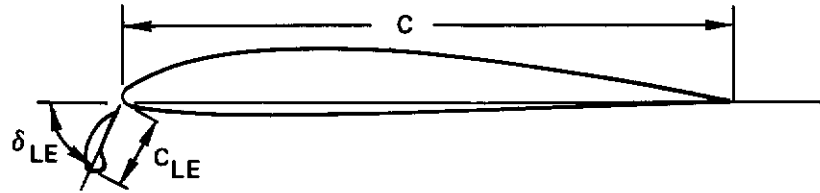
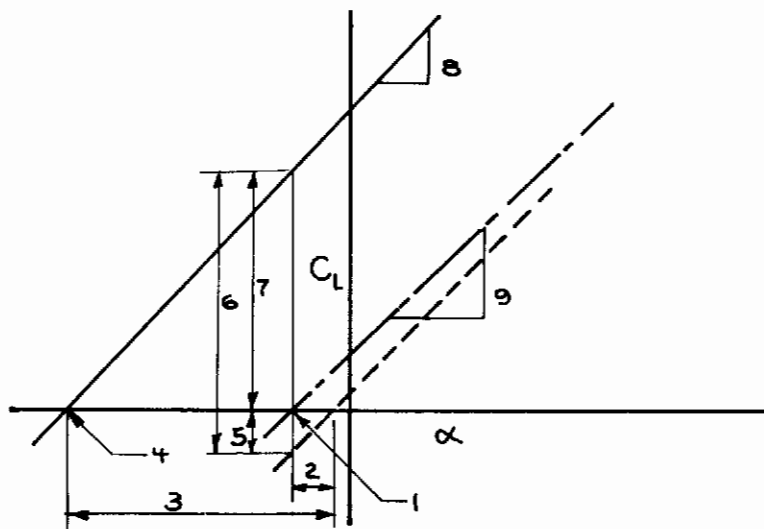


Figure 9: Leading Edge Flap Effectiveness

Contrails

2.1.1.4 Total Free Air Lift

The increments obtained, $\Delta\alpha_{OL}$ and ΔC_L and the slope of the flaps down lift curve may be combined with flaps up estimates from Datcom or other sources.



- (1) α_{OL} flaps up from Datcom or other source
- (2) $\Delta\alpha_{OL_{LE}}$
- (3) $\Delta\alpha_{OL_{TE}}$
- (4) α_{OL} flaps down = (1) + (2) + (3)
- (5) $\Delta C_{L_{LE}}$
- (6) $\Delta C_{L_{TE}}$
- (7) $\Delta C_{L_f} = (5) + (6)$
- (8) C_{L_α} flaps down
- (9) C_{L_α} flaps up Datcom

2.1.2 Maximum Lift

Many attempts have been made to develop methods for estimating the maximum lift of an airplane with a high lift system. No method has given consistently reliable results. The method given here should apply to the type of configuration likely to be considered for a STOL transport. Unfortunately, $C_{L_{max}}$ may vary widely from the values calculated by this method for particular configurations with unusual arrangements.

The approach taken divides the problem into the $C_{L_{max}}$ of the clean wing plus increments due to leading edge and trailing edge devices.

For the clean wing, the methods of Datcom may be used to estimate $C_{L_{max}}$. Next the increment in maximum lift due to leading edge devices will be added to the clean wing, then the trailing edge increment added. This technique has been chosen because of the availability of data in this form. It would be more satisfying to add a leading edge increment to the flaps-down maximum lift, since the shape and optimum deflection of the leading edge device is a function of the trailing edge lift increment. However, insufficient data is available to use this approach.

2.1.2.1 Leading Edge Devices

The maximum lift increment due to leading edge devices is a function of wing sweep, device chord, shape, deflection, and span. It is assumed that care will be taken in tailoring and fairing areas such as intersections of nacelle struts and wings, etc., where relatively large penalties may result from local flow separation and interference effects.

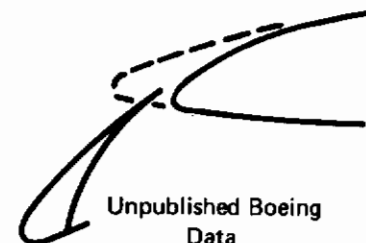
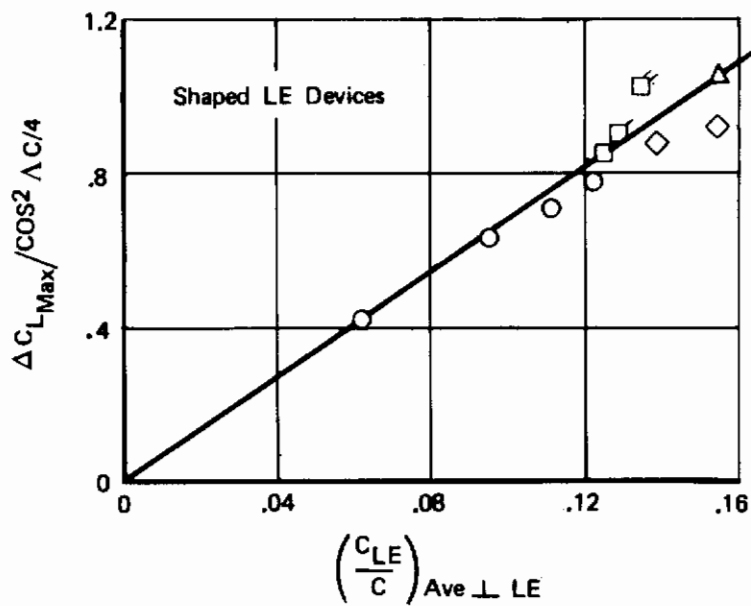
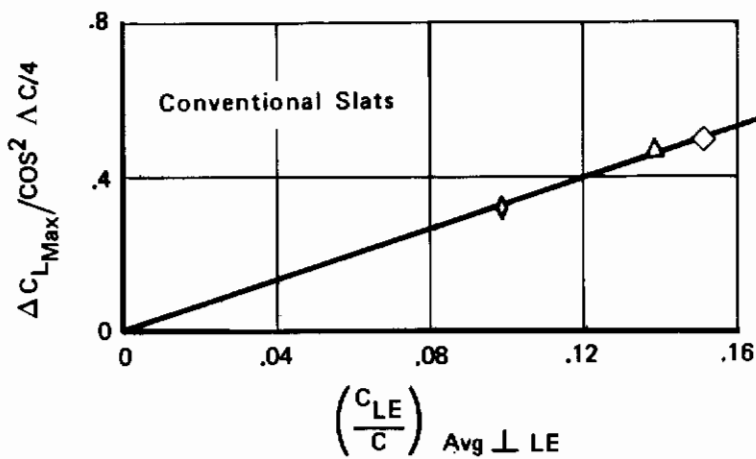
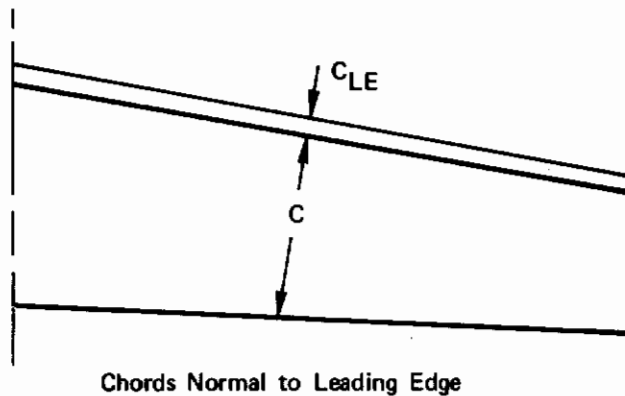
Correlations of $\Delta C_{L_{max}} / \cos^2 \Lambda_{c/4}$ versus leading edge device chord ratio are shown in Fig. 10 for conventional leading edge slats and for shaped leading edge devices representative of current state-of-the-art variable-camber Krueger flaps.

The maximum lift increment due to the leading edge device is then:

$$\Delta C_{L_{max_{LE}}} = \left(\frac{\Delta C_{L_{max}}}{\cos^2 \Lambda_{c/4}} \right) \cos^2 \Lambda_{c/4} \quad (2.1-15)$$

It should be noted that for this estimate the chord lengths are measured normal to the basic wing leading edge and that the gross area is the area of the basic wing extended to the body centerline.

Contrails



Unpublished Boeing Data

Sym	$\Delta \frac{1}{4}$	A
○	36°	6.964
□	32°	7.46
◻	20°	8.92
◻	9.5°	9.65
◇	37.5°	6.96
△	32°	7.48
◊	25°	8.83

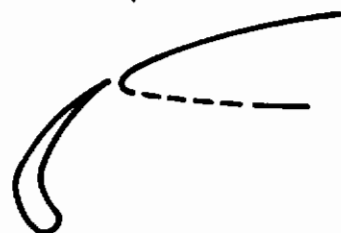


Figure 10: Effect of Leading Edge Device on Maximum Lift

SAMPLE PROBLEM, LEADING EDGE MAXIMUM LIFT

STAI Wind Tunnel Model, L.E. deployed, 15° sweep.

$$\frac{C_{LE}}{C} = .166$$

$$\Lambda_{c/4} = 15^\circ$$

from Fig. 10 and C_{LE}/C read

$$\frac{\Delta C_{L_{max}}}{\cos^2 \Lambda_{c/4}} = 1.14 \text{ (shaped leading edge)}$$

with Equation 2.1-15

$$\begin{aligned} \Delta C_{L_{maxLE}} &= (1.14) \cos^2 15.0 \\ &= 1.06 \end{aligned}$$

from test data

$$\Delta C_{L_{maxLE}} = .57$$

The calculated value is too high because the leading edge device tested was a compromise designed for several nacelle strut locations and leading edge sweep angles. A larger $\Delta C_{L_{max}}$ for a given configuration could normally be achieved by tailoring the leading edge.

2.1.2.2 Trailing Edge Devices

The increment in $C_{L_{max}}$ due to deploying trailing edge flaps is caused by two effects; increased area due to chord extension, if any, and increased camber. Assuming that the airfoil stalls when leading edge pressure distributions are similar for the flaps-up and -down cases, the theoretical maximum lift increment is related trailing edge flap lift increment by:

$$\Delta C_{L_{max}} = \left[\frac{\Delta C_{l_{max}}}{\Delta C_{l_{f\alpha=0}}} \right] \left(\frac{A+2}{A} \right) \Delta C_{L_{TE}} \quad (2.1-16)$$

where $\left[\frac{\Delta C_{l_{max}}}{\Delta C_{l_{f\alpha=0}}} \right]$, taken from Ref. 9, is given in Fig. 11.

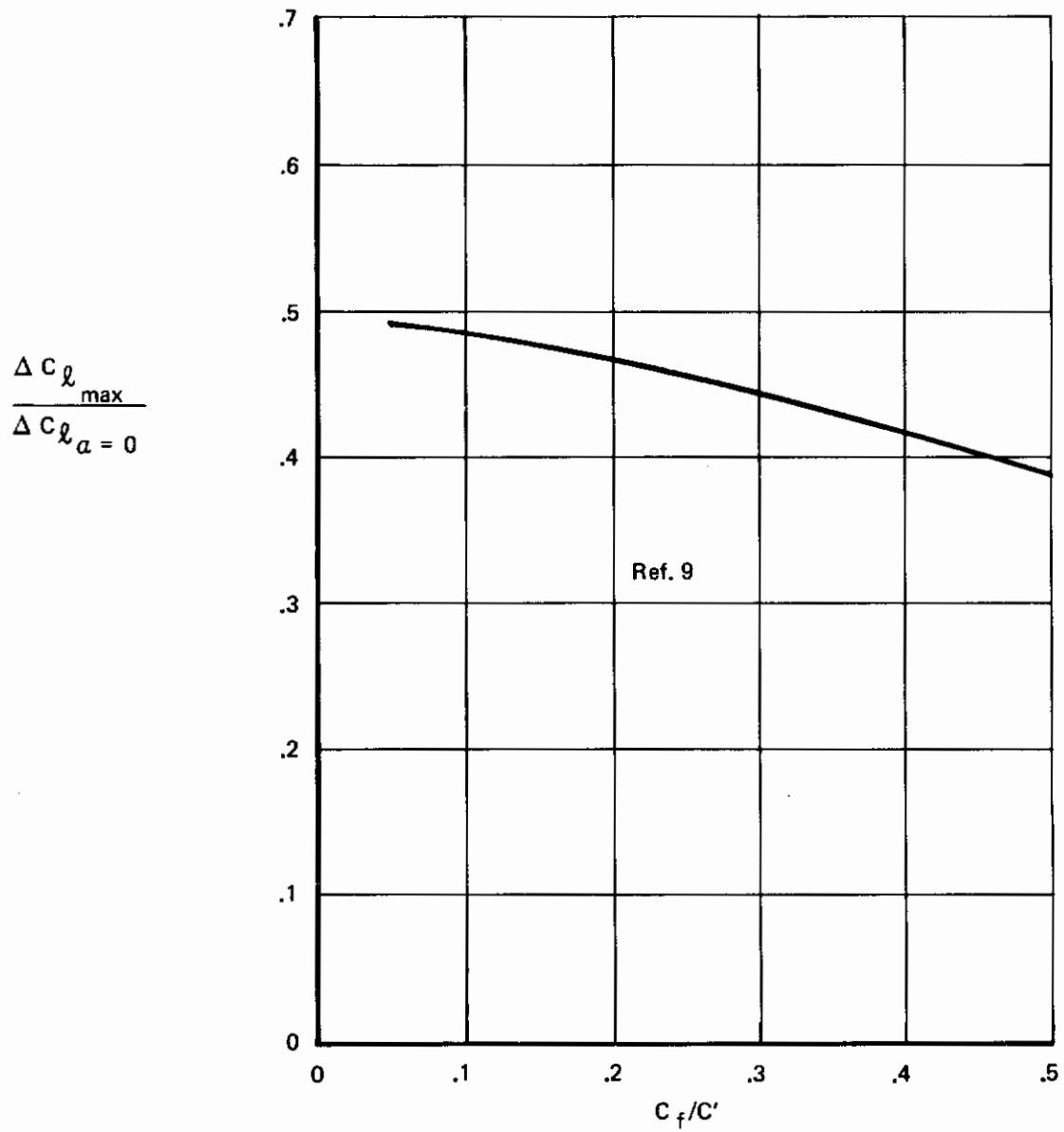


Figure 11: 2-D Maximum Lift Increment

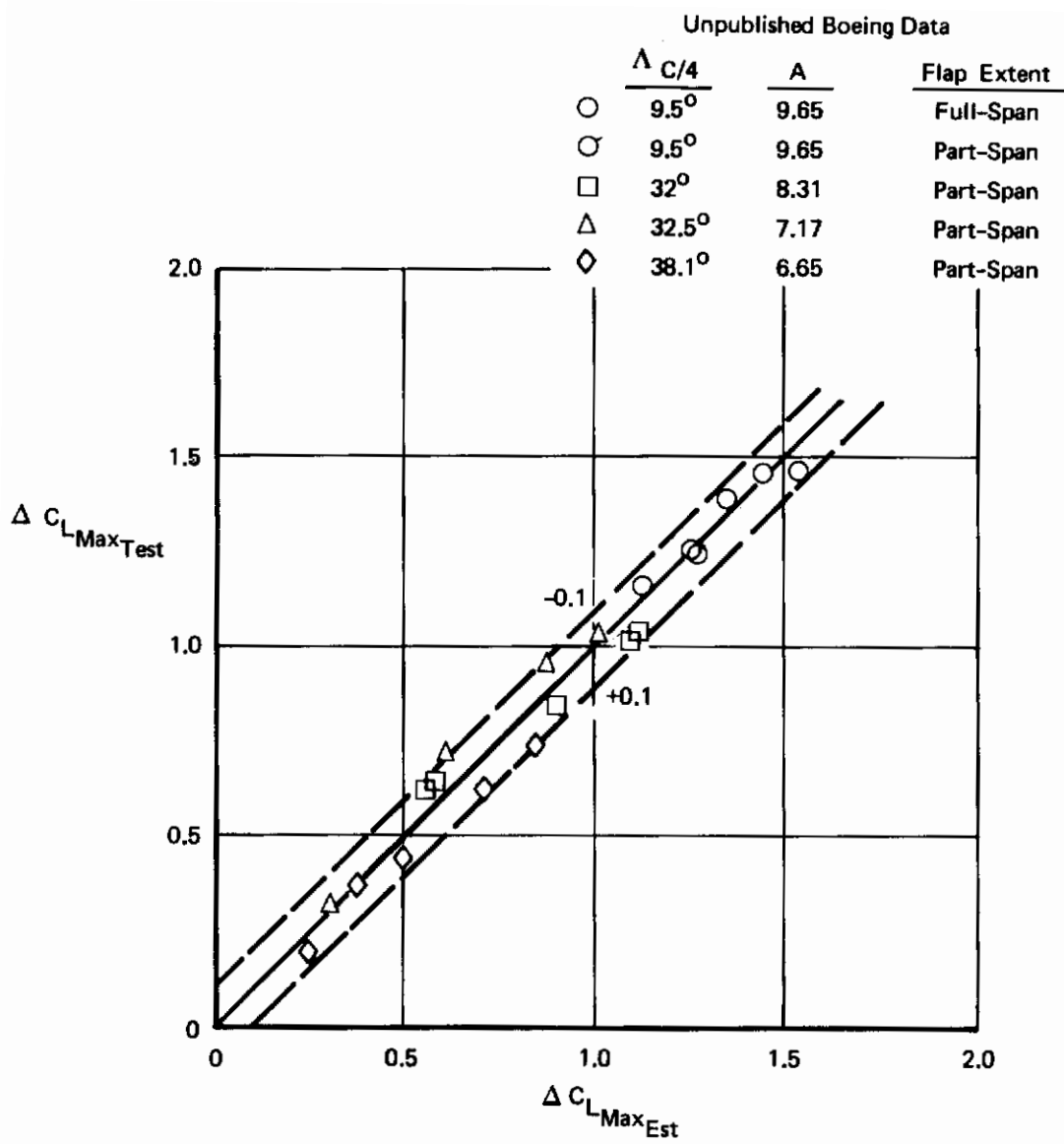


Figure 12: Trailing Edge Flap, Maximum Lift Increment

Contrails

SAMPLE PROBLEM, TRAILING EDGE MAXIMUM LIFT

STAI wind tunnel model L.E. and T.E. devices deployed, 15° sweep.

$$\lambda_{TE} = .666 \text{ (from Section 2.1.1.2)}$$

$$C'_f/C' = .323$$

$$A_G = 5.74$$

$$\Delta C_{L_{TE}} = .201 \text{ from Section 2.1.1.2}$$

$$\Delta S_{TE} = 1.104 \text{ SF}$$

$$S'_{Gross} = 5.119 \text{ SF}$$

$$\Delta S'_{LE} = .624 \text{ SF}$$

$$C_{LE}/C = .167$$

$$C_{LE}/C' = .130$$

$$\Lambda_{c/4} = 15.4^\circ$$

$$S_{REF} = 6.164 \text{ SF}$$

$$C_{L_{MaxFU}} = .98 \text{ flaps up (test data)}$$

$$\Delta C_{L_{mLE}} = 1.06 \text{ from Section 2.1.2.1}$$

from Fig. 11 and C'_f/C'

$$\frac{\Delta C_{L_{Max}}}{\Delta C_{L_{\alpha=0}}} = .438$$

maximum lift increment from camber, Equation 2.1-16

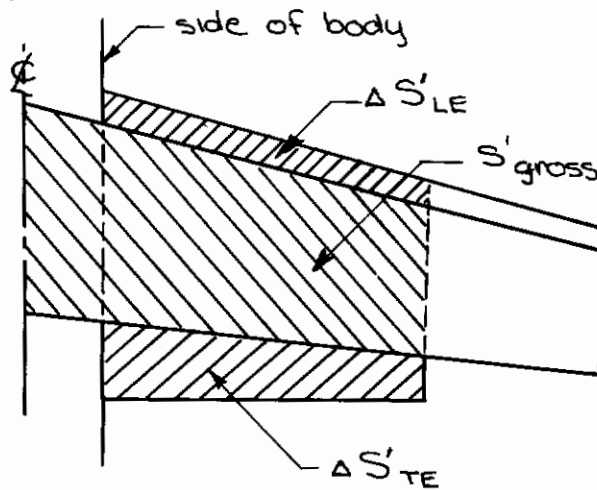
$$\Delta C_{L_{Max}} = (.438) \left(\frac{5.74 + 2}{5.74} \right) (2.01) = 1.19$$

maximum lift increment from chord extension, Equation 2.1-17.

$$\Delta C_{L_{Max}} = (.98 + 1.06) \left(\frac{1.104}{5.119 + .624} \right) (.666) = .27$$

From Fig. 10 at C_{LE}/C read slope of curve

$$\frac{d \left(\frac{\Delta C_{L_{Max}}}{\cos^2 \Lambda_{c/4}} \right)}{d \left(\frac{C_{LE}}{C} \right)} = 6.9$$



Contrails

Change in maximum lift increment for reduction in leading edge chord ratio, Equation 2.1-18

$$\Delta C_{L_{Max}} = (6.9)(\cos^2 15.)(.130 - .167)\left(\frac{5.119 + 1.104}{6.164}\right)(.666) = -.16$$

The total increase in maximum lift from the trailing edge flap

$$\begin{aligned}\Delta C_{L_{Max}} &= 1.19 + .26 - .16 \\ &= 1.29\end{aligned}$$

from test data

$$\Delta C_{L_{Max}} = 1.57$$

Total Estimated, leading edge and trailing edge flap

$$\begin{aligned}C_{L_{Max}} &= .98 + 1.29 + 1.06 \\ &= 3.33\end{aligned}$$

from test data

$$C_{L_{Max}} = 3.12$$

The comparison between the estimate and test data show a fortunate combination in the estimated data. The increment from the leading edge was low and the trailing edge increment high resulting in a better comparison with the total from test data.

2.1.2.3 Leading Edge Boundary Layer Control

The effectiveness of leading edge blowing boundary layer control is very configuration dependent. For example, a wing with large regions of separated flow near the leading edge would show large improvement in maximum lift with small amounts of blowing momentum. The correlation to be shown in this section does not include the effect of BLC as a cure for problem areas; e.g., separated flow in the wing/nacelle strut intersection region.

A correlation based on unpublished Boeing data is shown in Fig. 13 for leading edge devices designed specifically for blowing applications. The upper curve is based on configurations with uninterrupted leading edges; i.e., no wing mounted nacelles, and represents a design goal for a well-tailored configuration with wing mounted nacelles. The lower curve represents the level achieved with wing mounted nacelles with no additional system tailoring. An optimized leading edge device may achieve the lift levels indicated only to fall below this level when operated at off design conditions. The curves should yield reasonable, achievable, levels but no generalized information is available regarding best device shape or deflection or in what manner the blowing should be distributed on the wing.

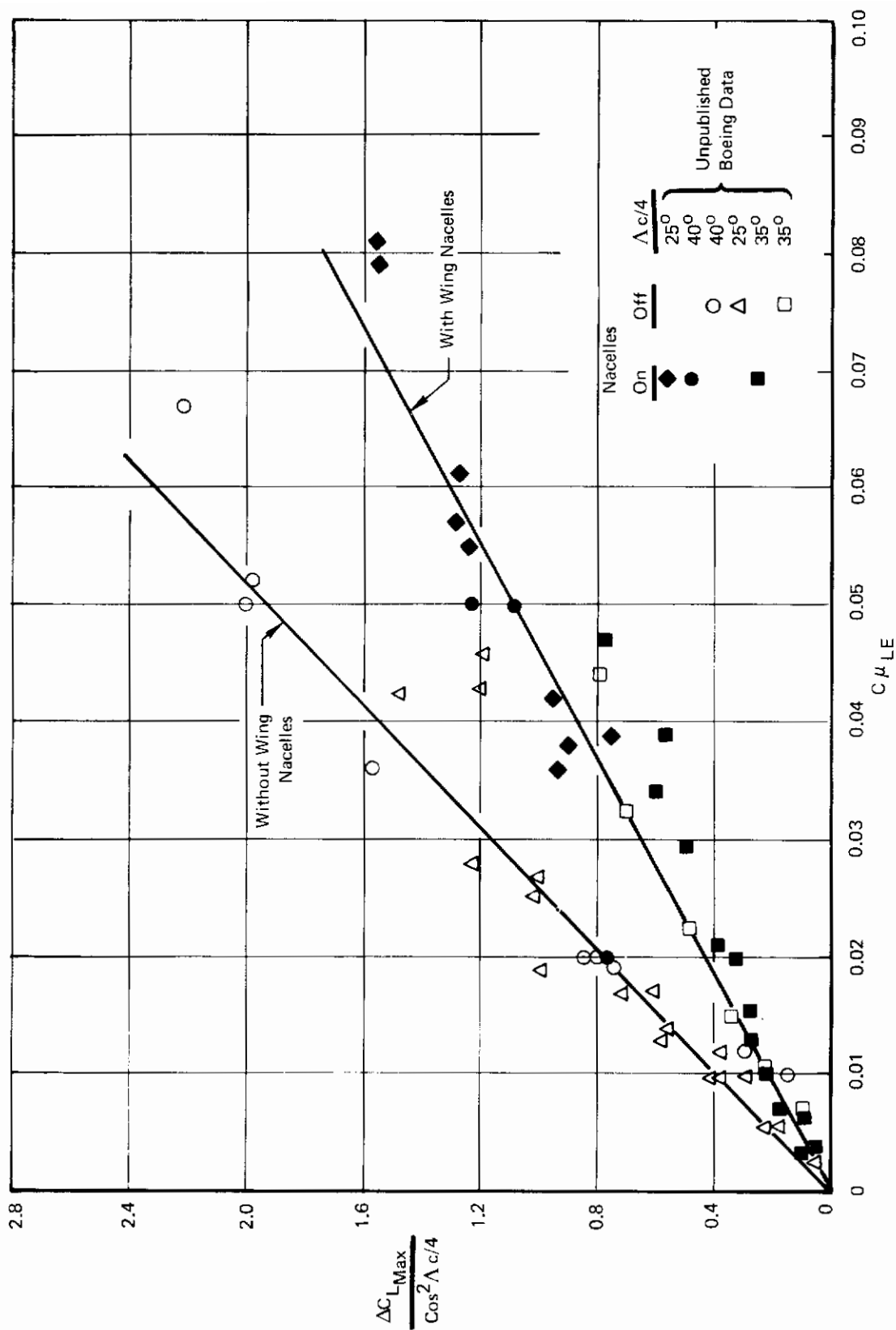


Figure 13: Leading Edge Blowing Boundary Layer Control Effectiveness

Leading edge blowing boundary layer control may also result in some increase in trailing edge effectiveness. This is a result of the thinner boundary layer that then exists ahead of the trailing edge flaps. Insufficient data exists to allow a rational correlation of this effect to be developed.

SAMPLE PROBLEM, MAXIMUM LIFT WITH L.E. BOUNDARY LAYER CONTROL

STAI Wind Tunnel Model, Nacelles On

$$C_{\mu_{LE}} = .06$$

$$\Lambda c/4 = 15.40$$

from Fig. 13 and $C_{\mu_{LE}}$

$$\frac{\Delta C_{L_{Max}}}{\cos^2 \Lambda c/4} = 1.3$$

Maximum lift increment for leading edge blowing

$$\begin{aligned}\Delta C_{L_{Max}} &= (1.3)(\cos^2 15.4) \\ &= 1.21\end{aligned}$$

from test data

$$C_{L_{Max}} = .29$$

This increment from test data is much too low, which may be the result of off-design operation of the leading edge devices, i.e. 15° rather than 30° sweep. Also, the model had not been tailored, and there were grounds to believe that there was trailing edge separation adjacent to the body. It would be expected with proper refinement of the model configuration the maximum lift increment from leading edge blowing would approach the predicted levels.

2.1.3 Drag

The approach will be to divide the drag into the clean airplane drag, the profile drag of the leading and trailing edge devices, the induced drag, and the pressure drag of the wing. Clean airplane drag can be found by conventional methods.

2.1.3.1 Trailing Edge Flap Parasite Drag

The parasite drag of trailing edge flaps is a function of flap type, area, and deflection. An empirical correlation for slotted flaps is given in Figure 14.

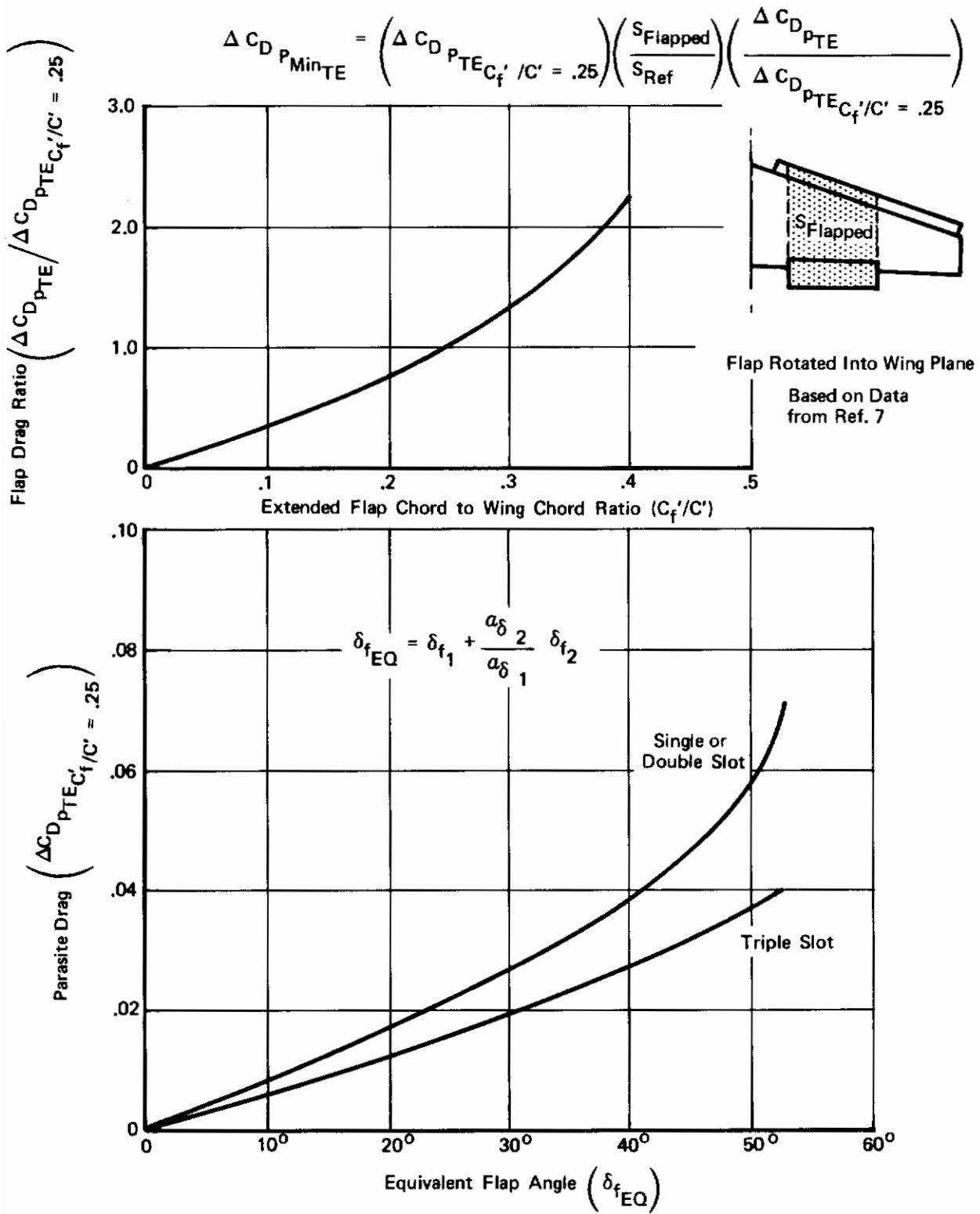


Figure 14: Parasite Drag of Trailing Edge Flaps

$$C_{DP\ min} = \left(\Delta C_{DP\ TE} \right)_{\frac{C'_f}{C} = .25} \left(\frac{S_{flapped}}{S_{REF}} \right) \left(\frac{\Delta C_{DP\ TE}}{\left[\Delta C_{DP\ TE} \right]_{\frac{C'_f}{C} = .25}} \right) \quad (2.1-20)$$

In this correlation the flapped area is the area forward (streamwise) of the trailing edge flap with the flaps, leading and trailing edge, extended and rotated into the plane of the wing.

2.1.3.2 Leading Edge Flap Parasite Drag

The parasite drag of leading edge devices is a function of device area and deflection. Insufficient data is available to establish an optimum leading edge deflection angle. However, unpublished Boeing data indicates that at the optimum angle

$$\Delta C_{DP\ min} = .154 \frac{S_{LE}}{S_{REF}} \quad (2.1-21)$$

where the leading edge area is the planform area of the leading edge device measured parallel to the device chord plane.

2.1.3.3 Change in Induced Drag from Trailing Edge Flaps

Deflecting trailing edge flaps results in a change in load distribution from that of the clean wing. Since the clean wing is normally designed to have a load distribution close to elliptic, the loading due to flaps will normally cause the load distribution to depart from elliptic, resulting in an additional induced drag. A. D. Young (Ref. 10) gives this drag for part-span flaps proportional to the square of the flap lift increment

$$\Delta C_{D_i} = K \left(\frac{C_{L_f}^2}{\pi A} \right) \quad (2.1-22)$$

where K is determined from Figure 15.

More accurate estimate of the polar shape may be determined by methods such as that in Ref. 1. However, these methods require the span loading to be determined.

2.1.3.4 Parasite Drag Variation with Lift

Both the friction and pressure drag vary with lift. It is impossible to estimate these variations precisely, yet some allowance should be made for them. The data from a number of wind tunnel tests of transport configurations with highly developed mechanical high lift systems have been correlated to obtain the curve shown in Figure 16. This curve is intended to give a reasonable preliminary design estimate of the parasite drag variation with lift with both leading and trailing edge devices deployed.

Contrails

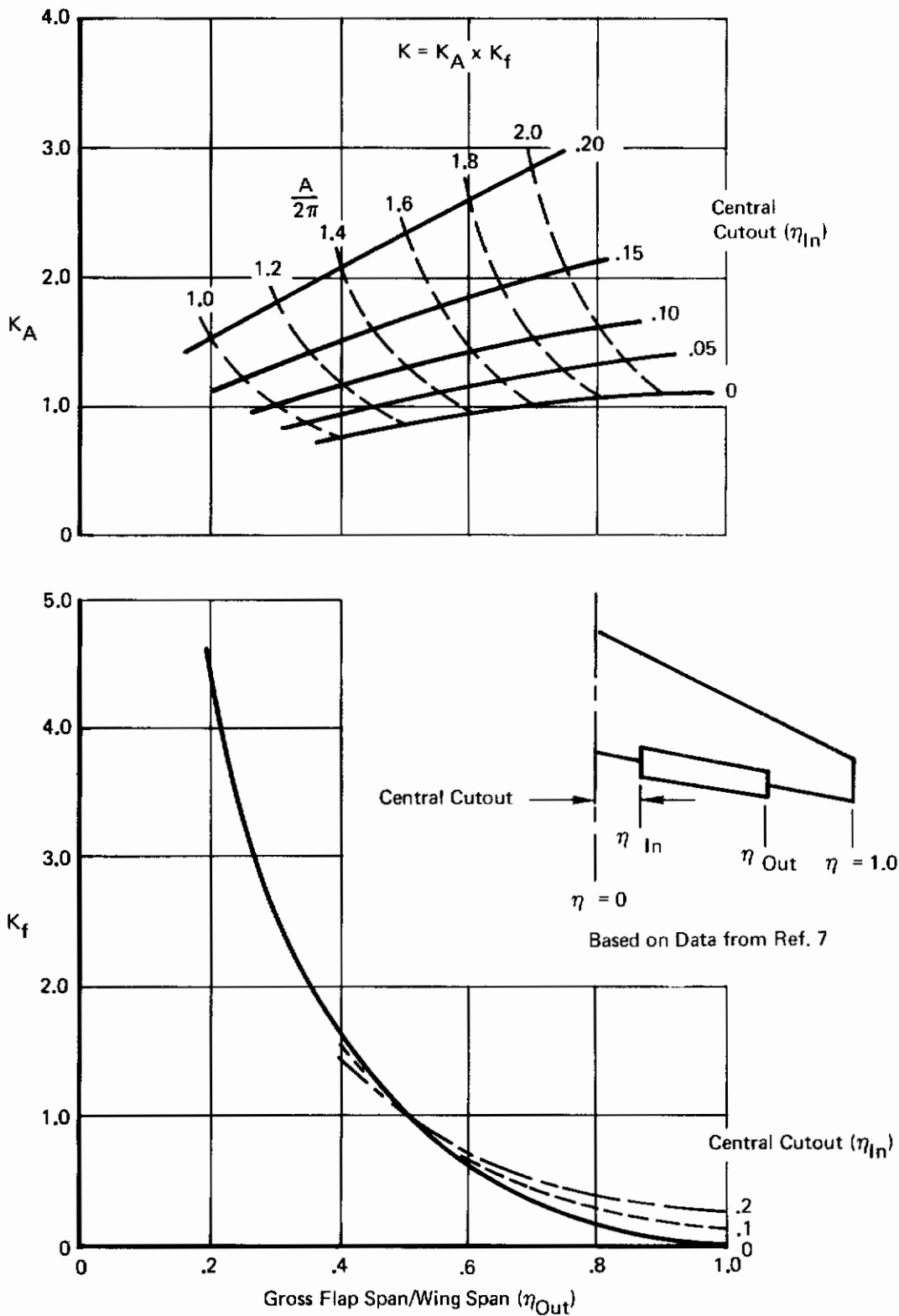


Figure 15: Part-Span Induced Drag Factors (Continuous Flaps with Central Cutout)

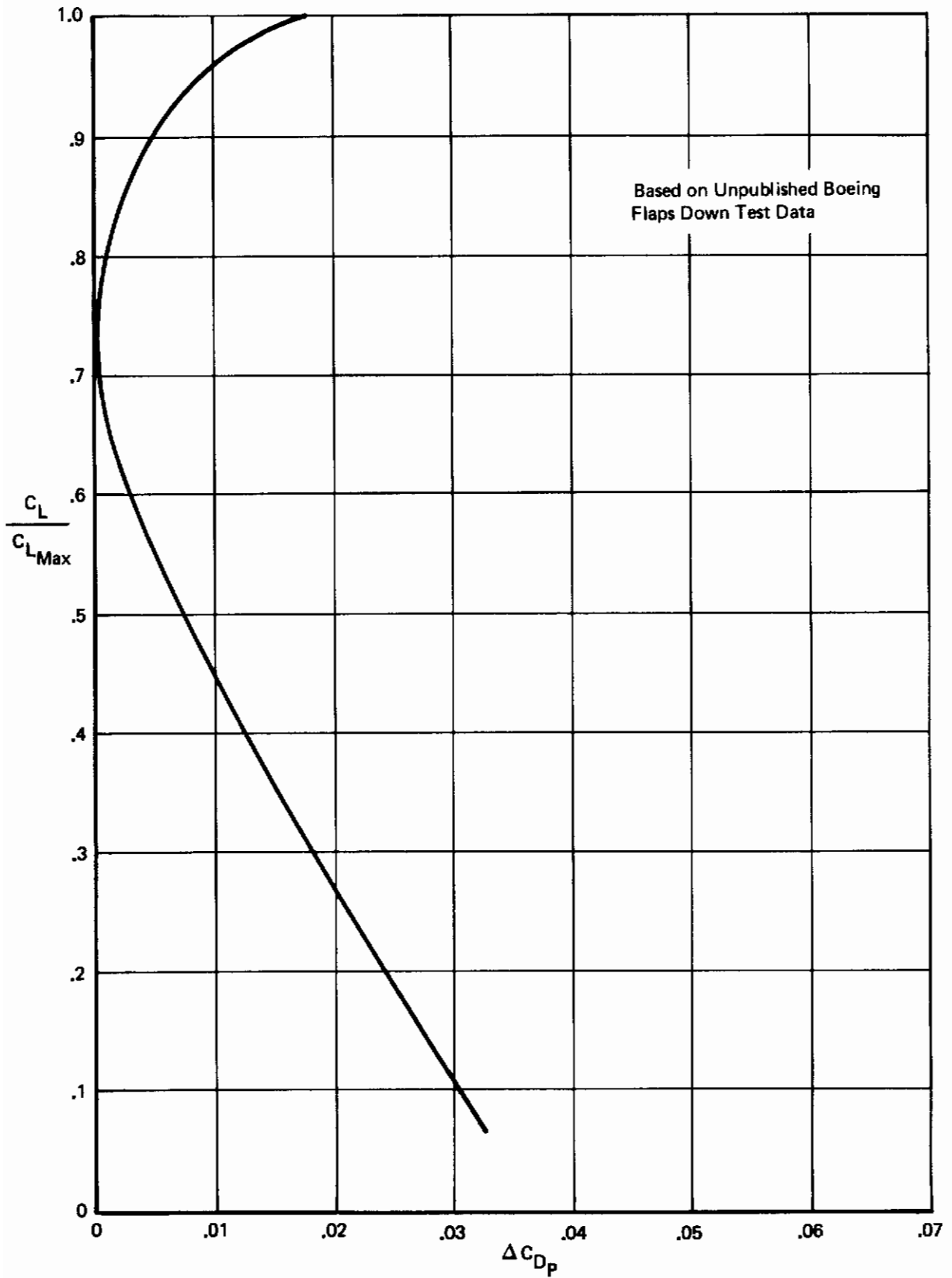


Figure 16: Profile Drag Variation with Lift

2.1.3.5 Induced Drag

The drag due to lift is estimated assuming elliptic load distribution.

$$C_{Di} = \frac{C_L^2}{\pi A} \quad (2.1-23)$$

This is used since the drag increments estimated in the previous sections are designed to account for the departure from an elliptic load.

A comparison between drag estimated by the methods described and drag obtained from the STAI wind tunnel test program is shown in Figure 17.

2.1.3.6 Leading Edge Boundary Layer Control

The effects of leading edge blowing boundary layer control on drag were obtained from the STAI wind tunnel test data. These data indicate that

$$\Delta C_{DBLC} = -.5 C_{\mu LE} \quad (2.1-24)$$

SAMPLE PROBLEM, FREE AIR DRAG

$$S_{\text{flapped}} = 5.577 \text{ SF}$$

$$S_{\text{Ref}} = 6.164 \text{ SF}$$

$$\delta_{f1} = 44.9^\circ$$

$$\delta_{f2} = 15.1^\circ$$

$$(\alpha_\delta)_1 = -.50$$

$$(\alpha_\delta)_2 = -.25$$

$$C'_{f1}/C' = .289 \text{ (includes leading edge extension)}$$

$$S_{LE} = .882 \text{ SF}$$

$$C_{L_{TEF}} = 1.73$$

$$A_G = 5.74$$

$$A = 8.00$$

$$\eta_{1B} = .145$$

$$\eta_{0B} = .75$$

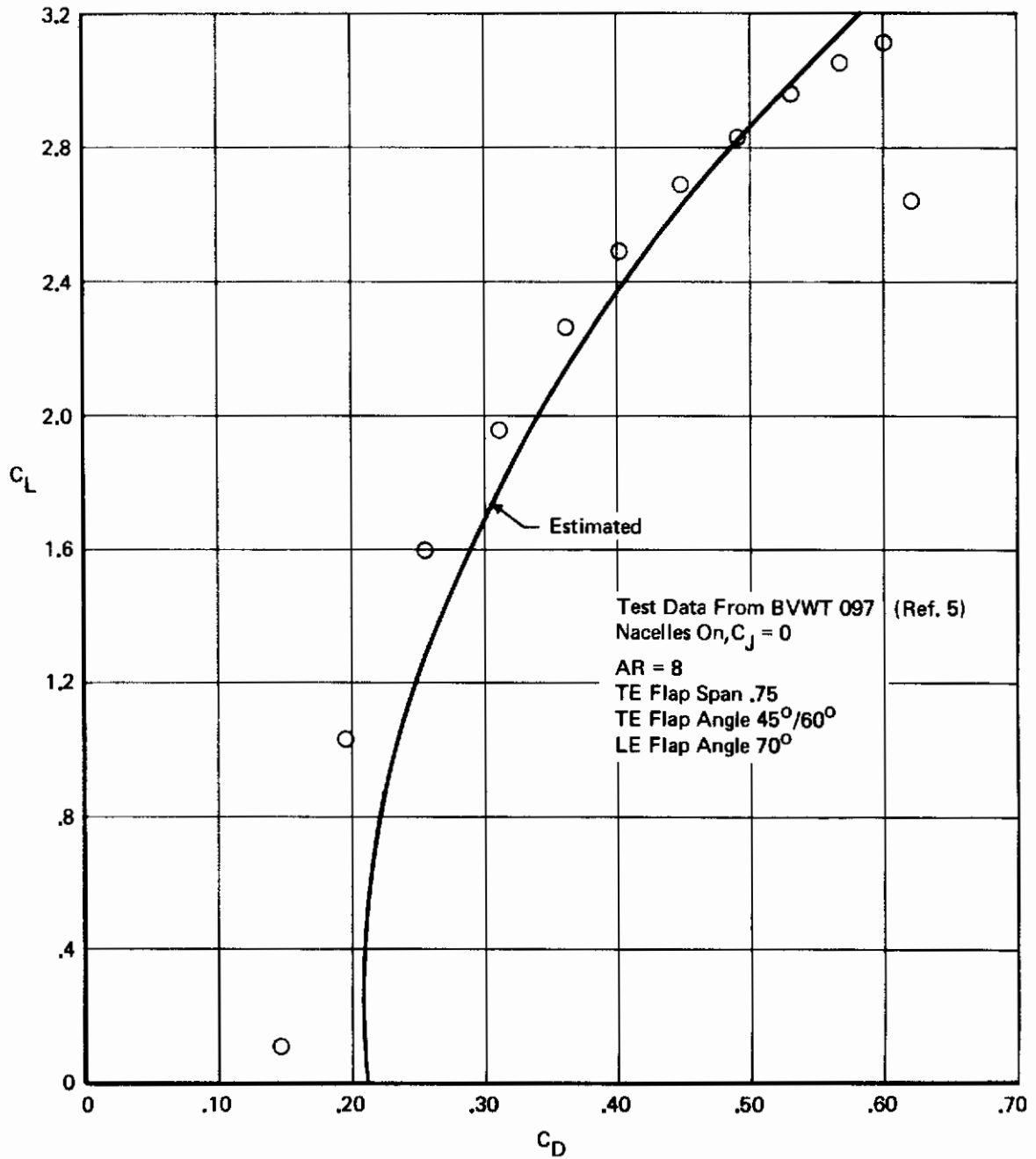


Figure 17: Comparison of Measured and Predicted Power-Off Drag Polars

Contrails

$$C_{L_{Max}} = 3.33 \text{ from Section 2.1.2.1 and 2.1.2.2}$$

$$C_{L_{Max}} = .98 \text{ test data flaps retracted}$$

$$C_{D_0} = .0600 \text{ test data, flaps retracted}$$

$$C_{H_{LE}} = 0$$

Calculate equivalent flap angle, Figure 14.

$$\delta_{f_e} = 45.14 + \left(\frac{.25}{.7485}\right) (15.13) = 52.94$$

Read from Figure 14 and $C'_{f/C}$ and δ_{f_e}

$$\left(\frac{\Delta C_{DP_{TE}}}{C}\right) C'_{f/C} = .25$$

$$\frac{\Delta C_{DT}}{C} = 1.25$$

Trailing Edge parasite drag, Equation 2.1-20

$$\Delta C_{D_{P_{MIN}}} = (.0395) \left(\frac{5.577}{6.164}\right) (1.0) = .0447$$

Leading edge parasite drag, Equation 2.1-21

$$\Delta C_{D_{P_{MIN}}} = (.154) \left(\frac{.882}{6.164}\right) = .0220$$

From Figure 15 and $A_G \eta_{1B}$ and η_{0B} read

$$K_a = 1.05$$

$$K_f = .4$$

$$K = (1.05) (.4) = .42$$

Change in induced drag from trailing edge flaps, Equation 2.1-22

$$\Delta C_{D_i} = (.42) \left(\frac{(1.73)^2}{(8)}\right) = .0500$$

at a $C_L = 2.4$ parasite drag variation with lift, with $C_{L_{Max}} = 3.33$

$$\Delta C_{D_P} = .0005$$

Induced drag

$$C_{D_i} = \frac{(2.4)^2}{(\pi)(8)} = .2290$$

Total Drag

$$\begin{aligned} C_D &= .0600 + .0447 + .0220 + .0500 + .0005 + .2290 \\ &= .4062 \end{aligned}$$

From Test Data at $C_L = 2.4$

$$C_D = .3880$$

2.1.4 Pitching Moment

Deflection of leading and trailing edge devices affects the tail-off airplane pitching moment characteristics by:

- (1) Moving the aerodynamic center location if chord extension is involved.
- (2) Changing the pitching moment at zero lift because of a change in camber.

An additional effect which influences the tail-on pitching moment is the change in the downwash field behind the wing. In the following sections these effects are examined. The methods for estimating the change in aerodynamic center location and pitching moment at zero lift are taken from Ref. 7. Methods for predicting the effects of high lift devices on the downwash field behind the wing are from Ref. 1 and 11.

2.1.4.1 Aerodynamic Center Shift Due to Leading Edge Devices

Leading edge devices without chord extension do not move the aerodynamic center as long as the flow remains attached. When chord extension is present, the a.c. shift may be calculated by considering the leading edge planform extension. The estimate of the aerodynamic center shift is made relative to the a.c. location of the basic trapezoidal wing.

An elliptical additional span load is assumed for the trapezoidal wing. The part span load of the wing panel where the chord is extended is λ . Using the Schrenk-Thorpe span load approximation, this panel load increases by half the fractional area increase upon addition of the chord extension covering a small fraction of the wing span. As the chord extension tends to full span, the panel load increment approaches the fractional chord extension.

Contrails

The inner wing panel loads are assumed to be centered at 50 percent of the panel span on the local aerodynamic center both for the original trapezoidal wing and the modified wing. The part of the wing planform contained within the body plan view is treated in a similar manner, letting the local load move forward (or aft for trailing edge devices) as dictated by the chord extension, but the load on the body is held constant.

Two different equations have been derived, for the leading edge devices extending to the side of the body, and for outboard devices which do not extend to the body.

In the following analysis it is assumed that the basic trapezoidal wing aerodynamic center position $(x_{ac})_{trap}$ is known (see Ref. 1 or 2) and the value of the load is unity, i.e.

$$L = 1.0 \quad (2.1-25)$$

Using Figures 5 and 18 and taking moments about A - A gives

$$M = \lambda_1 x_1 - \lambda_2 x_2 + M \Big|_{\eta=2}^{\eta=1} \quad (2.1-26)$$

In Equation 2.1-25 x_1 is the moment arm to the local aerodynamic center of the trapezoid where it intersects the body (use Figure 19 for correction to quarter chord location) and x_2 is the moment arm to the midspan of the wing panel with leading edge devices.

Assuming that M is a linear function of L and $M = 0$ at $L = 0$ leads to

$$\frac{\partial M}{\partial L} = \frac{M}{L} \quad (2.1-27)$$

Since

$$(x_{ac})_{trap} = - \frac{\partial M}{\partial L} = - \frac{M}{L} \quad (2.1-28)$$

it follows from Equation 2.1-25, 2.1-26, and 2.1-28 that

$$(x_{ac})_{trap} = \lambda_1 x_1 + \lambda_2 x_2 - M \Big|_{\eta=2}^{\eta=1} \quad (2.1-29)$$

and

$$-M \Big|_{\eta=2}^{\eta=1} = (x_{ac})_{trap} - \lambda_1 x_1 - \lambda_2 x_2 \quad (2.1-30)$$

The load of the wing with leading edge devices extended is

$$L = 1 + \mu_s \frac{\Delta S}{S_2} \lambda_2 \quad (2.1-31)$$

where $\mu_s \frac{\Delta S}{S_2} \lambda_2$ is the load increase based upon the Schrenk-Thorpe span load assumption. The area increase ΔS is shown in Figure 18 and the load factor is obtained from Figure 20.

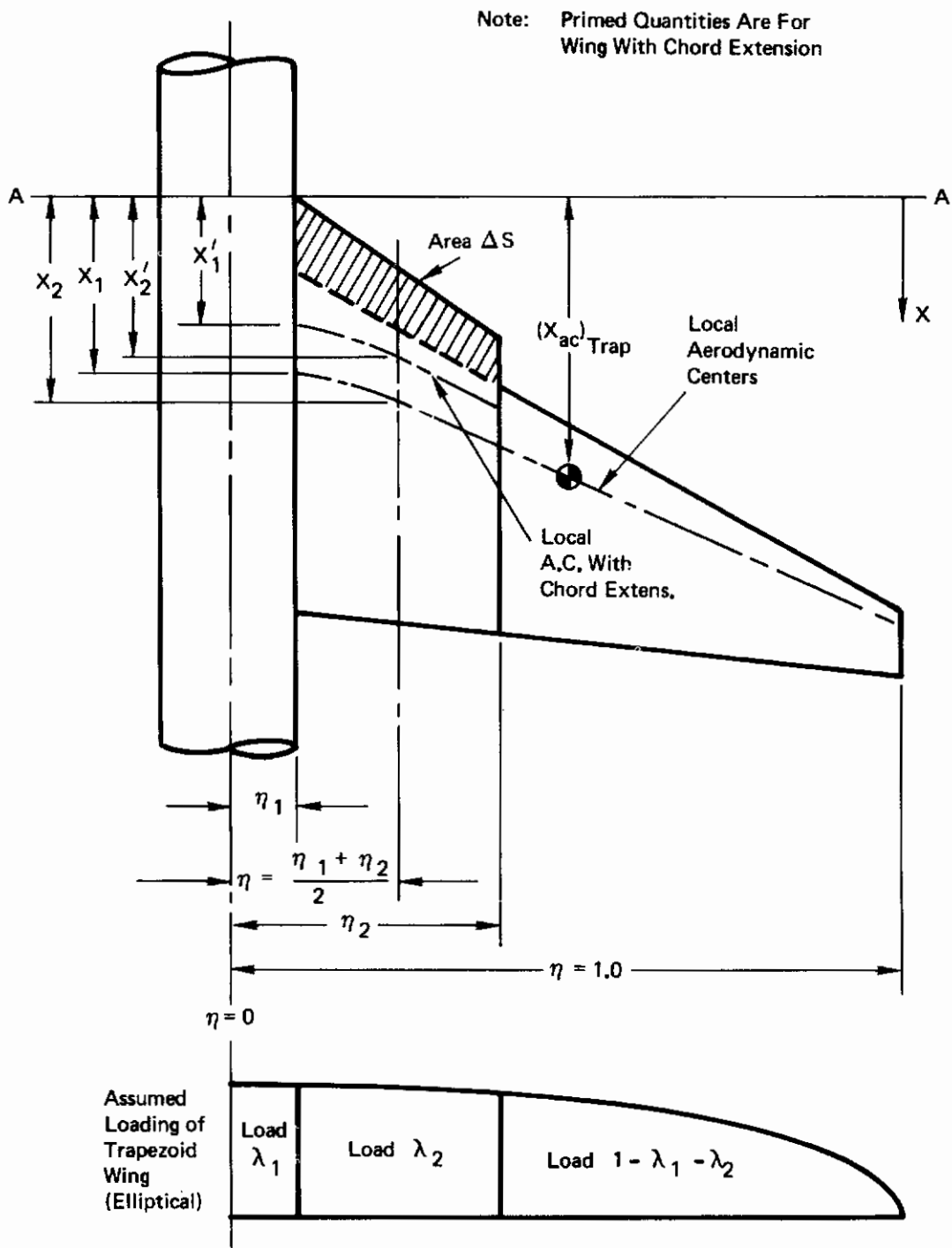


Figure 18: Nomenclature for ac Location with Inboard L.E. Devices

For High Wing Locations

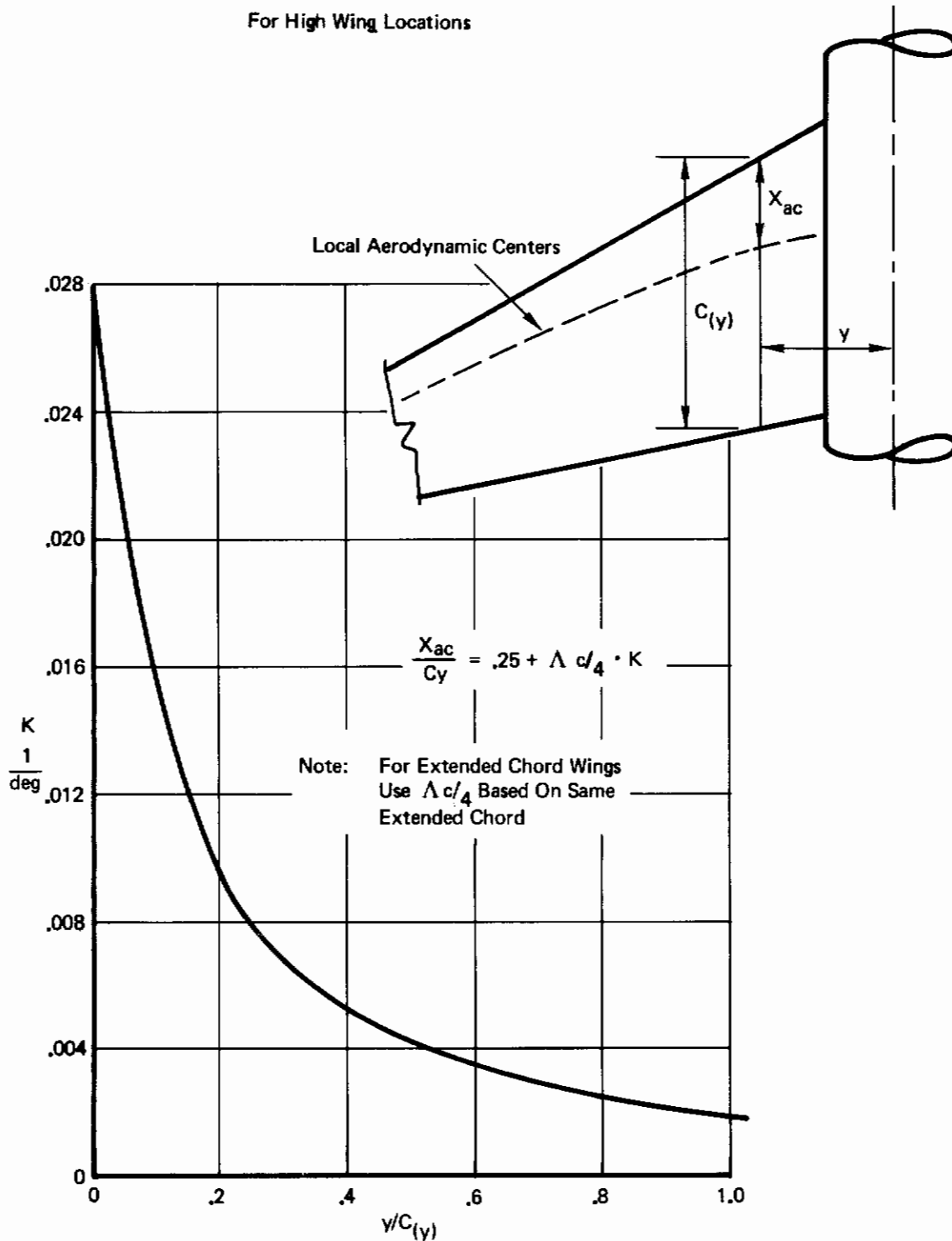


Figure 19: Local Aerodynamic Centers Near Middle Of Wing

Contrails

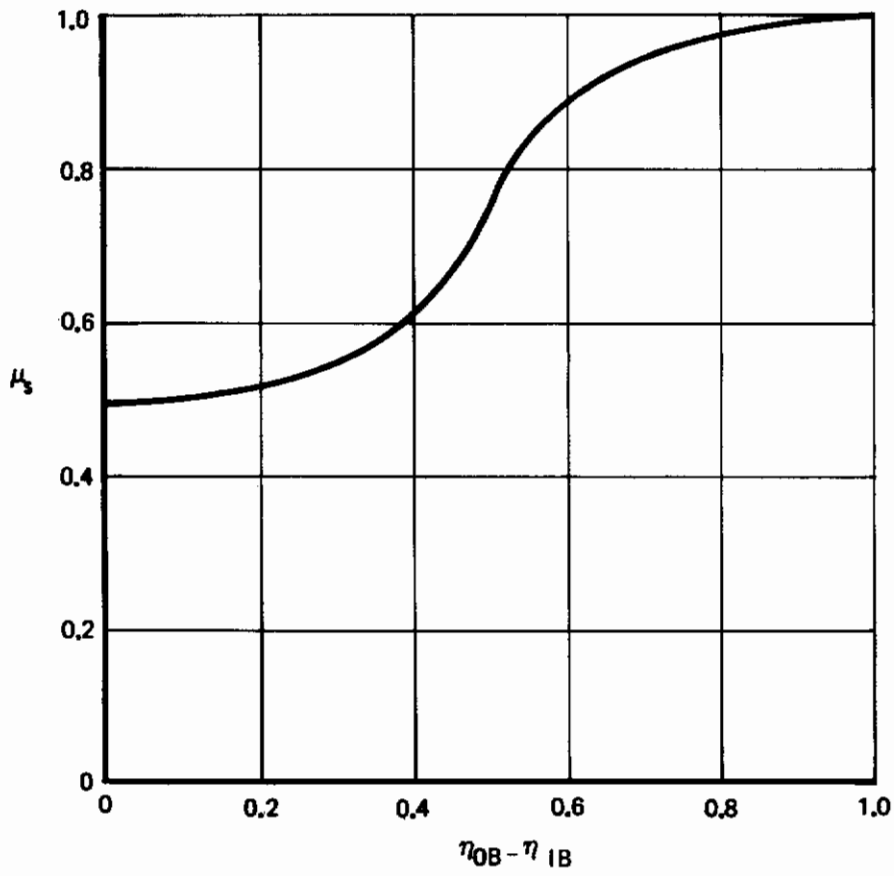
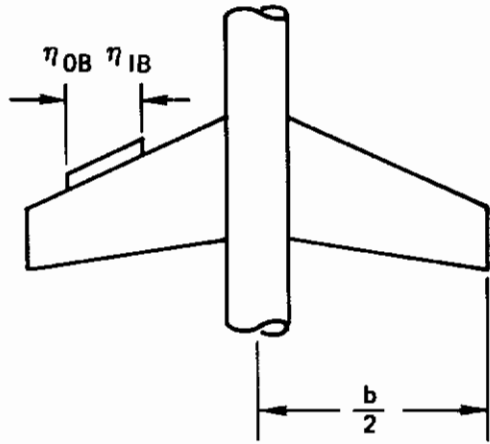


Figure 20: Load Effectiveness of Part Span Chord Extensions

Contrails

Again taking moments about A - A gives:

$$M = -\lambda_1 x'_1 - \lambda_2 x'_2 - \mu_s \frac{\Delta S}{S_2} \lambda_2 x'_2 + M \Big|_{\eta=2}^{\eta=1} \quad (2.1-32)$$

In Equation 2.1-32 x'_1 is the moment arm to the local aerodynamic center of the wing panel with the extended chord at the body side and x'_2 is measured to the extended chord wing local aerodynamic center at $\eta = \frac{\eta_1 + \eta_2}{2}$

The aerodynamic center for the wing with the leading edge devices extended follows from

$$\frac{\partial M}{\partial L} = (x_{ac})_{LE} = \frac{\lambda_1 x'_1 + \lambda_2 x'_2 \left(1 + \mu_s \frac{\Delta S}{S_2}\right) - M \Big|_{\eta=2}^{\eta=1}}{1 + \mu_s \frac{\Delta S}{S_2} \lambda_2} \quad (2.1-33)$$

Substituting Equation 2.1-30 into 2.1-33 gives:

$$(x_{ac})_{LE} = \frac{\lambda_1 (x'_1 - x_1) + \lambda_2 \left[1 + \mu_s \frac{\Delta S}{S_2}\right] (x'_2 - x_2) + (x_{ac})_{trap}}{1 + \mu_s \frac{\Delta S}{S_2} \lambda_2} \quad (2.1-34)$$

The analysis for the outboard leading edge devices is very similar to the one employed above. A simplification here is that the load on the body region does not require separate identification.

Assuming again a unity load

$$L = 1.0 \quad (2.1-35)$$

and taking moments about A-A (see Figure 21) leads to

$$M = M \Big|_{\eta=0}^{\eta=1} - \lambda_2 x_2 + M \Big|_{\eta=2}^{\eta=1} \quad (2.1-36)$$

Hence,

$$(x_{ac})_{trap} = \frac{\partial M}{\partial L} = \lambda_2 x_2 - M \Big|_{\eta=0}^{\eta=1} - M \Big|_{\eta=2}^{\eta=1} \quad (2.1-37)$$

and

$$-M \Big|_{\eta=0}^{\eta=1} - M \Big|_{\eta=2}^{\eta=1} = (x_{ac})_{trap} - \lambda_2 x_2 \quad (2.1-38)$$

Note: Applies To Either Leading Edge Or
Trailing Edge Chord Extensions

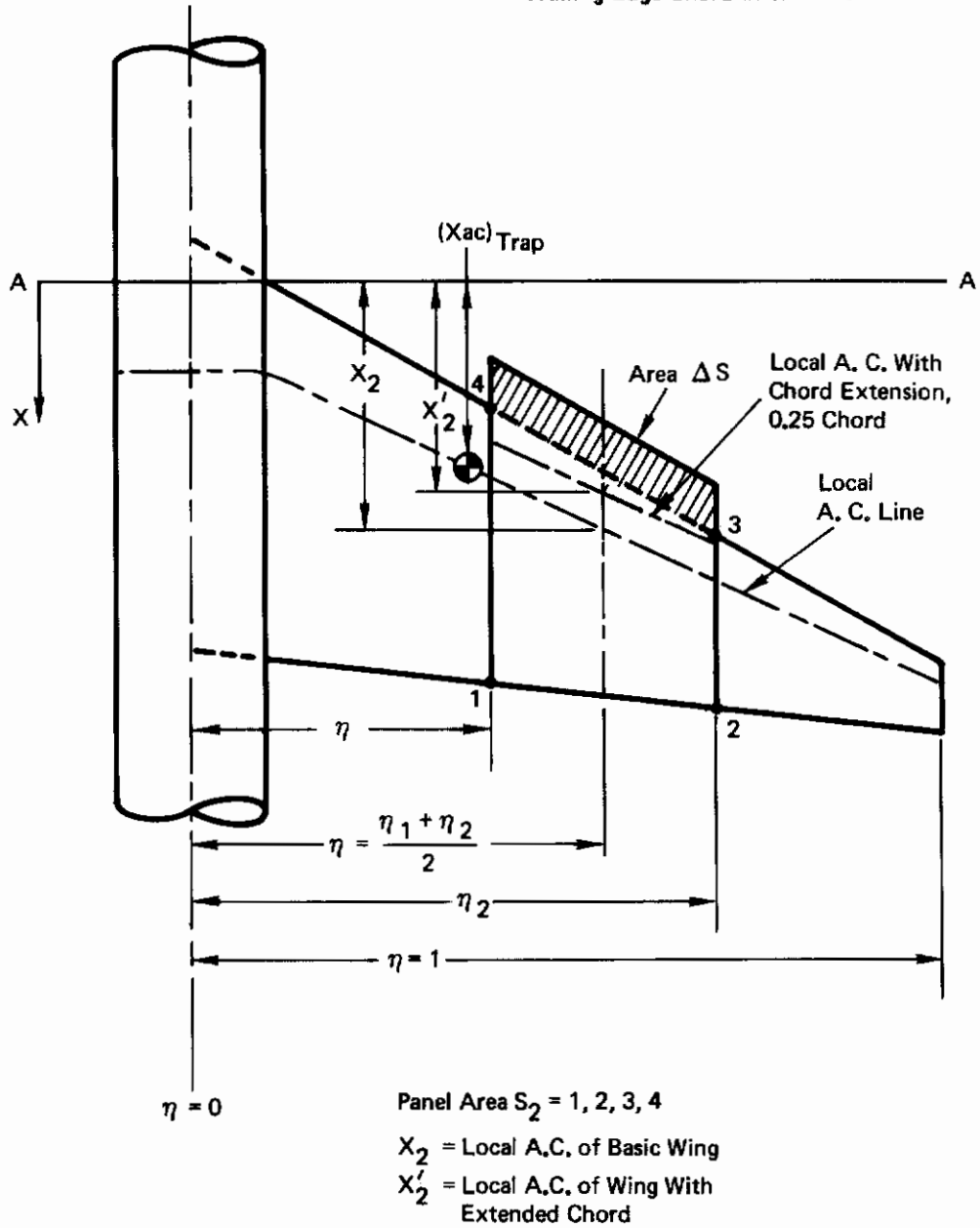


Figure 221: Nomenclature for ac Location with Outboard L.E. Devices

Contrails

$$L = 1 + \mu_5 \frac{\Delta S}{S_2} \lambda_2 \quad (2.1-39)$$

The moment is

$$M = M|_{n=0}^{n=1} + \lambda_2 \left(1 + \mu_5 \frac{\Delta S}{S_2} \right) x_2' + M|_{n=2}^{n=1} \quad (2.1-40)$$

Using the Equation 2.1-28 and 2.1-40 gives the a.c. location

$$(x_{ac})_{LE} = -\frac{\partial M}{\partial L} = \frac{-M|_{n=0}^{n=1} - M|_{n=2}^{n=1} + \lambda_2 \left(1 + \mu_5 \frac{\Delta S}{S_2} \right) \lambda_2'}{1 + \mu_5 \frac{\Delta S}{S_2}} \quad (2.1-41)$$

Substituting Equation 2.1-38 and 2.1-41 gives

$$(x_{ac})_{LE} = \frac{\lambda_1(x_1' - x_1) + \lambda_2 \left[\left(1 + \mu_5 \frac{\Delta S}{S_2} \right) x_2' - x_2 \right] + (x_{ac})_{trap}}{1 + \mu_5 \frac{\Delta S}{S_2} \lambda_2} \quad (2.1-42)$$

and the a.c. shift due to the leading edge devices becomes for the two cases:

(a) Leading edge devices extending to ~~the side~~ of the body:

$$(\Delta x_{ac})_{LE} = \frac{\lambda_1(x_1' - x_1) + \lambda_2 \left[\left(1 + \mu_5 \frac{\Delta S}{S_2} \right) x_2' - x_2 \right] + (x_{ac})_{trap}}{1 + \mu_5 \frac{\Delta S}{S_2} \lambda_2} - (x_{ac})_{trap} \quad (2.1-43)$$

(b) Outboard leading edge devices:

$$(\Delta x_{ac})_{LE} = \frac{\lambda_2 \left[\left(1 + \mu_5 \frac{\Delta S}{S_2} \right) x_2' - x_2 \right] + (x_{ac})_{trap}}{1 + \mu_5 \frac{\Delta S}{S_2} \lambda_2} - (x_{ac})_{trap} \quad (2.1-44)$$

SAMPLE PROBLEM, LEADING EDGE EXTENSION ac SHIFT

$$\eta_1 = .145$$

$$\eta_2 = 1.0$$

$$X_1 = 35.82 \text{ in.}$$

$$X_1' = 34.76 \text{ in.}$$

$$X_2 = 39.63 \text{ in.}$$

$$X_2' = 38.38 \text{ in.}$$

$$\Delta S = .882 \text{ SF}$$

$$S_2 = 4.945 \text{ SF}$$

$$(X_{ac})_{\text{Trap}} = 37.98 \text{ in.}$$

from chart Figure 20

$$\mu_S = .985$$

from Figure 5 read

$$\lambda_1 = .183$$

$$\lambda_2 = .817$$

with Equation 2.1-43 calculate shift on ac with leading edge extension

$$(X_{ac})_{LE} =$$

$$\frac{(.183)(34.76 - 35.82) + .817 \left\{ \left[1 + (.985) \left(\frac{.882}{4.945} \right) \right] (38.38) - 39.63 \right\} + 37.98}{1 + (.985) \left(\frac{.882}{4.945} \right) (.817)}$$
$$= \frac{-.194 + 4.488 + 37.98}{1.143} = 36.98 \text{ in.}$$

For the change in aerodynamic center, Equation 2.1-43

$$(\Delta X_{ac})_{LE} = 36.98 - 37.98 = 1.00 \text{ in.}$$

2.1.4.2 Aerodynamic Center Shift Due to Trailing Edge Flaps

Simple hinged flaps do not affect the aerodynamic center substantially so long as the air flow remains attached. Flaps with chord extension move the aerodynamic center back. Their effects may be determined by the methods developed for the leading edge devices in the preceding section. By using the appropriate values from Figures 19

Contrails

and 21. with μ_S from Figure 20 and λ from Figure 5 in Equation 2.1-43 and 2.1-44 the a.c. shift due to trailing edge flaps extending to the side of the body and outboard trailing edge flaps may be computed, respectively.

SAMPLE PROBLEM, TRAILING EDGE EXTENSION ac SHIFT

$$\eta_1 = .145$$

$$\eta_2 = .75$$

$$X_1 = 35.82 \text{ in.}$$

$$X_1' = 37.38 \text{ in.}$$

$$X_2 = 38.22 \text{ in.}$$

$$X_2' = 39.00 \text{ in.}$$

$$\Delta S = 1.104 \text{ SF}$$

$$S_2 = 3.881 \text{ SF}$$

$$(X_{ac})_{\text{Trap}} = 37.98 \text{ in.}$$

$$\lambda_1 = .183$$

$$\lambda_2 = .666$$

from Fig. 20 read

$$\mu_S = .89$$

The aerodynamic center with trailing edge extended equation, Equation 2.1-34

$$(X_{ac})_{\text{TE}} =$$

$$\frac{(.183)(37.38 - 35.82) + (.666) \left\{ \left[\left(1 + (.89) \frac{(1.104)}{(3.881)} \right) (39.00) - 38.22 \right] \right\} + 37.98}{1 + (.89) \left(\frac{1.104}{3.881} \right) (.666)}$$
$$= \frac{.285 + 7.095 + 37.98}{1.169} = \frac{45.36}{1.169} = 38.80$$

For the change in aerodynamic center (2.1-43)

$$(\Delta X_{ac})_{\text{TE}} = 38.80 - 37.98 = .820$$

2.1.4.3 Pitching Moment at Zero Lift Due to Trailing Edge Flap

ΔC_{mOL} is calculated by estimating the spanwise and chordwise position of the center of loading induced by the flap. ΔC_{mOL} is then equal to the estimated flap lift increment times the arm from the estimated flap load center to the flaps extended aerodynamic center.

Contrails

The flap load center is estimated as follows:

- (a) As a first approximation, assume the flap load center is along the wing half-chord line.
- (b) Along chordwise cuts normal to the half-chord line evaluate the flap chord ratio c'_f/c .
- (c) Determine the locus of chordwise flap load center positions using Figure 22.
- (d) Iterate if the new flap center of pressure line differs greatly from the initial approximation.
- (e) Locate the flap load center.

Finally,

$$(\Delta C_m)_{OL\ TE} = \frac{-(\Delta C_L)_{TE}}{C_{REF}} \left[x_{CP\ TE} - (x_{ac})_{\substack{\text{flaps} \\ \text{extended}}} \right] \quad (2.1-45)$$

SAMPLE PROBLEM, PITCHING MOMENT AT ZERO LIFT DUE TO TRAILING EDGE FLAP

$$C'_{f/C} = .323 \text{ (constant \% chord flap)}$$

$$\bar{c} = 11.179 \text{ in.}$$

$$A = 6.786$$

$$P = 98.831 \text{ in.}$$

$$\eta_{1B} = .145$$

$$\eta_{OB} = .75$$

$$\Delta C_{L\ TE} = 2.01$$

Calculate

$$\frac{C_{L\ \alpha}}{C_{L\ \alpha}} \sim \frac{6.786}{\left(\frac{98831}{84274} \right) (6.786) + 2} = .681$$

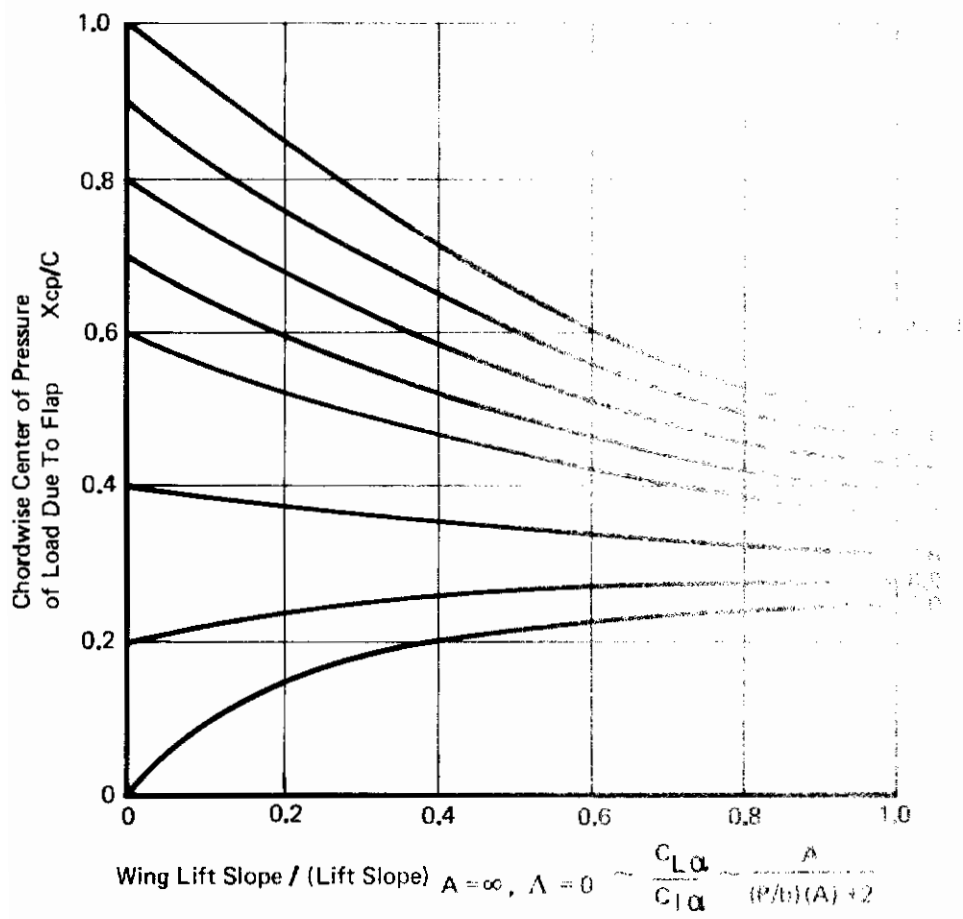


Figure 22: Chordwise Center of Load Due To Flaps

From Figure 22 obtain chordwise center of pressure

$$\frac{x_{cp}}{c} = .44, \text{ this is near enough to the original assumption of } X_{cp}/c = .50$$

that iteration will not result in a significant change. From Figure 23 determine spanwise center of pressure

$$\eta_{cp} = .422$$

The center of pressure is then located at the intersection of the .44 chord line and $\eta_{cp} = .422$. In the model longitudinal reference system

$$X_{cp \text{ TE}} = 41.47$$

The $(C_{m_{OL}})_{TE}$ is then calculated from equation 2.1-45

$$\begin{aligned} (C_{m_{OL}})_{TE} &= - \frac{2.01}{11.179} (41.47 - 38.88) \\ &= -.4637 \end{aligned}$$

2.1.4.4 Pitching Moment at Zero Lift Due to Leading Edge Devices

The pitching moment at zero lift increment due to leading edge flaps is much smaller than that due to trailing edge flaps so that a simpler approach can be adopted

$$(\Delta C_{m_{OL}})_{LE} = \frac{+(\Delta C_L)_{LE}}{C_{REF}} \left[X'_{c/4} - (X_{ac})_{LE \text{ extended}} \right] \quad (2.1-46)$$

Where $X'_{c/4}$ is the quarter chord of the mean aerodynamic chord determined with the leading edge extended in the plane of the wing.

SAMPLE PROBLEM, PITCHING MOMENT AT ZERO LIFT DUE TO LEADING EDGE

$$C_{L_{LE}} = -.15$$

$$C_{REF} = 11.179 \text{ in.}$$

$$X'_{c/4} = 36.867 \text{ in}$$

$$X_{ac_{LE}} = 36.98 \text{ in.}$$

calculate $(\Delta C_{m_{OL}})_{LE}$ with equation 2.1-46

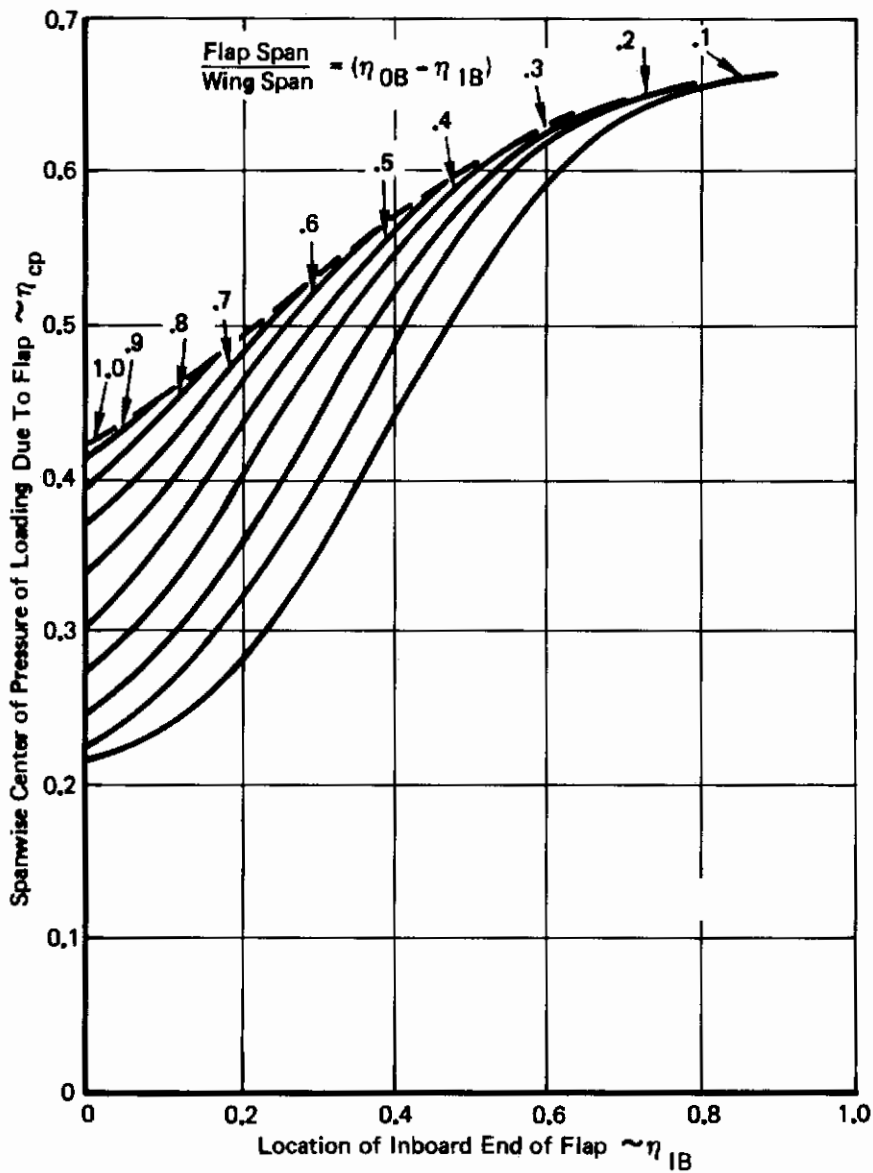
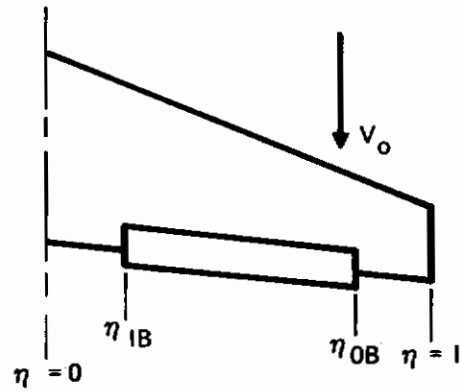


Figure 23: Spanwise Center of Load Due To Flaps

$$\begin{aligned} \Delta C_{L,LE} &= \frac{15}{11.179} (36.867 - 36.980) \\ &= + .0015 \end{aligned}$$

2.1.4.5 Change in Downwash Due to Leading Edge and Trailing Edge High-Lift Devices

Generally accepted methods for predicting the downwash variation behind the wing due to leading and trailing edge high lift devices are at present not available. However, qualitative design guidelines based on the analysis of large amount of experimental data are summarized in Ref. 11. Quantitative data for estimating the increment of downwash due to trailing edge flap deflection have also been obtained. All of the following discussion is based on Ref. 10.

Analysis of the air flow characteristics behind sweptback wings shows that before separation occurs the downwash remains unaffected by leading edge flaps. The increments of down wash due to deflecting trailing-edge flaps on air-body combinations are summarized in Figure 24. The ratio of measured effective downwash increment to the factor $\frac{\Delta C_{L_f}}{A(\eta_{OB} - \eta_{IB})}$ was found to give satisfactory correlation of the flap span effect and is shown in Figure 24 as a function of height of the horizontal tail. Only the lift increment due to trailing edge flap deflection is used in Ref. 10 indicates that leading edge devices have negligible effect on downwash.

The correlation of $\frac{\Delta \epsilon}{\frac{\Delta C_{L_f}}{A(\eta_{OB} - \eta_{IB})}}$ indicated in Figure 24 was found satisfactory as long as $\Delta \epsilon$ was smaller than 10° . When $\Delta \epsilon$ was larger than 10° , at low tail positions (close to the wing wake), the correlation was not as good.

SAMPLE PROBLEM, CHANGE IN DOWNWASH FROM TRAILING EDGE FLAPS

$$z_t = 17.566 \text{ in.}$$

$$b = 84.27 \text{ in.}$$

$$\eta_{IB} = .145$$

$$\eta_{OB} = .75$$

$$\Delta C_{L_{TE}} = 2.01$$

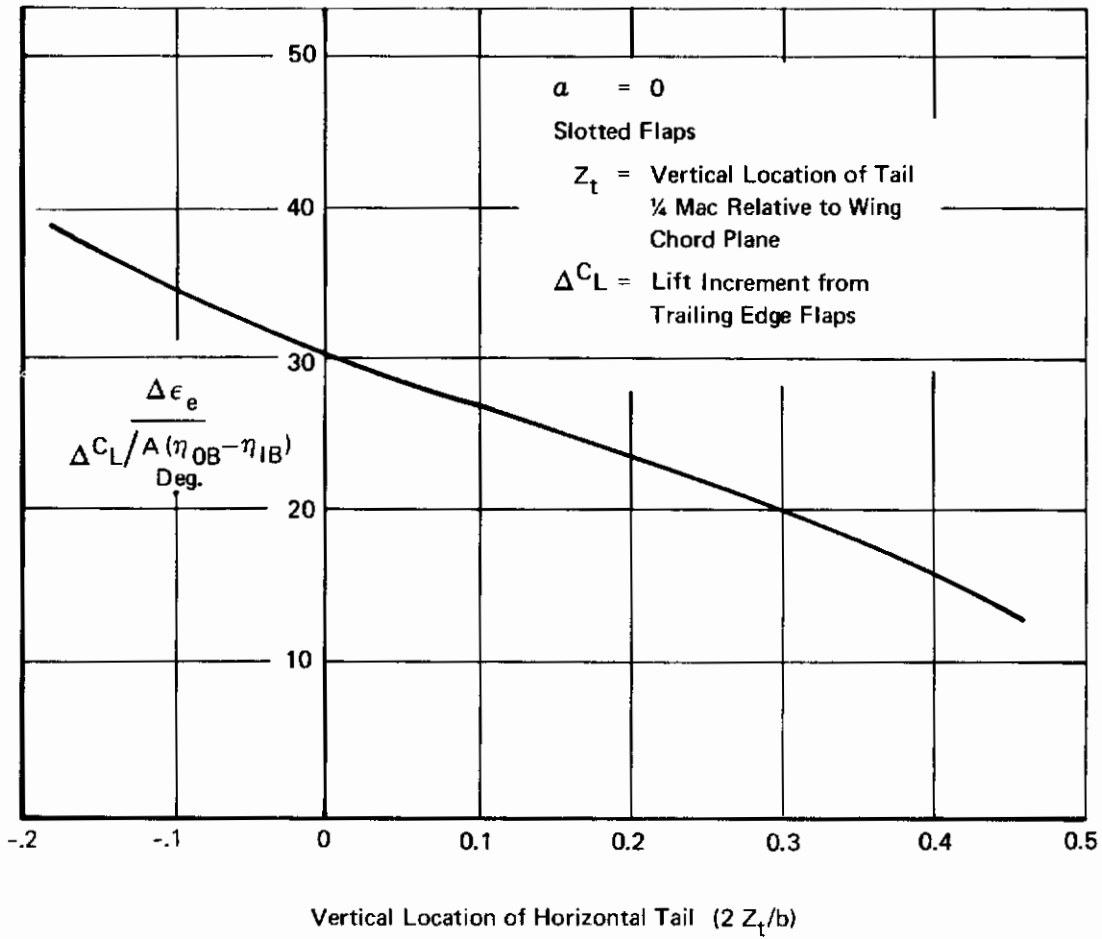


Figure 24: Change in Downwash at Horizontal Tail

from Figure 24 read @ $2h/b = .417$

$$\frac{\Delta \epsilon_e}{\Delta C_{L/A}(\eta_{OB} - \eta_{1B})} = 15.2$$

$$\Delta \epsilon_e = \frac{(15.2)(2.01)}{(8)(.75 - .145)} = 6.21$$

2.1.4.6 Total Free Air Pitching Moment

The increments in zero lift pitching moment and aerodynamic center from extension are combined with the flaps up data and provide pitching moment as a function of lift coefficient.

$$C_{m_{OL}} = C_{m_{OL}}^{\text{flaps up}} + \Delta C_{m_{OL}}^{\text{leading edge}} + \Delta C_{m_{OL}}^{\text{trailing edge}} \quad (2.1-47)$$

$$x_{ac} = x_{ac}^{\text{flaps up}} + \Delta x_{ac}^{\text{leading edge}} + \Delta x_{ac}^{\text{trailing edge}} \quad (2.1-48)$$

$$C_m = C_{m_{OL}}^{\text{flaps down}} + \left[\frac{x_{CG}}{C_{REF}} - \frac{x_{ac}}{C_{REF}^{\text{flaps down}}} \right] C_L \quad (2.1-49)$$

Figure 25 compares pitching moment estimated with the test data.

SAMPLE PROBLEM, PITCHING MOMENT

$$\begin{aligned} (C_{mo})_{\text{flaps up}} &= -.11 \\ (\Delta C_{mo})_{LE} &= +.0015 \\ (\Delta C_{mo})_{TE} &= -.4657 \\ (x_{ac})_{\text{flap up}} &= 37.98 \text{ in.} \\ (\Delta x_{ac})_{LE} &= -1.00 \text{ in.} \end{aligned}$$

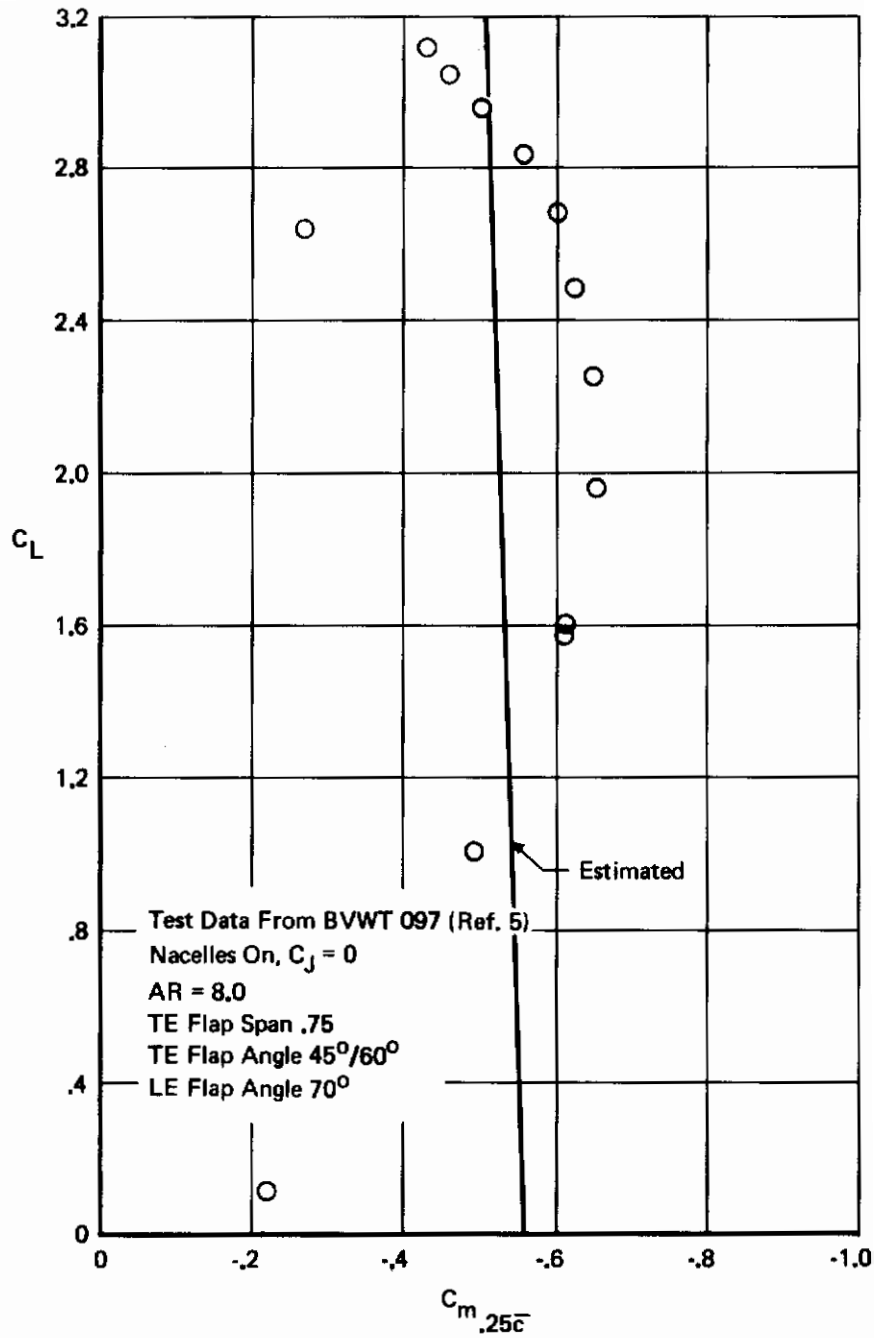


Figure 25: Comparison of Measured and Predicted Power-Off Pitching Moment

$$(X_{ac})_{TE} = + .820 \text{ in.}$$

$$X_{cg} = 37.98 \text{ in. } (.25 \text{ mac})$$

from equation 2.1-47

$$\begin{aligned} (C_{mo})_{\text{flap}} &= -.11 + .0015 - .4657 \\ \text{down} & \\ &= -.5742 \end{aligned}$$

from equation 2.1-48

$$\begin{aligned} (X_{ac})_{\text{flap}} &= 37.98 - 1.00 + .820 \\ \text{down} & \\ &= 37.80 \end{aligned}$$

Pitching moment from equation 2.1-49 @ a lift coefficient = 2.4

$$\begin{aligned} C_m &= -.5742 + \left(\frac{37.98}{11.179} - \frac{37.80}{11.179} \right) (2.4) \\ &= -.5742 + .0386 = -.5356 \end{aligned}$$

From Test Data

$$C_m = -.630$$

2.2 Ground Effect

Proximity to the ground affects the wing aerodynamic characteristics in three ways. There is a reduction in dynamic pressure at the wing, a reduction in induced angle of attack, and an induced camber.

The assumption is usually made (Ref. 1) that the effects of reduced q and induced camber are small and, since they are of opposite sign, can be ignored. While this assumption was reasonable prior to the advent of modern high lift systems, it is certainly not valid with today's very high lift STOL systems.

A very simple analysis has been performed using a single horseshoe vortex and its image in the ground plane. This will give a theoretical estimate of the induced change in angle of attack and the reduced dynamic pressure. The camber effect is assumed to be small compared to those effects for STOL configurations with high mounted wings.

2.2.1 Lift

To approximate an elliptically loaded wing by a single rectangular vortex, the vortex span should be $\pi b/4$. In this analysis a single horseshoe vortex with span $\pi b/4$ is used with the induced velocities

Contrails

averaged over the span. Consider the longitudinal velocity (see Figure 26) induced at any point along the wing span by the image bound vortex:

$$v(x) = \frac{\Gamma}{8\pi h} (\cos\theta_1 + \cos\theta_2) \quad (2.2-1)$$

It may be shown with the assumption of the same lift coefficient based on the local dynamic pressure in free air and in ground effect that the velocity ratio is

$$\frac{V_{FA}}{V_{FA} - V_{avg}} = 1 + \frac{2C_{LFA}}{\pi^3 A} \left\{ \left[1 + \left(\frac{\pi}{8h/b} \right)^2 \right]^{-1} \right\} \quad (2.2-2)$$

The ratio of lift coefficients must then be

$$\frac{C_{LGE}}{C_{LFA}} = \left[\frac{1}{1 + \frac{2C_{LFA}}{\pi^3 A} \left\{ \left[1 + \left(\frac{\pi}{8h/b} \right)^2 \right]^{-1} \right\}} \right] \quad (2.2-3)$$

This lift ratio is achieved at a reduced angle of attack due to the induced velocities from the image trailing vortices. The change in angle of attack is

$$\Delta\alpha = \frac{\omega_r}{V_{FA}} - \frac{\omega_r + \omega_i}{V_{FA} - V_{avg}} \quad (2.2-4)$$

and it may be shown that

$$\Delta\alpha = \frac{2C_{LFA}}{\pi^3 A} \ln \left[1 + \left(\frac{\pi}{8h/b} \right)^2 \right] \quad (\text{RAD}) \quad (2.2-5)$$

2.2.2 Drag

The ratio of drag in ground effect to that in free air is

$$\frac{C_{DGE}}{C_{DFA}} = \frac{\left[C_{DP} + C_{LFA} \left(\frac{\omega_r + \omega_i}{V_{FA} - V_{avg}} \right) \right] \frac{\rho}{8}}{C_{DP} + C_{LFA} \frac{\omega_i}{\omega_r}} \quad (2.2-6)$$

or

$$\frac{C_{DGE}}{C_{DFA}} = \left\{ 1 - \left(\frac{2}{\pi^3 A} \right) \left(\frac{C_{LFA}^2}{C_{DFA}} \right) \ln \left[1 + \left(\frac{\pi}{8h/b} \right)^2 \right] \right\} \frac{C_{LGE}}{C_{LFA}} \quad (2.2-7)$$

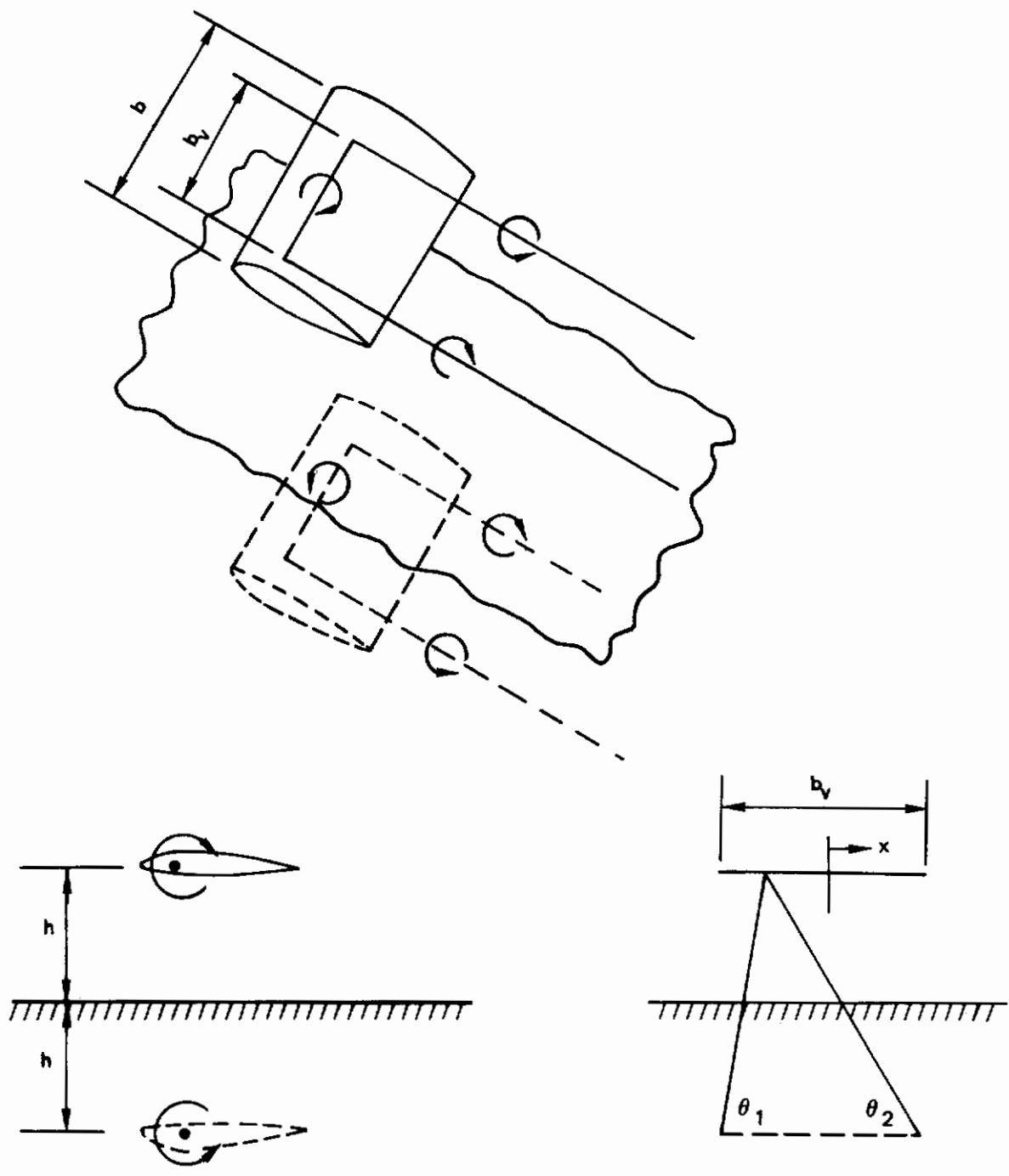


Figure 26: Wing in Ground Effect

2.2.3 Pitching Moment

The simple horseshoe vortex approximation cannot be used to find how the center of pressure of the wing changes from free air to ground effect. This would require a more sophisticated lifting surface analysis. As a first approximation we will assume that the location of the center of pressure does not change in ground effect. Therefore,

$$\frac{C_{m_{GE}}}{C_{m_{FA}}} = \frac{C_{L_{GE}}}{C_{L_{FA}}} \quad (2.2-8)$$

while this approach does not have any theoretical justification, it does correlate well with the test data, see Figures 27 and 28.

2.2.4 Downwash

Using a similar analysis to that for C_L , α and C_D it may be shown that the change in downwash at the horizontal tail in ground effect is

$$\Delta \epsilon_{GE} = -\frac{C_L b^2}{8\pi A} \left\{ \left(\frac{\ell_t}{\ell_t^2 + (2h - z_t)^2} \right) \left(\frac{1}{\left[\ell_t^2 + (2h - z_t)^2 + \frac{\pi^2 b^2}{64} \right]^{1/2}} \right) \right. \quad (2.2-9)$$

$$\left. + \left(\frac{1}{(2h - z_t)^2 + \frac{\pi^2 b^2}{64}} \right) \left(1 + \frac{\ell_t}{\left[\ell_t^2 + (2h - z_t)^2 + \frac{\pi^2 b^2}{64} \right]^{1/2}} \right) \right\} \quad (\text{RAD})$$

A comparison of free air test data corrected for ground effects, and test data in ground effect is shown in Figures 27 and 28.

SAMPLE PROBLEM, LONGITUDINAL CHARACTERISTICS IN GROUND EFFECT

$$C_L = 2.0$$

$$h/b = .209$$

$$b = 84.274 \text{ in.}$$

$$A = 8.0$$

$$\alpha = 2.33^\circ$$

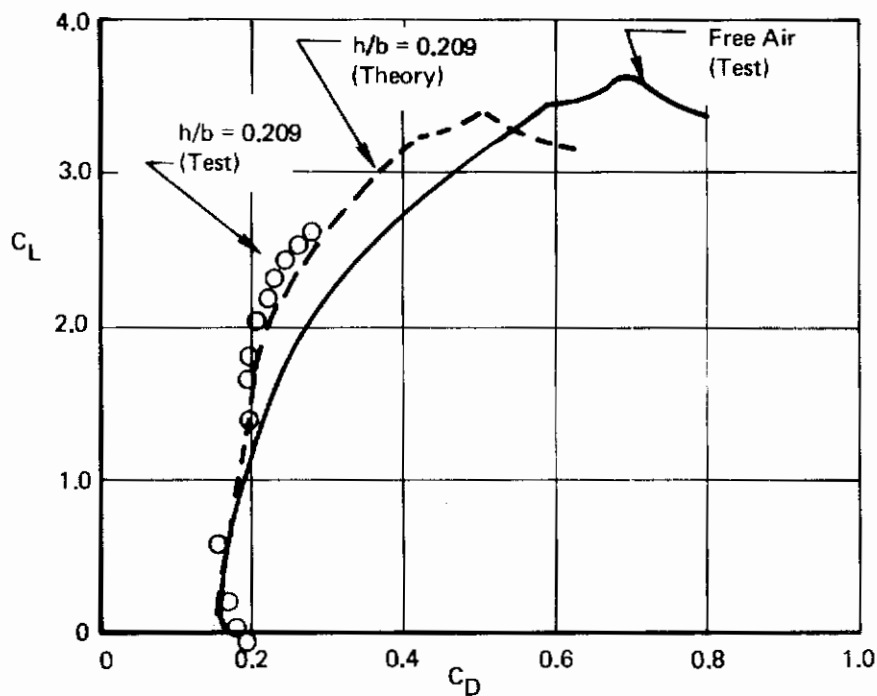
$$C_D = .3410$$

$$C_m = -.5273$$

$$z_t = 17.566 \text{ in.}$$

$$\ell_t = 49.171 \text{ in.}$$

Sweep = 15°, $C_j = 0$



Tail Off
 AR = 8.0
 TE Flap Span = 0.75
 TE Flap Angle = 35°
 LE Flap Angle = 70°
 $C_{\mu LE} = 0.06$
 Data from BVWT 099 (Ref. 5)

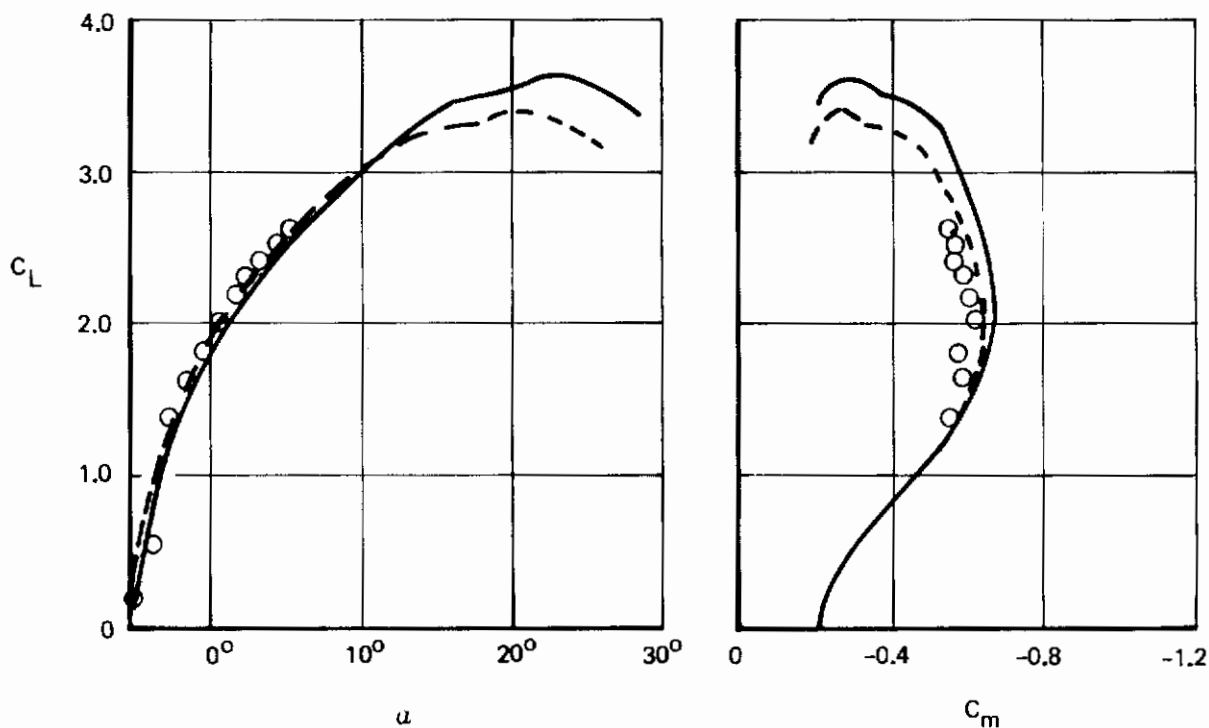


Figure 27: Ground Effect, Power Off, Test -- Estimate Comparison

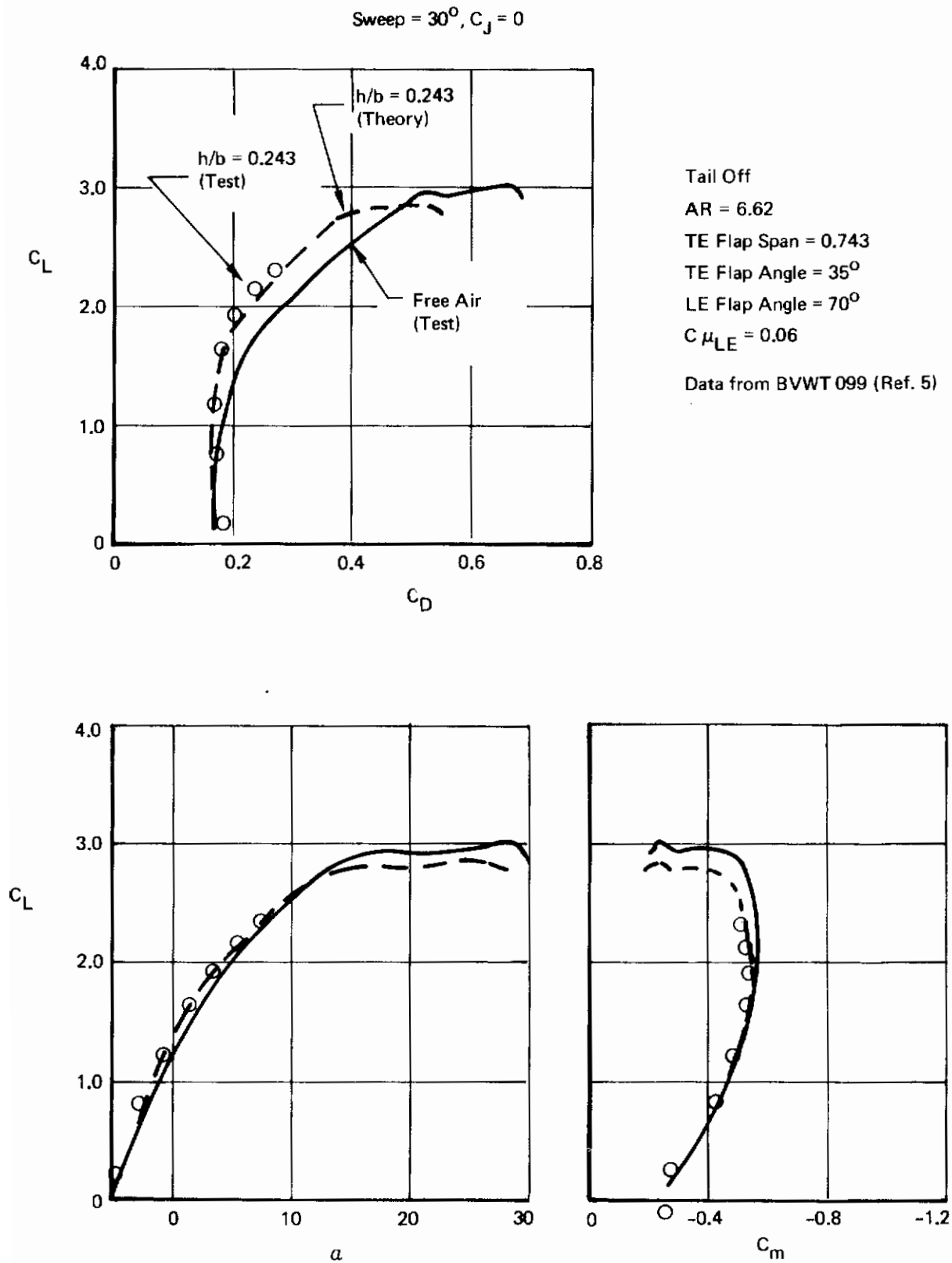


Figure 28: Ground Effect, Power Off, Test – Estimate Comparison

Contrails

For lift in ground effect, equation 2.2-3

$$C_{L_{GE}} = 2 \left[\frac{1}{1 + \frac{(2 \times 2)}{\pi^2 \times 8} \left[\left(\frac{\pi}{(8 \times 209)} \right)^2 + 1 \right]^{1/2} - 1} \right]^2$$

$$= 1.93$$

For angle of attack in ground effect 2.2-5

$$\alpha_{GE} = 2.33 - \left\{ \frac{(2 \times 2)}{\pi^2 \times 8} \arctan \left[1 + \left(\frac{\pi}{(8 \times 209)} \right)^2 \right] \right\} 57.3$$

$$= 2.33 - 1.40$$

$$= .93$$

For drag in ground effect, equation 2.2-6

$$C_{D_{GE}} = .341 \left\{ 1 - \left(\frac{2}{\pi^2 \times 8} \right) \left(\frac{2.0^2}{.341} \right) \arctan \left[1 + \left(\frac{\pi}{(8 \times 209)} \right)^2 \right] \right\} \frac{1.93}{2.0}$$

$$= .282$$

Pitching moment in ground effect, equation 2.2-8

$$C_{m_{GE}} = (-.5273) \frac{1.93}{2.00}$$

$$= -.5088$$

Change in downwash in ground effect, equation 2.2-9

$$\Delta \epsilon_{GE} = - \frac{(20 \times 84.27)^2}{(8 \times \pi \times 8)} \left\{ \left(\frac{49.17}{(49.17)^2 + [(2 \times 17.61) - 17.57]^2} \right) \left(\frac{1}{(49.17)^2 + [(2 \times 17.61) - 17.57]^2 + \frac{\pi^2 (84.27)^2}{64}} \right)^{1/2} \right. \\ \left. + \left(\frac{1}{[(2 \times 17.61) - 17.57]^2 + \frac{\pi^2 (84.27)^2}{64}} \right) \left(1 + \frac{49.17}{(49.17)^2 + [(2 \times 17.61) - 17.57]^2 + \frac{\pi^2 (84.27)^2}{64}} \right)^{1/2} \right\}$$

$$= -.1107 \text{ RAD}$$

$$= -6.34^\circ$$

2.3 Vectored Thrust

This section contains formulae for longitudinal force and moment coefficients incorporating thrust effects and a discussion of thrust interference effects on these coefficients. The longitudinal force and moment coefficients are presented below.

$$C_L = C_{L_{POWER}} + C_{L_{INT}} + C_J \sin(\alpha + \delta) \quad (2.3-1)$$

OFF

$$C_D = C_{D_{POWER}} + C_{D_{INT}} - C_J \cos(\alpha + \delta) + C_{D_{RAM}} \quad (2.3-2)$$

OFF

$$C_m = C_{m_{POWER}} + C_{m_{INT}} + C_J \left(\frac{x_E}{c} \sin \delta + \frac{z_E}{c} \cos \delta \right) \quad (2.3-3)$$

OFF

$$+ C_{D_{RAM}} \left(\frac{x_R}{c} \sin \alpha - \frac{z_R}{c} \cos \alpha \right)$$

The interference effects presented were obtained from the STAI wind tunnel test BVWT 099. These effects are the differences between the power-on and power-off test data with the appropriate thrust component removed from the power-on data. The interference corrections are shown as functions of thrust vector angle, angle of attack, nozzle longitudinal location and nozzle gross thrust coefficient.

The vertical and spanwise location effects are apparently negligible, although the available data was limited. Spanwise locations tested were from 27% to 60% of wing semi-span. The nacelle centerline heights tested were $h/\bar{c} = .371$ and $.453$ below chord plane. These variables are not included in the estimating procedure.

The vectored thrust interference data were analyzed to generalize the data with sufficient accuracy for preliminary design purposes. The methods will provide good results for configurations having reasonably high aspect ratios and engines located under the wing, since the data base for their derivation was so restricted. Application to other arrangements is subject to considerable uncertainty. Figure 29 shows the satisfactory agreement between measured forces and those predicted by the present methods which can be expected when this restriction is observed.

2.3.1 Lift Interference

Since the chordwise position of the exit centerline of the nozzle varies with vector angle, the data had to be crossplotted to obtain all of the vector angles at the same chordwise position. The limited data on spanwise location effects indicated that these were minimal.

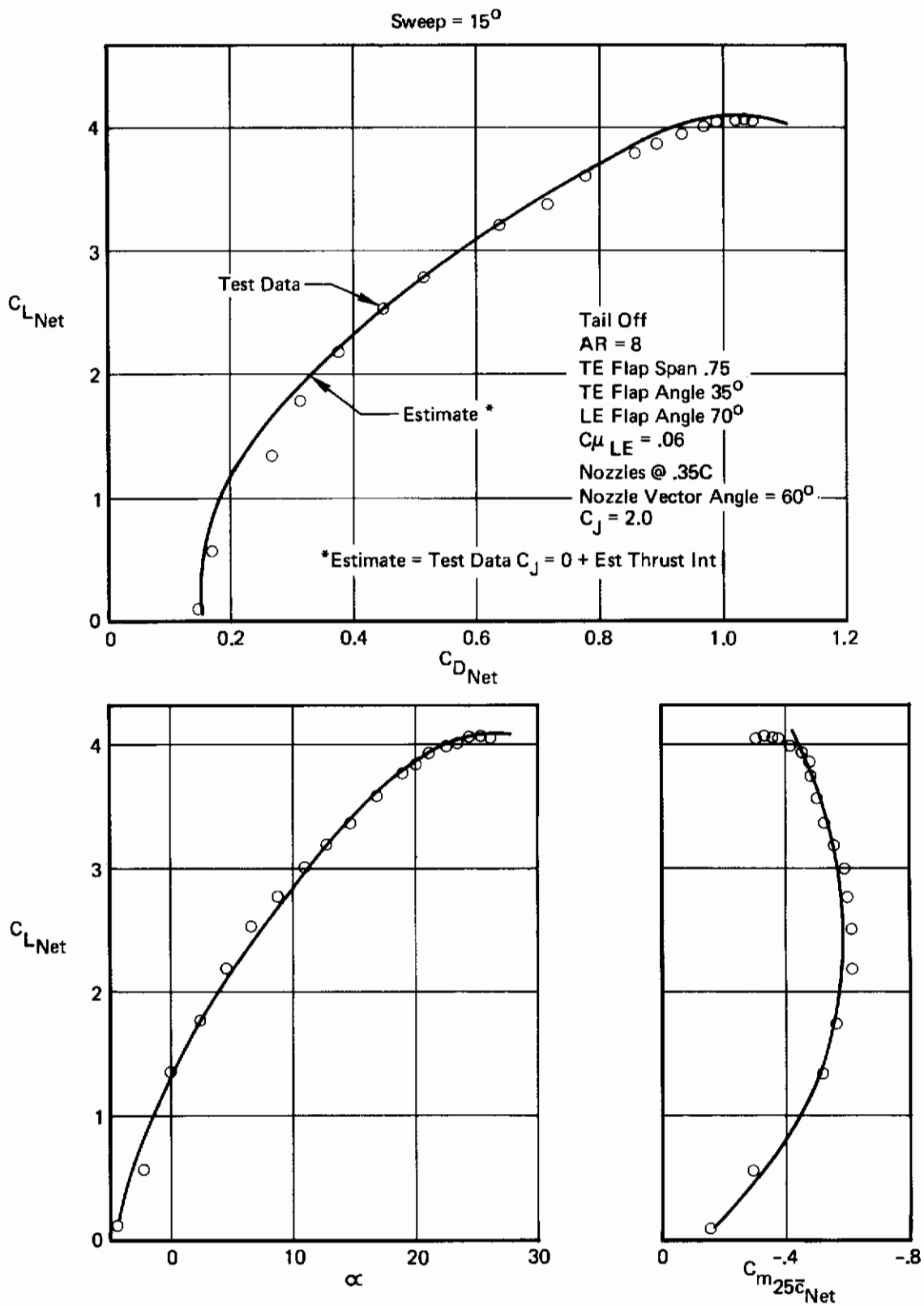


Figure 29: Vectored Thrust, Test – Estimate Comparison

Contrails

Free air lift interference due to vectored thrust may be found for $x/c = .35$ and $C_J = 2.0$ from Figure 30. An increment for other nozzle locations may be found from Figure 31. A parameter which has proved of some use in correlating vectored thrust and V/STOL aerodynamic interference effects is the equivalent jet velocity ratio,

$$V_e = \left(\frac{q_\infty}{q_{jet}} \right)^{1/2}$$
 V_e is directly proportional to $(1/C_J)^{1/2}$. It was found that the lift interference correlated directly with $C_J^{1/2}$ with sufficient accuracy for preliminary design purposes, though it begins to break down at high thrust coefficients or angles of attack.

The lift interference for any C_J and chordwise nacelle location is then

$$C_{LINT} = \left[C_{LINT} \text{ (FIG 30)} + \Delta C_{LINT} \text{ (FIG 31)} \right] \left[\frac{C_J}{2} \right]^{1/2} \quad (2.3-4)$$

For this analysis the nacelle longitudinal location is measured from the leading edge of the local wing chord at the engine centerline location, to the center of nozzle exit plane.

Symmetric thrust conditions have been assumed for the lift interference design charts developed. For nonsymmetric thrust conditions, the charts developed may be used assuming that each wing operates independently of the other. If one wing has $C_J = X$ and the other $C_J = Y$, the configuration will then have a lift interference given by

$$C_{LINT} = \frac{1}{2} [C_{LINT} @ C_J = 2X] + \frac{1}{2} [C_{LINT} @ C_J = 2Y] \quad (2.3-5)$$

2.3.2 Drag Interference

At a given nacelle location and nozzle vector angle, the free air drag interference could be correlated directly with the free air lift interference. This permitted a relatively simple procedure to be used. Free air drag interference is given in Figures 32 through 34.

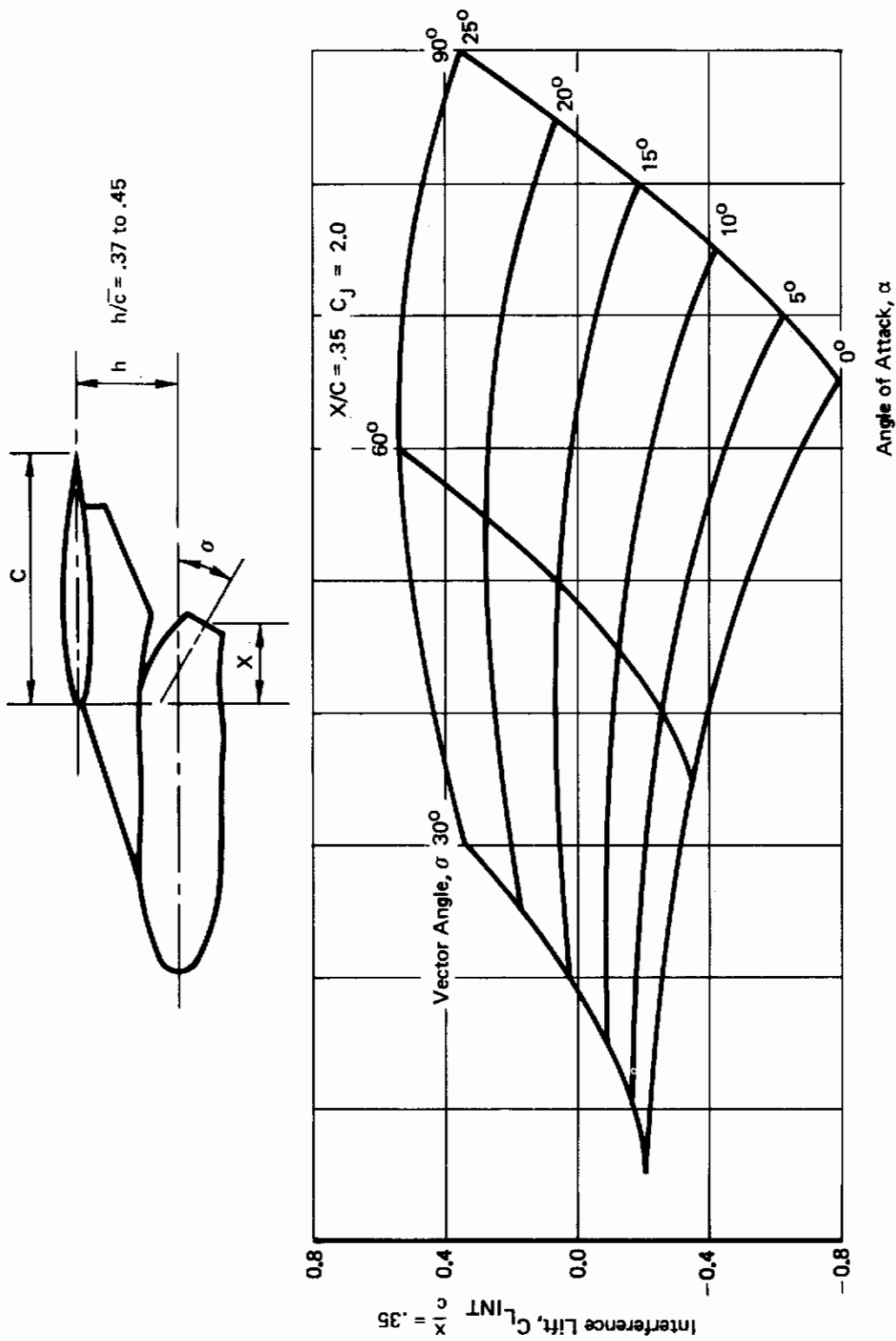


Figure 30: Vectored Thrust Lift Interference

Contrails

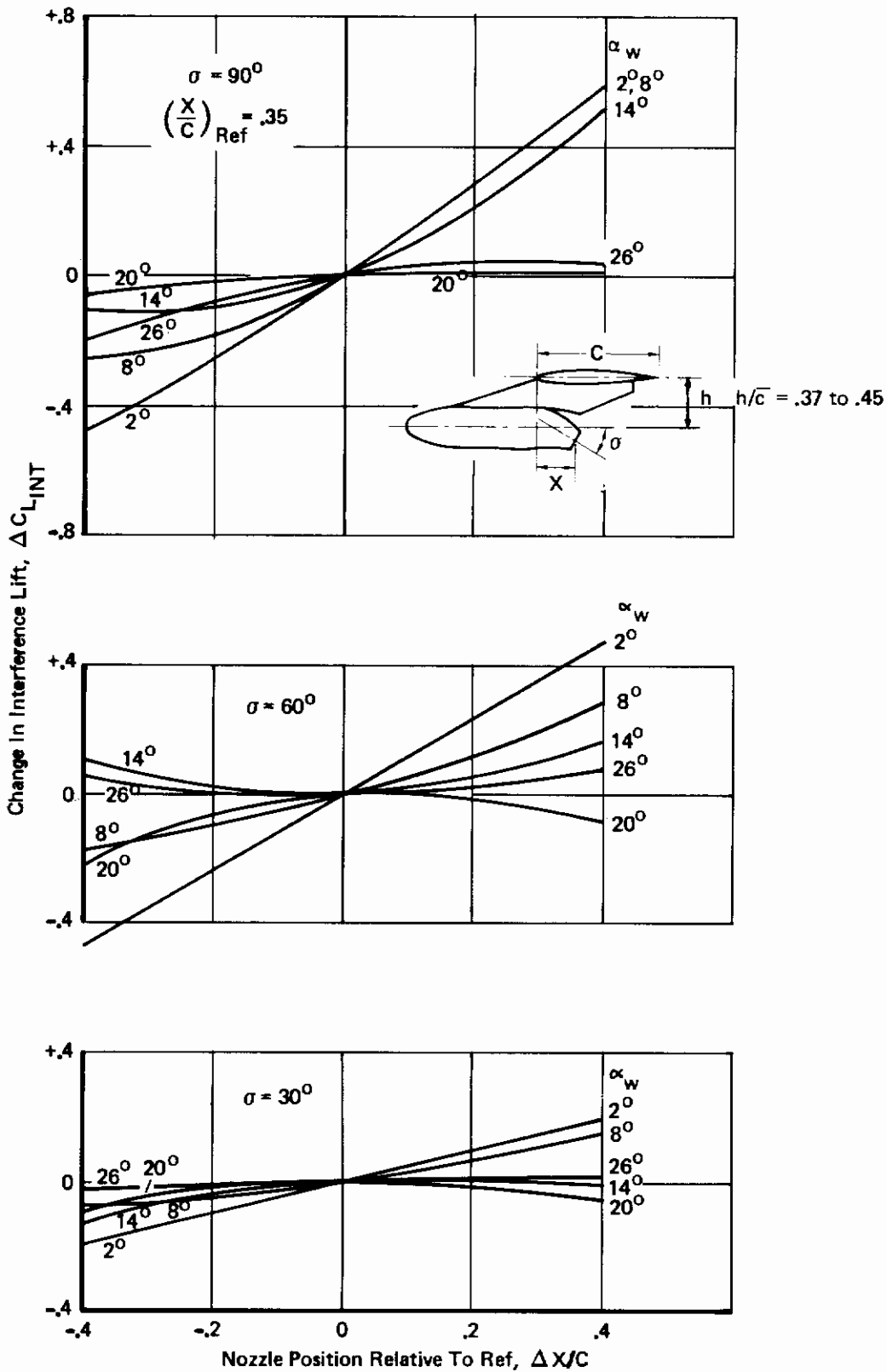
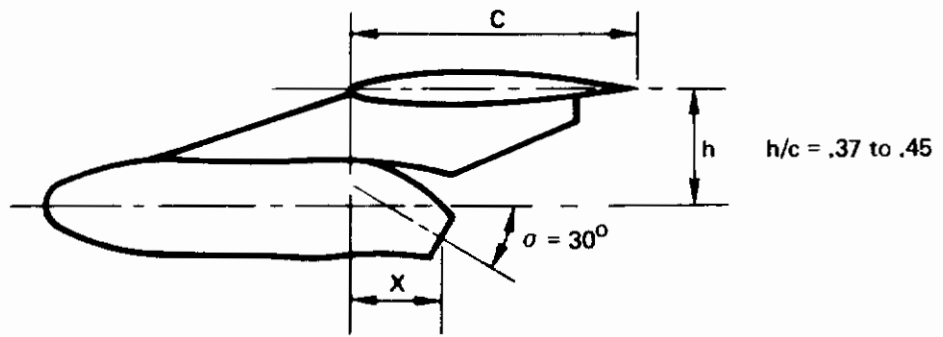


Figure 31: Vectored Thrust, Lift Interference, Effect of Nozzle Location

Contrails



$\sigma = 30^\circ$
All C_j

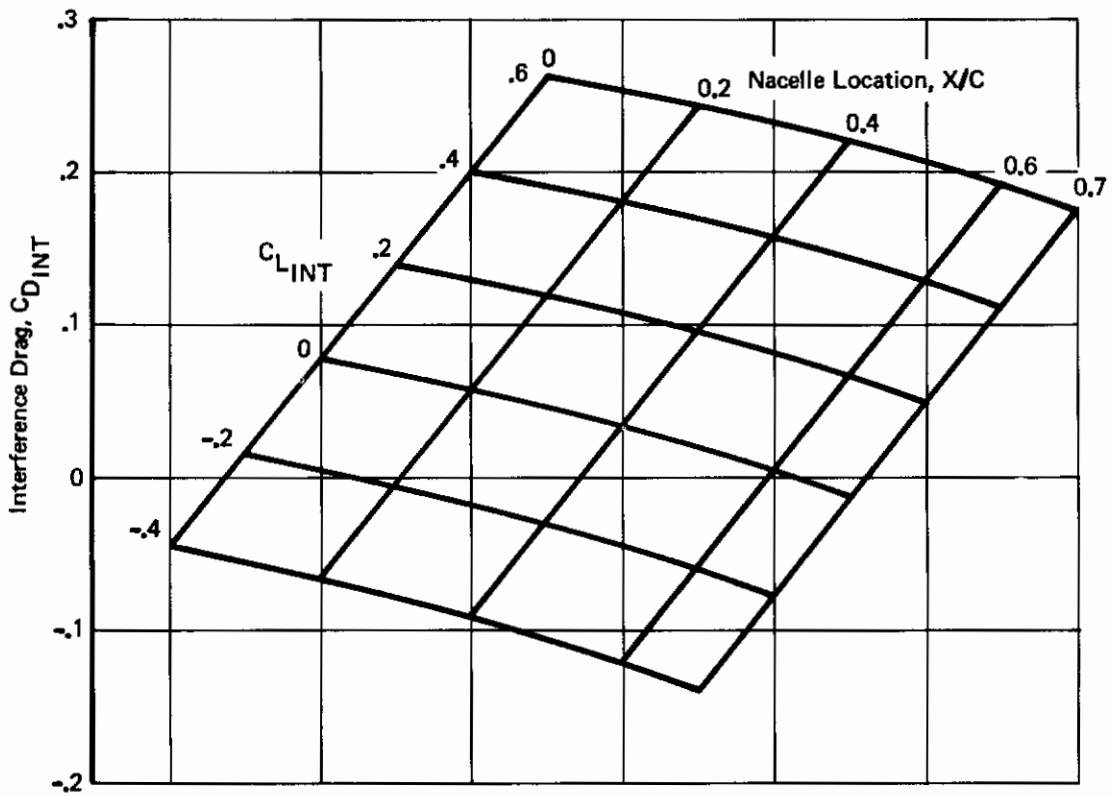


Figure 32: Vectored Thrust, Drag Interference, Vector Angle 30°

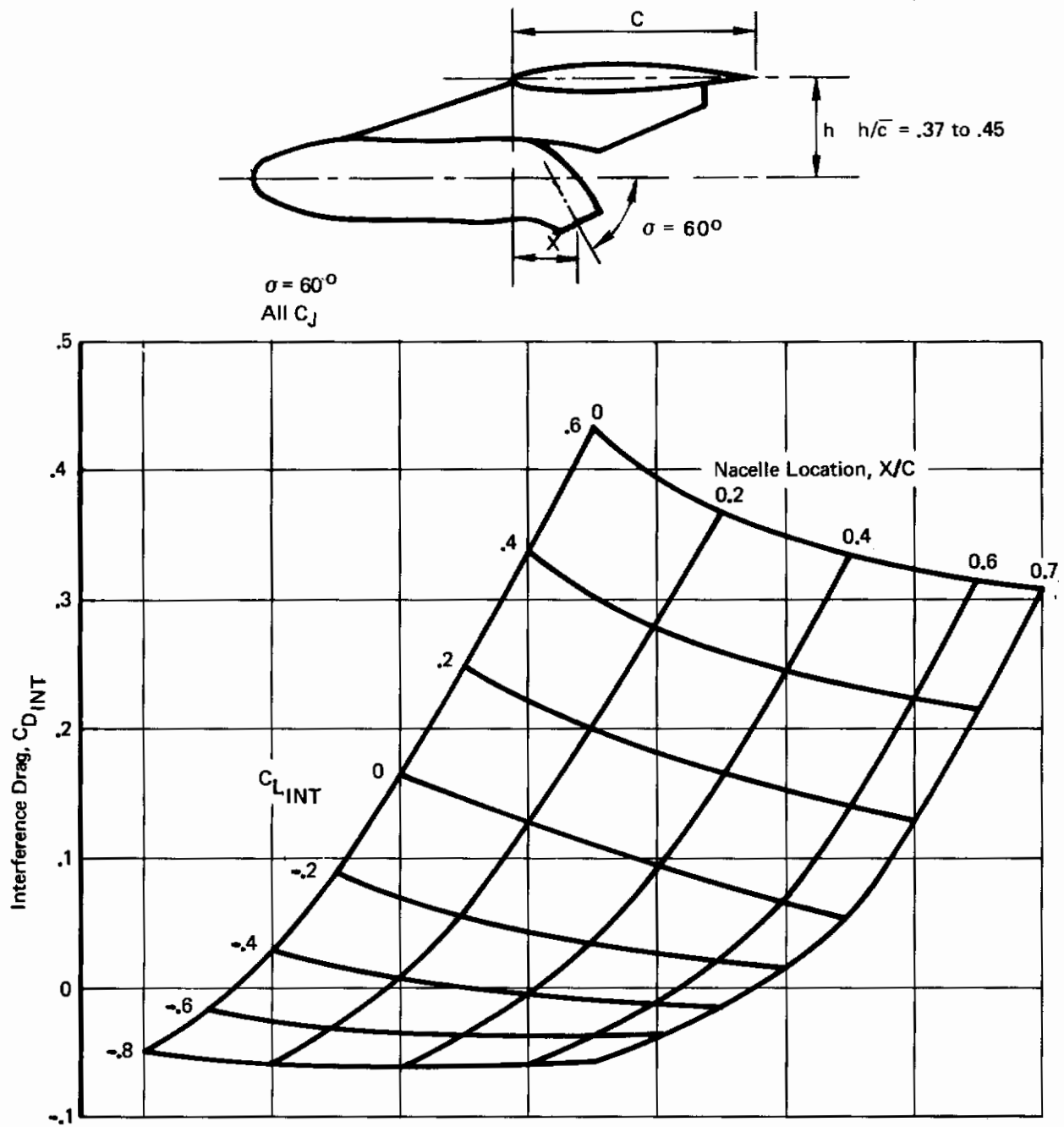
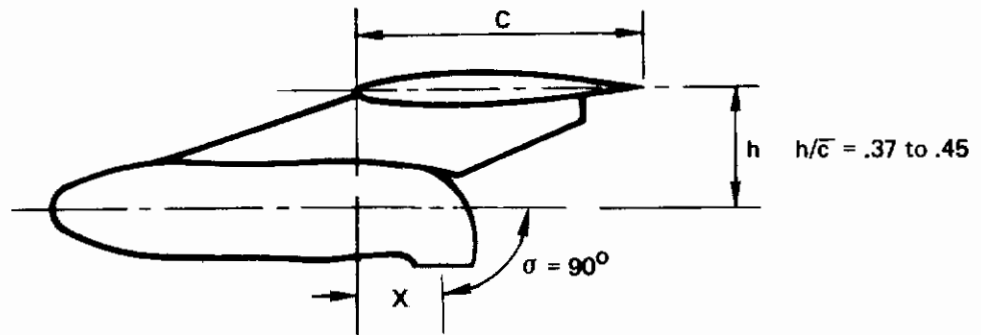


Figure 33: Vectored Thrust, Drag Interference, Vector Angle 60°

Contrails



$\sigma = 90^\circ$
All C_J

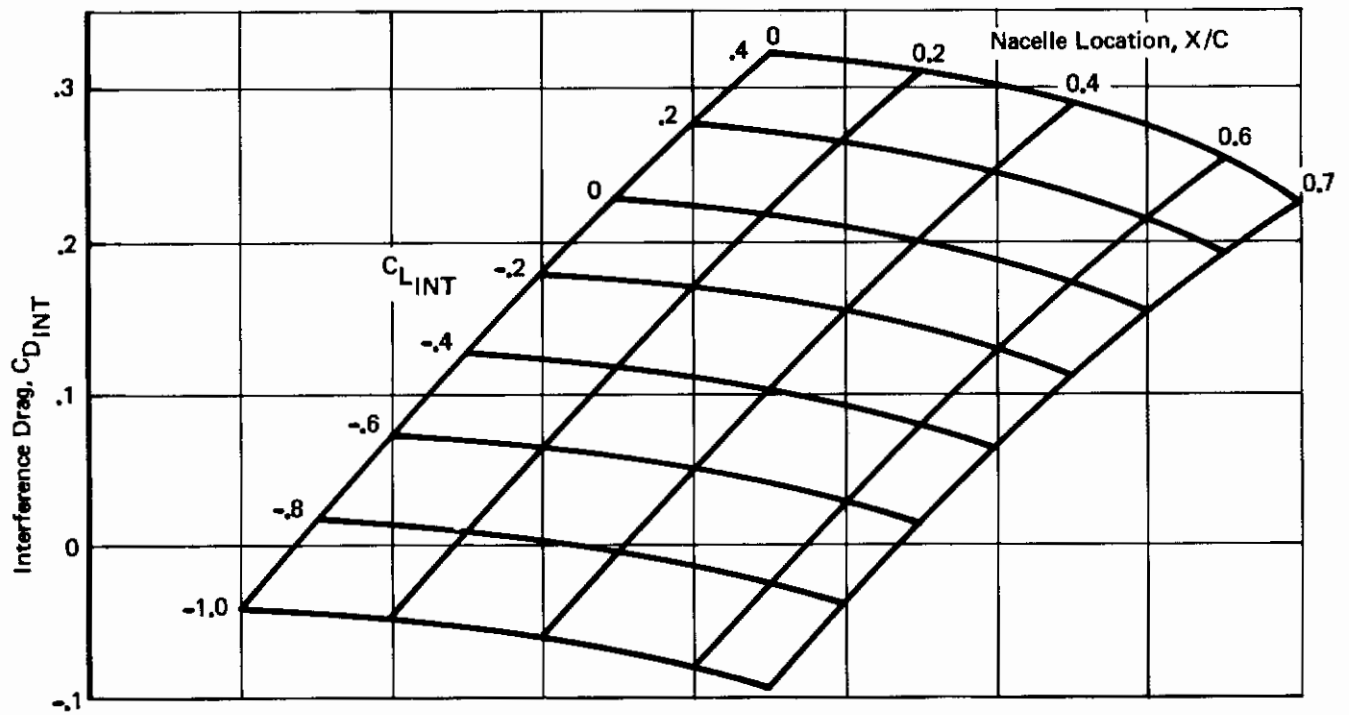


Figure 34: Vectored Thrust, Drag Interference, Vector Angle 90°

2.3.3 Pitching Moment Interference

Free air pitching moment interference also correlated well with the free air lift interference at a given nacelle location and nozzle vector angle. This indicates that the center of pressure of the induced lift remains constant with angle of attack for a given nacelle configuration. For pitching moments, the important length parameter is the distance from the center of pressure of the induced lift to the moment center. Therefore, for the pitching moment interference in free air, Figures 35 through 37, the nozzle location has been given as the distance from the center of the nozzle exit to the moment center. For a swept wing, the average nozzle location is used.

2.3.4 Downwash Interference

The effect of vectored thrust on downwash is shown in Figure 38.

SAMPLE PROBLEM - VECTORED THRUST, FREE AIR

$$\alpha = 5.46^\circ \text{ (estimated power-off aerodynamic characteristics)}$$

$$\sigma = 30^\circ$$

$$C_L = 2.4$$

$$C_D = .4062$$

$$C_{RAM} = 0 \text{ (model with blowing nozzles)}$$

$$C_J = .2.0$$

$$C_m = -.5356$$

$$\bar{c} = 11.179 \text{ in.}$$

$$X_E = -.066 \text{ in.}$$

$$Z_E = + 2.787 \text{ in.}$$

$$x/c = .35$$

Lift

from chart Figure 30 read $C_{L_{INT}}$

$$C_{L_{INT}} = -.15$$

from Figure 31 $C_{L_{INT}} = 0$

Total lift interference

$$C_{L_{INT}} = (-.15+0) \left(\frac{2.0}{2}\right)^{1/2} = -.15$$

Contrails

$$\sigma = 30^\circ$$

All C_J

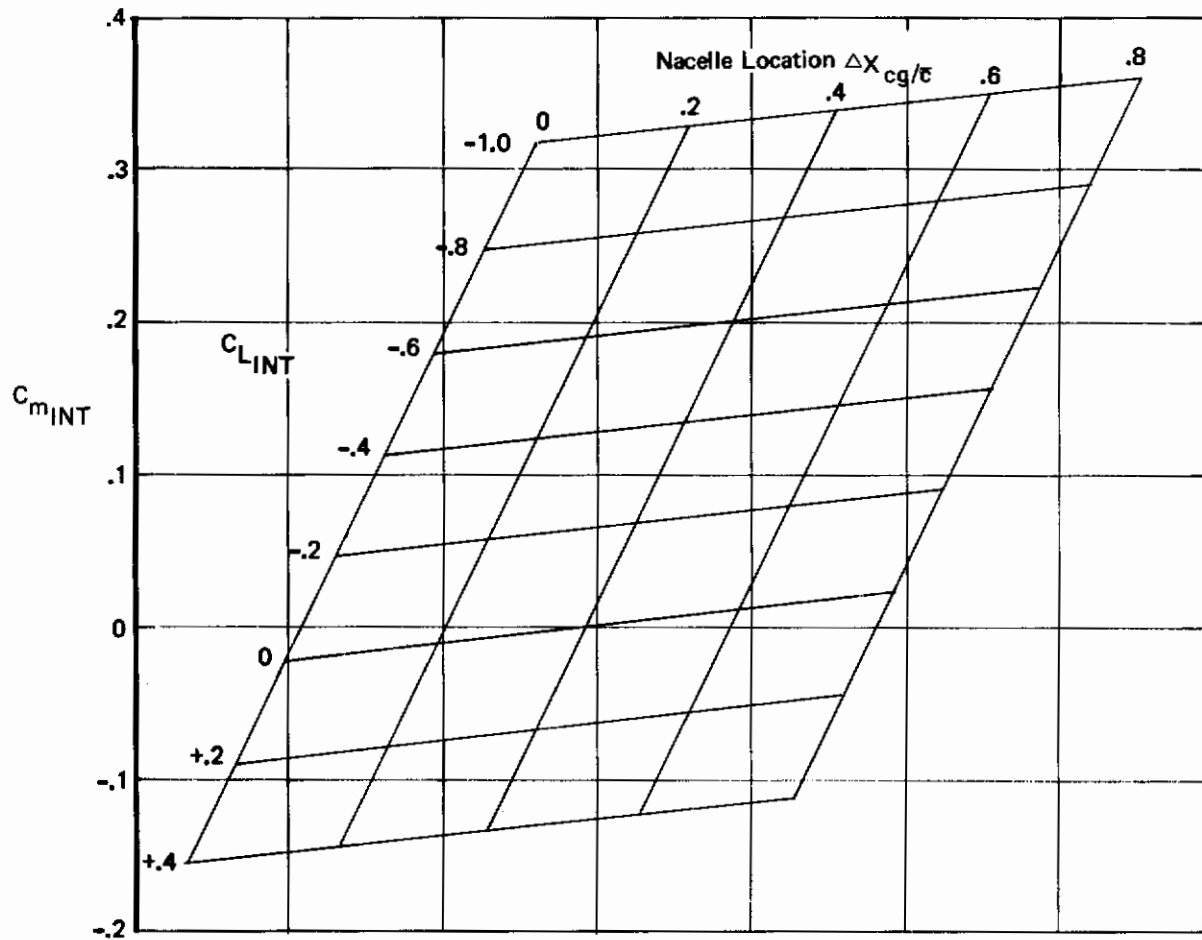
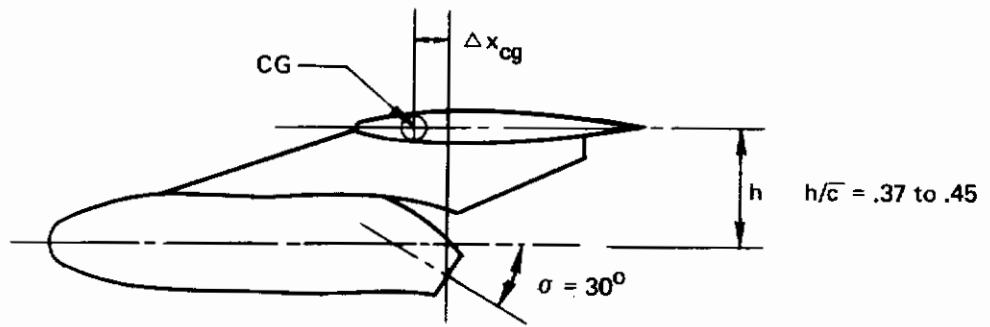


Figure 35: Vectored Thrust Pitching Moment Interference, Vector Angle 30°

Contrails

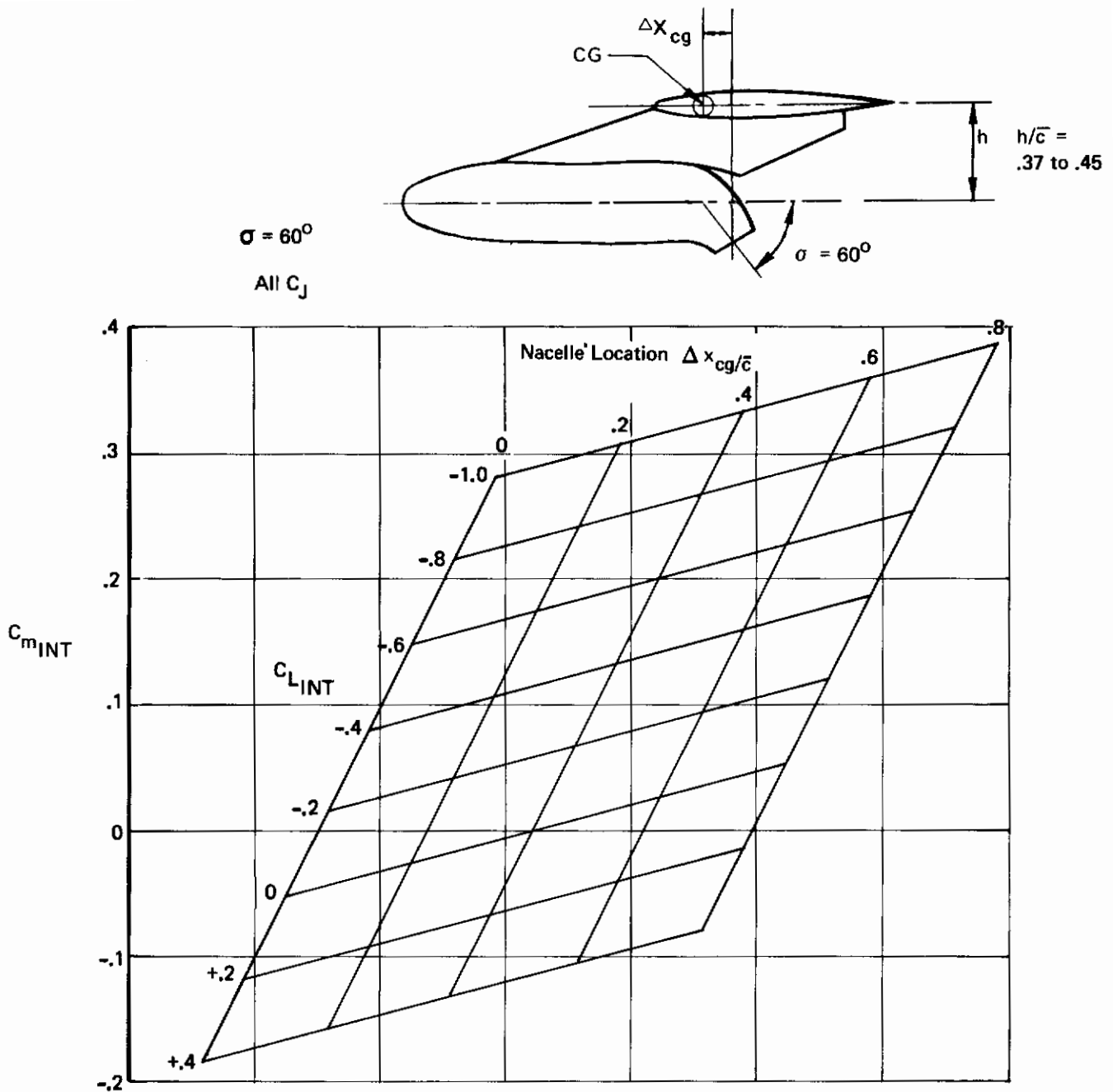


Figure 36: Vectored Thrust Pitching Moment Interference, Vector Angle 60°

Contrails

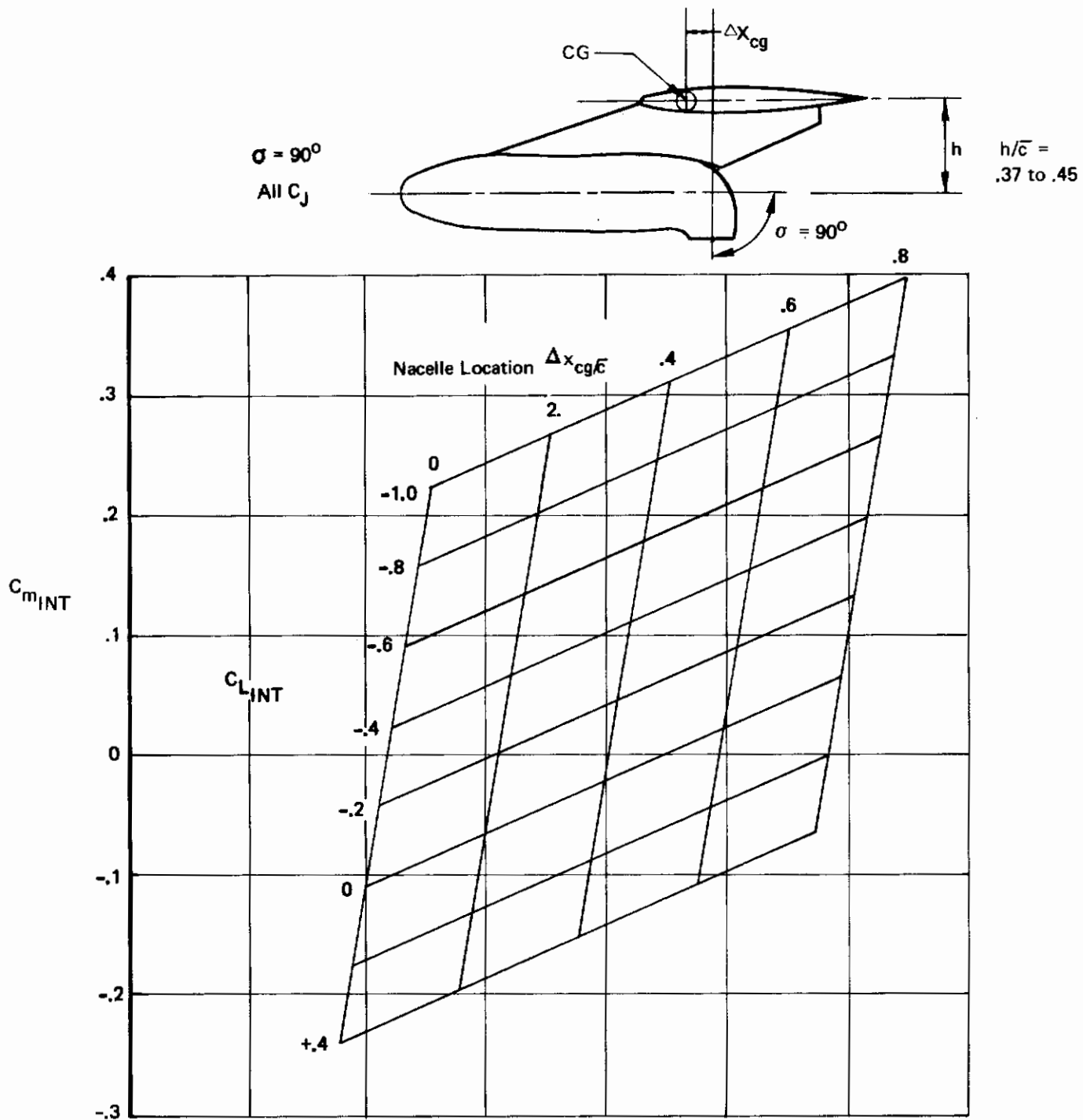


Figure 37: Vectored Thrust Pitching Moment Interference, Vector Angle 90°

Contrails

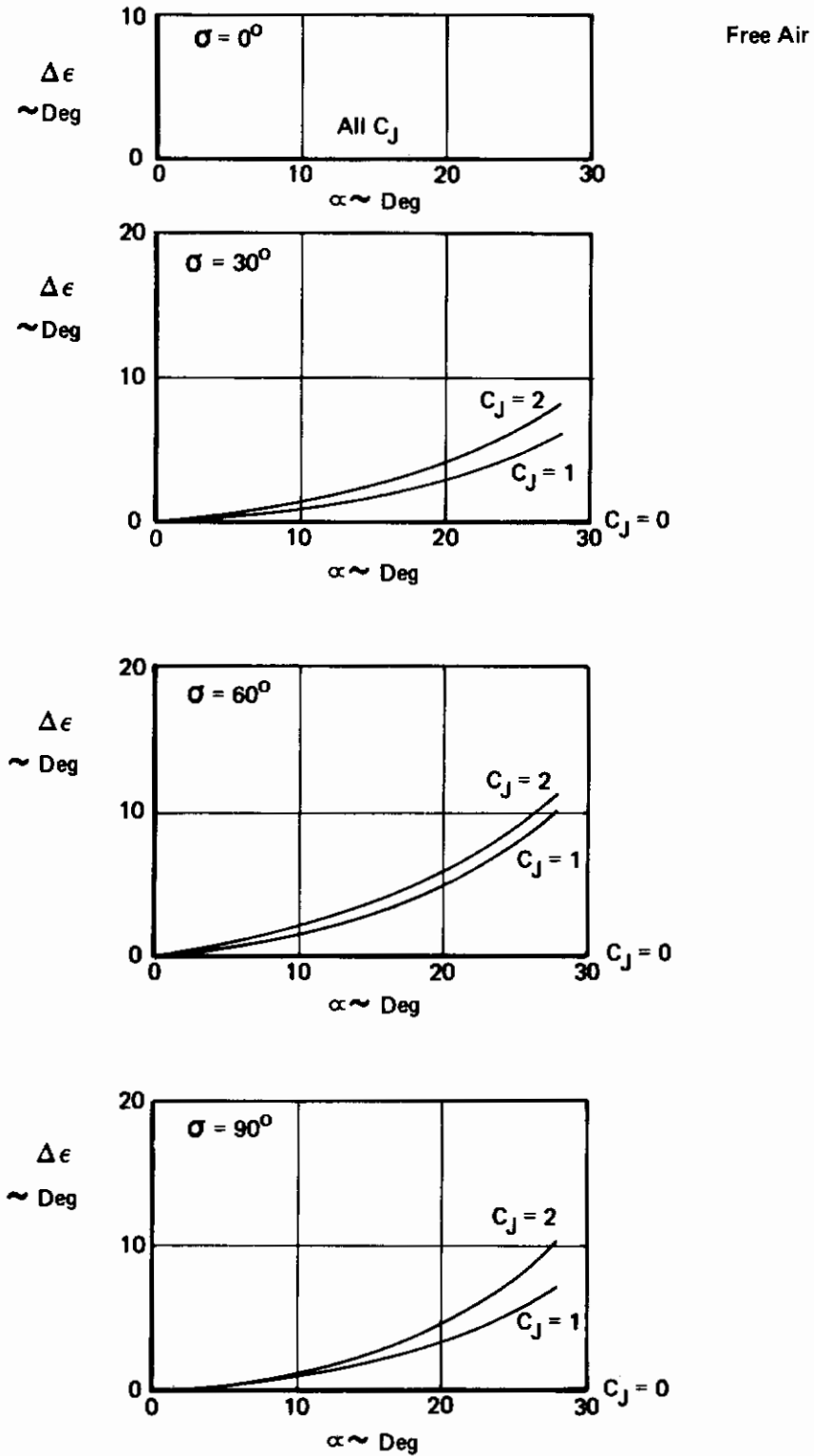


Figure 38: Vectored Thrust Downwash Change at Horizontal Tail

Contrails

With equation 2.3-1

$$\begin{aligned}C_L &= 2.4 - .15 + 2.0 \sin (30 + 5.46) \\ &= 3.43\end{aligned}$$

from wind tunnel test data

$$C_L = 3.63 @ \alpha = 5.46$$

Drag

from chart Figure 32 at $C_{L_{INT}}$ read

$$C_{D_{INT}} = -.010$$

calculate with equation 2.3.2

$$\begin{aligned}C_D &= .4062 - .010 - (2.0) \cos (30 + 5.46) + 0 \\ C_D &= -1.2852\end{aligned}$$

observed from TAI test data at $C_L = 3.43$

$$C_D = -1.28$$

Pitching Moment

from Figure 35 at $C_{L_{INT}}$ read

$$C_{m_{INT}} = +.0450$$

calculate C_m power on with equation 2.3-3

$$\begin{aligned}C_m &= -.5356 + .0450 + 2.0 \left[\frac{-.066}{11.179} \sin 30^\circ + \frac{2.787}{11.179} \cos 30^\circ \right] \\ &= -.074\end{aligned}$$

C_m observed at $C_L = 3.43$ wind tunnel test

$$C_m = -.190$$

Downwash

from Figure 38 read

$$\Delta \epsilon = +.09^\circ$$

2.4 Vectored Thrust in Ground Effect

Vectored thrust interference effects in the presence of the ground were also obtained from STAI wind tunnel test BVWT 099. Figure 39 presents a comparison of free air test data, free air test data corrected for ground influence and test data in ground effect. These show a good correlation between the corrected data and the test data in ground effect.

2.4.1 Lift Interference

As in the case of the power-off ground effect procedure, the C_L vs α curve in ground effect is determined from the free air curve by adjusting both C_L and α . Lift interference due to vectored thrust in ground effect is the sum of the lift interference due to vectored thrust in free air and an additional increment for the effect of ground proximity. This additional increment is presented in Figure 40. The angle of attack adjustment is the same as for the power off case (Eq. 2.2-5), but must be based on $C_{L_{NET}}$.

Lift in ground effect with vectored thrust is

$$C_L = C_{L_{GE}}^{\text{power off}} + C_{L_{INT}}^{\text{free air}} + \Delta C_{L_{INT}}^{\text{ground effect increment}} + C_J \sin(\alpha + \sigma) \quad (2.4-1)$$

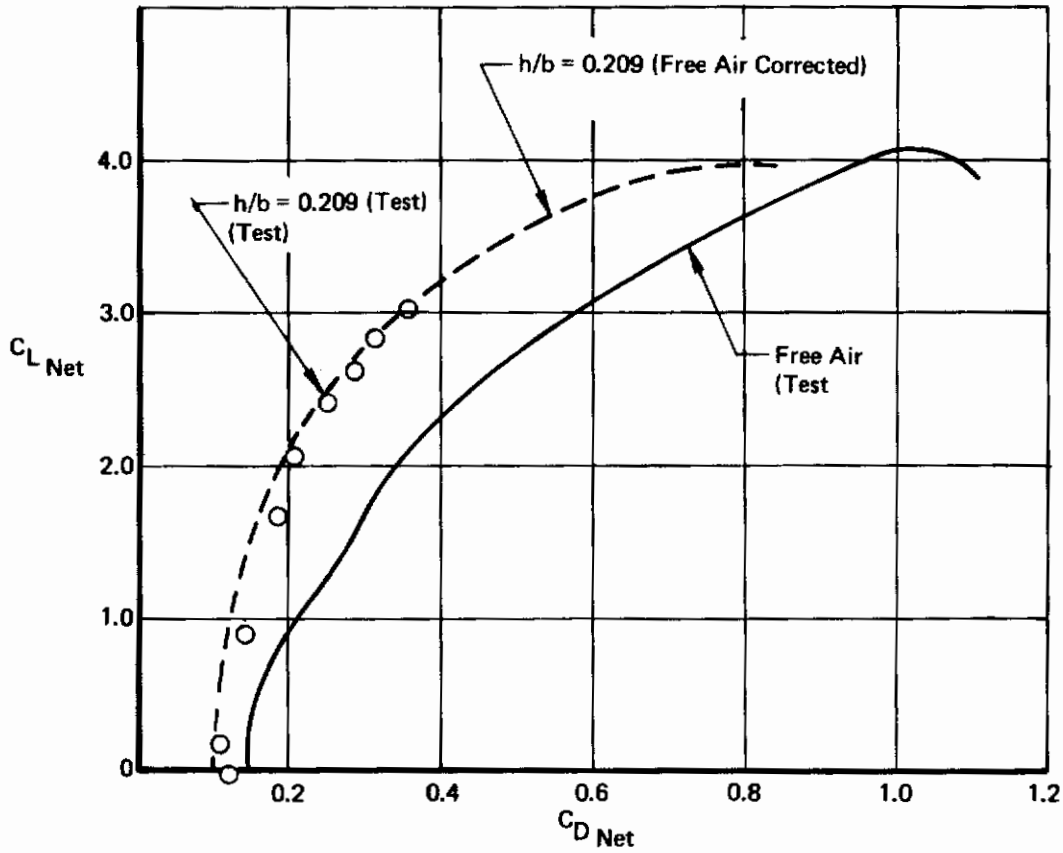
2.4.2 Drag Interference

Drag interference due to vectored thrust in ground effect is the sum of the drag interference due to vectored thrust in free air and an additional increment for the effect of ground proximity. The additional increment is presented in Figure 40.

Drag in ground effect with vectored thrust is

$$C_D = C_{D_{GE}}^{\text{power off}} + C_{D_{INT}}^{\text{free air}} + \Delta C_{D_{INT}}^{\text{ground effect increment}} + C_J (\cos \alpha + \sigma) + C_{D_{RAM}} \quad (2.4-2)$$

Sweep = 15° , $C_J = 2.0$



Tail Off
 Nozzles at
 35% Chord
 Nozzle Vector
 Angle = 60°
 $AR = 8.0$
 T.E. Flap Span
 = 0.75
 T.E. Flap Angle
 = 35°
 L.E. Flap Angle
 = 70°
 $C_{\mu\text{ L.E.}} = 0.06$
 Data From BWWT 099
 (Ref. 5)

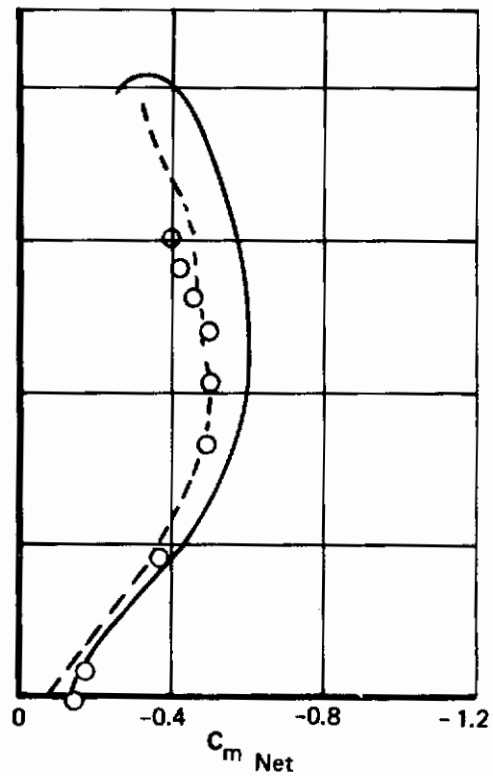
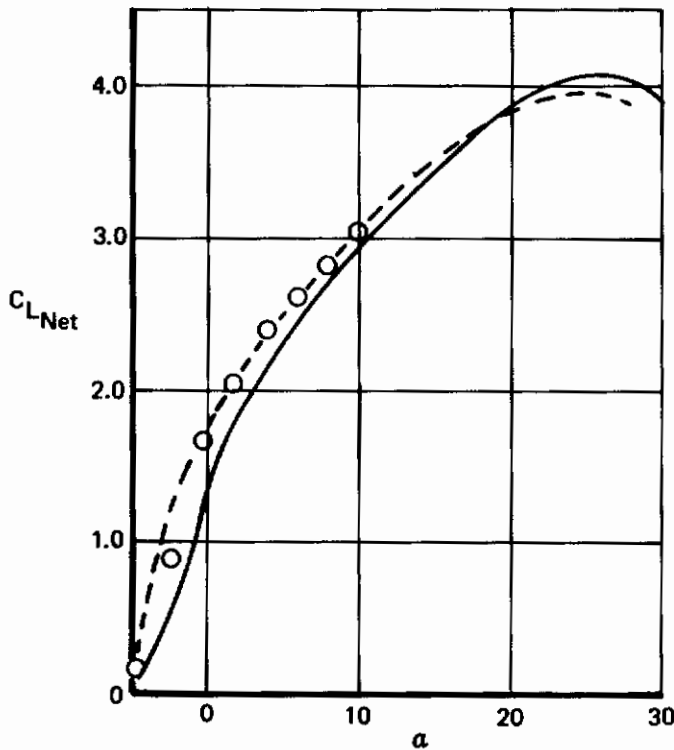
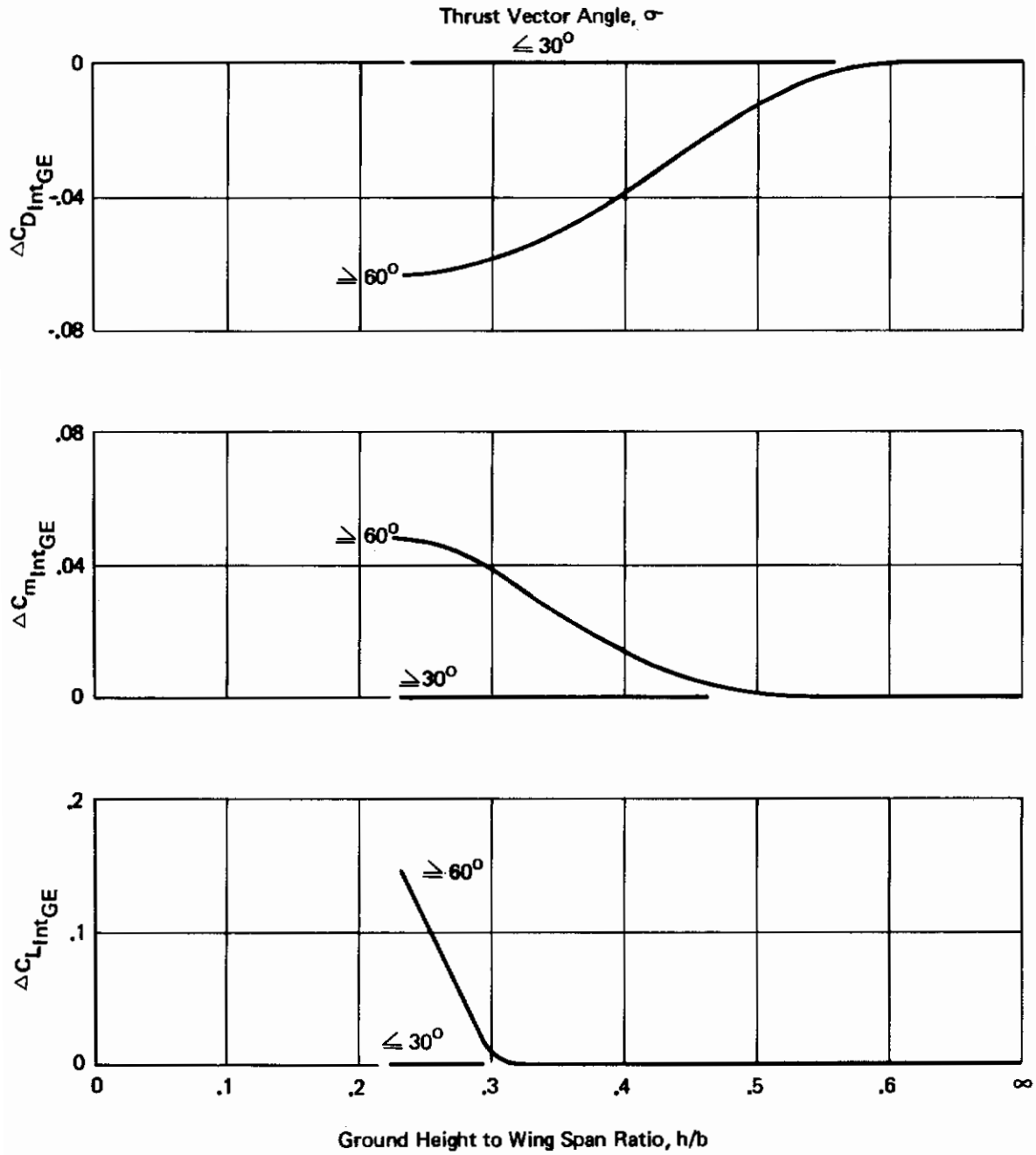


Figure 39: Vected Thrust in Ground Effect Test—Estimate Comparison



Obtained from Test Data $C_J = 0$ to 3.0 (BVWT 099, Ref. 5)

Figure 40: Change in Thrust Interference Effects Due to Ground Effect

2.4.3 Pitching Moment Interference

Pitching moment interference due to vectored thrust in ground effect is the sum of the pitching moment interference due to vectored thrust in free air and an additional increment for the effect of ground proximity. This additional increment is presented in Figure 40.

Pitching moment in ground effect with vectored thrust is

$$C_m = C_{m_{GE}} + C_{m_{INT}} + \Delta C_{m_{INT}} + C_J \left(\frac{x_E}{c} \sin \sigma + \frac{z_E}{c} \cos \sigma \right) + C_{DRAM} \left(\frac{x_R}{c} \sin \alpha + \frac{z_R}{c} \cos \alpha \right) \quad (2.4-3)$$

power off free air ground effect increment

2.4.4 Downwash Interference

Analysis of the test data did not show significant changes in downwash angle in ground effect with the addition of vectored thrust.

SAMPLE PROBLEM, THRUST INTERFERENCE IN GROUND EFFECT.

$$h/b = .208$$

$$\sigma = 30^\circ$$

From sample problem in Part 2.2 the test conditions in ground effect, power off

$$C_{L_{GE}} = 1.93$$

$$\alpha_{GE} = .93$$

$$C_{D_{GE}} = .282$$

$$C_{m_{GE}} = -.5088$$

The free air vectored thrust corrections at $\sigma = 30^\circ$, $C_J = 0$, nacelle $x/c = .35$.

Contrails

$$C_{L_{INT}} = -.2$$

$$C_{D_{INT}} = -.025$$

$$C_{m_{INT}} = +.065$$

For this example the thrust interference effects in ground effect are zero. Coefficients in ground effect are then, Lift equation 2.3-1

$$\begin{aligned} C_L &= 1.93 - .2 + 2.0 (\sin 30.93) \\ &= 2.76 \end{aligned}$$

Drag equation 2.3-2

$$\begin{aligned} C_D &= .282 - .025 - 2.0 (\cos 30.93) + 0 \\ &= -1.458 \end{aligned}$$

Pitching Moment equation 2.3-3

$$\begin{aligned} C_m &= -.5088 + .065 + .255 \\ &= -.1888 \end{aligned}$$

The comparable test values at this angle of attack

$$C_L = 2.88$$

$$C_D = -1.465$$

$$C_m = -.143$$

2.5 Trim

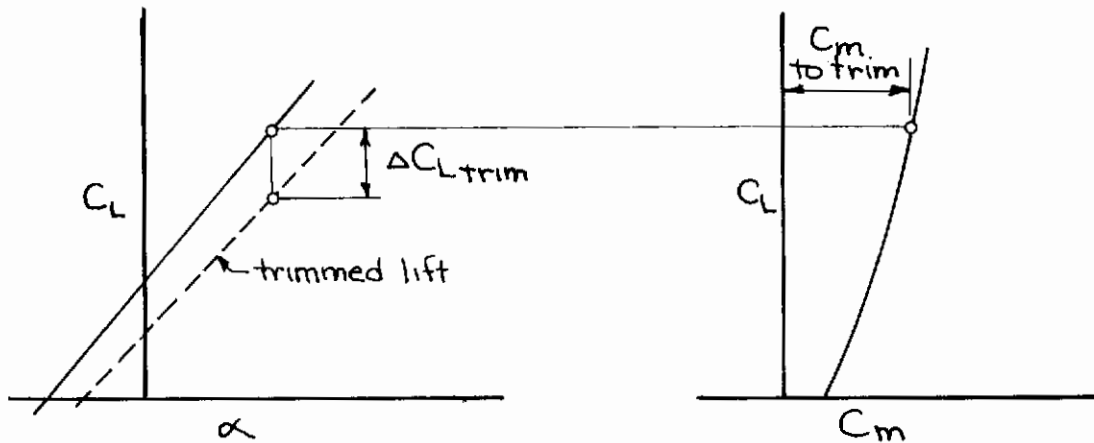
Any complete set of longitudinal data, lift, drag, pitching moment, and downwash at the tail may be reduced to trimmed lift and drag by the methods presented in this section. Note that these methods are valid for relating long tail arms; close coupled tails or canards would require a considerably more involved analysis.

2.5.1 Trimmed Lift

The lift increment required to trim is the increment required at the horizontal tail l/c to reduce the pitching about the center of gravity to zero.

$$\Delta C_{L_{trim}} = \frac{C_m}{l/c} \quad (2.5-1)$$

Contrails

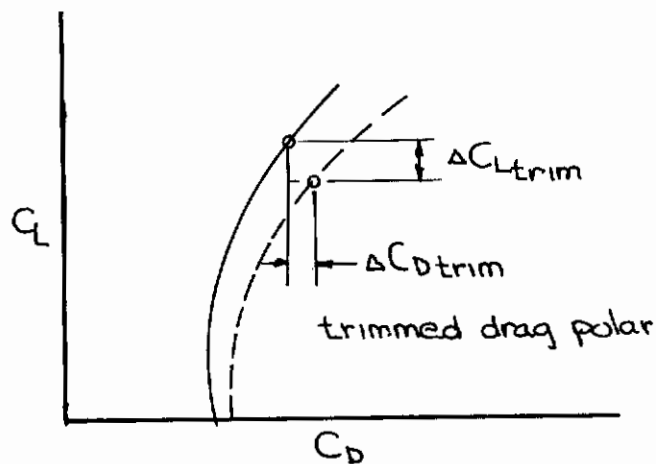


2.5.2 Trimmed Drag

The drag increment for trim is considered to be made up of two components. First, the inclination of the lift vector since it is in the downwash of the wing. Second, the tail drag both friction and the tail drag due to lift.

$$\Delta C_{Dtrim} = (\Delta C_{Ltrim})(e) + \left[(C_{Dmin})_{tail} + \left(\frac{\partial C_D}{\partial C_L^2} \right)_{tail} (C_L^2)_{tail} \right] \frac{S_{tail}}{S_{REF}}$$

(2.5-2)



SECTION III

STABILITY AND CONTROL DERIVATIVE PREDICTION METHODS

This section includes methods for predicting vectored thrust effects on stability derivatives, and a sensitivity study to determine the importance of each derivative. Methods are based on wind tunnel data from Reference 5. Accuracy adequate for preliminary design purposes is provided. This results in a simple, quick method.

Error charts and tables are included. These should be used in conjunction with the sensitivity study. The reader should guard against falling into the trap of thinking of errors only in terms of "percent error." Often it is the increment of error that is important. For instance, in predicting the tail-off $C_{n\beta}$, an error of 200% would be insignificant if the actual value were only $-.0001 \text{ deg}^{-1}$. On the other hand, if the tail-on $C_{n\beta}$ is $.008 \text{ deg}^{-1}$, a 15% error might be quite noticeable.

3.1 Stability Derivative Sensitivity Study

It is important in the study of an airplane's stability characteristics to understand the consequences of errors in estimating stability derivatives. When the sensitivity of the dynamic response to each parameter is known, effort to improve accuracy can be expended on the more important derivatives.

Such a sensitivity study was performed for the airplane shown in Figure 41.* A nominal STOL approach condition of 75 knots was selected, and stability derivatives were estimated. The derivatives, together with mass properties and reference dimensions, are given in Table I. Derivatives found to be the more important ones are listed in Table II.

Angle of attack and sideslip derivatives are based on wind tunnel data from Reference 5. Rotary derivatives were predicted using DATCOM methods.

Three degree of freedom equations of motion for longitudinal and lateral-directional stability were solved, using the nominal derivatives. Then each derivative was varied over a range of $\pm 150\%$, except in a few cases where this would have resulted in an unreasonably large increment.

*This airplane is the "Baseline Configuration" developed early in the STAI program and reported in detail in Appendix A of Volume I of the STAI Series (Ref. 12).

REFERENCE GEOMETRY

S = 1640 FT²

b = 114.5 FT

c̄ = 15.7 FT

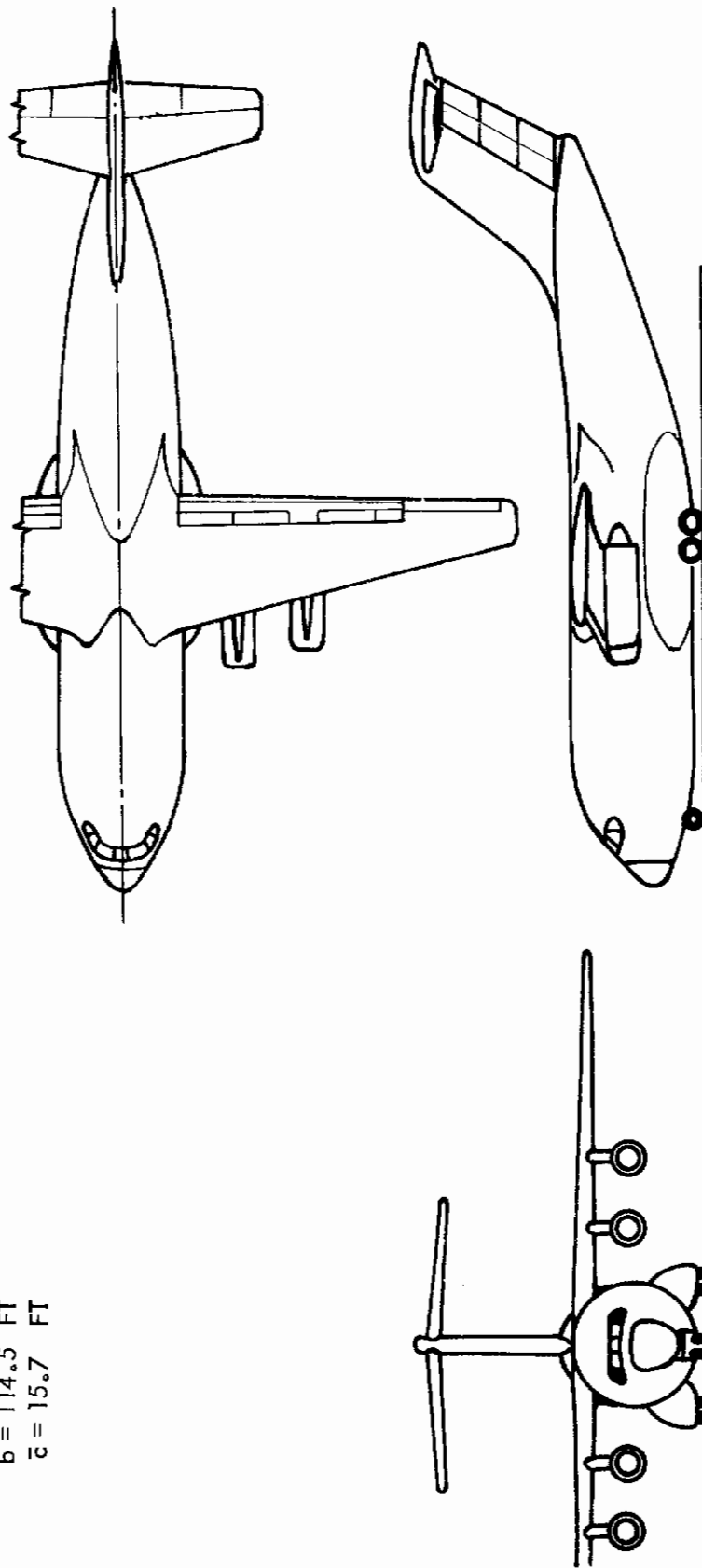


Figure 41: General Arrangement STOL Tactical Transport -- Model 953-801

TABLE I

Stability Derivatives, Mass Properties, and
Reference Dimensions of Example Airplane

All angles are in radians.

$C_{X_\alpha} = 1.297$	$C_{X_\alpha} = 0$	$C_{X_q} = 0$	$C_{X_u} = -1.77$
$C_{L_\alpha} = 7.84$	$C_{L_\alpha} = -8.18$	$C_{L_q} = 7.54$	$C_{L_u} = .0341$
$C_{m_\alpha} = -.496$	$C_{m_\alpha} = -6.06$	$C_{m_q} = -32.94$	$C_{m_u} = -.453$
$C_{Y_\beta} = -1.415$	$C_{Y_p} = .51$	$C_{Y_r} = .02$	
$C_{n_\beta} = .27$	$C_{n_p} = -.45$	$C_{n_r} = -.35$	
$C_{l_\beta} = -.191$	$C_{l_p} = -.59$	$C_{l_r} = 1.16$	
$S = 1640 \text{ ft}^2$	$W = 133,000 \text{ lbs.}$	$I_{ZZ} = 2.62 \times 10^6 \text{-slug-ft}^2$	
$\bar{c} = 15.7 \text{ ft}$	$I_{xx} = 1.26 \times 10^6 \text{-slug-ft}^2$	$I_{xz} = 1.4 \times 10^5 \text{-slug-ft}^2$	
$b = 114.5 \text{ ft.}$	$I_{yy} = 1.46 \times 10^6 \text{-slug-ft}^2$		

Angle of attack, $\alpha = .182$

Thrust deflection, $\sigma = 1.13$

Thrust coefficient, $C_J = 1.72$

TABLE II

Stability Derivatives With Important Influence
On Airplane Stability

Stability Derivative	Major Influence	
Longitudinal	$C_{L\alpha}$	neutral point (Note: when $C_{L\alpha}$ was varied, $C_{m\alpha}$ was held constant so the a.c. was moving.)
	$C_{m\alpha}$	neutral point, short period frequency and damping ratio, long period frequency and damping ratio
	$C_{m\dot{\alpha}}$	short period damping ratio
	$C_{m\dot{q}}$	short period damping ratio
	$C_{m\dot{u}}$	neutral point, long period frequency and damping
Lateral-Directional	$C_{n\beta}$	Dutch roll frequency, spiral stability
	$C_{l\beta}$	Dutch roll damping ratio, spiral stability
	$C_{n\dot{p}}$	Dutch roll frequency, spiral stability
	$C_{l\dot{p}}$	Dutch roll damping ratio, spiral stability
	$C_{n\dot{r}}$	Dutch roll damping ratio, spiral stability
	$C_{l\dot{r}}$	Dutch roll frequency and damping ratio, spiral stability

Roots of the longitudinal characteristic equation were plotted on the s-plane. Dutch roll mode roots are also presented on the s-plane. Spiral mode time constants were plotted versus the derivative being varied. These plots are shown, and significant trends discussed in the next sections.

3.1.1 Longitudinal

The influence of angle of attack, aerodynamic lag, pitch damping, and speed derivatives is shown in Figures 42, 43, 44, 45 and 46. These charts show that the derivatives critical to an accurate determination of the longitudinal characteristics are: $C_{L\alpha}$, $C_{m\alpha}$, C_{mq} , and $C_{m\dot{u}}$.

Sensitivity of longitudinal characteristics to variations of the pitching moment due to angle of attack, $C_{m\alpha}$, are shown in Figure 42. Even though $C_{m\alpha}$ is negative (the a.c. is more than 6% \bar{c} aft of the c.g.), the airplane is statically unstable. (There is a real root in the right half plane.) This is due to the large negative value of $C_{m\dot{u}}$. As $C_{m\alpha}$ is increased from its initial value, the unstable root moves to the left, toward the other real root, while the complex root moves upward. The short period frequency is increasing and the damping decreasing. At about 1.5 times the initial $C_{m\alpha}$, the previously unstable root goes to the origin and the airplane becomes neutrally stable. (The c.g. is at the neutral point.) When $C_{m\alpha}$ is further increased, the two real roots couple and form a long period oscillatory mode, the phugoid. If $C_{m\alpha}$ were further increased, the phugoid mode may go unstable but the airplane would still be statically stable (the neutral point would still be aft of the c.g.).

When $C_{m\alpha}$ is decreased the short period frequency decreases and the damping ratio increases. The unstable root goes more unstable and the other real root moves to the left. At about .57 times the initial $C_{m\alpha}$, the short period mode becomes critically damped. (The short period mode is now described by real roots.) As $C_{m\alpha}$ is increased more, one short period real root moves to the left while the other one moves toward the other stable real root. At about .53 times the initial $C_{m\alpha}$ these latter two roots couple and form an oscillatory mode.

It is necessary to know $C_{m\alpha}$ accurately for reasons other than longitudinal dynamics considerations. The aerodynamic center should be known within about $\pm 1\%$ MAC in order to design the tail, locate the c.g. envelope, compute control surface deflections for trim and maneuver, etc. In this case, a $\pm 1\%$ MAC error in the aerodynamic center location corresponds to about a $\pm 15\%$ error in $C_{m\alpha}$. Figure 42 shows that a 15% error in $C_{m\alpha}$ will only result in about a 5% error in natural undamped frequency and a .05 change in damping ratio.

Sensitivity to lift curve slope, $C_{L\alpha}$, and axial force due to angle of attack, $C_{X\alpha}$, is also shown in Figure 43. Varying $C_{X\alpha}$ had no noticeable effect on the unstable root and only a small effect on the others. A large error, $\pm 50\%$, in $C_{X\alpha}$, should cause no serious inaccuracies. It is hard to conceive of a 30% error in $C_{L\alpha}$ so this derivative

Approach Condition
 V = 74.6 Knots
 W = 133,000 Lbs
 $\sigma = 64.6$ Deg
 $\gamma = -6$ Deg
 $\dot{C}_J = 1.76$

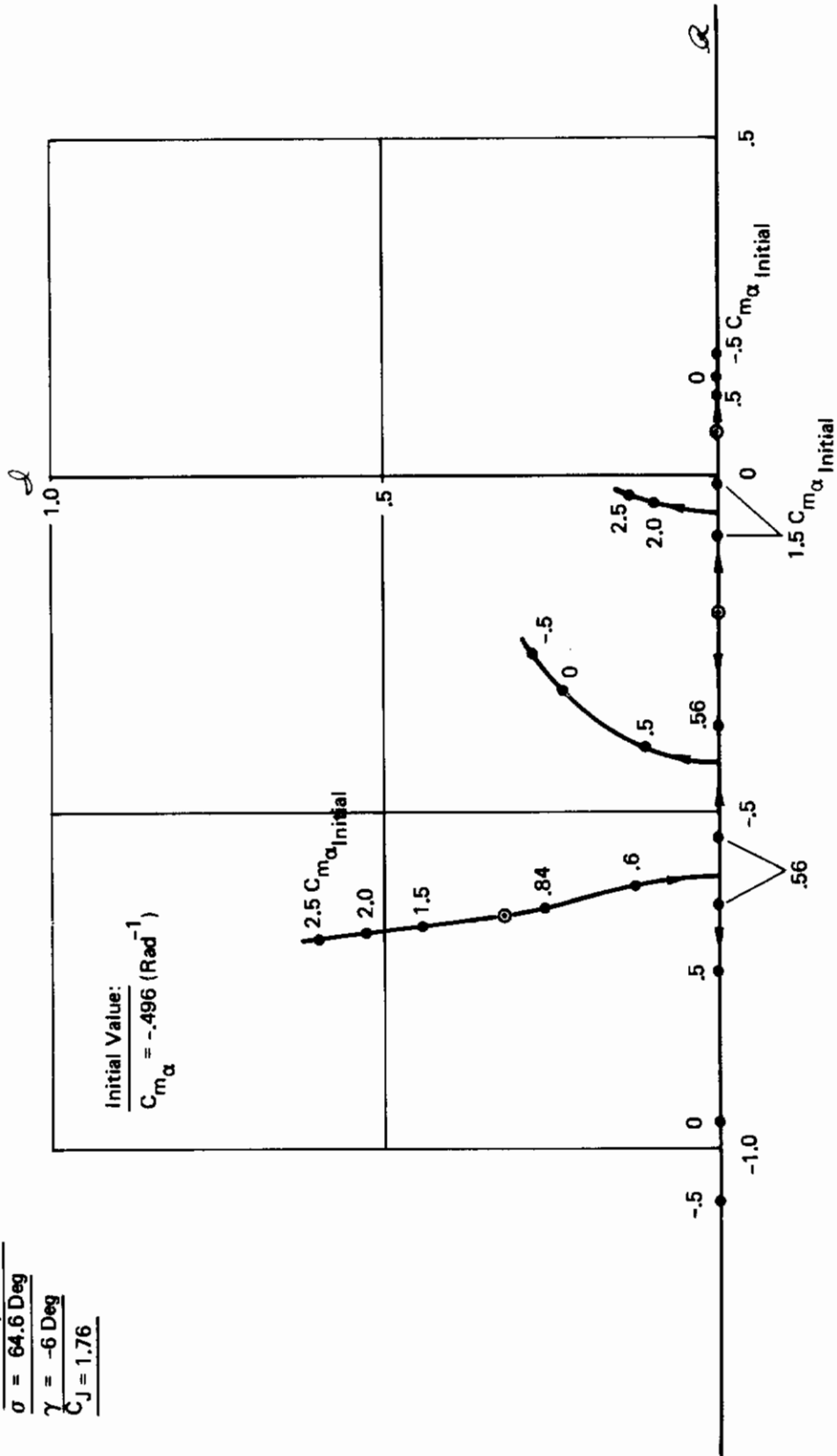


Figure 42 : Effect of Angle of Attack Derivative , $C_{m\alpha}$, on Longitudinal Dynamic Stability

Approach Condition
 $V = 74.6$ Knots
 $W = 133,000$ Lbs
 $\sigma = 64.6$ Deg
 $\gamma = -6$ Deg
 $C_J = 1.76$

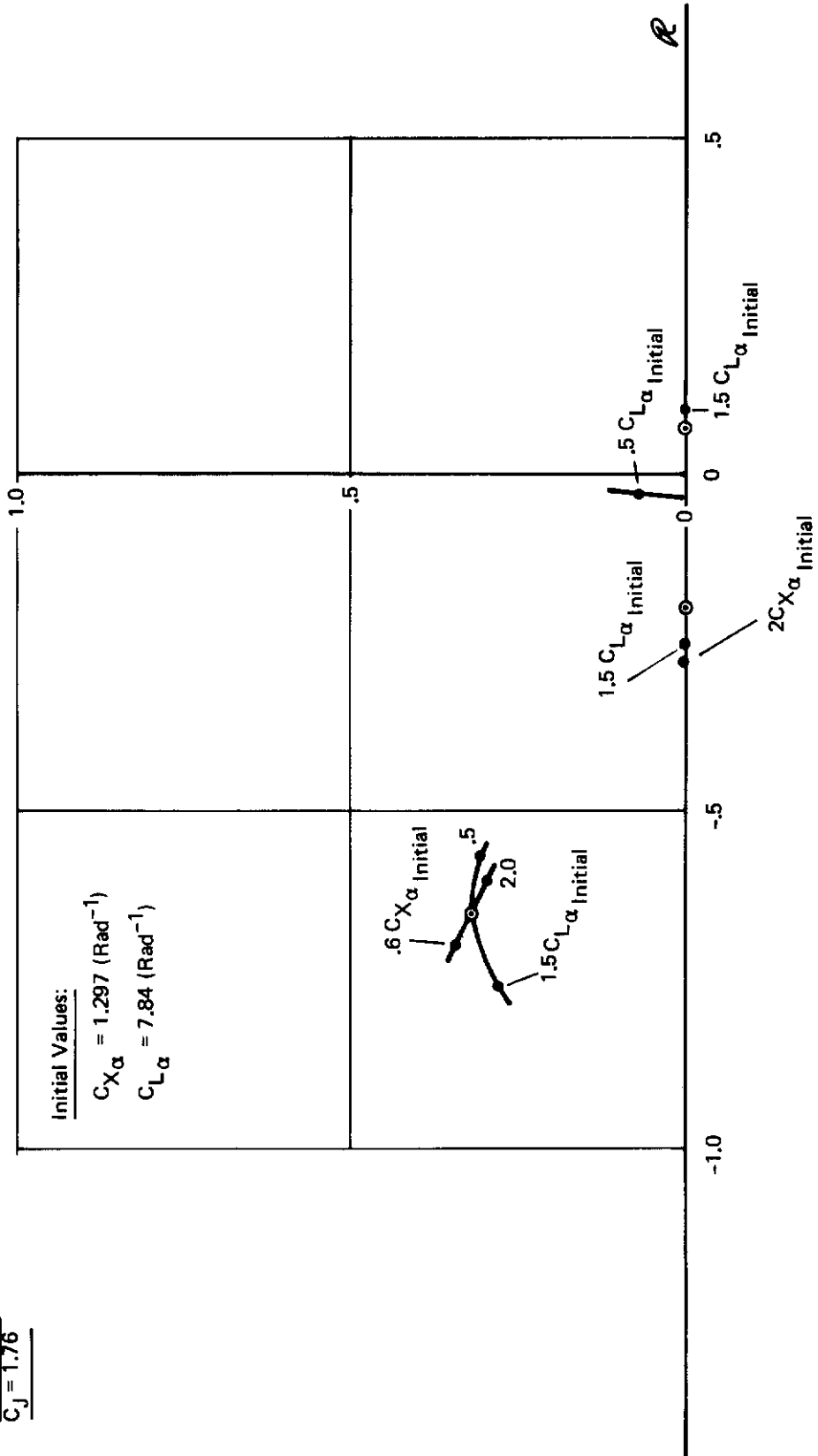


Figure 43 : Effect of Angle of Attack Derivatives, C_{X_α} and C_{L_α} , on Longitudinal Dynamic Stability

Approach Condition
V = 74.6 Knots
W = 133,000 Lbs
 $\sigma = 64.6$ Deg
 $\gamma = 6$ Deg
 $C_J = 1.6$

A Similar Variation
 of C_{L_u} Had No
 Noticeable Effect

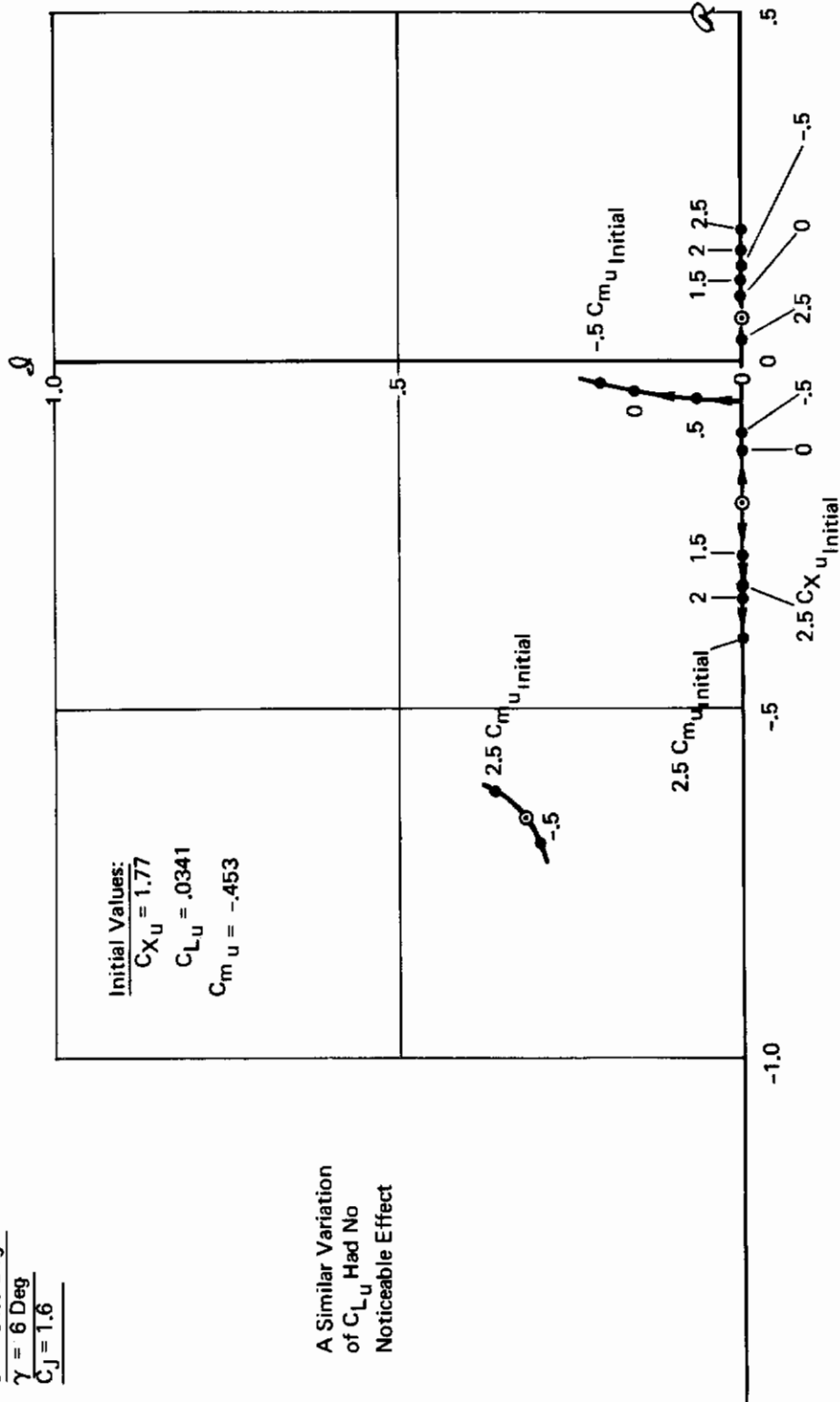


Figure 44 : Effect of Speed Derivatives on Longitudinal Dynamic Stability

Approach Condition
 $V = 74.6$ Knots
 $W = 133,000$ Lbs
 $\sigma = 64.6$ Deg
 $\gamma = -6$ Deg
 $C_J = 1.76$

Initial Values:
 $C_{X\dot{\alpha}} = 0$
 $C_{L\dot{\alpha}} = -8.18$ (Rad⁻¹)
 $C_{m\dot{\alpha}} = 6.06$ (Rad⁻¹)

A Similar Variation
of $C_{L\dot{\alpha}}$ Had No
Noticeable Effect

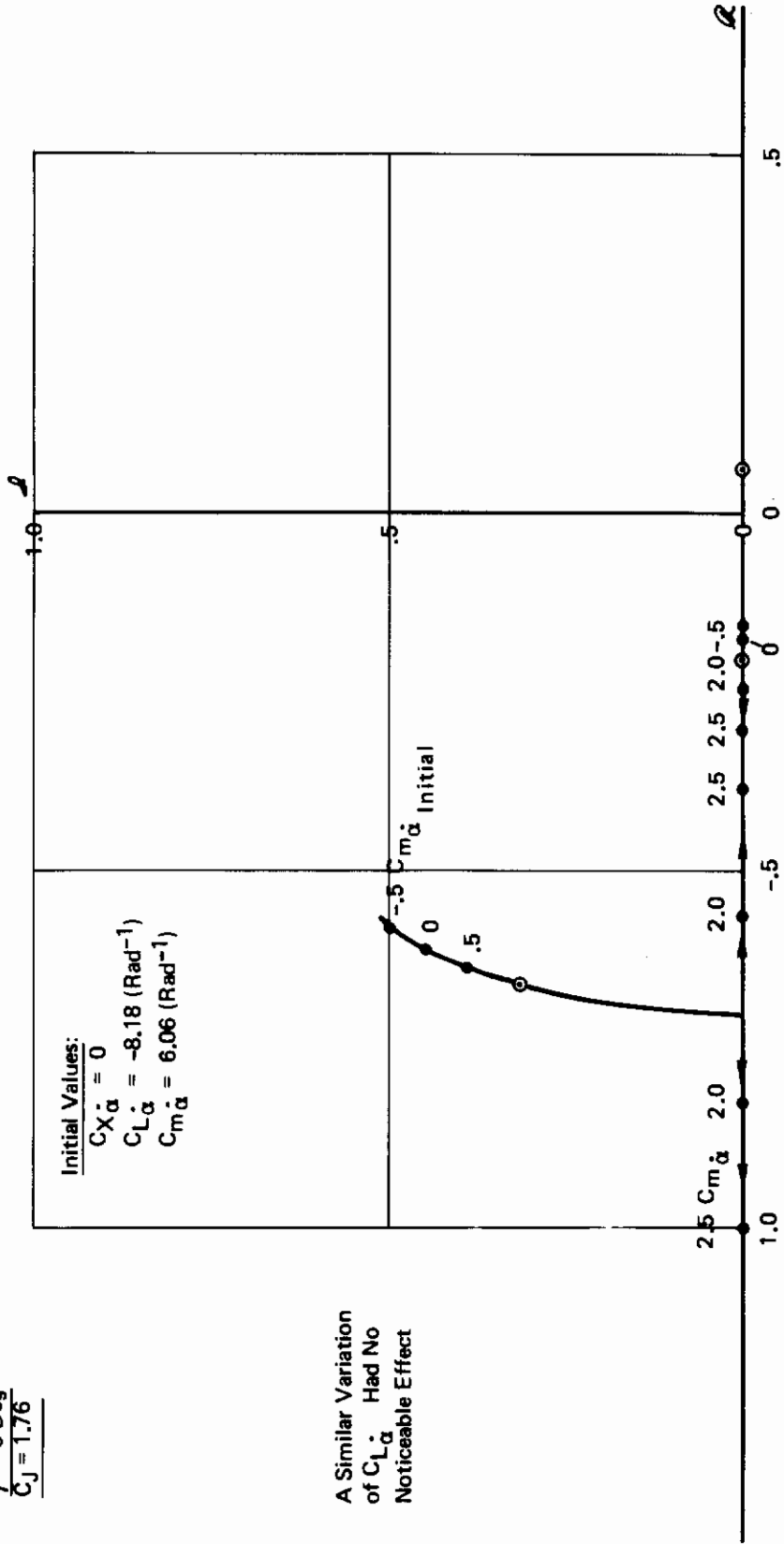


Figure #5 : Effect of Aerodynamic Lag Derivatives on Longitudinal Dynamic Stability

Approach Condition
 $V = 74.6$ Knots
 $W = 133,000$ Lbs
 $\sigma = 64.6$ Deg
 $\gamma = -6$ Deg
 $C_J = 1.76$

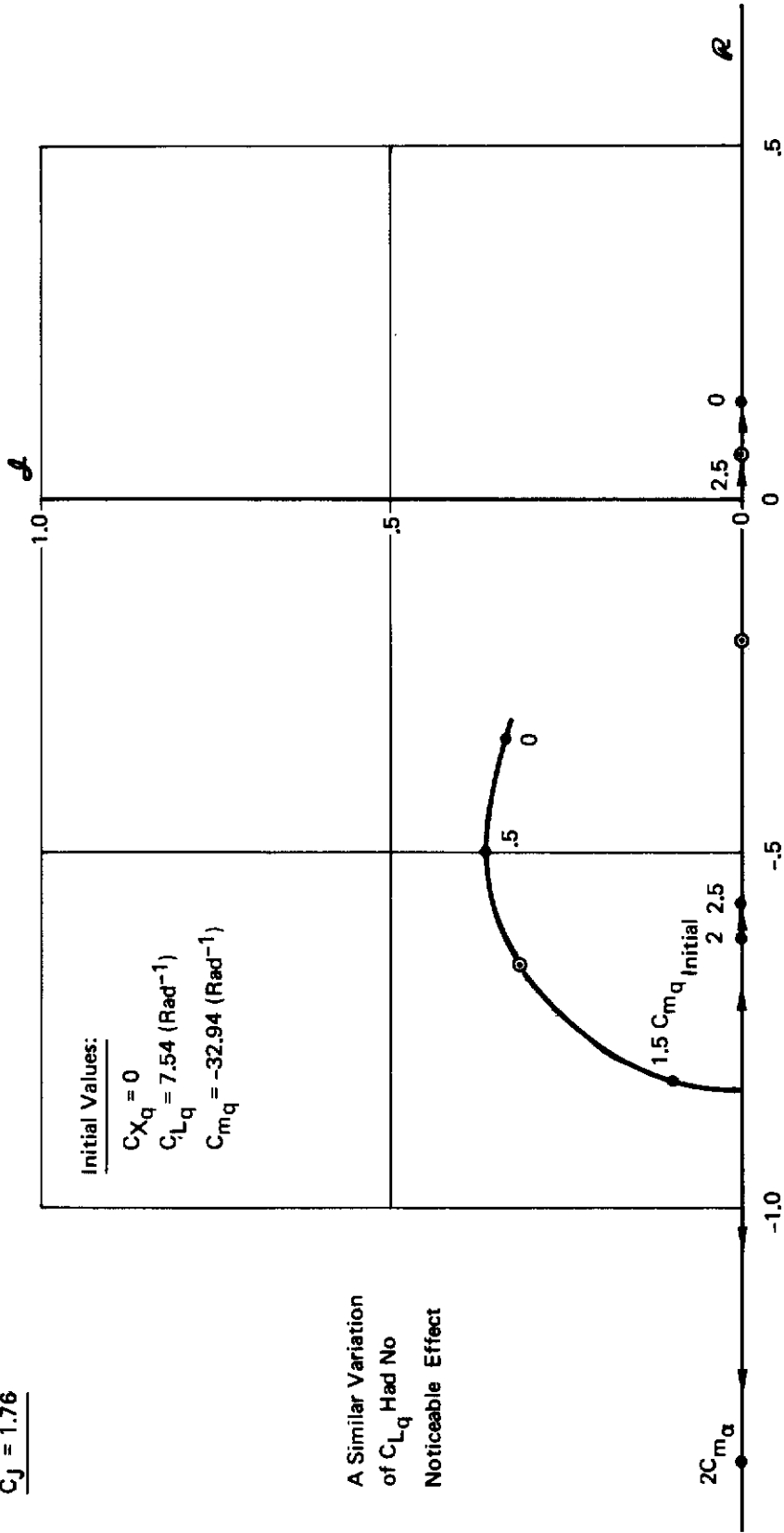


Figure 46 : Effect of Pitch Damping Derivatives on Longitudinal Dynamic Stability

was only varied $\pm 50\%$. A 30% error in lift curve slope would only affect the undamped natural frequency by about 6% and has a negligible effect on the damping ratio. Its greatest effect appears to be on the real roots. As $C_{L\dot{\alpha}}$ is reduced, the unstable root moves to the left, couples with the other real root, and forms the oscillatory phugoid mode. With a large unstable value for C_{m_u} , a 20% or 30% error in $C_{L\dot{\alpha}}$ could make the difference between whether or not the airplane was statically stable. Keep in mind that $C_{m\dot{\alpha}}$ was held constant while $C_{L\dot{\alpha}}$ varied, so changing $C_{L\dot{\alpha}}$ also implies a change in the aerodynamic center location.

The influence of speed derivatives is shown in Figure 44. Large errors in C_{x_u} and C_{L_u} will cause no problem. However, C_{m_u} should be accurately known, because large negative values of C_{m_u} cause the airplane to be statically unstable even though the c.g. is ahead of the aerodynamic center. C_{m_u} has only a small effect on the short period mode.

Powered lift airplanes are likely to have large values of C_{m_u} . In the trim condition a large aerodynamic pitching moment is required to balance the thrust moment. If a speed change occurs these two moments change at different rates causing a moment unbalance. There is another component, to C_{m_u} , due to thrust interference but this is generally small for a vectored thrust airplane.

Effects of aerodynamic lag or the $\dot{\alpha}$ derivatives, on longitudinal dynamics are shown in Figure 45. $C_{L\dot{\alpha}}$ has no noticeable effect. The real roots are not influenced by $C_{m\dot{\alpha}}$ but the damping ratio of the short period mode appears to be sensitive to this term. As $C_{m\dot{\alpha}}$ is increased the damping ratio increases and at two times the initial value the short period mode is critically damped. It would be desirable to know $C_{m\dot{\alpha}}$ within 40% in order to know the damping ratio within about 10%.

Sensitivity to the pitch rate derivatives is shown in Figure 46. Varying $C_{L\dot{q}}$ had no noticeable effect. A $\pm 200\%$ error would be negligible. However, dynamic characteristics are sensitive to $C_{m\dot{q}}$. As $C_{m\dot{q}}$ is increased from the initial value, the short period damping ratio is increased without much effect on undamped natural frequency. If $C_{m\dot{q}}$ is reduced, undamped natural frequency and damping ratio both are reduced. The real roots are only slightly affected, but if $C_{m\dot{q}}$ were increased still further than shown in Figure 46 a long period oscillatory mode would develop.

3.1.2 Lateral-Directional

The influence of sideslip, yaw rate, and roll rate derivatives on lateral-directional dynamics is shown in Figures 47 through 52. Derivatives that must be predicted with relative accuracy are: $C_{n\beta}$, $C_{l\beta}$, C_{n_p} , C_{l_p} , C_{n_r} , and C_{l_r} .

Sensitivity to variations in sideslip derivatives are shown in Figures 47 and 48. $C_{y\beta}$ has only a small influence on the Dutch roll mode and practically no effect on the spiral mode. Large errors in $C_{y\beta}$ would not seriously affect the Dutch roll characteristics. However, $C_{l\beta}$ and $C_{n\beta}$ strongly influence

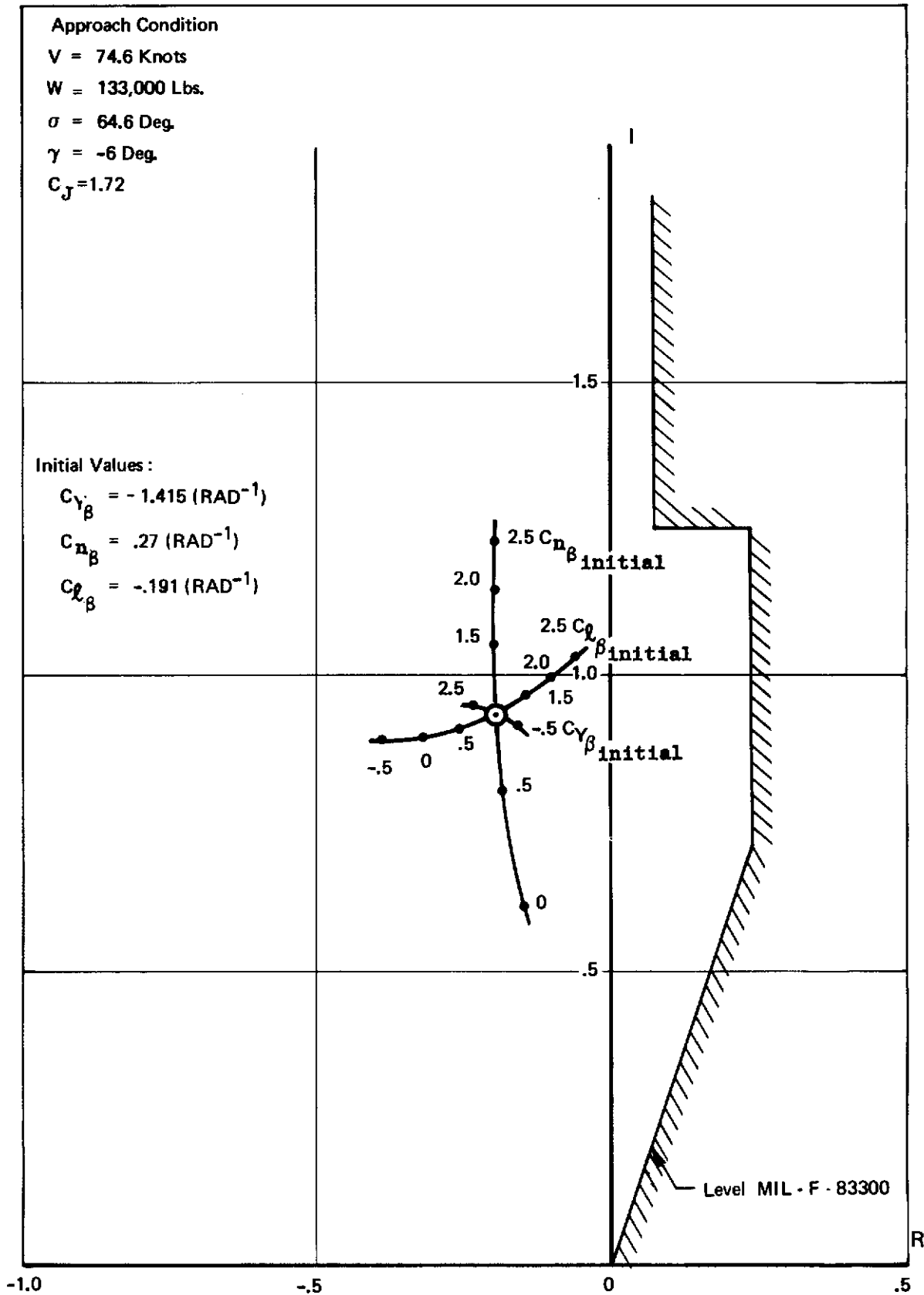


Figure 47 : Effect of Sideslip Derivatives on Dutch Roll Characteristics

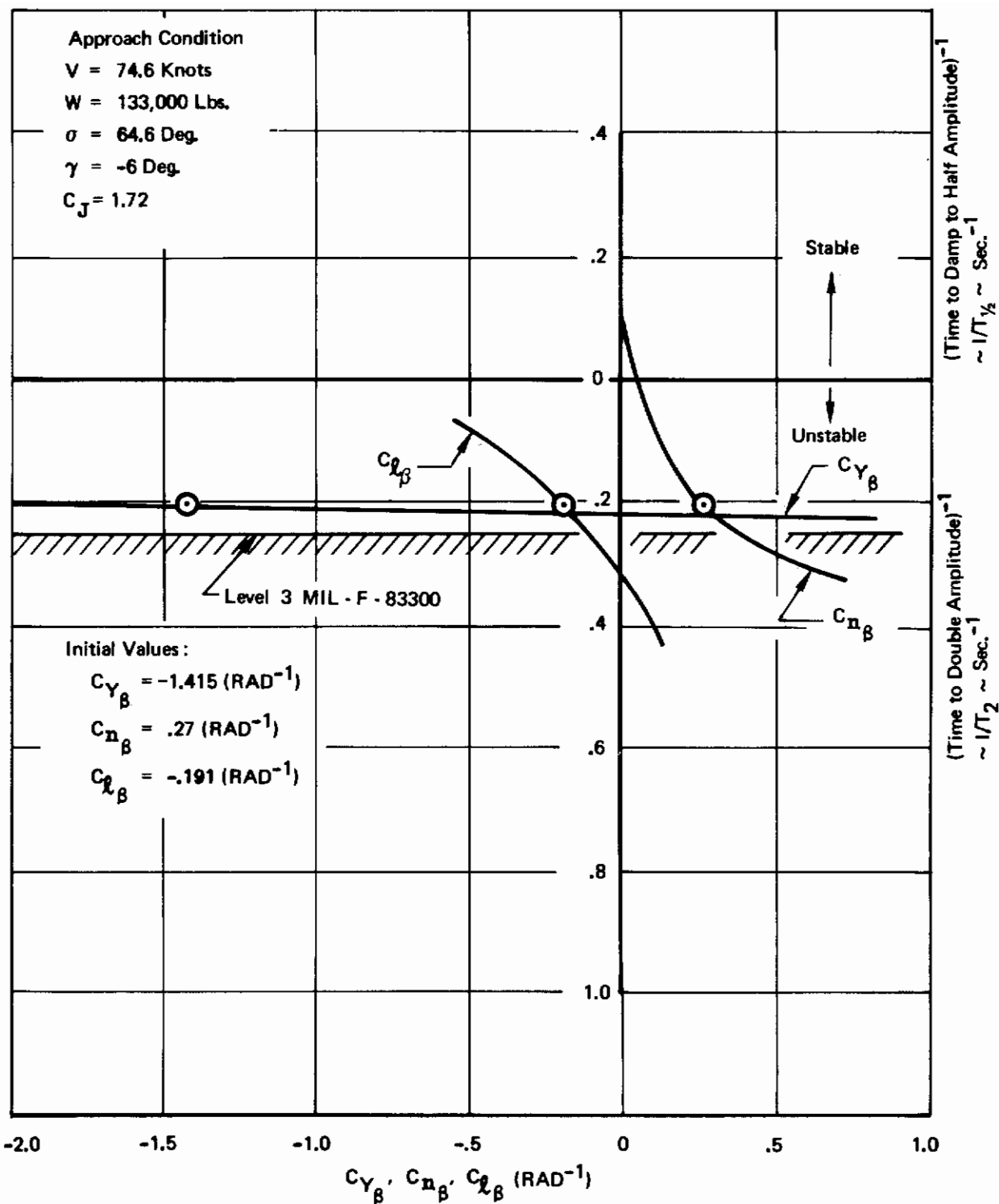


Figure 4B : Effect of Sideslip Derivatives on Spiral Mode Stability

Contrails

both the Dutch roll and spiral modes. It is desirable to know both of these derivatives within an increment of $\pm 0.03 \text{ rad}^{-1}$, about 10 to 15 percent. It is interesting to note that variations in $C_{n\beta}$ affect mainly the Dutch roll frequency while $C_{l\beta}$ changes affect primarily the Dutch roll damping ratio. When $C_{n\beta}$ is reduced to zero, the Dutch roll mode is still stable and the spiral mode becomes stable. If $C_{l\beta}$ is reduced to zero the Dutch roll mode remains stable but the spiral mode gets more unstable.

Accuracy of calculations relating to cross wind landings and engine-out conditions is directly related to the quality of the sideslip derivatives. This should be taken into account when deciding on the required accuracy of the derivatives.

Figures 49 and 50 show the effect of roll rate derivatives. $C_{y\dot{p}}$ has no effect on any of the roots of the characteristic equation and for this purpose can be ignored. $C_{n\dot{p}}$ and $C_{l\dot{p}}$ effect both the spiral and Dutch roll modes and should be known within an increment of $\pm 0.1 \text{ rad}^{-1}$, or about 20%. The cross derivative, $C_{n\dot{p}}$, affects mainly Dutch roll frequency and the roll damping derivative, $C_{l\dot{p}}$, affects mainly the Dutch roll damping ratio. When $C_{l\dot{p}}$ went to zero, the Dutch roll damping did too, even though $C_{n\dot{p}}$ and $C_{l\dot{\beta}}$ both have stable values.

The effects of yaw rate derivatives are shown in Figures 51 and 52. Again the side force derivative has no effect. The cross derivative, $C_{l\dot{r}}$, affects both Dutch roll damping ratio and frequency. The yaw damping derivative affects mainly Dutch roll damping. $C_{n\dot{r}}$ and $C_{l\dot{r}}$ both affect the spiral mode with $C_{l\dot{r}}$ having the greater influence. Reducing $C_{l\dot{r}}$ would stabilize the spiral mode while reducing the Dutch roll damping ratio. $C_{n\dot{r}}$ and $C_{l\dot{r}}$ should be determined within an increment of $\pm 0.1 \text{ rad}^{-1}$.

3.2 Stability and Control

This section presents a simple empirical method of predicting aerodynamic interference effects due to vectored thrust on stability and control derivatives. The method consists of applying a thrust correction factor to the tail-off derivative and taking into account the power effect on the downwash, sidewash, and dynamic pressure at the tail. It is assumed that the power-off characteristics are known, either estimated or from wind tunnel data. Correction factors are all based on wind tunnel data. The wind tunnel data are presented in Reference 5.

All derivatives and coefficients in this section are net values, that is; direct thrust forces are not included.

It is appropriate to state here some general observations and opinions regarding the wind tunnel yaw data.

- o Spanwise engine location has a negligible effect on lift curve slope.

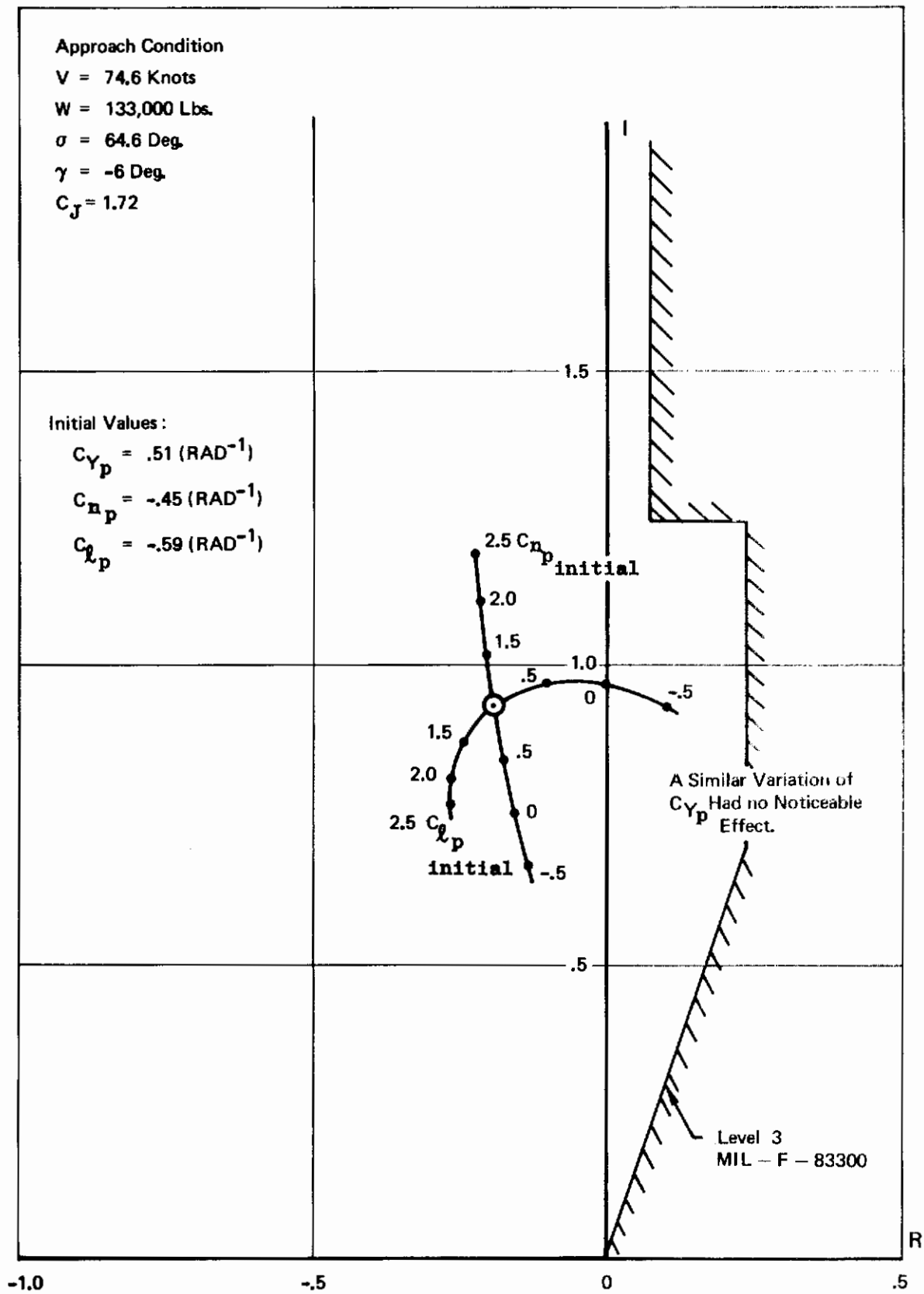


Figure 49 : Effect of Roll Rate Derivatives on Dutch Roll Characteristics

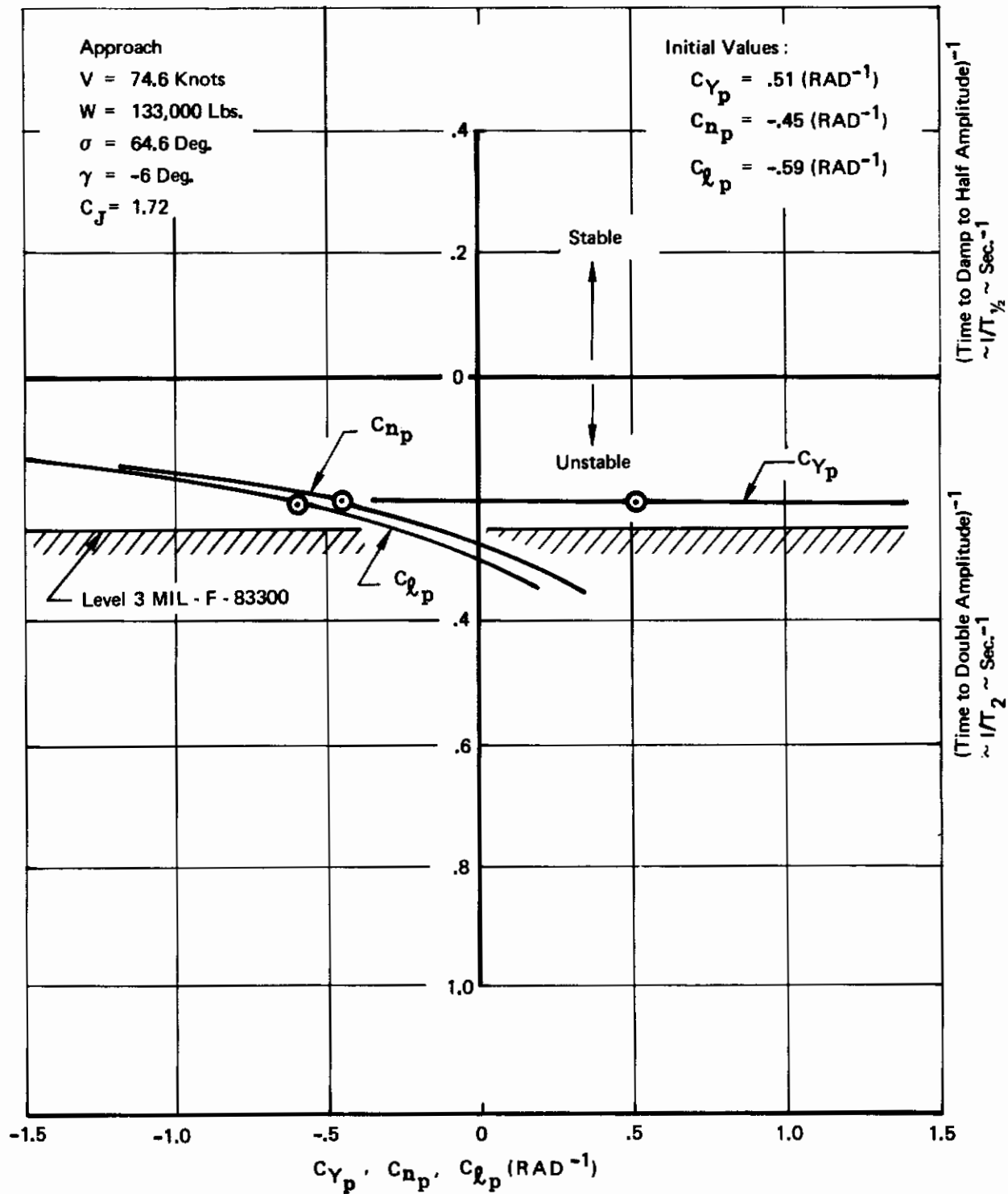


Figure 50 : Effect of Roll Rate Derivatives on Spiral Mode Stability

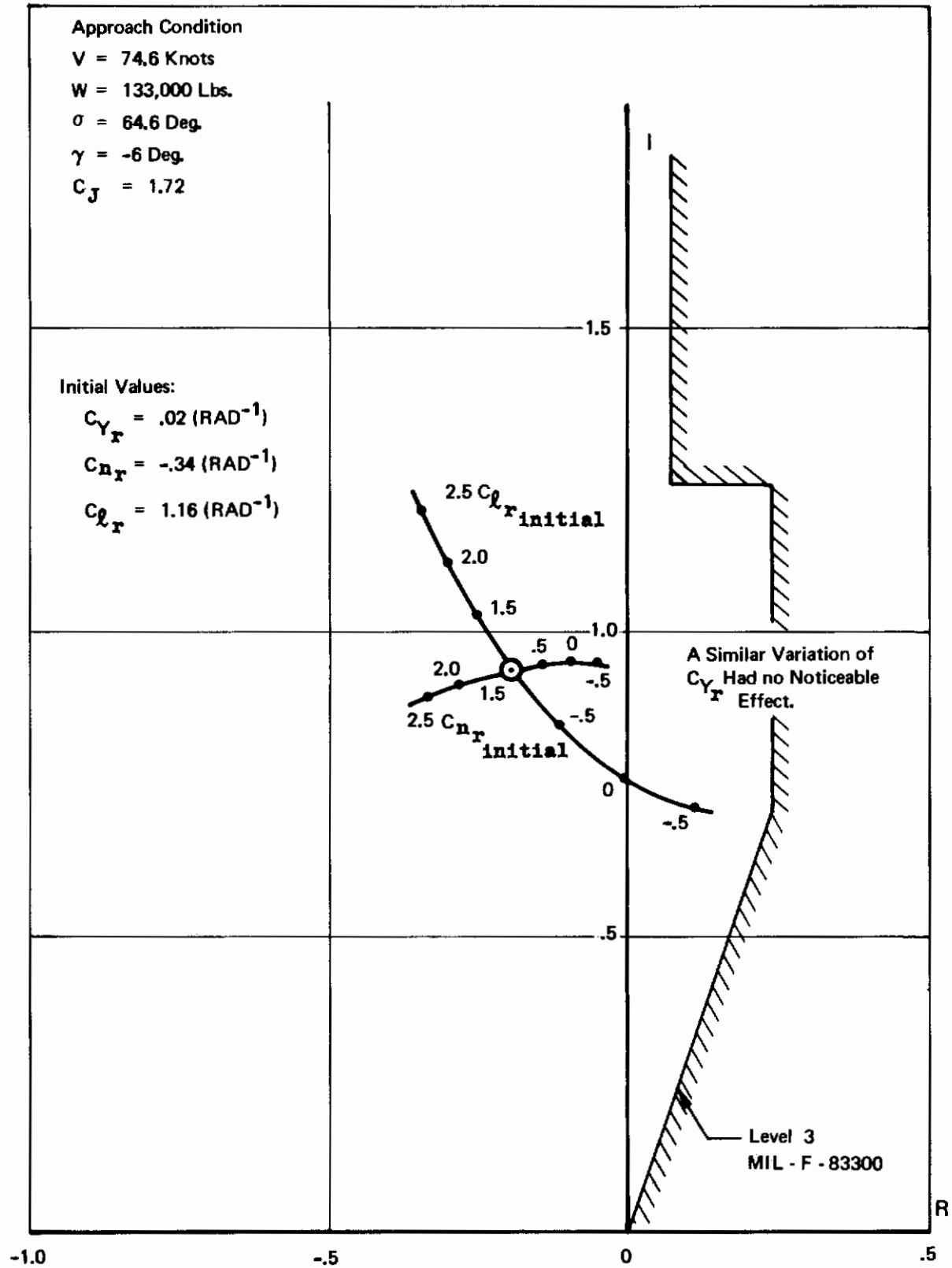


Figure 51 : Effect of Yaw Rate Derivatives on Dutch Roll Characteristics

Contrails

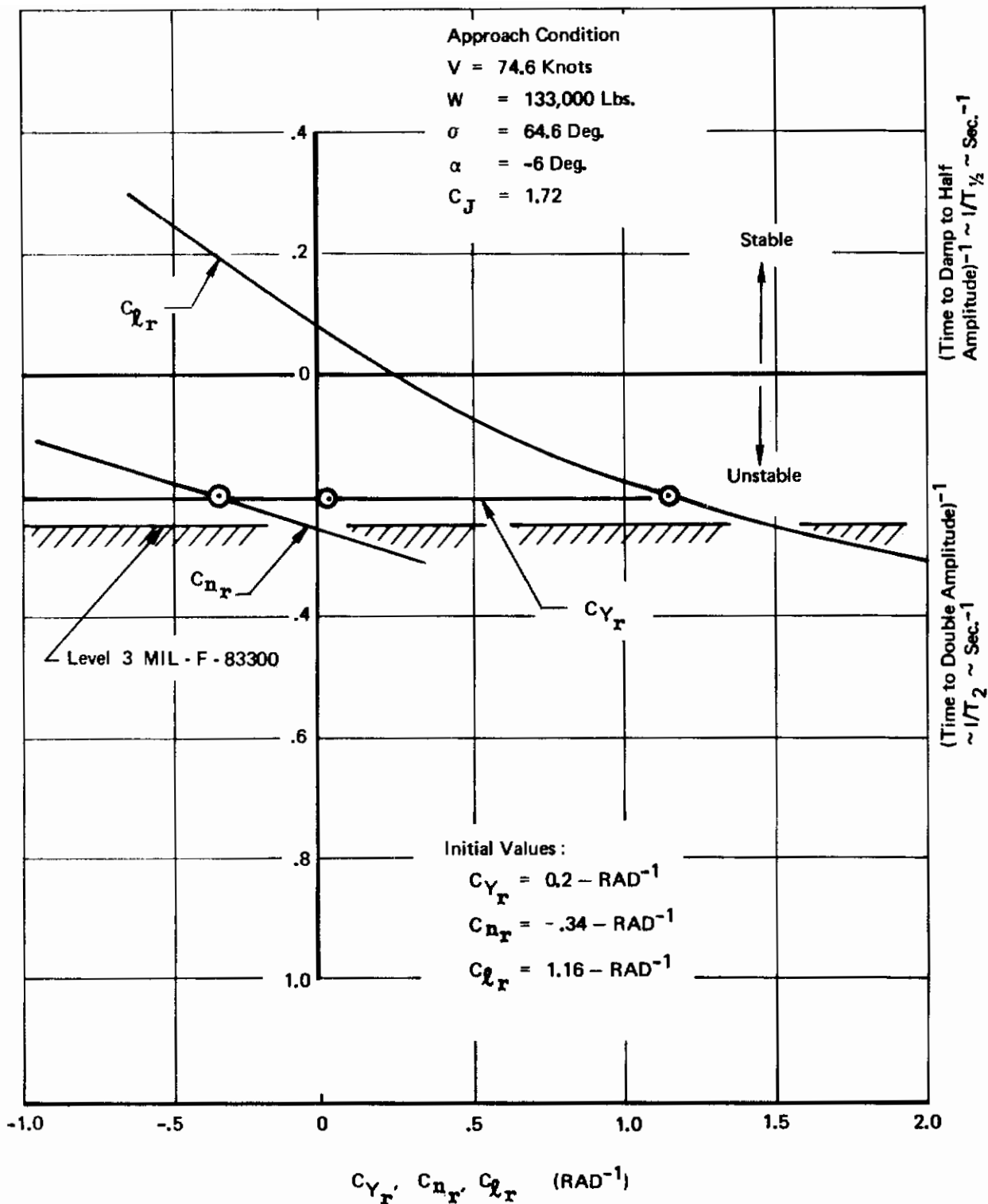


Figure 52 : Effect of Yaw Rate Derivatives on Spiral Mode Stability

Contrails

- o Engine-out has little effect on sideslip derivatives.
- o Thrust has small effect on sideslip derivatives except at high thrust deflection or when the nacelles are double podded inboard.
- o Angle of attack effects on sideslip derivatives are small, although a little greater at the higher wing sweep and in-ground effect.
- o Chordwise nozzle position has a negligible effect on sideslip derivatives.
- o Ground effects, on sideslip derivatives, are small except at high thrust settings with 90 degree thrust vector angle. There is apparently a flow breakdown at this condition.
- o Thrust has negligible effect with flaps up.

Thrust effects may be magnified by having poor flow on the model at zero thrust. With the leading edge flap deflected 70 degrees, flow is stalled on the bottom of the wing, so the trailing edge flaps are "seeing" stalled air. Tuft studies, in the wind tunnel, show that the trailing edge flaps are in turbulent flow up to about 12 degrees angle of attack. Also, the lift curve slope is very high at low angle of attack, indicating something (probably the wing undersurface) is becoming unstalled as angle of attack increases. All of the yaw runs were done at angles of attack less than or equal to 12 degrees. Therefore, the flaps never had "clean" air in any yaw run. The engines are located in this stalled air. They are an energy source that probably tends to straighten the stalled flow. This might mean that the power effects, presented here, are merely increments tending to swing the data back to where the power-off data would have been if the bottom of the wing had not been stalled.

3.2.1 Longitudinal Stability and Control

This section presents a method for estimating the aerodynamic interference effect of engine thrust on longitudinal stability and control derivatives. This method has an empirical basis and has been derived from the vectored thrust blowing test (BVWT 099, Reference 5). Methods for predicting lift and pitching moment are also presented in Section 2. However, the methods presented here, although less precise, are more appropriate for preliminary design purposes because they are faster.

3.2.1.1 Static Stability Derivatives

The test pitching moment and lift curves are quite nonlinear with respect to angle of attack. To obtain the results reported here, slopes were measured at 8° angle of attack, which is representative of takeoff and landing conditions. The method has been compared to test data at $\alpha=4^\circ$ and 8° and agreement is quite good at both angles of attack.

Contrails

Figures 53 through 55 show the effect of nozzle location, vector angle, and C_J on tail-off lift curve slope and aerodynamic center. These are corrections which should be applied to power off $C_{L\alpha}$ and ac by equations 3.1 and 3.2.

$$C_{L\alpha} = C_{L\alpha_{C_J=0}} + \left(\frac{\Delta C_{L\alpha}}{C_J} \right) C_J \quad (3.1)$$

$$ac = ac_{C_J=0} + \left[\left(\frac{\Delta ac}{C_J} \right)_a + \left(\frac{\Delta ac}{C_J} \right)_b \right] C_J \quad (3.2)$$

where:

$\Delta C_{L\alpha}$ - per degree

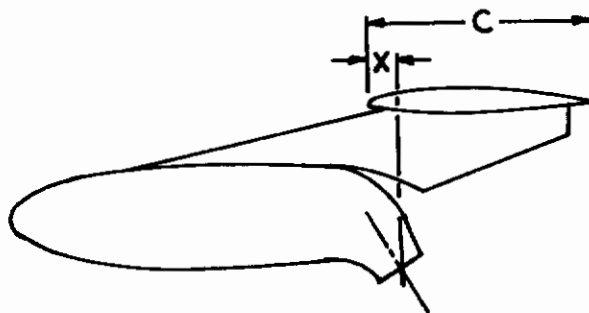
a.c. - aerodynamic center shift in fraction of MAC,
positive aft

Subscripts:

a - means at constant spanwise nacelle location

b - means at varying spanwise nacelle location

The nozzle chordwise location is the position of the center of the nozzle exit plane in percent of the wing local chord, as shown in the sketch below.



For ease of application data are shown for wing sweeps of 0° , 15° , and 30° . Power effects were measured in the wind tunnel at 15° and 30° only. the 0° sweep is an extrapolation of these data.

Figures 53 and 54 are for the engines at 27% and 43.5% semispan locations. To account for the effect of different spanwise positions Figure 55 has been developed. Figure 55 shows the effect of mean spanwise nacelle position (average between inboard and outboard) on a.c. The lift curve slope is not affected; however, inward movement of the nacelles has a stabilizing effect on a.c. shift due to interference.

The increments obtained from these figures are compared to the wind tunnel test results at $\alpha = 4^\circ$ and 8° and for several nacelle positions, both with single and double pods, in Table III and Figures 56 and 57.

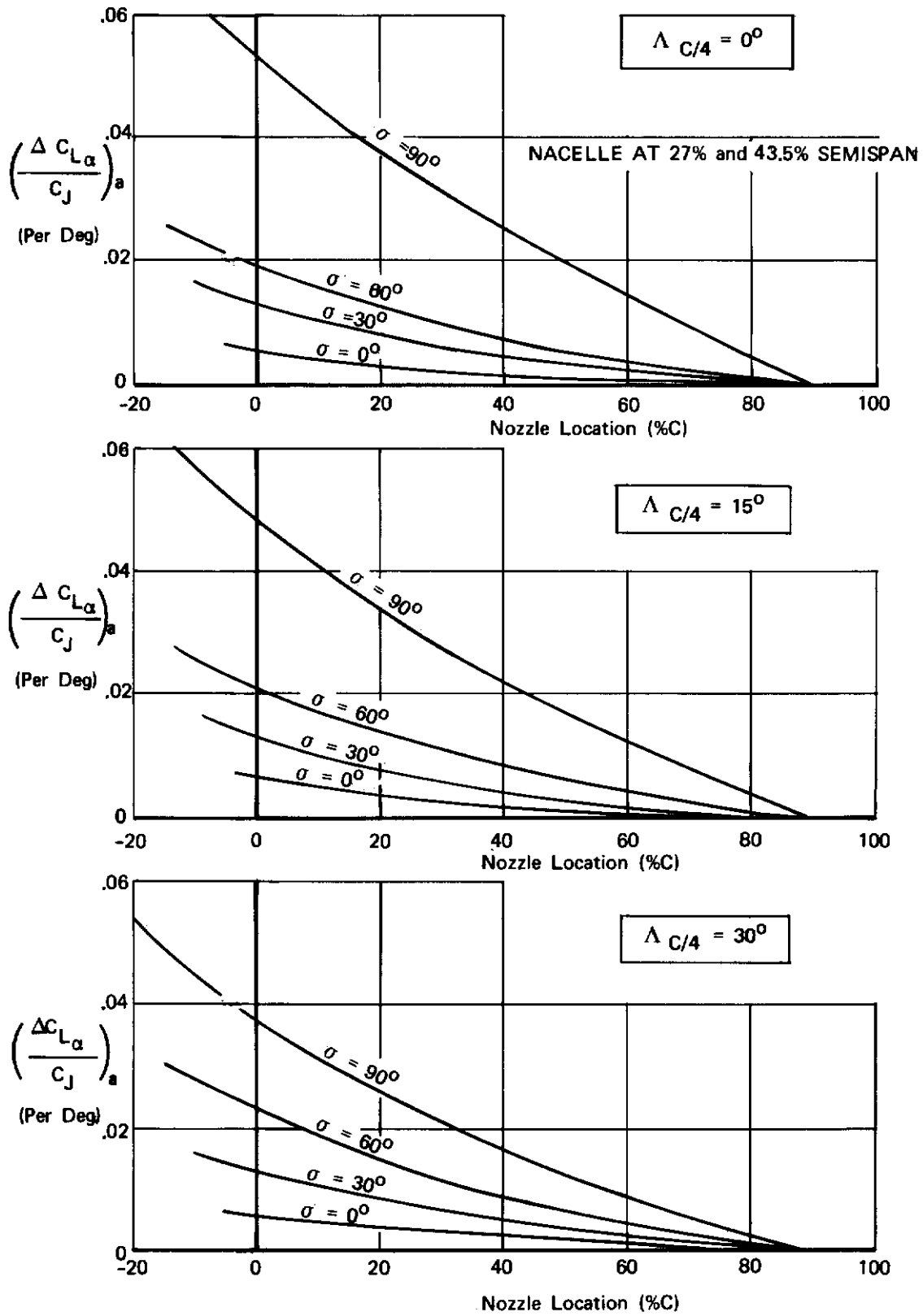


Figure 53 Effect of Vectored Thrust on Lift Curve Slope

NACELLES AT 27% and 43.5% SEMISPAN

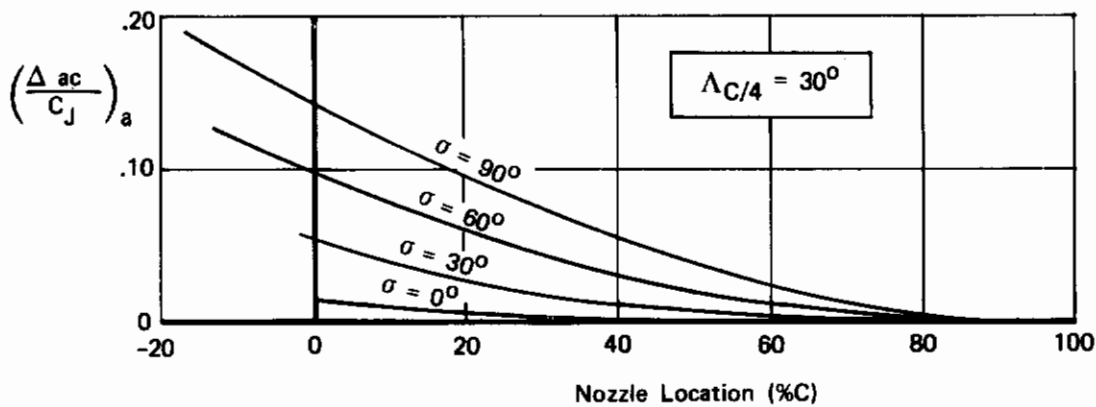
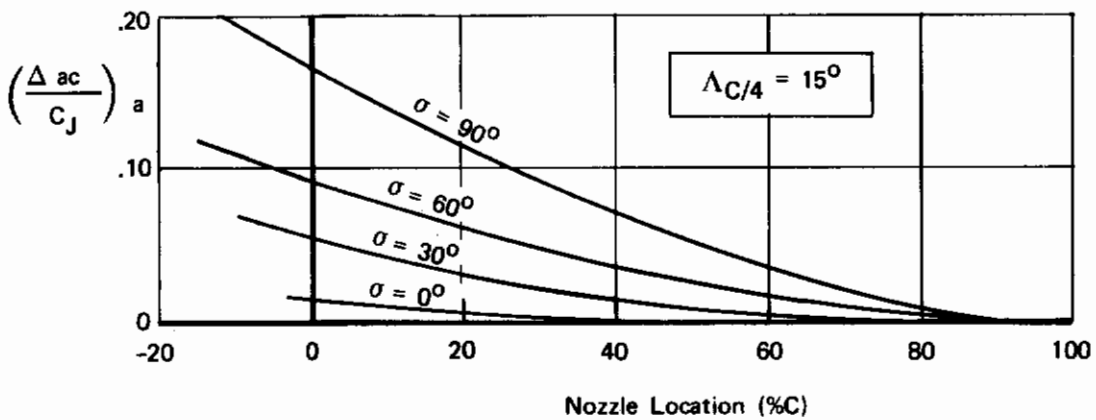
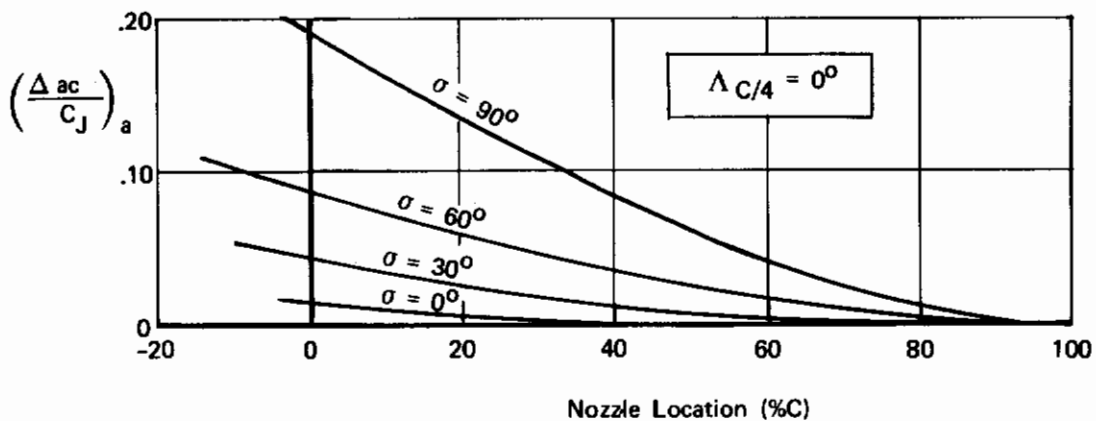


Figure 5A Effect of Vectored Thrust on Aerodynamic Center

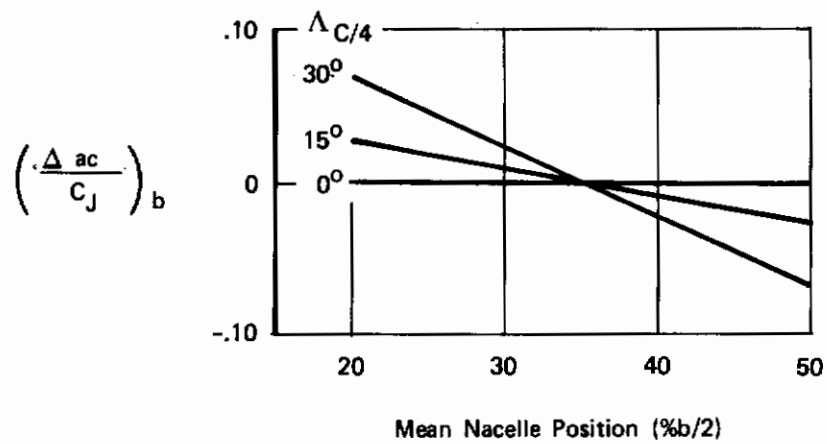


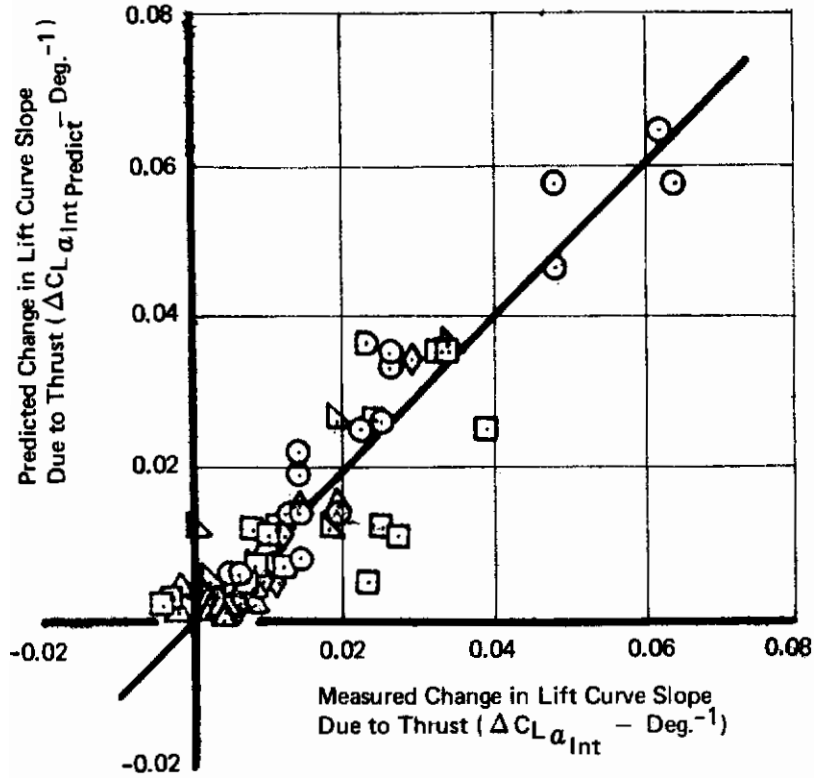
Figure 56 Effect of Nacelle Spanwise Location on Aerodynamic Center

TABLE III
TEST - PREDICTION COMPARISON, ANGLE OF ATTACK DERIVATIVES

Nacelle Location	Angle of Attack	Wing Sweep	Flap / Nozzle	$\frac{\Delta C_{L\alpha}}{C_J}$			$\frac{\Delta a_c}{C_J}$		
				Predicted	Measured	Error	Predicted	Measured	Error
P1 P4 - Engines at 27 and 43.5% semispan. Nozzles at 0% chord (nominal).	8°	15°	0° / 0°	.006	.006	0	.012	.010	.002
			20° / 30°	.014	.012	.002	.056	.023	.033
			35° / 30°	.014	.019	-.005	.056	.071	-.015
			35° / 60°	.025	.022	.002	.103	.097	.006
			35° / 90°	.064	.062	.002	.213	.217	-.004
	4°	30°	0° / 0°	.006	.005	.001	.012	.012	0
			20° / 30°	.014	.008	.006	.058	.038	.020
			35° / 30°	.014	.014	0	.058	.088	-.030
			35° / 60°	.026	.035	-.009	.112	.138	-.026
			35° / 90°	.048	.046	.002	.180	.170	.010
	8°	15°	0° / 0°	.014	.019	-.005	.056	.062	-.007
			20° / 30°	.025	.026	-.001	.103	.132	-.029
			35° / 30°	.064	.057	.007	.213	.123	.090
			35° / 60°	.014	.022	-.008	.058	.058	0
			35° / 90°	.026	.033	-.007	.112	.135	-.013
P2 P5 - Engines at 27 and 43.5% semispan. Nozzles at 35% chord (nominal).	8°	15°	0° / 0°	.002	-.004	.006	.002	-.005	.007
			20° / 30°	.005	.007	-.002	.017	.013	.004
			35° / 30°	.005	.006	-.001	.017	.005	.012
			35° / 60°	.011	.010	.001	.052	.045	.007
			35° / 90°	.035	.034	.001	.012	.011	.001
	4°	30°	0° / 0°	.003	-.003	.006	.002	.005	-.003
			20° / 30°	.007	.008	-.001	.015	.011	.004
			35° / 30°	.007	.008	-.001	.015	.013	.002
			35° / 60°	.012	.008	.004	.048	.028	.020
			35° / 90°	.025	.024	.001	.092	.086	.006
	8°	15°	0° / 0°	.012	.008	.004	.048	.027	.021
			20° / 30°	.005	.023	-.018	.017	.049	-.032
			35° / 30°	.011	.027	-.016	.052	.081	-.029
			35° / 60°	.035	.033	.002	.120	.070	.050
			35° / 90°	.007	.012	-.005	.015	.021	-.006
4°	30°	0° / 0°	.012	.025	-.013	.048	.050	-.002	
		20° / 30°	.025	.039	-.014	.092	.100	-.008	

TABLE III (Continued)
TEST - PREDICTION COMPARISON, ANGLE OF ATTACK DERIVATIVES

Nacelle Location	Angle of Attack	Wing Sweep	Flap / Nozzle	$\frac{\Delta C_L \alpha}{C_J}$			$\frac{\Delta c}{C_J}$						
				Predicted	Measured	Error	Predicted	Measured	Error				
P3 P6 - Engines at 27 and 43.5% semispan. Nozzles at 70% chord (nominal)	8°	15°	0° / 0°	0	.004	-.004	0	.028	-.028				
				.001	.003	-.002	.001	.001	0				
				.001	.004	-.003	.001	.034	-.033				
				.004	.008	-.004	.015	.022	-.007				
				.015	.019	-.004	.047	.042	.005				
				.001	.002	-.001	0	.022	-.022				
				.002	.006	-.004	.001	.001	0				
				.002	.002	0	.001	.004	-.003				
				.004	.005	-.001	.008	.015	-.007				
				.010	.010	0	.029	.025	.004				
				.004	.005	-.001	.008	-.010	.018				
				.001	-.002	.003	.001	-.002	.003				
P5 P8 - Engines at 43.5 and 60% semispan. Nozzles at 35% chord (nominal)	4°	15°	35° / 60°	.004	.006	-.002	.015	.009	.006				
				.004	.014	.001	.047	.007	.054				
				.015	.008	-.006	.001	.009	-.008				
				.002	.008	-.006	.008	.026	-.018				
				.004	.007	-.003	.008	.026	-.018				
				.010	.010	0	.029	.042	-.013				
				P12 - Double Podded Engines at 27% semispan. Nozzles at 35% chord (nominal)	8°	15°	0° / 0°	.002	.003	-.001	-.025	.022	-.047
								.005	.002	.003	-.010	.005	-.015
								.005	.010	-.005	-.010	.010	-.020
								.012	.018	-.006	.025	.014	.011
								.036	.034	.002	.098	.094	.004
								.007	.008	-.001	.058	.040	.018
.012	0	.012	-.025					-.015	-.010				
.026	.019	.007	.021					.055	-.034				
P13 - Double Podded Engines at 43.5% semispan. Nozzles at 35% chord (nominal)	8°	15°	0° / 0°					.002	.006	-.004	.017	.010	.007
								.005	.009	-.004	.034	.053	-.019
								.005	.011	-.006	.034	.085	-.051
								.011	.012	-.001	.069	.062	.007
				.034	.029	.005	.132	.124	.008				
				.055	.010	-.005	.003	.007	-.004				
				.012	.011	.001	.040	.037	.003				
				.036	.023	.013	.108	.076	.032				



- P₁ P₄ — Engines at 27 and 43.5% Semispan
Nozzles at 0% Chord
- P₂ P₅ — Engines at 27 and 43.5% Semispan
Nozzles at 35% Chord
- △ P₃ P₆ — Engines at 27 and 43.5% Semispan
Nozzles at 70% Chord.
- ◻ P₅ P₈ — Engines at 43.5 and 60% Semispan
Nozzles at 35% Chord
- ◇ P₁₂ — Double Podded Engines at 27%
Semispan. Nozzles at 35% Chord.
- ◻ P₁₃ — Double Podded Engines at 43.5%
Semispan. Nozzles at 35% Chord

Figure 56 : Lift Curve Slope Error

- P₁ P₄ — Engines at 27 and 43.5% Semispan
Nozzles at 0% Chord
- P₂ P₅ — Engines at 27 and 43.5% Semispan
Nozzles at 35% Chord
- △ P₃ P₆ — Engines at 27 and 43.5% Semispan
Nozzles at 70% Chord
- ▷ P₅ P₈ — Engines at 43.5 and 60% Semispan
Nozzles at 35% Chord
- ◇ P₁₂ — Double Podded Engines at 27%
Semispan Nozzles at 35% Chord
- ▷ P₁₃ — Double Podded Engines at 43.5%
Semispan Nozzles at 35% Chord

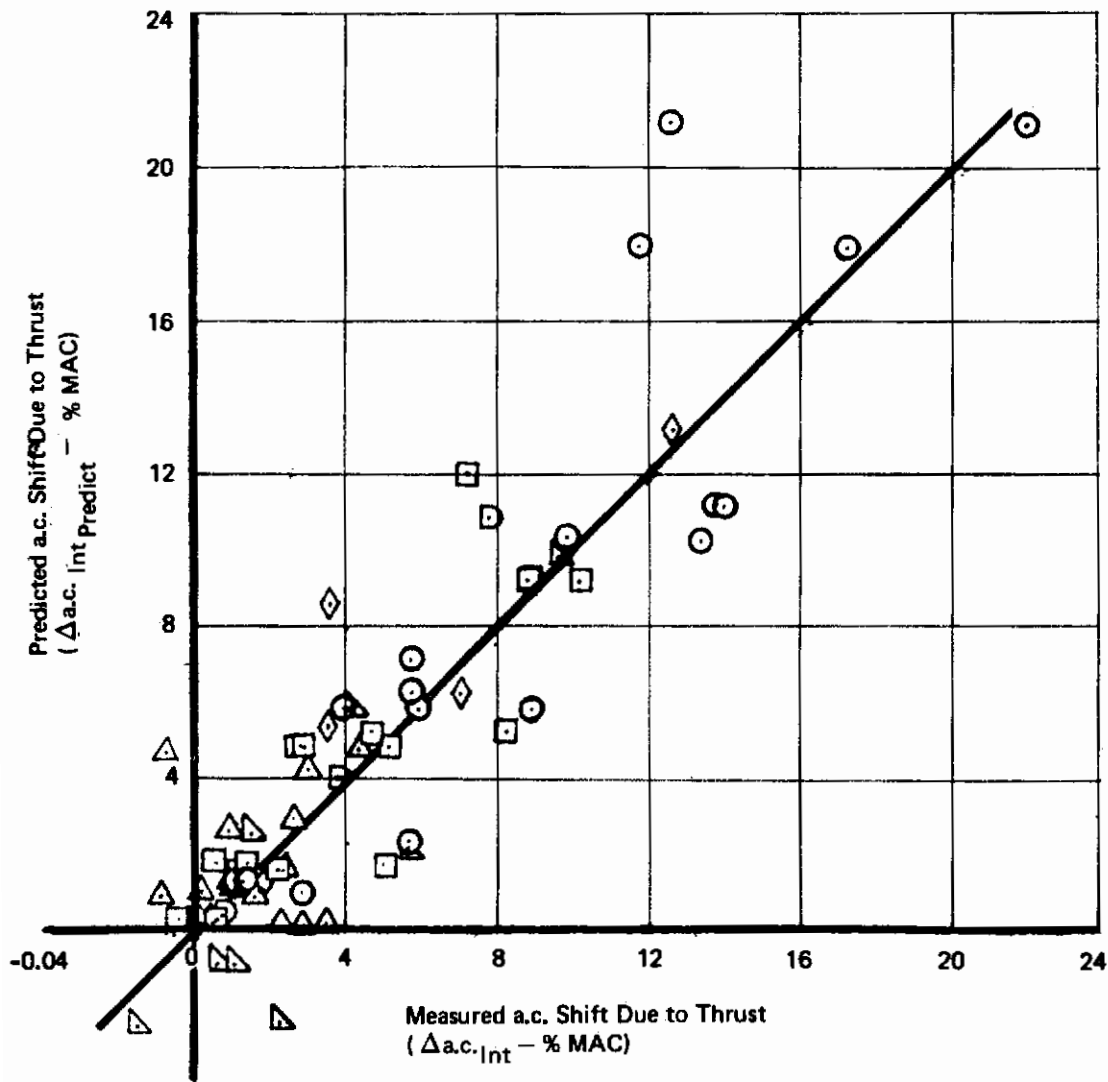


Figure 57 : Aerodynamic Center Error

Contrails

The interference drag term $\Delta C_{D\alpha}$ has also been derived from BVWT 099 (Reference 5) test data. Interference drag is a function of lift interference, vector angle, and nacelle chordwise location and is presented in Figures 32 through 34. From these figures an average

slope of $\frac{\partial C_{D\text{INT}}}{\partial C_{L\text{INT}}}$ is obtained. This term, when multiplied by $\Delta C_{L\alpha\text{INT}}$ from Figure 53 gives the $\Delta C_{D\alpha\text{INT}}$ term: $\Delta C_{D\alpha\text{INT}} = .3\Delta C_{L\alpha\text{INT}}$

The vectored thrust effect on horizontal tail input to lift curve slope and aerodynamic center is caused by a change in dynamic pressure and downwash at the tail. Power-off tail effectiveness should be corrected for thrust effects by Equations 3.3 and 3.4

$$\Delta C_{L\alpha_H} = \left(\Delta C_{L\alpha_H} \right)_{C_J=0} \left(\frac{q}{q_{C_J=0}} \right) \frac{\left(1 - \frac{\partial \epsilon}{\partial \alpha} \right)}{\left(1 - \frac{\partial \epsilon}{\partial \alpha} \right)_{C_J=0}} \quad (3.3)$$

$$\Delta a_{c_H} = \left(\Delta a_{c_H} \right)_{C_J=0} \left(\frac{q}{q_{C_J=0}} \right) \frac{\left(1 - \frac{\partial \epsilon}{\partial \alpha} \right)}{\left(1 - \frac{\partial \epsilon}{\partial \alpha} \right)_{C_J=0}} \quad (3.4)$$

$\frac{\left(1 - \frac{\partial \epsilon}{\partial \alpha} \right)_{C_J}}{\left(1 - \frac{\partial \epsilon}{\partial \alpha} \right)_{C_J=0}}$ is given in Figure 58. Downwash is based on tail-

on, tail-off, and tail control power test data from BVWT 099 (Reference 5). The downwash shown is the averaged value based on wing sweeps of 15° and 30° and on vector angles of 30°, 60° and 90°. This shows good agreement with downwash from wake rake data obtained in BVWT 101 (Reference 5).

An attempt to measure power effects on dynamic pressure at the tail proved unsatisfactory because of wind tunnel instrumentation problems. Figure 59 is presented instead, as a representative example of the effect of vectored thrust. This data was extracted from horizontal tail effectiveness tests at 60° vector angle.

Vectored thrust has an effect on the horizontal tail drag. However, this is only a small increment and for preliminary design purposes may be neglected.

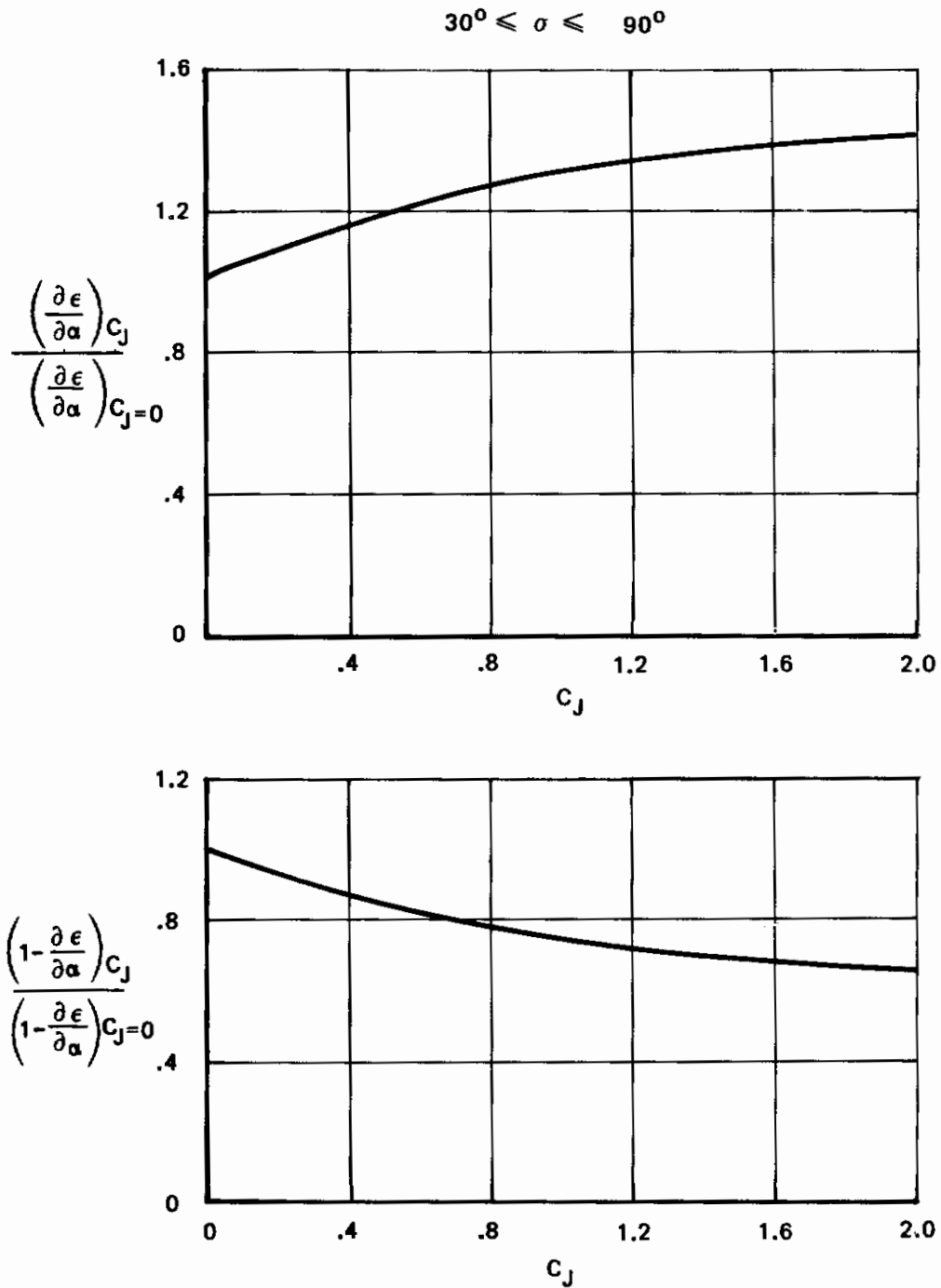


Figure 58 : Effect Of Vectored Thrust On Downwash

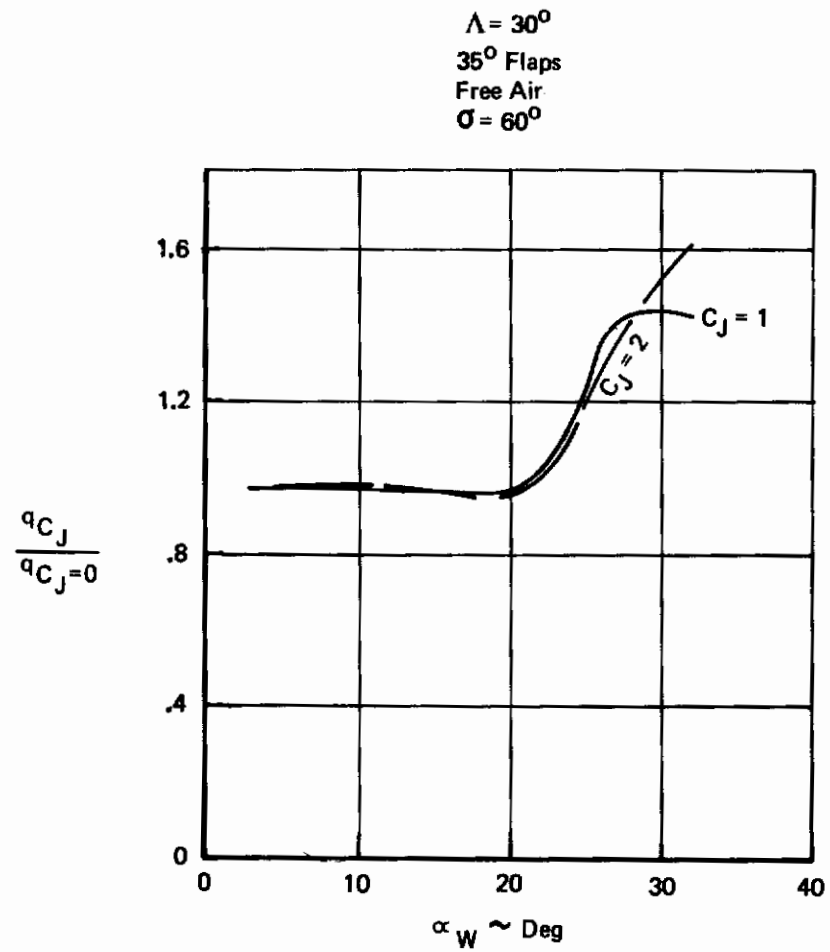


Figure 59 : Effect Of Vectored Thrust On Horizontal Tail Dynamic Pressure

3.2.1.2 Derivatives with Respect to Forward Speed

The speed derivatives C_{Z_u} , C_{X_u} , and C_{m_u} are a function of both direct thrust and thrust interference. The force and moment equations are:

$$C_Z = -C_{L_{C_J=0}} - \Delta C_{L_{INTERFERENCE}} - C_J \sin(\alpha + \sigma) \quad (3.5)$$

$$C_X = -C_{D_{C_J=0}} - \Delta C_{D_{INTERFERENCE}} + C_J \cos(\alpha + \sigma) \quad (3.6)$$

$$C_m = C_{m_{C_J=0}} + \Delta C_{m_{INTERFERENCE}} + C_J (Z_T \cos \sigma + X_T \sin \sigma) \quad (3.7)$$

Referenced to these equations the speed derivatives are:

$$C_{Z_u} = 2C_J \left[\frac{\partial(\Delta C_L)}{\partial C_J} \right]_{\alpha=\text{CONST}} \quad (3.8)$$

$$C_{X_u} = -2C_D + 2C_J \left[\frac{\partial(\Delta C_D)}{\partial C_J} \right]_{\alpha=\text{CONST}} \quad (3.9)$$

$$C_{m_u} = -2C_J (Z_T \cos \sigma + X_T \sin \sigma) - 2C_J \left[\frac{\partial(\Delta C_m)}{\partial C_J} \right]_{\alpha=\text{CONST}} \quad (3.10)$$

where $C_D = C_{D_{C_J=0}} + \Delta C_{D_{INTERFERENCE}}$

X_T = distance from c.g. to thrust vector in fraction of MAC,
positive fwd.

Z_T = distance from c.g. to thrust vector in fraction of MAC,
positive down.

Contrails

From the above equations, the thrust interference terms are

$$\Delta C_{z u_{\text{INTERFERENCE}}} = 2C_J \left[\frac{\partial(\Delta C_L)}{\partial C_J} \right]_{\alpha = \text{CONST}} \quad (3.11)$$

$$\Delta C_{x u_{\text{INTERFERENCE}}} = 2C_J \left[\frac{\partial(\Delta C_D)}{\partial C_J} \right]_{\alpha = \text{CONST}} \quad (3.12)$$

$$\Delta C_{m u_{\text{INTERFERENCE}}} = -2C_J \left[\frac{\partial(\Delta C_m)}{\partial C_J} \right]_{\alpha = \text{CONST}} \quad (3.13)$$

The terms $\left[\frac{\partial(\Delta C_L)}{\partial C_J} \right]$, $\left[\frac{\partial(\Delta C_D)}{\partial C_J} \right]$, and $\left[\frac{\partial(\Delta C_m)}{\partial C_J} \right]$

can be calculated from Equations 3.14 through 3.16.

$$\left[\frac{\partial(\Delta C_L)}{\partial C_J} \right]_{\alpha = \text{CONST}} = \frac{.35(C_{L_{\text{INT}}} + \Delta C_{L_{\text{INT}}})_{C_J=2}}{\sqrt{C_J}} \quad (3.14)$$

$$\left[\frac{\partial(\Delta C_D)}{\partial C_J} \right]_{\alpha = \text{CONST}} = \frac{.105(C_{L_{\text{INT}}} + \Delta C_{L_{\text{INT}}})_{C_J=2}}{\sqrt{C_J}} \quad (3.15)$$

$$\left[\frac{\partial(\Delta C_m)}{\partial C_J} \right]_{\alpha = \text{CONST}} = \frac{-.119(C_{L_{\text{INT}}} + \Delta C_{L_{\text{INT}}})_{C_J=2}}{\sqrt{C_J}} \quad (3.16)$$

where $[C_{L_{\text{INT}}} + \Delta C_{L_{\text{INT}}}]_{C_J=2}$ is obtained from Figures 29 and 30

Since this term varies with C_J by the equation:

$$\Delta C_L = [C_{L_{\text{INT}}} + \Delta C_{L_{\text{INT}}}] = [C_{L_{\text{INT}}} + \Delta C_{L_{\text{INT}}}]_{C_J=2} \sqrt{\frac{C_J}{2}} \quad (3.17)$$

Contrails

The term $\frac{\partial(\Delta C_L)}{\partial C_J}$ is obtained by differentiating with respect to C_J $\frac{\partial(\Delta C_D)}{\partial C_J}$

is obtained by multiplying $\frac{\partial C_D}{\partial C_L}$, based on Figures 30 through 32 by $\frac{\partial(\Delta C_L)}{\partial C_L}$. $\frac{\partial(\Delta C_m)}{\partial C_J}$ is obtained by multiplying $\frac{\partial C_m}{\partial C_L}$, based on Figures 33 through 35, by $\frac{\partial(\Delta C_L)}{\partial C_J}$

3.2.1.3 Pitch Rate and Angle of Attack Rate Derivatives

No testing was done to evaluate the effect of vectored thrust on the wing body contribution to the derivatives C_{m_q} , C_{Z_q} , $C_{m_{\dot{\alpha}}}$, and $C_{Z_{\dot{\alpha}}}$. However, this is expected to be small, and existing methods to predict the power off wing-body damping should provide sufficient accuracy. The horizontal tail contribution to pitch rate damping derivatives C_{m_q} and C_{Z_q} is influenced by engine thrust through the change in dynamic pressure at the tail. Power off C_{m_q} and C_{Z_q} should be obtained by existing methods and the tail contribution should be corrected for thrust effects by Equations 3.18 and 3.19.

$$C_{m_{q_H}} = (C_{m_{q_H}})_{C_J=0} \left(\frac{q}{q_{C_J=0}} \right) \quad (3.18)$$

$$C_{Z_{q_H}} = (C_{Z_{q_H}})_{C_J=0} \left(\frac{q}{q_{C_J=0}} \right) \quad (3.19)$$

The horizontal tail contribution to angle of attack rate damping derivatives $C_{m_{\dot{\alpha}}}$ and $C_{Z_{\dot{\alpha}}}$ is a function of both the dynamic pressure change and the downwash change due to vectored thrust. These derivatives should be predicted by existing methods, with the tail contribution corrected for thrust effects by:

$$C_{m_{\dot{\alpha}_H}} = (C_{m_{\dot{\alpha}_H}})_{C_J=0} \left(\frac{\frac{\partial \epsilon}{\partial \alpha}}{\frac{\partial \epsilon}{\partial \alpha}} \right) \left(\frac{q}{q_{C_J=0}} \right) \quad (3.20)$$

$$C_{Z_{\dot{\alpha}_H}} = (C_{Z_{\dot{\alpha}_H}})_{C_J=0} \left(\frac{\frac{\partial \epsilon}{\partial \alpha}}{\frac{\partial \epsilon}{\partial \alpha}} \right) \left(\frac{q}{q_{C_J=0}} \right) \quad (3.21)$$

3.2.1.4 Control Derivatives

The tail control derivatives $C_{m\delta_E}$, $C_{x\delta_E}$, and $C_{z\delta_E}$ are also a function of the dynamic pressure at the tail. Power off tail effectiveness should be predicted by existing methods such as DATCOM, and a power correction applied by Equations 3.22 through 3.24.

$$C_{m\delta_E} = (C_{m\delta_E})_{C_T=0} \left(\frac{q}{q_{C_T=0}} \right) \quad (3.22)$$

$$C_{x\delta_E} = (C_{x\delta_E})_{C_T=0} \left(\frac{q}{q_{C_T=0}} \right) \quad (3.23)$$

$$C_{z\delta_E} = (C_{z\delta_E})_{C_T=0} \left(\frac{q}{q_{C_T=0}} \right) \quad (3.24)$$

3.2.2 Lateral-Directional Stability Derivatives

This section presents a simple empirical method of predicting aerodynamic interference effects, due to vectored thrust, on lateral-directional stability derivatives. Correction factors are all based on wind tunnel data. The wind tunnel data are presented in Reference 5.

No large error would result in the tail-off sideslip derivatives if thrust effects were ignored. The data indicate that it is only in extreme conditions, like 90° thrust deflection in ground effect, that the thrust effects are large on the more important derivatives $C_{n\beta}$ and $C_{l\beta}$: This would probably only be a transient condition and for preliminary design purposes might be ignored.

3.2.2.1 Sideslip Derivatives

Thrust effect on sideslip derivatives can be accounted for by using the following five correction factors:

$$\left(\frac{C_{Y\beta}}{C_{Y\beta}_{C_T=0}} \right)_{T_0}, \left(\frac{C_{n\beta}}{C_{n\beta}_{C_T=0}} \right)_{T_0}, \left(\frac{C_{l\beta}}{C_{l\beta}_{C_T=0}} \right)_{T_0}, \frac{\partial \sigma}{\partial \beta} / \frac{\partial \sigma}{\partial \beta}_{C_T=0}, \frac{q_V}{q_{V_{C_T=0}}}$$

where

- β = sideslip angle
- C_Y = side force coefficient
- C_n = yawing moment coefficient

Contrails

- C_1 = rolling moment coefficient
 q = dynamic pressure
 σ = sidewash angle

subscripts

TO vertical tail, denotes tail-off

$C_J=0$ denotes thrust is zero

Values for these terms are presented in Figures 60 and 61. Side-slip derivatives are then computed using Equations 3.25 through 3.27.

$$C_{Y\beta} = \left(\frac{C_{Y\beta}}{C_{Y\beta, C_J=0, TO}} \right) C_{Y\beta, TO, C_J=0} - a_v \frac{S_v}{S} \left(1 - \frac{\frac{\partial \sigma}{\partial \beta}}{\frac{\partial \sigma}{\partial \beta}_{C_J=0}} \frac{\frac{\partial \sigma}{\partial \beta}}{\frac{\partial \sigma}{\partial \beta}_{C_J=0}} \right) \eta_v \frac{q_v}{q_{v, C_J=0}} \quad (3.25)$$

$$C_{n\beta} = C_{n\beta, TO, C_J=0} + a_v \frac{l_v S_v}{b S} \left(1 - \frac{\frac{\partial \sigma}{\partial \beta}}{\frac{\partial \sigma}{\partial \beta}_{C_J=0}} \frac{\frac{\partial \sigma}{\partial \beta}}{\frac{\partial \sigma}{\partial \beta}_{C_J=0}} \right) \eta_v \frac{q_v}{q_{v, C_J=0}} \quad (3.26)$$

$$C_{l\beta} = \left(\frac{C_{l\beta}}{C_{l\beta, C_J=0}} \right) C_{l\beta, C_J=0} + a_v \frac{z_v S_v}{b S} \left(1 - \frac{\frac{\partial \sigma}{\partial \beta}}{\frac{\partial \sigma}{\partial \beta}_{C_J=0}} \frac{\frac{\partial \sigma}{\partial \beta}}{\frac{\partial \sigma}{\partial \beta}_{C_J=0}} \right) \eta_v \frac{q_v}{q_{v, C_J=0}} \quad (3.27)$$

where

- S = wing area
 b = wing span
 a = vertical tail lift curve slope
 S_v = vertical tail area
 l_v = distance from c.g. aft to vertical tail a.c.
 z_v = distance from c.g. down to vertical tail a.c.
 η_v = ratio of dynamic pressure at the tail to free stream dynamic pressure at $C_J = 0$

Nacelles at 27%
and 43.5% Semi-Span

FLAPS DOWN

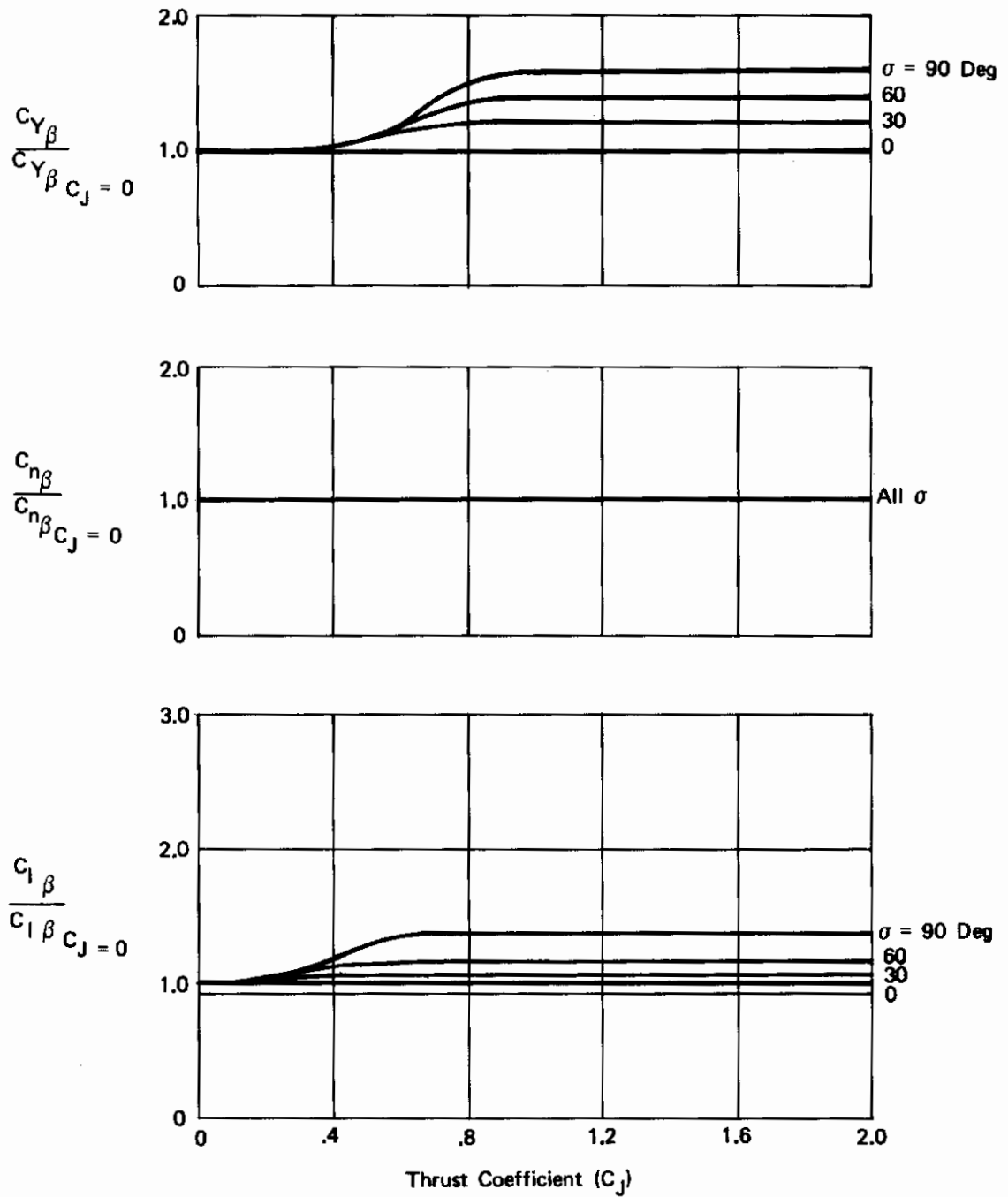


Figure 60 Vected Thrust Effect Factors for Sideslip Derivatives Tail Off

FLAPS DOWN

Nacelles at 27%
and 43.5% Semi-Span

In Ground Effect, $h/b = .21$

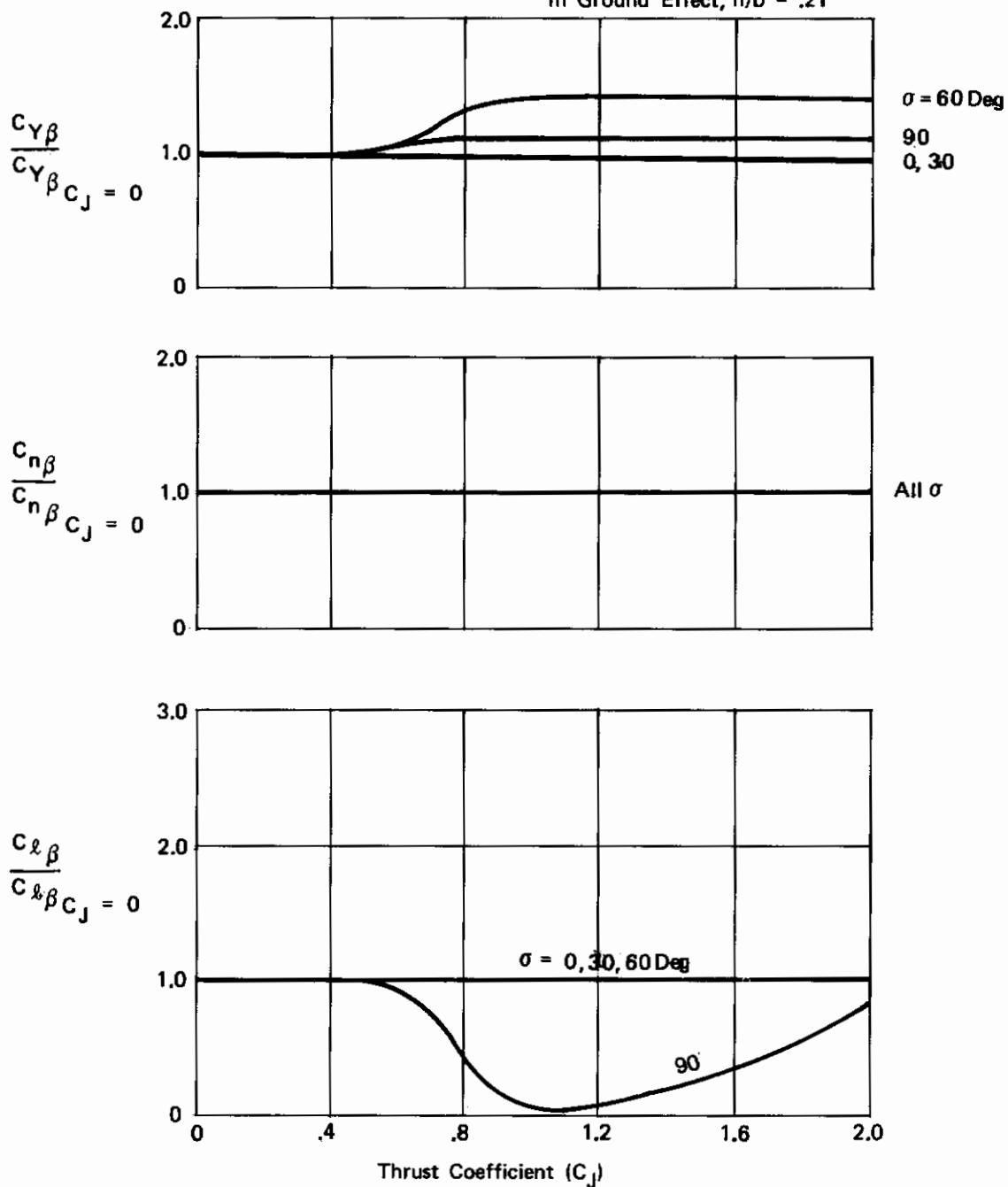


Figure 61 Vectored Thrust Factors for Sideslip Derivatives in Ground Effect, Tail Off

The biggest correction factor is for the sideforce derivative which is the least important of the three. See Section 3.1, Stability Derivative Sensitivity Study. The more important yawing moment derivative has no correction due to thrust. The other important derivative, rolling moment due to sideslip, has a correction factor of only 1.17 up to a thrust deflection of 60 degrees. It can be seen from the derivative sensitivity study, Section 3.1, that these corrections are not large.

Sidewash data are shown in Figure 62 . For this particular model, thrust had no influence so $\frac{\partial \sigma}{\partial \beta} / \frac{\partial \sigma}{\partial \beta}_{C_T=0} = 1$. However, it may be too much of a generalization to extrapolate this result to other configurations so the term is left in the equations. In the absence of additional data, assume no vectored thrust effect on sidewash.

An attempt to measure power affects on dynamic pressure at the vertical tail failed due to wind tunnel instrumentation problems. It is suggested that the values given in Figure 59 , for the horizontal tail, be used until more applicable data are available.

Table IV and Figure 63 show typical errors resulting from the application of the correction factors, presented in Figures 60 and 61 , to the power-off, tail-off data. While the percent error is sometimes large, the increment is usually small. These errors, when viewed in conjunction with the derivative sensitivity study presented in Section 3, are seen to be small.

3.2.2.2 Roll Rate and Yaw Rate Derivatives

No dynamic testing was done in the wind tunnel upon which to base any corrections. Although the sideslip data obtained during the wind tunnel test program is not directly applicable to the yaw or roll rate case, it does provide a little insight upon which to base an opinion that the effect is small.

The quality of the roll damping derivative, C_{l_p} , can be improved by multiplying it by the lift curve slope correction factor, as given in Equation 3.28.

$$C_{l_p} = \left[1 + \left(\frac{\Delta C_{L\alpha}}{C_T} \right) \frac{C_T}{C_{L\alpha}_{C_T=0}} \right] C_{l_p}_{C_T=0} \quad (3.28)$$

This correction is applicable because the roll damping is proportional to the local lift curve slope which should be proportional to the 3-dimensional lift curve slope. The tail contribution should be ignored when computing C_{l_p} unless data on sidewash due to roll rate are available.

The vertical tail contribution to the damping derivatives can be improved by applying the dynamic pressure ratio factor, Equations 3.29 through 3.33.

Contrails

Symbol	α (Deg)	C_T	σ (Deg)	h/b	Run	Engine-Out
○	8.0	.5/.5/0/.5	30	∞	138	Right Inboard
△	8.0	.5/.5/.5/0	30	∞	139	Right Outboard
□	8.0	2.0	30	∞	140	None
◇	8.0	2.0	30	.242	141	None
○	0	.5/.5/.5/0	30	.242	142	Right Outboard
△	8.0	.5/.5/.5/0	30	.242	142	Right Outboard
△	8.0	.5/.5/0/.5	30	.242	143	Right Inboard
▷	8.0	0	60	.242	144	—
▷	8.0	2.0	60	.242	145	None
◇	6.0	2.0	30	.242	147	None

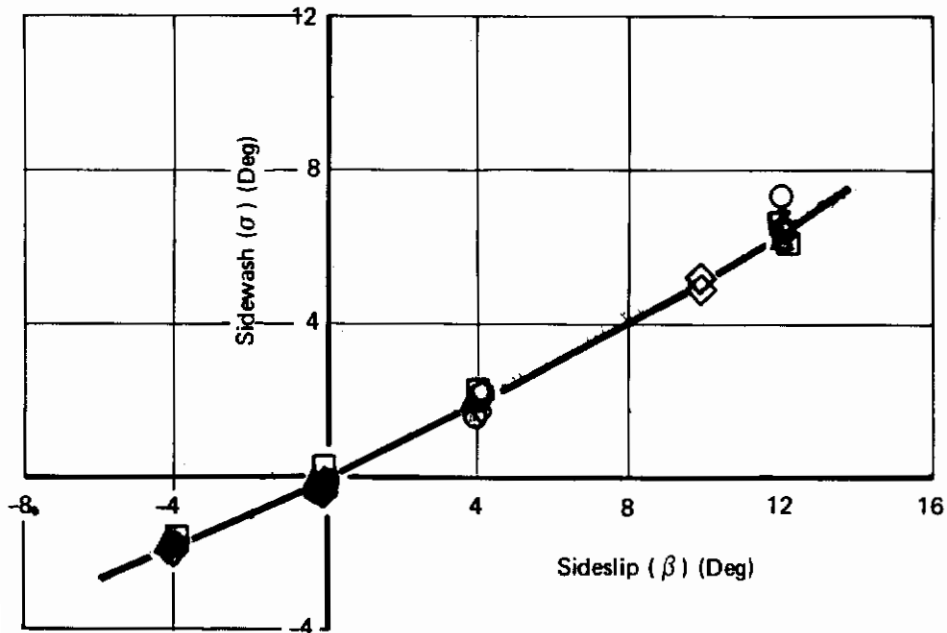


Figure 62: Sidewash at the Vertical Tail

Contrails

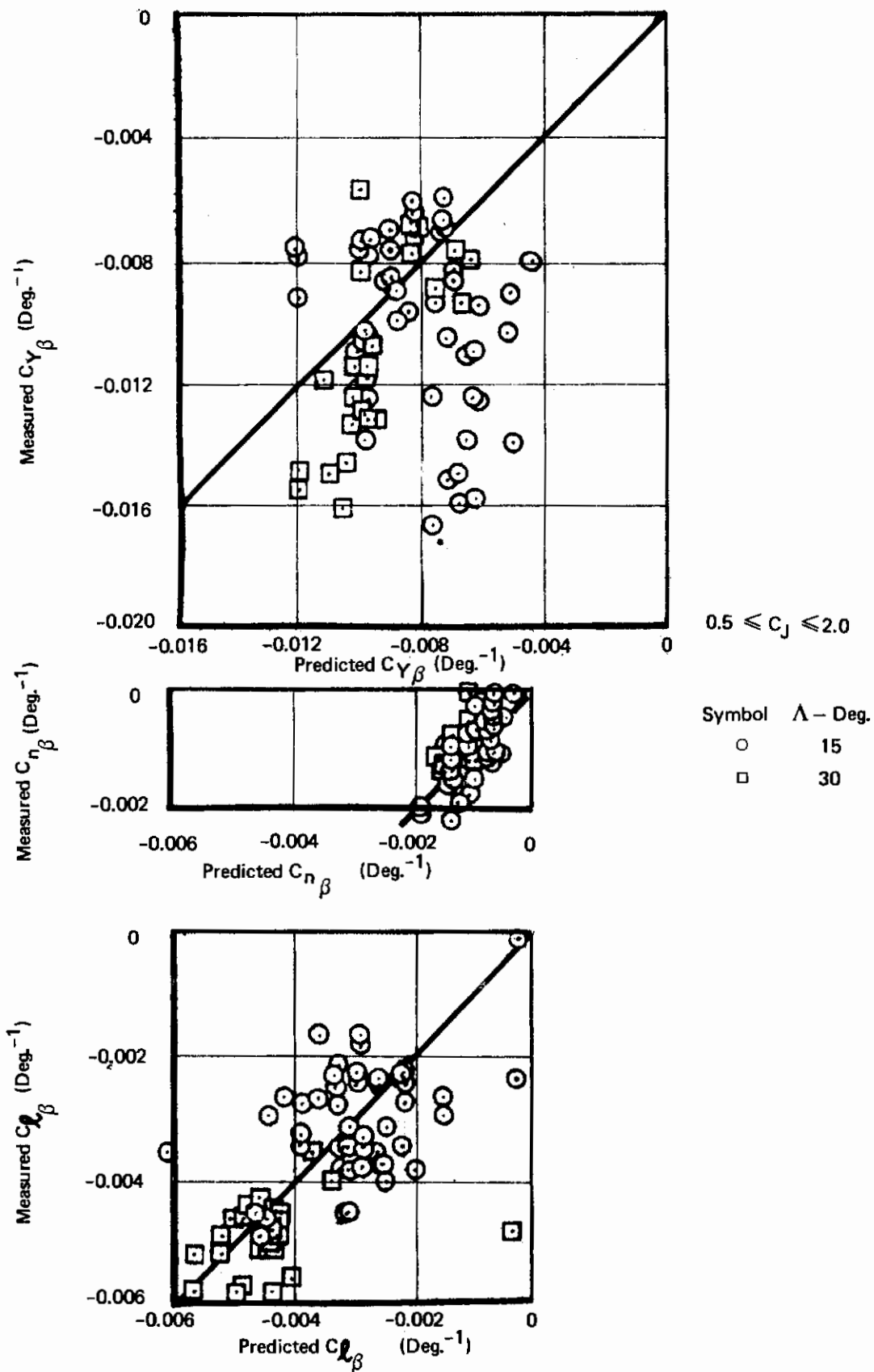


Figure 63 : Powered Sideslip Derivatives Error

TABLE IV
TEST-PREDICTION COMPARISON, SIDESLIP DERIVATIVES

TAIL-OFF
A = 15 DEG
NACELLES: AT .35C
27 AND 43.5%^b/₂

				TEST				PREDICT					
δ_f -DEG	σ -DEG	h/b	α -DEG	C_J	$C_{Y\beta}$ -DEG ⁻¹	$C_{n\beta}$ -DEG ⁻¹	$C_{l\beta}$ -DEG ⁻¹	$C_{Y\beta}$ -DEG ⁻¹	$C_{n\beta}$ -DEG ⁻¹	$C_{l\beta}$ -DEG ⁻¹	ERROR _{C_{Yβ}}	ERROR _{C_{nβ}}	ERROR _{C_{lβ}}
35	30	∞	8	0	-.0075	-.0009	-.0029	-.0075	-.0009	-.0029	0	0	0
	60			1.0	-.0077	-.0011	-.00275	-.0090		-.0031	-.0013	.0002	-.00035
				2.0	-.0070	-.0009	-.0021	-.0090		-.0031	-.0020	0	-.0010
				0	-.0070	-.00095	-.0021	-.0070	-.00095	-.0021	0	0	0
				.5	-.0094	-.0008	-.0023	-.00749		-.00244	.00191	-.00015	-.00014
				1.0	-.0107	-.0008	-.0024	-.0098		-.00244	.0009	-.00015	-.00004
				2.0	-.0104	-.0009	-.0023	-.0098		-.00244	.0006	-.00005	-.00014
		.208		0	-.0042	-.0010	-.0020	-.0042	-.0010	-.0020	0	0	0
				.5	-.0081	-.0010	-.0022	-.00437		-.0020	.00373	0	.0002
				1.0	-.0095	-.00095	-.0024	-.00609		-.0020	.00341	-.00005	.0004
				2.0	-.0127	-.00085	-.0027	-.00609		-.0020	.00661	-.00015	.0007
	90	∞		0	-.0061	-.00075	-.0017	-.0061	-.00075	-.0017	0	0	0
				1.0	-.0119	-.0007	-.0031	-.00976		-.0023	.00214	-.00005	.0008
				2.0	-.0126	-.00085	-.0040	-.00976		-.0023	.00284	.0001	.0017
		.21		0	-.0060	-.0010	-.0023	-.0060	-.0010	-.0023	0	0	0
				1.0	-.0087	-.0011	0	-.0069		-.0012	.0018	.0001	-.00012
				2.0	-.0083	0	-.0038	-.0069		-.00309	.0014	-.0010	-.00076
	60	∞	4	0	-.0072	-.00095	-.0017	-.0072	-.00095	-.0017	0	0	0
			8		-.0070	-.0009	-.0020	-.0070	-.0009	-.0020	0	0	0
			12		-.0071	-.0008	-.0020	-.0071	-.0008	-.0020	0	0	0
			4	2.0	-.011	-.0005	-.0037	-.01008	-.00095	-.00238	.00092	-.00045	.00132
			8		-.0108	-.0009	-.0022	-.0098	-.0009	-.0028	.0010	0	-.0006
			12		-.0123	-.0008	-.0024	-.00994	-.0008	-.0028	.00236	0	-.0004
	30		8	0	-.0076	-.0014	-.0019	-.0076	-.0014	-.0019	0	0	0
				2.0	-.0087	-.0012	-.0023	-.00912	-.0014	-.00203	-.00042	-.0002	.00027
				0	-.0098	-.0015	-.0028	-.0098	-.0015	-.0028	0	0	0
		.21		2.0	-.0079	-.0011	-.0033	-.0098	-.0015	-.0028	-.0019	-.0004	.0005
			4	0	-.0061	-.0014	-.0017	-.0061	-.0014	-.0017	0	0	0
		∞	8		-.0075	-.0015	-.0019	-.0075	-.0015	-.0019	0	0	0
			12		-.0070	-.00135	-.0023	-.0070	-.00135	-.0023	0	0	0
	4		4	2.0	-.0071	-.0013	-.0028	-.00732	-.0014	-.00182	-.00022	-.0001	.00098
			8		-.0086	-.0011	-.0024	-.0090	-.0015	-.00203	-.0004	-.0004	.00037
			12		-.0097	-.0007	-.0025	-.0084	-.00135	-.00246	-.0013	-.00065	.00004

Contrails

TABLE IV
TEST-PREDICTION COMPARISON, SIDESLIP DERIVATIVES (Continued)

TAIL-OFF
Λ = 15 DEG.
NACELLES AT .35C

NACELLE LOC. -y/2	TEST						PREDICT							
	δ _f -DEG	σ-DEG	h/b	α-DEG	C _J	C _{Yβ} -DEG ⁻¹	C _{Nβ} -DEG ⁻¹	C _{Lβ} -DEG ⁻¹	C _{Yβ} -DEG ⁻¹	C _{Nβ} -DEG ⁻¹	C _{Lβ} -DEG ⁻¹	ERROR _{C_{Yβ}}	ERROR _{C_{Nβ}}	ERROR _{C_{Lβ}}
.27	20	30	∞	8.0	0	-.0042	-.0013	-.0013	-.0042	-.0013	-.0013	0	0	0
					1.0	-.0091	-.0011	-.0013	-.00504	-.0013	-.0013	.00406	-.0002	.00121
					2.0	-.0140	-.0009	-.0013	-.00504	-.0013	-.0013	.00896	-.0004	.00151
			.21		0	-.0068	-.0010	-.0010	-.0068	-.0010	-.0010	0	0	0
					1.0	-.015	-.0009	-.0010	-.0068	-.0010	-.0010	.0082	-.0001	.00045
.435/.60			∞		2.0	-.016	-.0007	-.0010	-.0068	-.0010	-.0010	.0092	-.0003	.00085
					0	-.0060	-.0018	-.0018	-.0060	-.0018	-.0018	0	0	0
					1.0	-.0067	-.0019	-.0018	-.0072	-.0018	-.0018	-.0005	.0001	-.0009
					2.0	-.0070	-.0020	-.0018	-.0072	-.0018	-.0018	-.0002	.0002	-.0007
.27	35		.219		0	-.0063	-.0006	-.0006	-.0063	-.0006	-.0006	0	0	0
					1.0	-.011	-.0004	-.0006	-.0063	-.0006	-.0006	.0047	-.0002	.0002
					2.0	-.0158	-.0003	-.0006	-.0063	-.0006	-.0006	.0095	-.0003	.0002
			∞		0	-.006	-.0009	-.0009	-.0060	-.0009	-.0009	0	0	0
					1.0	-.016	-.0006	-.0009	-.0072	-.0009	-.0009	.0034	-.0003	-.00082
					2.0	-.0152	-.0002	-.0009	-.0072	-.0009	-.0009	.0080	-.0007	-.00182
	60				0	-.0047	-.0007	-.0007	-.0047	-.0007	-.0007	0	0	0
					1.0	-.0113	-.0005	-.0007	-.00658	-.0007	-.0007	.00472	-.0002	-.00104
					2.0	-.0139	-.0006	-.0007	-.00658	-.0007	-.0007	.00732	-.0001	-.00034
.435					0	-.0059	-.0007	-.0007	-.0059	-.0007	-.0007	0	0	0
					1.0	-.0061	-.0010	-.0007	-.00826	-.0007	-.0007	-.00216	.0003	.00071
					2.0	-.0065	-.00095	-.0007	-.00826	-.0007	-.0007	-.00176	.00025	.00056
.435/.60					0	-.0071	-.0013	-.0013	-.0071	-.0013	-.0013	0	0	0
					1.0	-.0077	-.0015	-.0013	-.00994	-.0013	-.0013	-.00224	.00025	.0002
					2.0	-.0074	-.0021	-.0013	-.00994	-.0013	-.0013	-.00254	.0008	.00015
.27			.219		0	-.0068	-.0003	-.0003	-.0068	-.0003	-.0003	0	0	0
					1.0	-.0103	-.0004	-.0003	-.00986	-.0003	-.0003	.00044	.0001	-.0005
					2.0	-.0139	-.0004	-.0003	-.00986	-.0003	-.0003	.00404	.0001	-.0010
			∞		0	-.0048	-.0006	-.0006	-.0048	-.0006	-.0006	0	0	0
					.5	-.0104	-.0005	-.0006	-.00514	-.0006	-.0006	.00526	-.0001	-.00137
					1.0	-.0125	-.0006	-.0006	-.00768	-.0006	-.0006	.00482	0	-.00135
					2.0	-.0167	-.0010	-.0006	-.00768	-.0006	-.0006	.00902	.0004	.00035
.435					0	-.0055	-.0006	-.0006	-.0055	-.0006	-.0006	0	0	0
					1.0	-.0090	-.0002	-.0006	-.0088	-.0006	-.0006	.0002	-.0004	.00039
					2.0	-.0100	0	-.0006	-.0088	-.0006	-.0006	.0012	-.0006	.00169
.435/.60					0	-.0075	-.0013	-.0013	-.0075	-.0013	-.0013	0	0	0
					1.0	-.0092	-.0013	-.0013	-.0120	-.0013	-.0013	-.0028	0	-.00094
					2.0	-.0080	-.0014	-.0013	-.0120	-.0013	-.0013	-.0040	.0001	-.00114
.27			.21		0	-.0055	-.0003	-.0003	-.0055	-.0003	-.0003	0	0	0
					1.0	-.0125	0	-.0003	-.00633	-.0003	-.0003	.00617	-.0003	.00211
					2.0	-.0080	-.0008	-.0003	-.00633	-.0003	-.0003	.00167	.0005	.00154
.435/.60			∞		0	-.0060	-.0009	-.0009	-.0060	-.0009	-.0009	0	0	0
					2.0	-.0060	-.0014	-.0009	-.0072	-.0009	-.0009	-.0012	.0005	.00051
					0	-.0069	-.0012	-.0009	-.0069	-.0012	-.0012	0	0	0
					2.0	-.0073	-.0018	-.0012	-.00966	-.0012	-.0012	-.00236	.0006	.00009
					0	-.0076	-.0013	-.0013	-.0076	-.0013	-.0013	0	0	0
					2.0	-.0076	-.0013	-.0013	-.01216	-.0013	-.0013	-.00456	0	-.00239

Contrails

TABLE IV
TEST-PREDICTION COMPARISON, SIDESLIP DERIVATIVES (Continued)

TAIL-OFF
 $\Lambda = 30 \text{ DEG}$
NACELLES AT: .35C
27 AND $43.5\% \frac{b}{2}$

δ_f -DEG	σ -DEG	h/b	α -DEG	C_J	TEST			PREDICT			ERROR $C_{L\beta}$	ERROR $C_{N\beta}$	ERROR $C_{Y\beta}$	ERROR $C_{1\beta}$ -DEG $^{-1}$	ERROR $C_{1\beta}$ -DEG $^{-1}$	ERROR $C_{1\beta}$ -DEG $^{-1}$	
					$C_{Y\beta}$ -DEG $^{-1}$	$C_{N\beta}$ -DEG $^{-1}$	$C_{1\beta}$ -DEG $^{-1}$	$C_{Y\beta}$ -DEG $^{-1}$	$C_{N\beta}$ -DEG $^{-1}$	$C_{1\beta}$ -DEG $^{-1}$							
35	30	∞	8	0	-.0083	-.00085	-.0038	-.0083	-.00085	-.0038	0	0	0	0	0	0	0
	60	∞		1.0	-.0057	-.0010	-.0046	-.0095	-.00095	-.0046	-.00425	0	0	-.00425	0	0	0
		∞		2.0	-.0084	-.0010	-.0045	-.0095	-.00095	-.0045	-.00155	0	0	-.00155	0	0	0
		∞		0	-.0070	-.0012	-.0036	-.0070	-.0012	-.0036	0	0	0	0	0	0	0
		.242		.5	-.0089	-.0011	-.0050	-.0075	-.0011	-.0050	.0014	-.0001	-.0001	.0014	-.0001	0	0
		∞		1.0	-.0115	-.00085	-.0058	-.0098	-.00085	-.0058	.0017	-.00035	-.00035	.0017	-.00035	0	0
		.242		2.0	-.0132	-.00090	-.0048	-.0098	-.00090	-.0048	.0034	-.00030	-.00030	.0034	-.00030	0	0
		∞		0	-.0066	-.0010	-.0041	-.0066	-.0010	-.0041	0	0	0	0	0	0	0
		∞		.5	-.0077	-.0012	-.0049	-.0066	-.0012	-.0049	.00084	-.0002	-.0002	.00084	-.0002	0	0
		∞		1.0	-.010	-.0017	-.0045	-.00957	-.0017	-.0045	.00043	-.0007	-.0007	.00043	-.0007	0	0
		∞		2.0	-.0132	-.0011	-.0051	-.00957	-.0011	-.0051	.00363	-.0001	-.0001	.00363	-.0001	0	0
		∞		0	-.0060	-.0012	-.0040	-.0060	-.0012	-.0040	0	0	0	0	0	0	0
		.242		1.0	-.0132	-.0010	-.0052	-.0096	-.0010	-.0052	.0036	-.0002	-.0002	.0036	-.0002	0	0
		∞		2.0	-.0108	-.0009	-.0058	-.0096	-.0009	-.0058	.0012	-.0003	-.0003	.0012	-.0003	0	0
		∞		0	-.0072	-.0007	-.0044	-.0072	-.0007	-.0044	0	0	0	0	0	0	0
		∞		1.0	-.0078	-.0011	-.0048	-.00828	-.0011	-.0048	0	0	0	0	0	0	0
		∞		2.0	-.0068	-.00115	-.0035	-.00828	-.00115	-.0035	-.00148	-.00045	-.00045	-.00148	-.00045	0	0
		∞		0	-.0073	-.0012	-.0040	-.0073	-.0012	-.0040	0	0	0	0	0	0	0
		∞		4	-.0070	-.0013	-.0036	-.0070	-.0013	-.0036	0	0	0	0	0	0	0
		∞		8	-.0086	-.0010	-.0042	-.0086	-.0010	-.0042	0	0	0	0	0	0	0
		∞		12	-.0115	-.0008	-.0057	-.0102	-.0008	-.0057	.0013	-.0004	-.0004	.0013	-.0004	0	0
		∞		4	-.0130	-.0008	-.0050	-.0098	-.0008	-.0050	.0032	-.0005	-.0005	.0032	-.0005	0	0
		∞		8	-.0148	-.0007	-.0046	-.01205	-.0007	-.0046	.00275	-.0003	-.0003	.00275	-.0003	0	0
		∞		12	-.0056	-.0013	-.0032	-.0056	-.0013	-.0032	0	0	0	0	0	0	0
		∞		8	-.0094	-.0008	-.0040	-.00663	-.0008	-.0040	.00277	-.0005	-.0005	.00277	-.0005	0	0
		.242		2.0	-.0063	-.0015	-.0042	-.0063	-.0015	-.0042	0	0	0	0	0	0	0
		∞		0	-.0080	-.0012	-.0048	-.0063	-.0012	-.0048	0	0	0	0	0	0	0
		∞		4	-.0073	-.0014	-.0033	-.0073	-.0014	-.0033	0	0	0	0	0	0	0
		∞		8	-.0075	-.0012	-.0040	-.0075	-.0012	-.0040	0	0	0	0	0	0	0
		∞		12	-.0076	-.0009	-.0043	-.0076	-.0009	-.0043	0	0	0	0	0	0	0
		∞		4	-.0125	-.00085	-.0056	-.01022	-.00085	-.0056	.00228	-.00055	-.00055	.00228	-.00055	0	0
		∞		8	-.0146	-.0008	-.0046	-.0105	-.0008	-.0046	.0041	-.0004	-.0004	.0041	-.0004	0	0
		.242		12	-.0161	-.0006	-.0049	-.01064	-.0006	-.0049	.00546	-.0003	-.0003	.00546	-.0003	0	0
		∞		8	-.0083	-.0010	-.0050	-.0083	-.0010	-.0050	0	0	0	0	0	0	0
		∞		2.0	-.0115	-.0014	-.0052	-.01205	-.0014	-.0052	0	0	0	0	0	0	0
		∞		0	-.0068	-.0008	-.0041	-.0068	-.0008	-.0041	0	0	0	0	0	0	0
		∞		4	-.0069	-.0009	-.00425	-.00817	-.0009	-.00425	0	0	0	0	0	0	0
		∞		8	-.0072	-.0011	-.0047	-.00817	-.0011	-.0047	0	0	0	0	0	0	0
		.242		12	-.0112	-.0008	-.0043	-.00817	-.0008	-.0043	0	0	0	0	0	0	0
		∞		4	-.0119	-.0012	-.0051	-.0112	-.0012	-.0051	0	0	0	0	0	0	0
		∞		8	-.0070	-.0011	-.0041	-.0070	-.0011	-.0041	0	0	0	0	0	0	0
		∞		12	-.0074	-.0009	-.0036	-.0074	-.0009	-.0036	0	0	0	0	0	0	0
		∞		4	-.0079	-.0011	-.0039	-.0079	-.0011	-.0039	0	0	0	0	0	0	0
		∞		8	-.0118	-.0009	-.0058	-.0098	-.0009	-.0058	0	0	0	0	0	0	0
		∞		12	-.0134	-.0009	-.0052	-.01038	-.0009	-.0052	.0020	-.0002	-.0002	.0020	-.0002	0	0
		∞		4	-.0150	-.0007	-.0044	-.01108	-.0007	-.0044	.00302	0	0	.00302	0	0	0
		∞		8							.00392	-.0004	.00392	-.0004	0	0	
		∞		12											0	0	

Contrails

Contrails

$$C_{YRV} = C_{YRV_{C_J=0}} \frac{q}{q_{C_J=0}} \quad (3.29) \quad C_{YPV} = C_{YPV_{C_J=0}} \frac{q}{q_{C_J=0}} \quad (3.32)$$

$$C_{NRV} = C_{NRV_{C_J=0}} \frac{q}{q_{C_J=0}} \quad (3.30) \quad C_{NPV} = C_{NPV_{C_J=0}} \frac{q}{q_{C_J=0}} \quad (3.33)$$

$$C_{IRV} = C_{IRV_{C_J=0}} \frac{q}{q_{C_J=0}} \quad (3.31)$$

where

r is the yaw rate angle, $\frac{Rb}{2V}$

p is the wing tip helix angle, $\frac{Pb}{2V}$

subscript V denotes vertical tail contribution.

The power effect on sidewash due to roll rate and yaw rate is not accounted for, since there are no data upon which to base a correction.

3.2.2.3 Control Derivatives

3.2.2.3.1 Thrust Effect on Rudder Power

The effect of thrust on rudder power is shown in Figure 64. Side force, due to rudder deflection, goes down with thrust at 8 degrees angle of attack. At 20 degrees angle of attack, sideforce increases with thrust.

3.2.2.3.2 Thrust Effect on Aileron Power

With no aileron BLC, thrust has little effect on aileron power, see Figures 65 and 66. However, Figure 67 shows that when the ailerons are blown, the presence of thrust ($C_J=2.0$) increases the rolling moment coefficient by about .01. Figure 65 shows that sideslip can have a strong influence on the effect of thrust on aileron power.

3.2.2.3.3 Thrust Effect on Spoiler Power

Thrust has a strong influence on spoiler effectiveness. This is shown in Figures 68 and 69. Thrust effect is low at zero angle of attack and increases with angle of attack. This is probably because thrust induces more lift for the spoilers to operate on. See $C_{L\alpha}$ effects on Figure 53.

Contrails

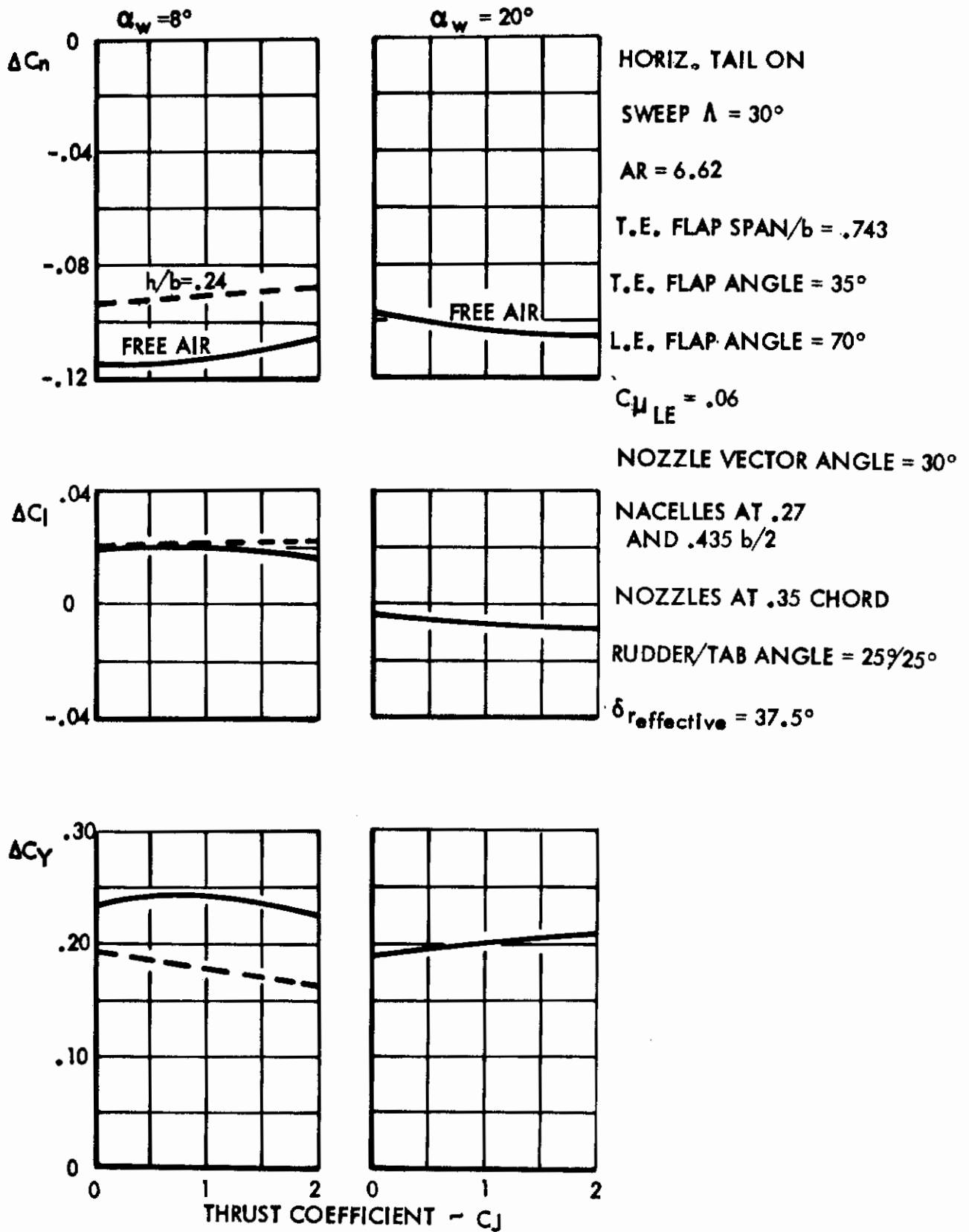
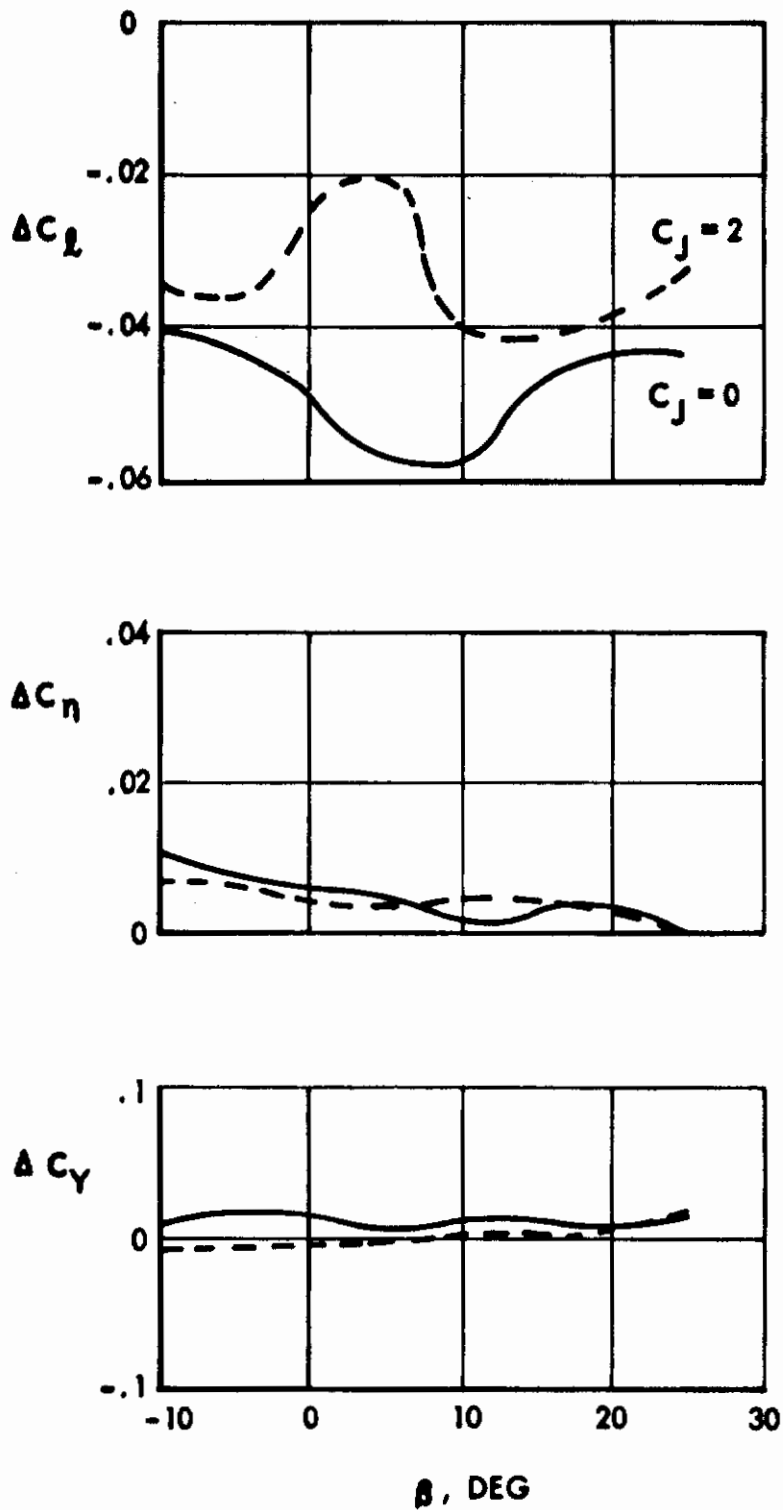


Figure 64 THRUST EFFECT ON RUDDER POWER

$\delta_{\text{AIL RIGHT}} = 40^\circ \text{ DOWN}, \alpha_W = 0 \text{ DEG.}$

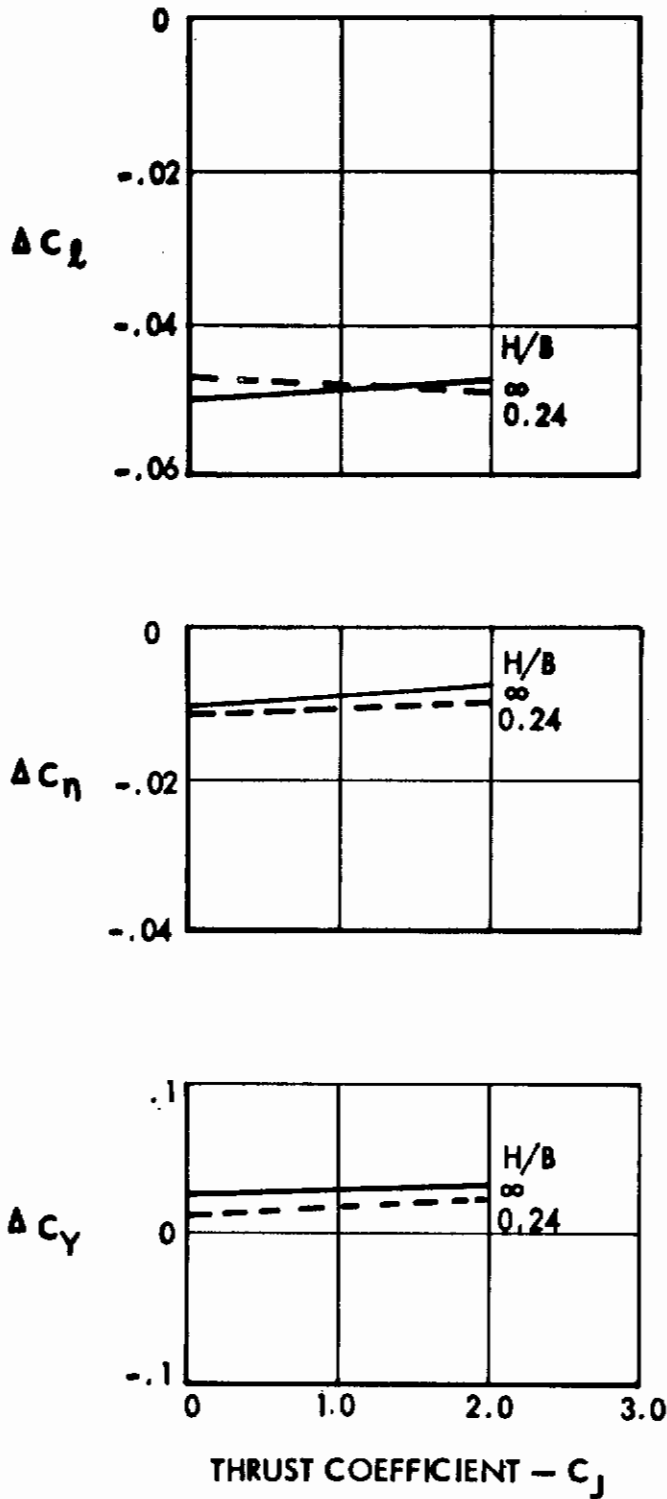


FREE AIR
 TAIL OFF
 NACELLES AT .27 AND
 .435 $b/2$
 NOZZLES AT .35 CHORD
 SWEEP = 30°
 AR = 6.62
 T. E. FLAP SPAN $\sqrt{b} = .743$
 T. E. FLAP ANGLE = 35°
 L. E. FLAP ANGLE = 70°
 $C_{\mu_{LE}} = .06$
 $C_{\mu_{AIL}} = .005$
 NOZZLE VECTOR
 ANGLE = 60°

Figure 65 EFFECT OF SIDESLIP ON AILERON POWER

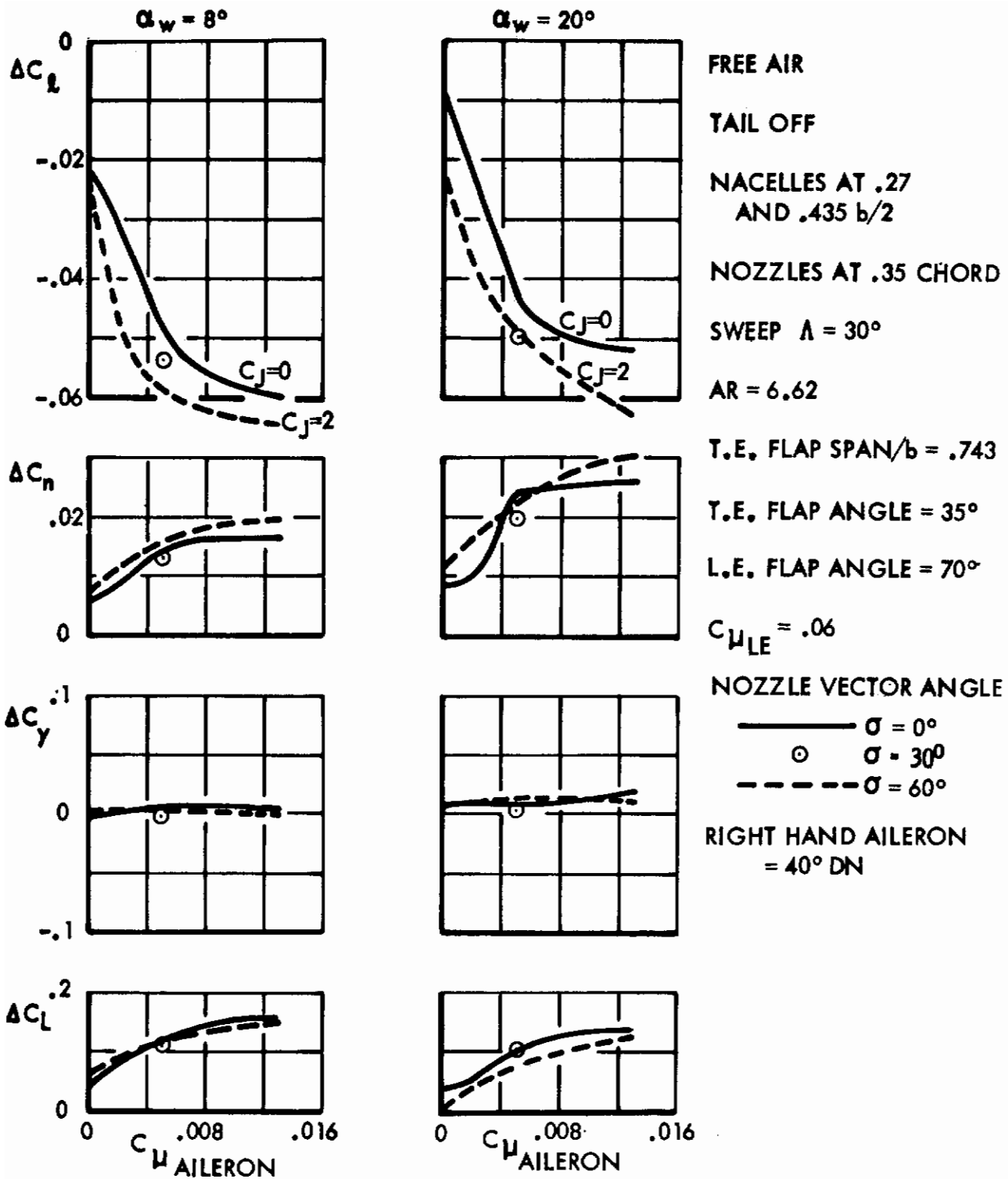
Contrails

$\delta_{AIL LEFT} = 40^\circ UP, \alpha_W = 8^\circ$



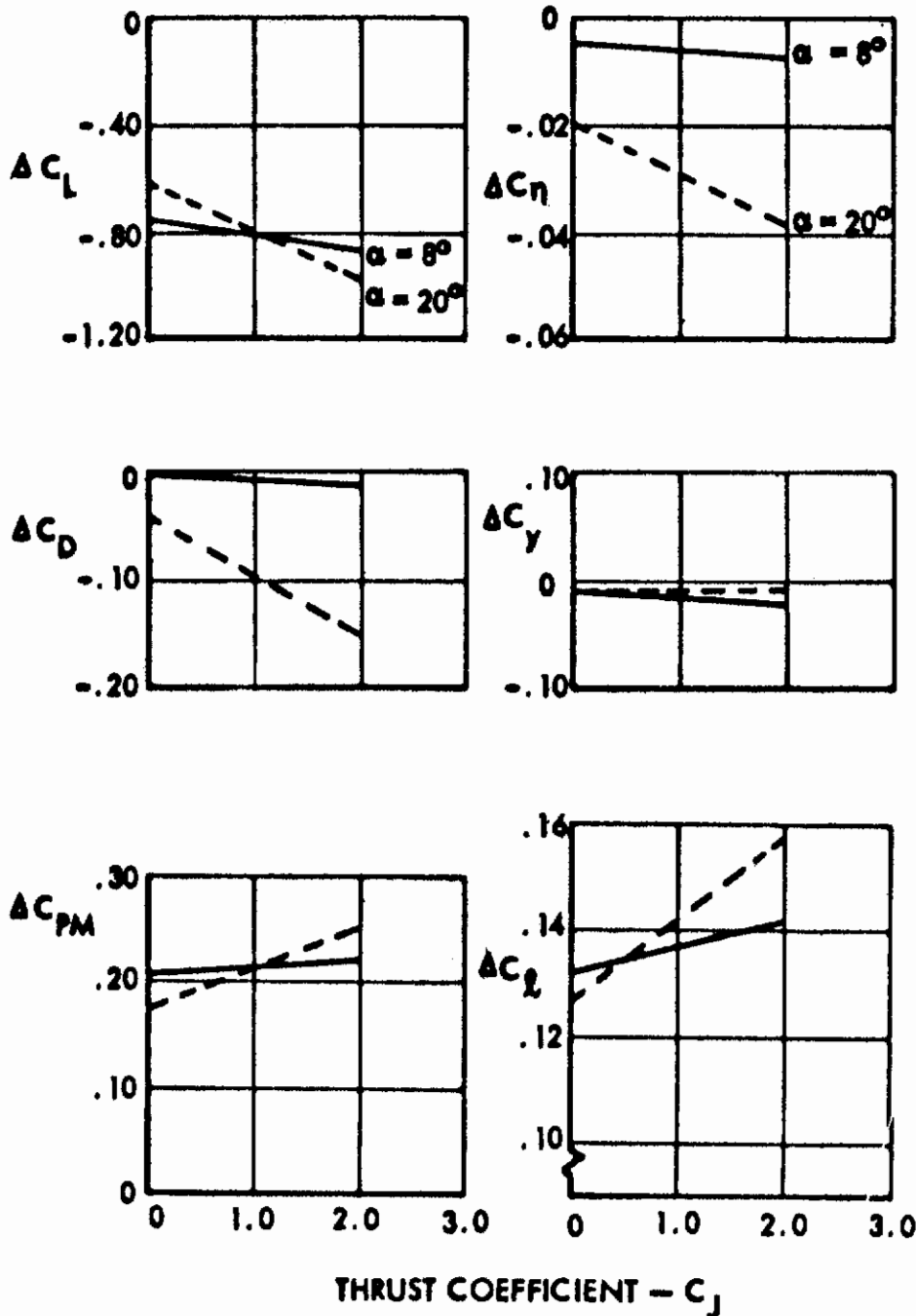
TAIL OFF
 NACELLES AT .27 AND
 .435 $b/2$
 NOZZLES AT .35 CHORD
 SWEEP $\Lambda = 30^\circ$
 AR = 6.62
 T.E. FLAP SPAN/ $b = .743$
 T.E. FLAP ANGLE = 35°
 L.E. FLAP ANGLE = 70°
 $C_{\mu LE} = .06$
 NACELLE VECTOR
 ANGLE = 30°
 $C_{\mu AIL} = 0$

Figure 66 EFFECT OF THRUST ON AILERON EFFECTIVENESS IN FREE AIR AND IN GROUND EFFECT



EFFECT OF AILERON BLOWING AND ENGINE THRUST ON AILERON EFFECTIVENESS
 Figure 67 133

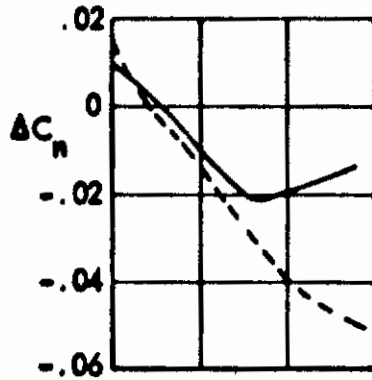
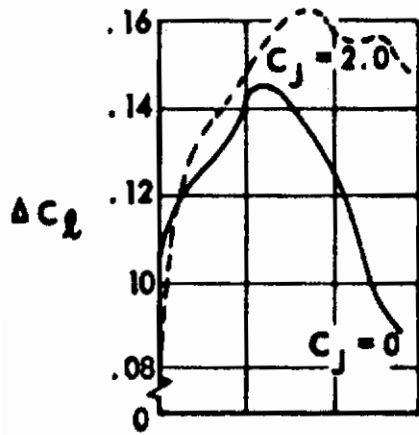
δ SPOILER = 49°
RIGHT



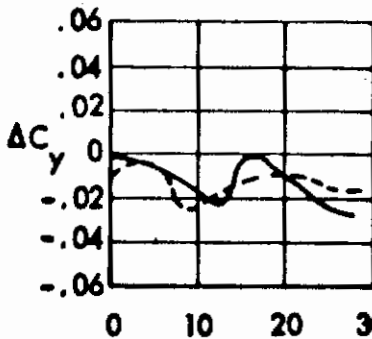
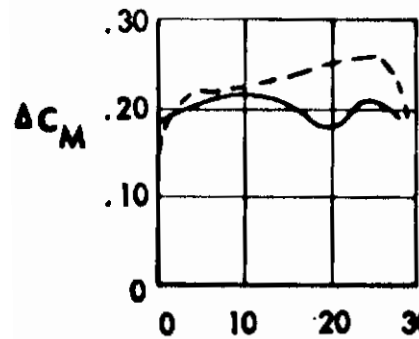
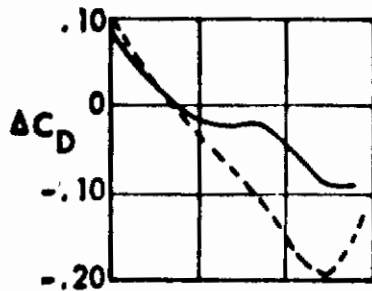
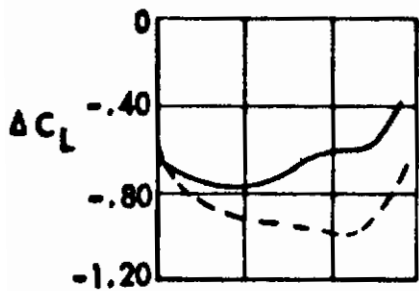
TAIL OFF
NACELLES AT .27
AND .435 $b/2$
NOZZLES AT .35
CHORD
SWEEP = 30°
AR = 6.62
T. E. FLAP
SPAN/ b = .743
T. E. FLAP
ANGLE = 35°
L. E. FLAP
ANGLE = 70°
 $C_{M_{L.E.}}$ = .06
 $C_{M_{AIL}}$ = 0
NOZZLE VECTOR
ANGLE = 60°

Figure 68 EFFECT OF THRUST ON SPOILER EFFECTIVENESS

$\delta_{\text{SPOILER}} = 49^\circ$
RIGHT



FREE AIR
TAIL OFF
NACELLES AT .27 AND
.435 b/2
NOZZLES AT .35 CHORD
SWEEP = 30°
AR = 6.62
T.E. FLAP SPAN/b = .743
T.E. FLAP ANGLE = 35°
L.E. FLAP ANGLE = 70°
 $C_{\mu_{LE}} = .06$
 $C_{\mu_{AIL}} = 0$
NOZZLE VECTOR
ANGLE = 60°



α_W - DEG.

Figure 69 SPOILER EFFECTIVENESS

3.3 Engine Out

This section presents methods for calculating the pitching moment, rolling moment, and yawing moment due to engine failure for a vectored thrust airplane. These methods are based on test data from BVWT 099 (Reference 5).

In order to obtain the pitching moment on the airplane for engine out conditions, the pitching moment for the all engine case is calculated using methods previously outlined in Section 3.2.1.1. From this the direct thrust pitching moment is subtracted by the Equation:

$$\Delta C_{m_{\text{FAILED ENGINE}}} = \Delta C_{J_{\text{FAILED ENGINE}}} (X_T \sin \sigma + Z_T \cos \sigma) \quad (3.34)$$

where

X_T = Distance from moment center to thrust vector in fraction of MAC, positive forward

Z_T = Distance from moment center to thrust vector in fraction of MAC, positive down

Figures 70 and 71 show the effect of engine failure on rolling moment and yawing moment. These data are presented in the form

of $\frac{\Delta C_l}{\Delta C_L}$ and $\frac{\Delta C_n}{\Delta C_D}$ where ΔC_L and ΔC_D are the lift and drag changes due to engine failure and include both direct thrust and interference effects. The rolling and yawing moments are calculated by Equations 3.35 and 3.36.

$$\Delta C_{l_{\text{FAILED ENGINE}}} = \frac{\Delta C_l}{\Delta C_L} \left[\Delta C_{J_{\text{FAILED ENGINE}}} \sin(\alpha + \sigma) + C_{L_{\text{INT}_{\text{FAILED ENGINE}}}} \right] \quad (3.35)$$

$$\Delta C_{n_{\text{FAILED ENGINE}}} = \frac{\Delta C_n}{\Delta C_D} \left[\Delta C_{J_{\text{FAILED ENGINE}}} \cos(\alpha + \sigma) + C_{D_{\text{INT}_{\text{FAILED ENGINE}}}} \right] \quad (3.36)$$

Contrails

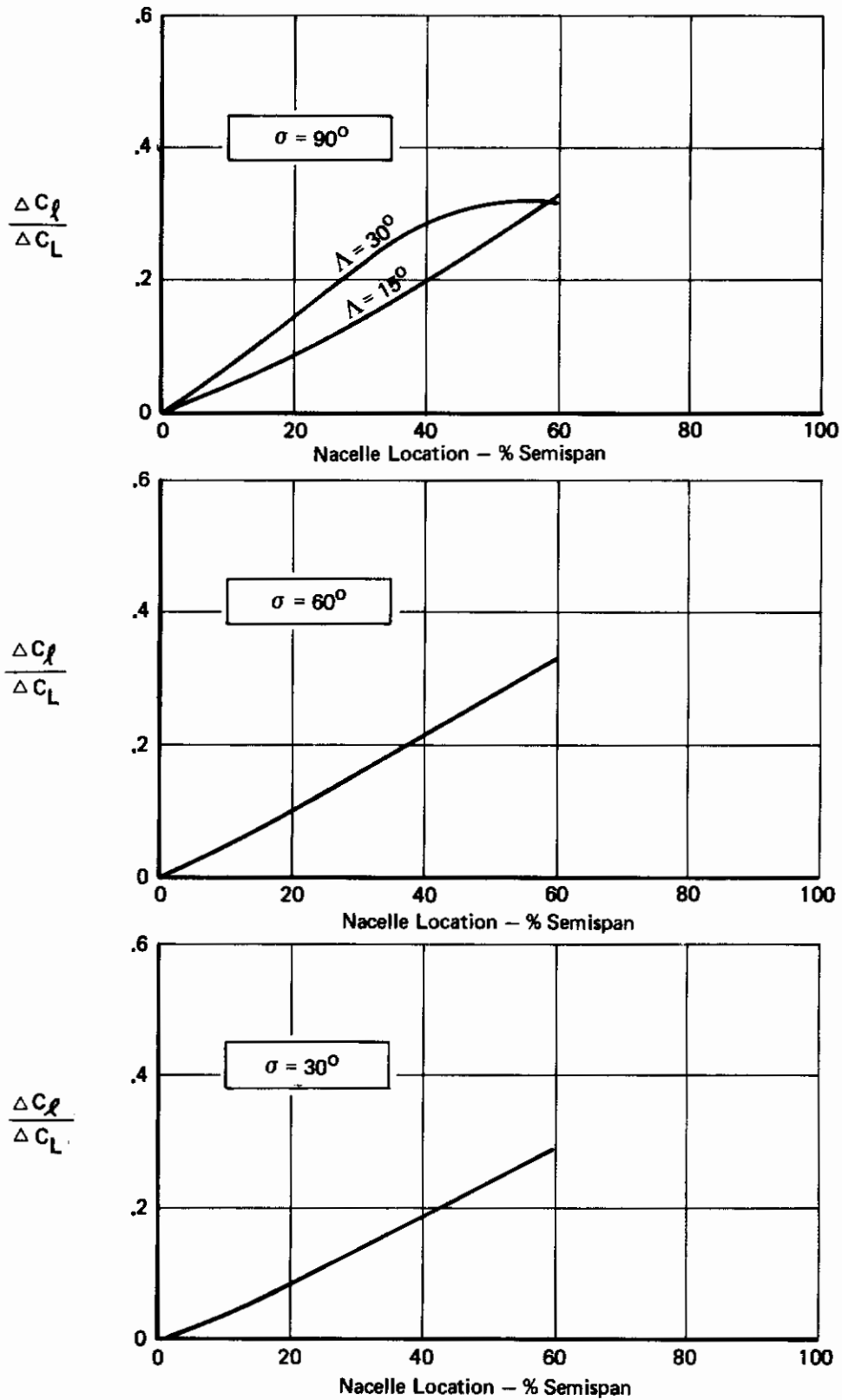


Figure 70 : ROLLING MOMENT DUE TO THRUST LOSS

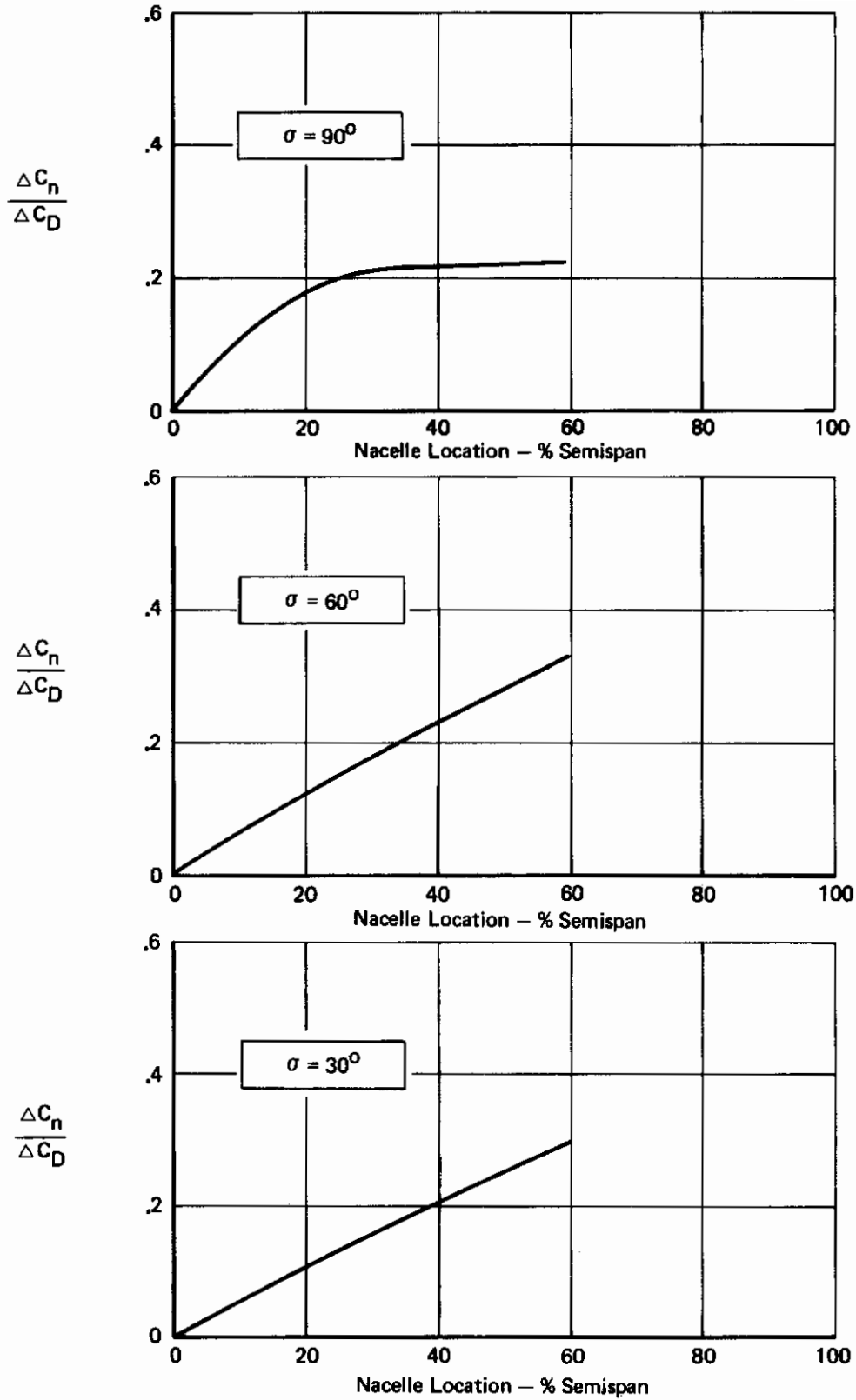


Figure 71: YAWING MOMENT DUE TO THRUST LOSS

APPENDIX

USERS' MANUAL FOR COMPUTER PROGRAM

1. INTRODUCTION

1.1 Program Description

The program calculates the aerodynamic characteristics of an airplane with various types and combinations of high lift devices. These characteristics include the additional lift, drag, and pitching moments of the high lift devices and the resultant trimmed totals. The high lift devices include leading edge flaps with and without boundary layer control (BLC), single slotted, double slotted, double slotted/double hinged, and triple slotted/double hinged trailing edge flaps.

The program is in FORTRAN IV source code compatible with the Control Data Corp. (CDC) FTN compiler on the SCOPE 3.3 operating system for the CDC 6000/7000 series computers. Eight general purpose mathematical routines from the BCS mathematical library used for interpolation (INTAB, OUTTAB, TBL, SEARCH, TBLU3, TERP1, TERP2, and TERP3) are included in FTN binary form only. The deck also includes the basic data tables developed in the main body of this document.

The program requires a number of tabular functions to be maintained on a permanent storage device file. The contents of this file, called the "permanent tables", actually form a substantial part of the data comprising the methodology defined in this report. The permanent tables may be permanently updated or temporarily modified if the user wishes to change the methodology. Input procedures for such changes are beyond the scope of this report, but are discussed in Reference 13.

1.2 Input Sequence

Any number of cases may be done on a single computer run. Input data for the whole batch begins with a "starter" card. Next comes the first case's title card. Data cards for that case follow. Next comes the title card for the second case, and so forth.

1.3 Output Summary

A printout of all permanent tables on the storage device is user selectable. When a table is modified, it is printed for verification, whether it is a temporary or permanent modification. The title for each case is printed, followed by all the input data for that case.

The coefficients of lift, drag, and pitching moment are printed following the input data for each case for free air, with ground effect, and vectored thrust. A single run may include several thrust coefficients, flap angles and wing/ground distances. The outputs for ground effect are repeated for each wing height. This output is repeated for each flap angle, and the entire output is repeated for each thrust coefficient.

2. INPUT CARD PUNCHING INSTRUCTIONS

The STARTER card must be punched with one-digit integers in specified columns. Title cards are punched as 72 columns of freely arranged alphameric data. With two exceptions noted in the discussion below, all other data are to be punched in 10-field seven digit format. This format requires all numbers to have a decimal point but permits arbitrary placement in the seven digit field.

2.1 Input Card Order

"STARTER" Card

1st Case	TITLE CARD	C01
	FLAP TYPE	C02
	Balance of Data	C04-C26
2nd Case	TITLE CARD	C01
	FLAP TYPE	C02
	Balance of Data	C04-C26

2.2 Input Card Formats

"STARTER" Card

<u>Column</u>	<u>Variable</u>	<u>Description</u>
7	IU	Input/output unit for permanent tabular data*
	= 2 - Permanent disk/scratch disk	
	= 4 - Magnetic tape/scratch disk	
14	NTBL	Number of permanent tables to be modified (Use 0)*
21	IP	Print option
	= 0 - Formal output printed	
	= 1 - Tables and formal output printed	
	= 2 - Tables, detailed intermediate computations, and formal output printed	
28	ICR	Permanent tables on card reader (Use 0)*
72-80	May be used for identification	

*Modification or updation of tables requires nonzero inputs. This situation is discussed in Reference 13.

Contrails

Card C01

<u>Column</u>	<u>Name</u>	<u>Description</u>
1-72		Title

Card C02

<u>Field</u>	<u>Name</u>	<u>Description</u>
1	AFLAP	Flap type identification. 1. Type 1 single slotted 2. Type 2 double slotted 3. Type 3 double slotted 4. Type 4 triple slotted (Refer to Figure 6 for description of the flap types.)
2	ATTBL	Number of temporary table updates. 0. To use existing tables in storage.

Card C03 - Temporary tables (Not normally used.)

Card C04

<u>Field</u>	<u>Name</u>	<u>Description</u>
1	WGROSS	Gross wing area, sq ft
2	WREF	Reference wing area, sq ft
3	SPAN	Wing span, ft
4	WPERMT	Wing semi-perimeter, ft (For example, refer to sample problem, Page 5.)

Card C05

<u>Field</u>	<u>Name</u>	<u>Description</u>
1	CPRIME	Extended wing chord length normal to extended wing half chord line, ft (Extended chord definition on Figure 6.)
2	CFLAP	Flap chord Types 1 and 2 flap normal to wing half chord line, ft
3	AQCORD	Sweep angle of wing quarter chord line, deg
4	AHCORD	Sweep angle of wing half chord line, deg

Contrails

Card C05 (Continued)

<u>Field</u>	<u>Name</u>	<u>Description</u>
5	AHLAFT	Sweep angle of aft flap hinge line, deg. This is the hinge line for Types 1 and 2 flap or the aft hinge line for Types 3 and 4.

Card C06

<u>Field</u>	<u>Name</u>	<u>Description</u>
1	ADFLAP	Number of flap deflections, maximum of 4.

Card C07 (For Flap Type 1 or 2)

<u>Field</u>	<u>Name</u>	<u>Description</u>
1	DFLP ₁	First flap deflection, Type 1 or 2 flap, deg
2	DFLP ₂	Second flap deflection, deg
3	DFLP ₃	Third flap deflection, deg
4	DFLP ₄	Fourth flap deflection, deg

Card C07 (For Flap Type 3 or 4)

<u>Field</u>	<u>Name</u>	<u>Description</u>
1	DFFW ₁)	First flap deflection, Type 3 or 4 flap, deg
2	DFAF ₁)	
3	DFFW ₂)	Second flap deflection.
4	DFAF ₂)	
5	DFFW ₃)	Third flap deflection.
6	DFAF ₃)	
7	DFFW ₄)	Fourth flap deflection.
8	DFAF ₄)	

Card C08 (For Flap Type 3 or 4)

<u>Field</u>	<u>Name</u>	<u>Description</u>
1		Not used.

Contrails

Card C08 (Continued)

<u>Field</u>	<u>Name</u>	<u>Description</u>
2	CPFLAP	Forward flap chord (includes aft flap rotated into forward flap chord plane) ft - see Figure 6 for definition.
3	CAFT	Aft flap chord measured normal to wing half chord line, ft
4	AHLFWD	Sweep angle of forward flap hinge line, deg

Card C09

<u>Field</u>	<u>Name</u>	<u>Description</u>
1	ETEIN	Distance from airplane centerline to inboard edge of trailing edge flap, semispans
2	ETEOUT	Distance from airplane centerline to outboard edge of trailing edge flap, semispans

Card C10

<u>Field</u>	<u>Name</u>	<u>Description</u>
1	CLEDGE	Leading edge flap chord measured normal to wing quarter chord line, ft
2	CHORD	Wing chord normal to wing quarter chord line, ft
3	DLEDGE	Leading edge flap deflection normal to flap hinge line, deg
4	ELEIN	Distance from airplane centerline to inboard edge of leading edge flap, semispans
5	ELEOUT	Distance from airplane centerline to outboard edge of leading edge flap, semispans

Contrails

Card C11

<u>Field</u>	<u>Name</u>	<u>Description</u>
1	CLAFU	Lift curve slope, flaps up, per degree
2	AOFLU	Angle of zero lift, flaps up, deg
3	CLMAXU	Maximum lift coefficient, flaps up
4	ALPHAI	Initial angle of attack for which data is desired, deg
5	DALPHA	Increment in angle of attack for which data is desired, deg
6	CHDLE	Extended wing chord length normal to wing leading edge with trailing edge flap extended, ft

Card C12

<u>Field</u>	<u>Name</u>	<u>Description</u>
1	CLENLE	Chord length of leading edge device normal to wing leading edge, ft
2	CRDNLE	Wing chord length normal to wing leading edge, ft
3	DWTE	Increase in wing area due to trailing edge flap extension, sq ft
4	DWLE	Increase in wing area due to leading edge flap extension (including only the area forward of trailing edge flaps) sq ft
5	WPGROS	Basic wing area inboard of outboard edge of trailing edge flap, sq ft
6	CULE	Leading edge boundary layer control blowing momentum coefficient
7	AEDGE	Leading edge flap type. 1. Shaped leading edge devices. 2. Conventional slats.

Contrails

Card C13

<u>Field</u>	<u>Name</u>	<u>Description</u>
1	WGFLAP	Wing area including leading and trailing edge flap extension between the inboard and outboard edge of the trailing edge flap, sq ft
2	SPANLE	Planform area of leading edge device, sq ft
3	CRDDPM	Wing chord including leading and trailing edge extension normal to wing half chord line, ft
4	CDPMFU	Minimum drag flap ^s up

Card C14

<u>Field</u>	<u>Name</u>	<u>Description</u>
1		Not used, leave blank
2	APQCHD	Sweep angle of quarter chord with leading edge extended, deg
3	XAC	Longitudinal location of aerodynamic center of basic trapezoidal wing, ft (Note, all longitudinal distances must be from a common reference point.)
4	S2	Wing area between the inboard and outboard edges of the leading edge flaps, sq ft
5	DSLE	Increase in wing area from extension of leading edge flaps, sq ft
6	S3	Wing area between the inboard and outboard edges of the trailing edge flaps, sq ft

Card C15

<u>Field</u>	<u>Name</u>	<u>Description</u>
1	ALE	Location of inboard edge of leading edge flaps: 1. Start at side of body. 2. Start outboard of side of body.

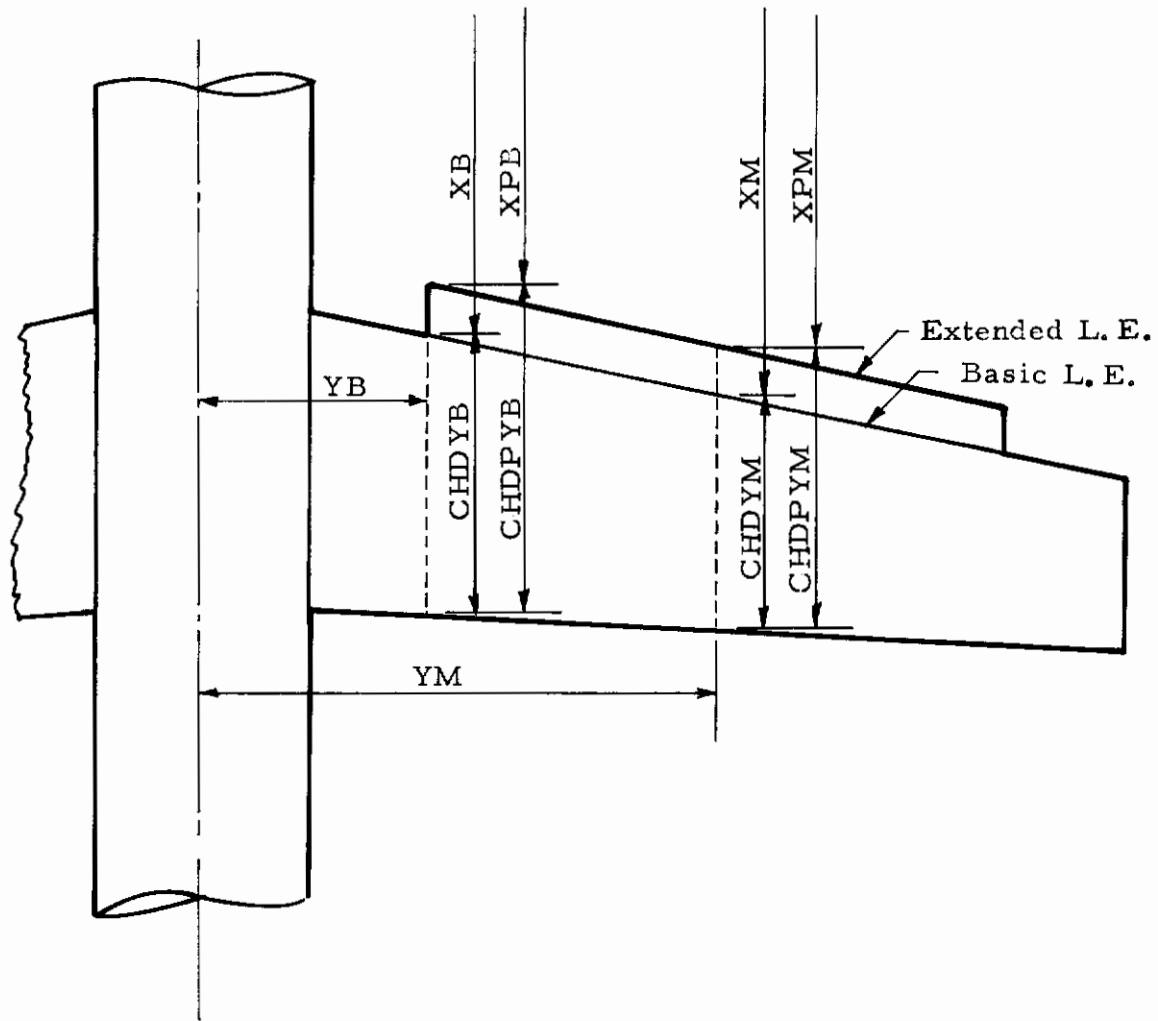


Figure 72: Nomenclature for Leading Edge Flap

Contrails

Card C15 (Continued)

<u>Field</u>	<u>Name</u>	<u>Description</u>
2	ATE	Location of inboard edge of trailing edge flaps. 1. Start at side of body. 2. Start outboard of side of body.

Card C16 (For additional description of geometry on Cards C16 and C17 refer to Figure 72.)

<u>Field</u>	<u>Name</u>	<u>Description</u>
1	CHDYB	Streamwise wing chord length at inboard edge of leading edge flap, ft.
2	XB	Longitudinal location of leading edge of streamwise wing chord (CHDYB) at inboard edge of leading edge flaps, ft Measured from the common reference point.
3	CHDPYB	Streamwise chord length at inboard edge of leading edge flaps with leading edge extended, ft
4	XPB	Longitudinal location of leading edge of streamwise chord (CHDPYB) with leading edge flaps extended, chord at inboard edge of leading edge flaps, ft
5	YB	Spanwise location of inboard edge of leading edge flaps, ft
6	YM	Spanwise location of leading edge flap semispan, ft

Card C17

<u>Field</u>	<u>Name</u>	<u>Description</u>
1	CHDYM	Streamwise chord at mid span of leading edge flap, ft
2	XM	Longitudinal location of leading edge of chord CHDYM, ft
3	CHDPYM	Extended streamwise chord at midspan of leading edge flap, ft
4	XPM	Longitudinal location of leading edge of chord CHDPYM, ft

Contrails

Card C18 (For additional description of geometry on Cards C18 and C19, refer to Figure 73.)

<u>Field</u>	<u>Name</u>	<u>Description</u>
1	CHDYBT	Streamwise chord at inboard edge of trailing edge flap, ft
2	XBTE	Longitudinal location of leading edge of chord CHDYBT, ft
3	CDPYBT	Streamwise chord length at inboard edge of trailing edge flaps with trailing edge extended, ft
4	XPBTE	Longitudinal location of leading edge of chord CHPYBT, same as XBTE, ft
5	YBTE	Spanwise location of chord CHDYBT, ft
6	YMTE	Spanwise location of midspan of trailing edge flap, ft

Card C19

<u>Field</u>	<u>Name</u>	<u>Description</u>
1	CHDYMT	Streamwise chord at trailing edge flap semispan, ft
2	XMTE	Longitudinal location of leading edge of CHDYMT, ft
3	CPYMTE	Streamwise chord at trailing edge flap semispan, includes trailing edge flap extension, ft
4	XPMTE	Longitudinal location of leading edge of CPYMTE, same as XMTE, ft

Card C20

<u>Field</u>	<u>Name</u>	<u>Description</u>
1	CREF	Reference chord length for pitching moment, ft
2	CFLIB	Streamwise flap chord at inboard edge of trailing edge flap, flap type 1 or 2, ft
3	CFLOB	Streamwise flap chord at outboard edge of trailing edge flap, flap type 1 or 2, ft

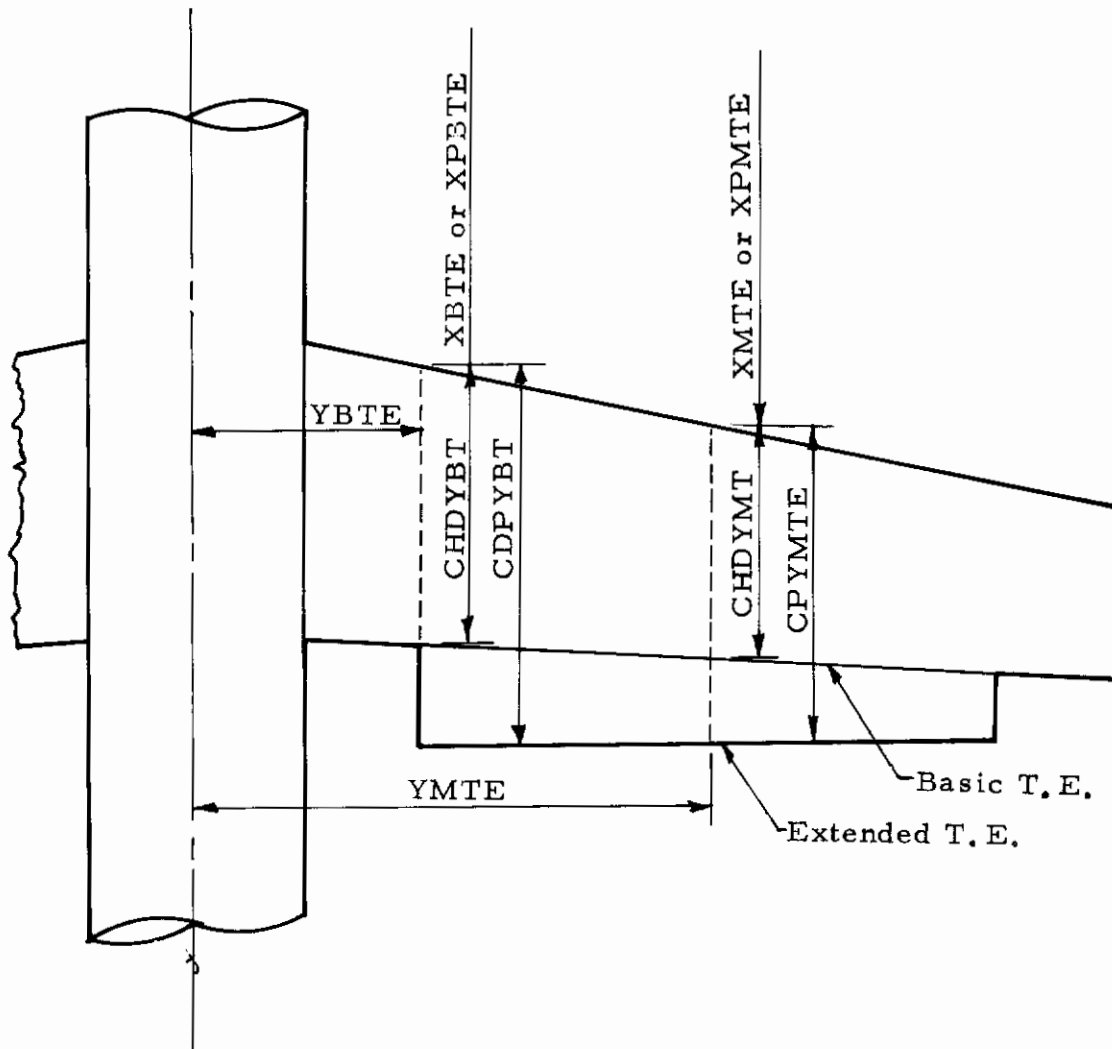


Figure 73: Nomenclature for Trailing Edge Flap

Contrails

Card C20 (Continued)

<u>Field</u>	<u>Name</u>	<u>Description</u>
4	CPMIB	Streamwise wing chord at inboard edge of trailing edge flap (including trailing edge flap extension), ft
5	CPMOB	Streamwise wing chord at outboard edge of trailing edge flap (including trailing edge flap extension), ft

Card C21

<u>Field</u>	<u>Name</u>	<u>Description</u>
1	CPFLIB	Streamwise flap chord at inboard edge of trailing edge flap, includes aft flap rotated about hinge line into forward flap chord plane, flap type 3 or 4, ft
2	CPFLOB	Streamwise flap chord at outboard edge of trailing edge flap (includes aft flap rotated about hinge line into forward flap chord plane), flap type 3 or 4, ft
3	XIB	Longitudinal intersection of CPMIB and wing half chord line, ft
4	XOB	Longitudinal intersection of CPMOB and wing half chord line, ft
5	XPQCRD	Longitudinal location of wing quarter mac with the leading edge flap extended, ft
6	XCG	Longitudinal location of center of gravity, ft

Card C22

<u>Field</u>	<u>Name</u>	<u>Description</u>
1	CMOLFU	Pitching moment coefficient at zero lift, flaps up
2	EPTEIB	Distance from airplane centerline to intersection of CPMIB and wing half chord line, semispans

Contrails

Card C22 (Continued)

<u>Field</u>	<u>Name</u>	<u>Description</u>
3	EPTEOB	Distance from airplane centerline to intersection of CPMOB and wing half chord line, semispans

Card C23

<u>Field</u>	<u>Name</u>	<u>Description</u>
1	THQM	Height of horizontal tail quarter mac above wing chord plane, ft
2	TLQM	Tail length, from wing quarter mac to tail quarter mac, ft
3	NWINGH	Number of ground heights to be considered, maximum of 4 (must be right adjusted integer in Column 21)
4	WHQM ₁	First ground height, ground to wing quarter mac, ft
5	WHQM ₂	Second ground height, ft
6	WHQM ₃	Third ground height, ft
7	WHQM ₄	Fourth ground height, ft

Card C24

<u>Field</u>	<u>Name</u>	<u>Description</u>
1	STAIL	Horizontal tail area, sq ft
2	EPSO	Downwash angle at horizontal tail, flaps up, zero angle of attack, deg
3	DEPDAL	Rate of change of downwash with angle of attack, flaps up, degrees/degree
4	DCPDM	Horizontal tail minimum drag coefficient, referred to horizontal tail area
5	DCDDCL	(dC_D/dC_L^2) , tail induced drag factor referred to tail lift coefficient and tail area

Contrails

Card C25

<u>Field</u>	<u>Name</u>	<u>Description</u>
1	CDRAM	Ram drag coefficient
2	ENGVEC	Engine vector angle referred to wing chord plane, deg
3	XNACEL	Longitudinal distance from wing leading edge to nozzle exit divided by wing chord length at the same stream-wise station
4	XNOZLE	Longitudinal distance from center of gravity to nozzle exit centerline, ft
5	ZNOZLE	Vertical distance from center of gravity to nozzle exit centerline, ft
6	ZINLET	Longitudinal distance from center of gravity to centerline of inlet face, ft
7	ZINLET	Vertical distance from center of gravity to centerline of inlet face, ft

Note: For multi-engine configurations use average values for nozzle and inlet locations.

Card C26

<u>Column</u>	<u>Name</u>	<u>Description</u>
7	NCG	Number of engine thrust coefficients; (integer 5)

<u>Field</u>	<u>Name</u>	<u>Description</u>
2-NCJ+1	CJ _i	Array of engine thrust coefficients; NCJ fields are used.

3.0 EXECUTING FROM CARDS

To execute the program from the FORTRAN source deck with the tables on cards, saving the tables on a magnetic tape file, TAPE4, and printing the tables, the deck setup required is shown on Figure 74.

3.1 Using the External Table File

The deck is stacked with the REQUEST control card as in Section 3.0 for magnetic tape. The tables are retrieved from the tape without

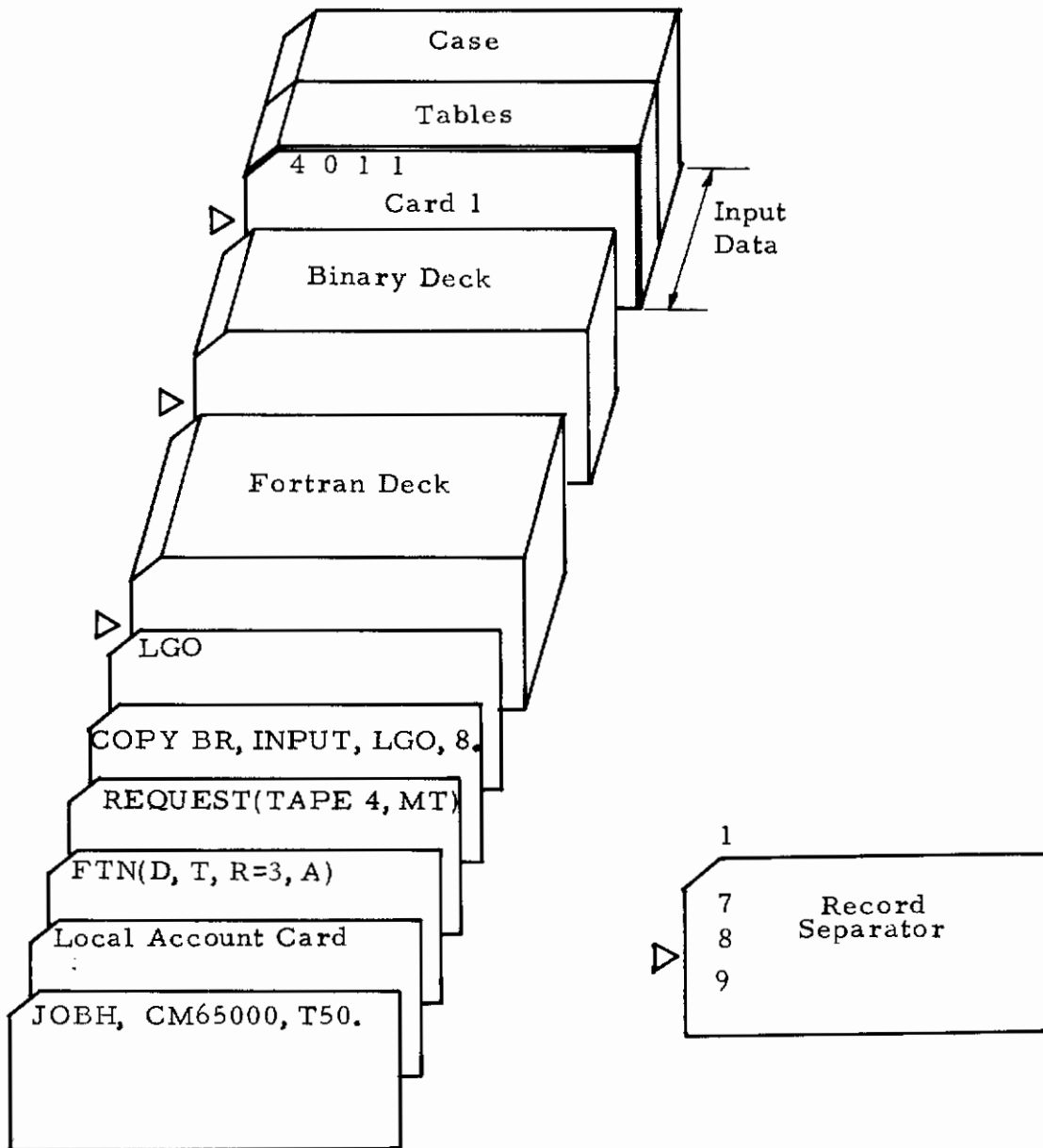


Figure 74: Program Deck Stacking

Contrails

the full set of tables in the data. The installation convention for identification of the tape is required on the REQUEST card. A permanent disk file can be used instead of the magnetic tape file and permanent or temporary table updates may be supplied as discussed in Reference 13, Section 2. Column 28 of Card 1 is zero.

If execution without the FORTRAN source deck is desired, consult a programmer for the most desirable approach for your installation. This would be preferred in a production situation where no changes are being made to the program.

4. SAMPLE INPUT AND OUTPUT

The sample problem used in this document is presented on an input data form in Table V, followed by the corresponding output.

The output data begins with a recapitulation of the input data. The constants defining the power off lift, moment and drag curves are then stated, followed by tabulated tail-off lift, moment and drag, and by tabulated trimmed lift and drag, for both power-off and power-on conditions. If ground effect data is called for, tabulated characteristics in ground effect come next.

5. PROGRAM LISTING

A FORTRAN IV source code listing of the program begins on page 163.

TABLE V
SAMPLE INPUT

TEN FIELD, SEVEN DIGIT CRD FORMAT

1	7	8	14	15	21	22	28	29	33	36	42	43	49	50	56	57	63	64	70	71	72	IDENT	80
	4		0		2		1															STARTER	
	SAMPLE	PROBLEM																				CO1	
	4.0	0.																				CO2	
		(NOT	USED	FOR	THIS	PROBLEM)																CO3	
	8.592	6.164	7.02284	8.41267																		CO4	
	1.0722	.346	15.	11.652	3.525																	CO5	
	1.0																					CO6	
	45.14	15.13																				CO7	
	.145	.750																				CO8	
	.13975	.83567	70.	.145	1.																	CO9	
	.076	0.	.98	0.	2.																	C10	
	.13889	.83567	1.104	.624	5.199	.06	1.0															C11	
	5.577	.882	1.2119	.060																		C12	
		15.0	3.165	4.945	.882	3.881																C13	
	1.	1.																				C14	
	1.14508	2.61417	1.284	2.47325	.50833	2.01																C15	
	.82333	3.097	.96225	2.958																		C16	
	1.14508	2.6142	1.4692	2.61417	.50833	1.57133																C17	
	9.1767	2.9558	1.17742	2.9558																		C18	
	93158		1.46917	.88567																		C19	
	4.745	2.8608	.33488	3.7398	3.064	3.165																C20	
	-.110	.145	.75																			C21	
	1.46383	4.0976	1	1.46775																		C22	
	1.624	0.	.25	.0075	.0999																	C23	
	0.	30.	.02917	-.0055	.23225	1.007	2.3225															C24	
	1	2.																				C25	
	TITLE	SAMPLE PROBLEM										NAME	DATE	PAGE	OF								

SAMPLE PROBLEM

TRIPLE SLOTTED FLAP TYPE 4

WING S	WING REF	SPAN	PERIMETER		
8.59	6.16	7.02	8.41		
CPRIME	C FLAP	SWEEP 1/4C	SWEEP 1/2C	SWEEP AFT	
1.07	.35	15.00	11.65	3.53	
NO FLAP ANGLES					
1	OFFWD(1)	DFAFT(1)	OFFWD(1)		
	45.14	15.13			
C FWD	C PRIME FWD	C AFT	SWEEP FWD		
-0.00	.35	.10	7.29		
ETA IB TE	ETA OB TE				
.145	.750				
CHORD LE	C CHORD	DELTA LE	ETA IB LE	ETA OB	
.14	.84	70.00	.145	1.000	
GL ALPHA FU	ALPHA ZERO L	CLMAX FU	ALPHA	DALPHA	CPRIME NLE
.076	0.0	.980	0.00	2.00	1.07
C LE NLE	CHORD NLE	DELS TE	DELS LE	S PRM GROSS	CU LE
.14	.84	1.10	.62	5.20	.060
S FLAPPED	SPAN LE	C DBL PM	CDPMFU		
5.577	.882	1.212	.060		
GMO	SWEEP PM G/4	XAC TRAP	S2	DSLE	S3
-0.00	15.00	3.17	4.94	.88	3.88

ARE THE FLAP EDGES ADJACENT TO THE BODY SIDE OR NOT.
 IF FLAG = 1, YES, = 2, NO. FLAG LE = 1 FLAG TE = 1

LEADING EDGE

CHORD Y BODY	X BODY	C PRM BUY	X PM BDY	Y BODY	Y MID SPAN
1.15	2.61	1.28	2.48	.51	2.01
CHORD Y MID	X MID	C PRM MID	X PM MIU		
.82	3.10	.96	2.96		

SAMPLE PROBLEM

TRAILING EDGE										
CHORD Y BODY	X BCDY	C PRM BUDY	X PM BUDY	Y BODY	Y MID SPAN					
1.15	2.61	1.47	2.61	.51	1.57					
CHORD Y MID	X MID	C PRM MID	X PM MID							
.92	2.96	1.18	2.96							
REF CHORD	C FLAP IB	C FLAP OB	C PRM IB	C PRM OB						
.93	-0.00	-0.00	1.47	.89						
CPRM FLAP IB	CPRM FLPOB	X IB	X OB	XPRM C/4	XCG					
.47	.29	3.35	3.74	3.07	3.17					
CM OLFU	ETAPRM TE IB	ETAPRM TE OB								
-.110	.145	.750								
TAIL H	TAIL LENGTH	NO. WING H,S	WING(1)	WING H(2)	WING H(3)	WING H(3)	WING H(3)	WING H(3)	WING H(3)	WING H(3)
1.46	4.10	1	1.47							
S TAIL	EPSILON 0	D EPS/D ALP	DCPD MIN	CU/CL TAIL						
1.624	0.000	.250	.008	.100						
RAM DRAG	SIGMA ENG	X NACELLE	X NOZZLE	Z NOZZLE	X INLET	Z INLET	X INLET	Z INLET	X INLET	Z INLET
0.00	30.00	.03	-.01	.23	1.01	.23	1.01	.23	1.01	.23
NO. OF CJ	CJ(1)	CJ(2)	CJ(3)	CJ(4)	CJ(5)					
1	2.00									

SAMPLE PROBLEM

ANGLES OF ATTACK - ZERO LIFT

FLAP UP	LE DOWN	TE DOWN	BOTH DOWN
0.00000	1.67830	-19.91228	-18.23398

LIFT PARAMETERS

SLOPE	SLOPE	COEF	COEF	COEF
FLAPS UP	FLAPS DOWN	DEL CL FD	CLMAX FU	CLMAX FD
.07600	.09885	1.80249	.98000	4.37882

DRAG COEFFICIENTS

MINIMUM FLAPS UP	DEL MIN TE	DEL MIN LE
.06000	.04380	.02204

PITCHING MOMENT COEFFICIENTS

ZERO LIFT	DEL OL TE	DEL OL LE
-.11000	-.48886	.00266

SAMPLE PROBLEM

UNPOWERED CHARACTERISTICS

F R E E A I R

GROSS THRUST COEFFICIENT 0.00
 FLAP ANGLES 45.14 15.13
 WING HEIGHT (SPANS) 0.00

ALPHA	T A I L O F F				T R I M M E D			
	CL	CD	CM	CD	CL	CD	CM	CD
0.00	1.80249	.29141	-.56894	.29141	1.67314	.28570		.28570
2.00	2.00019	.31918	-.56595	.31918	1.87152	.31345		.31345
4.00	2.19790	.35005	-.56296	.35005	2.06991	.34431		.34431
6.00	2.39560	.38403	-.55996	.38403	2.26830	.37828		.37828
8.00	2.59331	.42113	-.55697	.42113	2.46668	.41537		.41537
10.00	2.79102	.46236	-.55398	.46236	2.66507	.45659		.45659
12.00	2.98872	.50691	-.55099	.50691	2.86345	.50113		.50113
14.00	3.18643	.55458	-.54800	.55458	3.06184	.54879		.54879
16.00	3.38413	.60657	-.54501	.60657	3.26023	.60078		.60078
18.00	3.58184	.66287	-.54202	.66287	3.45861	.65706		.65706
20.00	3.77955	.72227	-.53903	.72227	3.65700	.71646		.71646
22.00	3.97725	.78554	-.53604	.78554	3.85538	.77973		.77973
24.00	4.17496	.85531	-.53305	.85531	4.05377	.84948		.84948
26.00	4.37266	.92818	-.53006	.92818	4.25216	.92235		.92235

SAMPLE PROBLEM

POWER-ON CHARACTERISTICS

F R E E A I R

GROSS THRUST COEFFICIENT 2.00
 FLAP ANGLES 45.14 15.13
 WING HEIGHT (SPANS) 0.00

T A I L O F F

T R I M M E D

ALPHA	CL	CD	CM	CL	CD
0.00	2.37815	-1.49835	-.02305	2.37291	-1.49693
2.00	2.71206	-1.41312	-.04576	2.70166	-1.41226
4.00	3.03429	-1.32546	-.06487	3.01954	-1.32511
6.00	3.34316	-1.23544	-.07997	3.32498	-1.23555
8.00	3.64101	-1.14225	-.09185	3.62013	-1.14278
10.00	3.91463	-1.04979	-.09611	3.89278	-1.05060
12.00	4.19503	-.94944	-.10317	4.17157	-.95064
14.00	4.48215	-.84157	-.11303	4.45645	-.84330
16.00	4.76921	-.72730	-.12344	4.74115	-.72964
18.00	5.07039	-.60236	-.13917	5.03874	-.60557
20.00	5.38322	-.47019	-.15975	5.34690	-.47457
22.00	5.70765	-.32781	-.18491	5.66561	-.33353
24.00	6.04363	-.17162	-.21389	5.99500	-.17917
26.00	6.39110	-.00573	-.24656	6.33504	-.01570

SAMPLE PROBLEM

UNPOMEREC CHARACTERISTICS

G R O U N D E F F E C T

GROSS THRUST
COEFFICIENT 0.00

WING
HEIGHT (SPANS)
 .21

FLAP ANGLES
45.14 15.13

T A I L O F F

T R I M M E D

ALPHA	CL	CD	CM	CL	CD
-1.26	1.74479	.24378	-.55073	1.61959	.23800
.60	1.92934	.26087	-.54590	1.80523	.25508
2.47	2.11257	.27991	-.54110	1.98955	.27410
4.33	2.29450	.30088	-.53633	2.17257	.29506
6.19	2.47514	.32376	-.53160	2.35428	.31793
8.05	2.65450	.34951	-.52689	2.53472	.34367
9.91	2.83259	.37732	-.52221	2.71387	.37148
11.78	3.00942	.40698	-.51756	2.89176	.40113
13.64	3.18500	.43960	-.51294	3.06838	.43375
15.50	3.35934	.47514	-.50835	3.24377	.46928
17.36	3.53245	.51244	-.50379	3.41791	.50658
19.22	3.70433	.55220	-.49926	3.59083	.54633
21.09	3.87501	.59681	-.49475	3.76253	.59095
22.95	4.04448	.64312	-.49028	3.93302	.63725

SAMPLE PROBLEM

POWER-ON CHARACTERISTICS

G R O U N D E F F E C T

GROSS THRUST COEFFICIENT 2.00
 FLAP ANGLES 45.14 15.13
 WING HEIGHT (SPANS) .21

ALPHA	T A I L O F F		T R I M M E D	
	CL	CD	CL	CD
-1.26	2.22885	-1.58380	2.23227	-1.58145
.60	2.54738	-1.51099	2.54591	-1.50918
2.47	2.85451	-1.43915	2.84891	-1.43778
4.33	3.15021	-1.36532	3.14116	-1.36432
6.19	3.43260	-1.29043	3.42092	-1.28970
8.05	3.70410	-1.21259	3.69042	-1.21206
9.91	3.95281	-1.13712	3.93867	-1.13664
11.78	4.20615	-1.05584	4.19098	-1.05547
13.64	4.46406	-.96775	4.44731	-.96754
15.50	4.72040	-.87503	4.70197	-.87499
17.36	4.98674	-.77522	4.96566	-.77545
19.22	5.26199	-.66922	5.23731	-.66979
21.09	5.54609	-.55348	5.51689	-.55448
22.95	5.83902	-.43038	5.80439	-.43187

```

PROGRAM HTLIFT(INPUT,OUTPUT,TAPE1=INPUT,TAPE2,TAPE3=OUTPUT,TAPE4,
1 TAPE7,TAPE5=INPUT)
TAPE7  BACKUP FILE FOR TABULAR FUNCTIONS
SW7    SENSE SWITCH IF ON BACKUP FILE IS TO BE SAVED.
CR     PERMANENT TABLES ON CARD
CR     NE 0 E.G. YES - PERMANENT TABLES ON CARD READER.=BLANK- ON PERM FILE
HIGHLIFT PROGRAM WRITTEN IN SUPPORT OF D162-10050-1, PARAGRAPHS
2.3.2.1.3 AND 3.6. FOR THE AIRFORCE FLIGHT DYNAMICS LABRATORY
WRIGHT PATTERSON AIR FORCE BASE,OHIO.
THE PROGRAM CALCULATES THE AERODYNAMIC CHARACTERISTICS OF A WING
WITH VARIOUS TYPES AND COMBINATIONS OF HIGH LIFT DEVICES
LIFT AND DRAG COEFFICIENTS OF THE FLAPS AS WELL AS TOTAL WING
LIFT AND DRAG COEFFICIENTS
P.J. REIDIG AND B.A. PAQUETTE    SEPTEMBER, 1972
    
```

NOMENCLATURE

```

IU     INPUT UNIT FOR TABULAR DATA  =1-CARD KDR, 2-PERM DISK,4-MAG TAPE
NPTBL  NUMBER OF PERMANENT TABLES TO BE MODIFIED
NTTPL  NUMBER OF TEMPORARY TABLES TO BE MODIFIED
TP     PRINT OPTION =0 BRIEF PRINT OPTION NE 0 FULL PRINT - TABLES
IN     STANDARD INPUT STREAM
IO     STANDARD OUTPUT STREAM

REAL KFAP12,KF1502,LAMETA
COMMON ACRFS2(77),ACRFD2(77),ADCRA2(77),LAMEGA(30),
1ADLFCR(30),DCLACC(30),DCLACS(30),DCLKCR(30),DCLACM(30),
2DCDTED(30),DCDTFT(30),FDKCR(30),KFAP12(77),KEFEU2(77),DCDCLA(30),
3AMSBR(30),XCPAR2(77),ECP12(77),DCAUT(30),AKRYCY(30),DKULL2(77),
4CLIAS2(77),DCL13(182),CD13(231),DEPS3(182),DCLIG2(77),
5DCMIG2(77),DCDIG2(77)
TABLE LENGTH 2 INDEF VAR 6 POINTS =56 WORDS 7=71 8= 128
TABLE LENGTH 1 INDEPENDENT VAR 6PTS=18 WORDS, 7=20, 10 =26
DIMENSION TRLS(3000)
EQUIVALENCE (ACRF2,TBLS)
COMMON /INTARC/II,IN,IO,ICR,NPTBL,IP
COMMON/CJ/NCJ,ACJ(5)
COMMON /COMPUTE/ D(2),V(2)
COMMON /TROM/ ILOST
COMMON /OUTARG/ IOT
COMMON /CASEIN/ TITLE(18),IFLAP,WGRUSS,WKEF,wPERMIT,INDFLAP,
    
```

```

ACPRIME,CFLAP,DFLP(4),CFWD,CPFLAP,CAFT,DFEWD, DFAFT,AMCGRD,AMCGRU,
1AHLFWD,AHLAFT,FTFIN,FTFOUT,CLEDGE,CGRD,DLEDGE,ELEIN,ELEOUT,CLAFU,
2ACLFU,CLENLE,CRDNLE,WPGROS,DWTE,DWLE,CLMAXU,ALPHA1,CULE,DALPHA,
3WGFAP,SPANLE,CHROLE,XCP1,XCPLE,XCP2,XCP2TE,XAC,52,DSLE,53,CPMUB
4,XCG,CREF,CFLP,CFLOR,CPMIB,CPFLP,CPFLUB,XIB,XUB,FTEIN,XPGCND,
5CMOLF,WHQM(3),NWINCH,THMM,MPAN,TLWM,STAIL,EPSEFU,DCPDMM,DCDDCL
6,CHDYR,CHDPYB,CMO,APUCHP,XPRB,XB,YR,YM,CHDYM,XM,CHDPYM,XPM,IEDGE
7,CHDYPT,XBTE,COPYRT,XPRTE,YBTE,YMTE,CHDYMT,XMTE,CYMT,XPMTE
8,DFLAP,DFEW(4),DEAF(4),CRDUPM,CDPMFU,EPTUOB,EPSO,DEPDAL
9,CJ,ENGVEC,XNACEL,XNOZLE,ZNOZLE,XINLET,ZINLET,CDKAM,ILE,ITE
COMMON /OUTPUT/ NALPHA,CLAFD,AULLEF,AULTFD,AULBFD
1,DCLBFD,CLMAXD,UCUTE,DCULE,DCMULF,DCMULL,CUFATR(20),
2CVOBFD,CLMAXG(2),ALPHA(20),CLTU(20),CUTU(20),CMTU(20),CLTK(20),
3COTR(20),ALPHAG(20),CLTUG(20),COTUG(20),CMFUG(20),CLTKG(20)
1,CDTRG(20),CLPOFA(20),CLINI(20),CDPOFA(20),CMPOFA(20),DEPOFA(20),
5CLPOGE(20),CDPOGE(20),CMPUGE(20),CLGETK(20),CDGETK(20),CLFATR(20)
COMMON/BASIC/RATIO,PI,RAD,ARFF
COMMON/IPAGE/IPAGE,ICASE
DATA 0,TL0ST /3*1.0,
1 FORMAT( 10F7.0)
2 FORMAT( 10I7 )
3 FORMAT( 75H1 YOU HAVE HAD IT. THE TABULAR FUNCTIONS ABOVE COULD NO
4 1T BE READ. YOU LOST , I3, 7H TIMES.)
5 FORMAT(19HITABLE INPUT UNIT =, I3, I2H THERE ARE, I3,
6 1 26H PERMANENT TABLE UPDATES. //15H PRINT OPTION =, I3,50H PERMA
7 2NENT TABLES ON CARD READER,IF CR NE 0. CR=,I2)
8 IN = 1
9 5FORMAT(45H1* * * * INTERPOLATION ERKOR IN LIFT. IFR = ,I2 )
10 6FORMAT(45H1* * * * INTERPOLATION ERKOR IN MXLIFT. IFR = ,I2 )
11 7FORMAT(45H1* * * * INTERPOLATION ERKOR IN DRAG. IFR = ,I2 )
12 8FORMAT(45H1* * * * INTERPOLATION ERKOR IN PITCH. IFR = ,I2 )
13 9FORMAT(45H1* * * * INTERPOLATION ERKOR IN VIFREE IFR = ,I2 )
14 10FORMAT(45H1* * * * INTERPOLATION ERKOR IN VIGE IFR = ,I2 )
15 11FORMAT(44H1PARITY OR EOF ON BUFFER STATEMENT IN HILIFT // )
RAD=57.20578
PI=3.141593
ICASE=0
IO = 3
IOT = IO
RFAD(IN,2) IU,NPTRL,IP,ICR
WRITE(10,4) IU,NPTRL,IP,ICR

```

```

IF (ICR.NF.0) GO TO 16
IF (ICR.EQ.0) RIJFFK IN(IU,1) (TRLS(1),TBL5(3000))
IF (UNIT(IU)) 16,15,15
15 WRITE(10,11)
16 CALL TRLEIN
18 IF(NPTRL.EQ.0) GO TO 20
PERMANENT TABLE MODS REQUIRED
CALL PTBUDT(NPTBL)
C IF ILOST = 1, PERMANENT TABLES NOT READ CORRECTLY. STOP 1
20 IF(ILOST.NE.0) 22,22
22 WRITE(10,3) ILOST
STOP 1
C READ IN THE NEXT CASE OF DATA
23 CALL CASIN1
ICASE=ICASE+1
C *** ENGINE THRUST COEFFICIENT
C
DO 300 J=1,NCJ
CJ=ACJ(J)
C
DO 200 IF=1,NDFLAP
IF (IFLAP.GT.2) GO TO 50
C STUFF FLAP DEFLECTIONS TYPE 1 AND 2
DFLAP = DFLP(IF)/RAD
GO TO 60
C
50 CONTINUE
C STUFF FLAP DEFLECTIONS TYPE 3 AND 4
DFFWD = DFFW(IF)/RAD
DFAFT = DFAF(IF)/RAD
60 CONTINUE
C ** FREE AIR
CALL LIFT (IFR)
IF (IFR.NF.0) WRITE(10,5) IER
CALL MXLIFT(IFR)
IF (IFR.NF.0) WRITE(10,6) IER
CALL DRAG (IFR)
IF (IFR.NE.0) WRITE(10,7) IER
CALL PITCH (IFR)

```

```

IF (IER.NE.0) WRITE(10,8) IER
CALL VTRFE(IER)
IF (IER.NE.0) WRITE(10,9) IER

C ** GROUND EFFECT
C
C DO 100 I=1,NWINGH
C
C *** WING HEIGHTS FOR GROUND EFFECT
C
CALL GRNDE(I)
CALL VTGF(I,IFR)
IF (IER.NE.0) WRITE(10,10) IER
CALL CASOUT(I,WHQM(I))
100 CONTINUE
200 CONTINUE
300 CONTINUE
C NEXT CASE
GO TO 23
END
SURROUTINE TRLEIN
C 1P TABLE PRINT OPTION. IF .NE. 0, PRINT TABLES.
C
C * * TABULAR NOTATION * * * * *
C
C NTXX TABLE NUMBER FROM NT1 - NTXX
C
C NUMBER OF POINTS ALLOWED IN TABLES9
C NI = 1 7 POINTS FOR A DIMENSION OF 20
C NI = 2 6 BY 5 FOR ARRAY OF 56
C NI = 3 7 BY 6 FOR ARRAY OF 63
C NI = 4 7 BY 7 FOR ARRAY OF 71
C
C ACRES2 ALPHA FLAP EFFECTIVENESS VS CORD RATIO VS DELTA FLAP SINGLE SLOT TB 1
C 1. 57.2958 TB 1
C ACRES2 ALPHA FLAP EFFECTIVENESS VS CORD RATIO VS DELTA FLAP DOUBLE SLOT TB13
C 1. 57.2958 TB 13
C ADCRA2 RATIO FLAP EFFECTIVENESS VS CORD RATIO VS INVERSE A TB 2
C LAMETA SPAN LOADING FACTOR LAMBDA VS ETA TB 3
C ADLECR ALPHA DELTA LEADING EDGE VS CORD RATIO TB 4
C PKCLE2 BODY LIFT CARRYOVER K VS CLTE VS ETAIB TB 21

```

C DCLACC DELTA CLMAX / COSSQ ALPHA VS CORD RATIO CONVENTIONAL SLATS TB 19
 C DCLACS DELTA CLMAX / COSSQ ALPHA VS CORD RATIO SHAPED LEADING EDGE TB 5
 C DCLRCR DELTA CL RATIO VS CORD RATIO TB 6
 C DCLACM DEL CL MAX / COSSQ ALPHA VS CNOLE -LE BOUNDARY LAYER EFFITVNSS TB 7
 C DCDTFD DEL CD TF VS FLAP ANGLE, DOUBLE SLOTTED TB 8
 C1. 57.2958 TB 8
 C DCDTFT DEL CD TF VS FLAP ANGLE, TRIPLE SLOTTED TB 9
 C1. 57.2958 TB 9
 C DFCR DRAG RATIO VS CORD RATIO TB 10
 C KEAPI2 KA VS ETA IB VS ALPHA / 2 PI TB 11
 C KEIFO2 KE VS ETA OB VS ETA IH TB 12
 C DCDCLP DEL CDCLP VS CLIFT RATIO TB 14
 C AVSPR MU S VS SPAN RATIO TB 15
 C XCPAR2 XCP/CPRIVE VS A/(PA/B+2) VS CORD RATIO TB 16
 C FCPEI2 ETA CENTER OF PRESSURE VS ETA IB VS ETA OB - ETA IB TB 17
 C DCART DEL CLF/ARF/R VS 2H/B VERTICAL LOCATION OF HORIZONTAL TAIL TB 18
 C.01745 1. TB 18
 C AKRYCY K VS RATIO Y/CY FOR PITCHING MOMENT TB 18
 C57.2958 1. TB 20
 C TABLES 21 AND 19 FOLLOW TABLE 4 TB 22
 C CLIAS2 CLINT VS ALPHA VS SIGMA, ENGINE VECTOR ANGLE. TB 22
 C1. 57.2958 57.2958 TB 22
 C DCLI3 DELTA CLINT VS ALPHA VS SIGMA VS DELTA X/C, U NOZZLE POSITION TB 23
 C1. 57.2958 57.2958 TB 23
 C CCI2 CPINT VS NACELLE COORDINATE XNACEL VS SIGMA VS CLINT TB 24
 C1. 1. 57.2958 TB 24
 C CMI2 CMINT VS NACELLE COORDINATE XNACEL VS ISGMA VS CLINT TB 25
 C1. 1. 57.2958 TB 25
 C DEPS3 DEPSILON, DOWNWASH INTERFERENCE VS ALPHA VS SIGMA VS CJ, INKJ TB 26
 C.01745 57.2958 57.2958 TB 26
 C DCLIG2 DCINT, CHANGE IN CLINT VS SIGMA VS RATIO OF WING HEIGHT TO SPAN TB 27
 C1. 57.2958 1. TB 27
 C DCMIG2 DCMINT, CHANGE IN CMINT VS RATIO WING HEIGHT/WSPAN VS SIGMA TB 28
 C1. 57.2958 1. TB 28
 C DCDIG2 DCDINT, CHANGE IN CDINT VS RATIO WING HEIGHT/WSPAN VS SIGMA TB 29
 C1. 57.2958 1. TB 29
 C * * * * * END TABLE NOMENCLATURE
 COMMON /INTARC/IU, IN, IO, ICR, NPTRL, IP
 REAL KEAPI2, KEIFO2, LAMETA
 COMMON
 ACRES2(77), ACRFD2(77), ADCRA2(77), LAMETA(30),
 1ADLFCK(30), DCLACC(30), DCLACS(30), DCLCKR(30), DCLACM(30),

```

2DCDTEF(30),DCDTFT(30),FDRCR(30),KEAPI2(77),NEIEU2(77),DCDCLR(30),
3AMSR(30),XCPAR2(77),ECPFI2(77),DCABT(30),ANKYCY(30),BNCLE2(77),
4FLTAS2(77),DCLT3(182),CMI3(231),CMT3(231),DEPS3(182),DCLIG2(77),
5DCMIG2(77),DCDIG2(77)
DIMENSION TRLS(1000)
EQUIVLFNCF(ACRES2,TRLS)
IUTMP = IU
IH = IN
CALL TBLRP(NT1,1,ACRES2)
CALL TBLRP(NT13,13,ACRF2)
CALL TBLRP(NT2,2,ADGRA2)
CALL TBLRP(NT3,3,LAMETA)
CALL TBLRP(NT4,4,ADLECR)
CALL TBLRP(NT21,21,PKCLE2)
CALL TBLRP(NT19,19,DCLACC)
CALL TBLRP(NT5,5,DCLACS)
CALL TBLRP(NT6,6,DCLRCR)
CALL TBLRP(NT7,7,DCLACM)
CALL TBLRP(NT8,8,DCDTFD)
CALL TBLRP(NT9,9,DCDTFT)
CALL TBLRP(NT10,10,FDRCR)
CALL TBLRP(NT11,11,KEAPI2)
CALL TBLRP(NT12,12,KEIEO2)
TABLE 13 FOLLOWS TABLE 1
CALL TBLRP(NT14,14,DCDCLR)
CALL TBLRP(NT15,15,AMBR)
CALL TBLRP(NT16,16,XCPAR2)
CALL TBLRP(NT17,17,ECPFI2)
CALL TBLRP(NT18,18,DCABT)
TABLE 19 FOLLOWS TABLE 5
CALL TBLRP(NT20,20,AKRYCY)
TABLE 21 FOLLOWS TABLE 4
CALL TBLRP(NT22,22,CLIAS2)
CALL TBLRP(NT23,23,DCLIA)
CALL TBLRP(NT24,24,CMI3)
CALL TBLRP(NT25,25,CMI3)
CALL TBLRP(NT26,26,DEPS3)
CALL TBLRP(NT27,27,DCLIG2)
CALL TBLRP(NT28,28,DCMIG2)
CALL TBLRP(NT29,29,DCDIG2)
TABLES READ FROM PERM FILE. DO NOT RECREATE PERM FILE.

```

```

111 = IUTMP
IF(ICR.EQ. 0) RETURN
REWIND 111
BUFFER OUT (IU,1) (TRLS(1),TRLS(3000))
IF (UNIT(IU)) 50,60,60
50 REWIND IU
60 RETURN
END
SUBROUTINE TRLRP(NTX,NTI,TARLF)
C THIS ROUTINE CALLS ROUTINES INTAB AND OUTTAB TO READ AND PRINT TABLES
C NTX INTEGER VARIARLF WHERE X IS THE TABLE NUMBER -INPUT
C NTT INTEGER CONSTANT, TARLF NUMBER -INPUT
C TARLF ARRAY IN WHICH THE TABLE IS STORED -OUTPUT
COMMON /INTARC/IU,IN,IU,ICR,NPTBL,IP
C IF TABLES ARE READ FROM TAPE OR DISK, PRINT THEM ONLY.
IF (ICR .EQ. 0) GO TO 10
NTX = INTAR(TARLF)
IF(NTX .LE. 0) CALL TBOMB(NTX,TABLE,NTI)
10 IF(IP .NE. 0) IFR = OUTTAB(0,TABLE)
IF(IP .NE. 0 .AND. IER .NE. 0) WRITE(IU,1) NTI,IER
1 FORMAT(50H1TROUBLE HAS BEEN ENCOUNTERED WITH PRINTING TABLE ,I3,
1/20HOUTAR ERROR FLAG = ,I2 )
RETURN
END
SUBROUTINE PTRINT(NT)
C THIS ROUTINE CREATES A BACKUP FILE FOR TABULAR FUNCTIONS, STORED IN
COMMON. IT UPDATES THE PERMANENT FILE OF TABLES OR SAVES A BACKUP
C FILE, IF PROBLEMS OCCUR IN READING TABLE MODS IN SUBROUTINE RDEFTB.
C
REAL KEAPI2,KEIEO2,LAMETA
COMMON
ACRES2(77),ACRFD2(77),ADCRA2(77),LAME1A(30),
1ADLFER (30),DCLACC(30),DCLACS(30),DCLKCK(30),DCLACM(30),
2DCDTEF(30),DCDTEI(30),FORCK(30),KEAPI2(77),KEIEJ2(77), DCDCLK(30),
3AMSBR(30),XCPAR2(77),FCPEI2(77),DCABT(30),AKRYCY(30),BKCLE2(77),
4CLIAS2(77),DCLI3(182),CMI3(231),CMT3(231),DEPS3(182),DCLIG2(77),
5DCMIG2(77),DCDIG2(77)
COMMON /INTARC/IU,IN,IU,ICR,NPTBL,IP
DIMENSION TRLS(3000)
EQUIVALENCE (ACRES2,TRLS)
C TRLS IS USED TO TRANSFER ENTIRE BLOCK OF TABLES IN COMMON

```

```

1  FORMAT(61H)THE FOLLOWING PERMANENT TABLES ARE BEING REVISED AS FOL
1  LWS )
2  FORMAT(44H)PARITY OR EOF ON RUFFER STATEMENT IN PTRUDT (// )
   REWIND IU
   REWIND 7
   IF(ICR .NE. 0) GO TO 10
   BUFFERIN(IU,1) (TRLS(1),TBL5(3000))
   IF(UNIT(IU))10,8,8
R   WRITE(IO,2)
10  BUFFER OUT (7,1)(TRLS(1),TBL5(3000))
C   READ TABLES TO BE CHANGED
   WRITE(IO,1)
   CALL RDEFTR(NT,IEF)
   IF(IEF .EQ. 1) GO TO 20
C   WRITE MODIFIED PERMANENT TABLES TO IU
   REWIND IU
14  BUFFER OUT (IU,1)(TRLS(1),TRLS(3000))
15  IF(UNIT(IU)) 15,14,14
16  WRITE(IO,2)
17  RETURN
20  CALL ONSW(7)
C   SWITCH TO BACKUP FILE 7 FOR TABLES
   IU = 7
   RETURN
   END
SURROUTINE TRUMR(NPTS,ARY,NT)
C   THIS ROUTINE SETS A FLAG, ILOST, TO 1, IF AN ERROR OCCURRED WHILE
C   READING A TABLE FROM CARDS.
C
C   NPTS   ERRONEOUS NUMBER OF POINTS, RETURNED BY INTAR.
C   ARY    ARRAY CONTAINING TABLE (INCORRECT)
C   NT     TABLE NUMBER
C   ILOST  FLAG IN COMMON. = 0, NO PROBLEM. = 1 - JOB MUST BE ABORTED.
C
   REAL XFAPI2,KFTFO2,LAMETA
   COMMON      ACRES2(77),ACRFD2(77),ADCRA2(77),LAMETA(30),
1ADLECR (30),DCLACC(30),DCLACS(30),DCLRCR(30),DCLACM(30),
2DCDTFD(30),DCDTFT(30),FDRCR(30),KEAPI2(77),KEIEU2(77), DCDCLK(30),
3AMSPR(30),XCPAR2(77),FCPI2(77),DCABT(30),AKKYCY(30),RKCCLF2(77),
4CLTAS2(77),DCLJ3(182),CMI3(231),DEPS3(182),DCLIG2(77),
5DCMIG2(77),DCDIG2(77)

```

```

COMMON /TROMR/ ILOST
COMMON /INTARC/IO,IN,IO,ICK,NPBL,IP
COMMON /OUTAPG / IOT
ILOST = 1
WRITE(IO,1) NT,NPTS
FR = OUTTAB(50,ARY)
RETURN
FORMAT(25HIERROR IN INPUT DATA, TABLE NUMBER ,13,16FIDAL POINT COUNT
IT , 15, /20H TABLF FOLLOWS (50 LOCATIONS) )
END
SURROUTINE (ASIN1)

```

HILIFT INPUT ROUTINE P.J. REIG 12/72

CARD C01 TITLE

TITLE 72 CHARACTER TITLE FOR EACH CASE

PART 1 - FREE AIR SECTION 1, COEFFICIENT OF LIFT

CARD C02 FLAP TYPE

FLAP FLAP TYPE 1-SINGLE SLOT, 2-DOUBLE SLOT, 3-DOUBLE SLOT, DBLE HINGE
4-TRIPLE SLOTTED

ATTBL = NTTBL - NUMBER OF TEMPORARY TABLE UPDATES

CARDS C03 TEMP TABLES

** SEE SECTION 2 FOR FORMAT OF TABULAR DATA

CARD C04 GEOM CL

WGROSS GROSS WING AREA
WREF REFERENCE WING AREA
WSPAN WING SPAN
WPERMT SEMI PERIMETER OF WING GROSS AREA

CARD C05 TYP 1 - 4

C CPRTIME WING CHORD NORMAL TO 1/2 CHORD LINE WITH FLAPS
 C CFLAP FLAP CHORD NORMAL TO 1/2 CHORD LINE SINGLE SLOT
 C ACORD ALPHA SWEEP ANGLE OF WING 1/4 CHORD LINE.
 C AHCORD ALPHA SWEEP ANGLE OF WING 1/2 CHORD LINE.
 C AHLAFT ALPHA SWEEP ANGLE OF AFT HINGE LINE.
 C CARD C06 NO. FLAP ANGLES
 C ADFLAP = NDFLAP - NUMBER OF FLAP DEFLECTIONS - MAXIMUM OF 4.
 C ** CARD C07 TYPE 1+2
 C DFLAP FLAP DEFLECTION, TYPE 1 AND 2. ARRAY
 C CARD C07 TYPE 3+4
 C OFFWD FWD FLAP DEFLECTION, TYPE 3 AND 4. ARRAY
 C REAFT AFT FLAP DEFLECTION, TYPE 3 AND 4. ARRAY
 C ** CARD C08 TYPE 3+4
 C CARD 9 NEEDED FOR FLAP TYPES 3 AND 4
 C CFWD FORWARD FLAP CHORD MEASURED STREAMWISE.
 C CPFLAP FORWARD FLAP CHORD MEASURED NORMAL TO 1/2 CHORD LINE.
 C CAFT AFT FLAP CHORD MEASURED NORMAL TO 1/2 CHORD LINE.
 C AHLEND ALPHA SWEEP ANGLE OF FORWARD HINGE LINE.
 C CARD C09 TYPE 1 - 4
 C ETEIN NON DIMENSIONAL WING SEMI SPAN TO INBOARD FLAP EDGE (ETA) T.E.
 C ETEOUT NON DIMENSIONAL WING SEMI SPAN TO OUTBOARD FLAP EDGE (ETA) T.E.
 C CARD C10 1 CL 1
 C CLFEDGE LEADING EDGE FLAP CHORD NORMAL TO 1/4 CHORD LINE
 C CHORD WING CHORD NORMAL TO 1/4 CHORD LINE
 C DLEDGE LEADING EDGE FLAP DEFLECTION, NORMAL TO HINGE LINE (DELTA)
 C FLEIN NON DIMENSIONAL WING SEMI SPAN TO INBOARD EDGE OF LEADING EDGE GLAPS
 C FLEOUT NON DIMENSIONAL WING SEMI SPAN TO OUTBOARD EDGE OF LEADING EDGE GLAPS
 C CARD C11 1 CL 2
 C CLAFU COFF OF LIFT FLAPS UP

C ACLEU ANGLE OF ZERO LIFT FLAPS UP
 C CLMAXJ MAX LIFT FLAPS UP
 C ALPHAI INITIAL ANGLE OF ATTACK
 C DALPHA INCREMENT TO ALPHA TO CLMAX
 C CHRDLF WING CHORD INCL FOWLER ACTION OF TE NORMAL TO LE

 C CARD C12 2 CLMAX

 C PART I FREE AIR, SECTION 2 CLMAX

 C CLENLF CHORD LFNGLTH OF LEADING EDGE DEVICE, NORMAL TO L.E.
 C CRONLF TOTAL WING CHORH LENGTH, NORMAL TO L.E.
 C DWTE DELTA (INCREASE) IN WING AREA T.E. FLAP
 C DWLF DELTA (INCREASE) IN WING AREA L.E. FLAP
 C WPGROS BASIC WING AREA INBOARD OF OUTBOARD EDGE OF T.E. FLAP
 C CULE LEADING EDGE FLC MOMENTUM COEFFICIENT
 C AEDGE = IEDGE LEADING EDGE TYPE =1 CONVENTIONAL =2 SHAPED

 C CARD C13 3 CDRAE

 C PART I FREE AIR, SECTION 3 DRAG

 C WGFELAP FLAPPED WING AREA
 C SPANLF AREA OF L.E. DEVICE
 C CRDDPM CHORD, C FOURLF PRIME, INCLUDING LEADING EDGE EXT, NORMAL TO LE
 C CDPMFU MINIMUM DRAG, FLAPS UP

 C CARD C14 4 CM 1

 C PART I FREE AIR SECTION 4 PITCHING MOMENT

 C CM0 PITCHING MOMENT FOR ZERO LIFT
 C APOCHD SWFFP ANGLE, PRIME OF QUARTER CHORD
 C XAC AERODYNAMIC CENTER OF BASIC WING TRAPEZOID
 C S2 AREA OF TRAPEZOID BETWEEN IB AND OB FLAP EDGES OF LEADING EDGE FLAPS.
 C DSLE DELTA S, CHANGE IN AREA LE
 C S2 AREA OF TRAPEZOID BETWEEN IB AND OB FLAP EDGES OF TRAILING EDGE FLAPS

 C CARD C15 4 CM 2

C ALE FLAPS ADJACENT TO BODY SIDE OR WOT. =1, YES, =2,NO LE
 C ATF FLAPS ADJACENT TO BODY SIDE OR WOT. =1, YES, =2,NO TE
 C
 C CARD C16 4 CM 3
 C
 C * * LEADING EDGE DEVICE DATA FOR AERODYNAMIC CENTERS OF PRESSURE
 C
 C CHDYB STREAMWISE CHORD AT THE BODY SIDE
 C XB LOCATION OF LEADING EDGE OF CHDYB FROM THE STANDARD ORIGIN
 C CHDPYB STREAMWISE CHORD AT THE BODY SIDE WITH THE LE FLAP EXTENDED
 C
 C XPR X PRIME BODY SIDE - LOCATION OF THE LEADING EDGE OF CHDPYB WITH LE EXT
 C YB Y BODY SIDE - SPANWISE LOCATION OF THE LEADING EDGE AT THE BODY SIDE
 C YM Y MID SPAN SPANWISE LOCATION OF THE LEADING EDGE AT MIDSPAN LE FLAP
 C
 C CARD C17 4 CM 4
 C
 C CHDYM STREAMWISE CHORD THROUGH YM AT MIDSPAN
 C XM X MID SPAN - LOCATION OF LEADING EDGE OF CHDYM
 C CHDPYM STREAMWISE CHORD PRIME AT MID SPAN WITH LE EXTENDED
 C XPM X PRIME MID SPAN - LOCATION OF LEADING EDGE OF CHDPYM
 C
 C * * TRAILING EDGE DEVICE DATA FOR AERODYNAMIC CENTERS OF PRESSURE
 C
 C CARD C18 4 CM 5
 C
 C CHDYBT STREAMWISE CHORD AT BODY SIDE = CHDYB
 C XRTE XB - LOCATION OF THE LEADING EDGE OF CHDYBT
 C CDPYBT STREAMWISE CHORD PRIME BODY SIDE WITH TE EXTENDED
 C XPBTE X PRIME BODY SIDE - LOCATION OF LEADING EDGE OF CDPYBT = XBTE
 C YBTE Y BODY SIDE -SPANWISE LOCATION OF THE STREAMWISE BODYSIDE CHORD,CHDYBT
 C YMBTE Y MID SPAN - SPANWISE LOCATION OF THE STREAMWISE MIDSPAN CHORD,CHDYMT
 C
 C CARD C19 4 CM 6
 C
 C CHDYMT STREAMWISE CHORD MID SPAN OF TE FLAP
 C XMTE X MID SPAN - LOCATION OF LEADING EDGE OF CHDYMT
 C CPMTE CHORD PRIME AT MID SPAN WITH TE EXTENDED
 C XPMTE X PRIME MID SPAN - LOCATION OF LE OF CPMTE = XMTE

CARD C20 4 CM 7

CREE REFERENCE CHORD LENGTH
 CFLIR FLAP CHORD NORMAL TO HALF CHORD LINE AT INBOARD EDGE OF TE FLAP
 CFLOR FLAP CHORD NORMAL TO HALF CHORD LINE AT OUTBOARD EDGE OF TE FLAP
 CPMOR C PRIME - CHORD NORMAL TO 1/2 CHORD LINE OUT BOARD EDGE OF TE FLAP, I
 CPMIR C PRIME - CHORD NORMAL TO 1/2 CHORD LINE IN BOARD EDGE OF TE FLAP, INCL

CARD C21 4 CM 8

CPFLIR FLAP CHORD I.B. NORMAL TO 1/2 CHORD LINE
 CPFLOR FLAP CHORD O.B. NORMAL TO 1/2 CHORD LINE
 XIB LONGITUDINAL INTERSECTION CPMIR AND WING 1/2 CHORD LINE I.B.
 XOR LONGITUDINAL INTERSECTION CPMOR AND WING 1/2 CHORD LINE O.B.
 XPCORD X PRIME - LOCATION OF 1/4 AERODYNAMIC CHORD, INCL LEAPING EDGE
 XCG LONGITUDINAL LOCATION OF CENTER OF GRAVITY

CARD C22 4 CM 9

CMOLEFU PITCHING MOMENT ZERO LIFT, FLAPS UP.
 CPTEOR ETA PRIME TE OR, WING SEMISPAN, LONGITUDINAL LOCATION OF CPMOB
 AND HALF CHORD LINE
 CPTEIR ETA PRIME TE IR, WING SEMISPAN, LONGITUDINAL LOCATION OF CPMIB
 AND HALF CHORD LINE

CARD C23 5 6 7 GE

THGM HEIGHT OF TAIL 1/4 MAC ABOVE OR BELOW WING CHORD PLANE

PART II GROUND EFFECT SECTION 6 LIFT
 PART II GROUND EFFECT SECTION 7 MAX LIFT

TLGM TAIL LENGTH WING 1/4 MAC TO TAIL 1/4 MAC

NMWHM NUMBER OF WING HEIGHTS TO BE CONSIDERED. MAXIMUM OF FOUR.
 WHQM ARRAY OF WING HEIGHTS 1/4 MAC

CARD C24 8 TRIMGE

PART II GROUND EFFECT SECTION 8 DRAG

STATL HORIZONTAL TAIL AREA
 FPSC DOWNWASH ANGLE AT TAIL AT ZERO ALPHA.
 DFPDAL RATE OF CHANGE OF DOWN WASH ANGLE AT TAIL, FLAPS UP VS DALPHA.
 DCPOMN TAIL MINIMUM DRAG COEFF
 DCDDCL CHANGE IN TAIL DRAG DUE TO TAIL LIFT

CARD C25 0 POWER 1

CDRAM RAM DRAG
 ENGVFC SIGMA, ENGINE VECTOR ANGLE FROM THE HORIZONTAL IN DEG
 XNACEL X COORDINATE OF NACELLE FROM AN ARBITRARY ORIGIN
 XNOZLF X COORDINATE OF NOZZLE FROM AN ARBITRARY ORIGIN
 ZNOZLF Z COORDINATE OF NOZZLE FROM AN ARBITRARY ORIGIN
 XINLET X COORDINATE OF INLET FROM AN ARBITRARY ORIGIN
 ZINLET Z COORDINATE OF INLET FROM AN ARBITRARY ORIGIN

CARD C26 0 POWER 2

NCJ NUMBER OF ENGINE THRUST COEFFICIENTS ON INPUT CARD (MAX 5)
 ACJ ARRAY OF VALUES OF ENGINE THRUST COEFFICIENTS

COMMON /CASEIN/ TITLE(18), IFLAP, WGRUSS, WKEF, WPERMT, INDFLAP,
 ACPRIME, CFLAP, DFLP(4), CFWD, CPFLAP, CAFT, OFFWD, DPAFT, ACCORD, AHCURD,
 1AHLFWD, AHLAFT, ETEIN, ETEOUT, CLEDGE, CHORD, DLEDGF, ELEIN, ELEOUT, CLAFU,
 2ADLFU, CLENLF, CRDNLF, WPGROSS, DWTE, DWLE, CLMAXU, ALPHA1, CULE, DALPHA,
 3WGLAP, SPANLE, CHRDLE, XCP1, XCPLE, XCP2, XCP2TE, XAC, S2, DSLE, S3, CPMOB
 4, XCG, CREF, CFLIR, CFLOH, CPMIB, CPHLIR, CPFLUB, XIB, XV8, EPTTEIN, XPCCKD,
 5CMOLFU, WHQM(3), NWTNGH, THUM, WSPAN, TLUM, STAIL, EPSFU, DCPDMN, DCDDCL
 6, CHDYR, CHDPYR, CMO, APJCHD, XPB, XB, YB, YM, CHDYM, XM, CHDPYM, XPM, IEDGE
 7, CHDYPT, XBTE, CDPYRT, XPBTF, YBTE, YMTF, CHDYMT, XMTTE, CPMTE, XPMTE
 8, DFLAP, DFFW(4), DPAF(4), CRDUPM, CDPMFU, EPTTECB, EP50, DFPDAL
 9, CJ, ENGVFC, XNACEL, XNOZLE, ZNOZLE, XINLET, ZINLET, CDRAM, ILE, ITE
 COMMON /INTARC/ IU, IN, IG, ICR, NPTBL, IP
 COMMON /IPAGE/ IPAGE, ICASE
 COMMON /CJ/ NCJ, ACJ(5)
 COMMON TRLS(3000)

COMMON/BASIC/ARATIO,PI,RAD,ARFF

DATA IPAGE/1/

1 FORMAT(10F7.0)

2 FORMAT(10I7)

3 FORMAT(J8A4)

4 FORMAT(1H1,/,115X,4HPAGE,13)

5 FORMAT(1H0,50X,18A4////)

6 FORMAT(43H0 WING S WING REF SPAN PERIMETER)

7 FORMAT(1X, 10(F7.2,4X))

8 FORMAT(1X,10(FR.2,2X))

9 FORMAT(1X,10(FR.3,3X))

10 FORMAT(1X, 3(F7.2,4X), 7(F7.3,4X))

11 FORMAT(1X, F9.3, F14.1,6X,F7.3,4F10.2)


```

60 READ(IN,1) WGRSS,WREF,WSPAN,WPERMT
   WRITE(IO,6)
   WRITE(IO,8)WGRSS,WREF,WSPAN,WPERMT
   WRITE(IO,17)
   READ(IN,1) CPRIME,CFLAP,AGCORD,AHCORD,AHLAFT
   WRITE(IO,7) CPRIME,CFLAP,AGCORD,AHCORD,AHLAFT
   READ(IN,1) ADFLAP
   NDFLAP=ADFLAP
   IF (IFLAP.GT.2) GO TO 70
   WRITE(IO,36) (I,I=1,NDFLAP)
   READ(IN,1) (DFLP(I),I=1,NDFLAP)
   WRITE(IO,37) NDFLAP, (DFLP(I),I=1,NDFLAP)
   GO TO 80

70 WRITE(IO,35) (I,I=1,NDFLAP)
   READ(IN,1) (DFFW(I),DFAF(I),I=1,NDFLAP)
   WRITE(IO,37) NDFLAP,(DFFW(I),DFAF(I),I=1,NDFLAP)
   WRITE(IO,29)
   READ(IN,1) CFWD,CPELAP,CAFT,AHLEWD
   WRITE(IO,7) CFWD,CPELAP,CAFT,AHLEWD
   CONTINUE

80 WRITE(IO,18)
   READ(IN,1) ETEIN,ETEOUT
   WRITE(IO,9) ETEIN,ETEOUT
   WRITE(IO,19)
   READ(IN,1) CLEDGE,CHORD,DLEDGE,ELEIN,ELEOUT
   WRITE(IO,10) CLEDGE,CHORD,DLEDGE,ELEIN,ELEOUT
   WRITE(IO,31)
   READ(IN,1) CLAFU,AULFU,CLMAXU,ALPHA1,DALPHA,CHRDLE
   WRITE(IO,11) CLAFU,AULFU,CLMAXU,ALPHA1,DALPHA,CHRDLE
   WRITE(IO,20)
   READ(IN,1) CLENLF,CRDNLE,DWTE,DWLE,WPKRUS,CULE,AEDGE
   WRITE(IO,30) CLENLF,CRDNLE,DWTE,DWLE,WPKRUS,CULE,AEDGE
   IEDGE=AEDGE
   WRITE(IO,21)
   READ(IN,1) WGFLAP,SPANLE,CRDDPM,CDPMFU
   WRITE(IO,9) WGFLAP,SPANLE,CRDDPM,CDPMFU
   WRITE(IO,38)
   READ(IN,1) CMO,APQCHD,XAC,S2,DSLF,S3
   WRITE(IO,8) CMO,APQCHD,XAC,S2,DSLF,S3
   READ(IN,1) ALF,ATF
   ILF=ALF

```

```

ITF=ATF
WRITE(IO,41) ILF,ITF
WRITE(IO,39)
WRITE(IO,32)
READ(IN,1) CHDYB,XR,CHDPYB,XPB,YB,YM
WRITE(IO,7) CHDYB,XR,CHDPYB,XPB,YR,YM
WRITE(IO,22)
RFAD(IN,1) CHDYM,XM,CHDPYM,XPM
WRITE(IO,7) CHDYM,XM,CHDPYM,XPM
IPAGE=IPAGE+1
WRITE(IO,4) IPAGE
WRITE(IO,5) TITLE
WRITE(IO,40)
WRITE(IO,32)
RFAD(IN,1)
WRITE(IO,7) CHDYRT,XRTF,CDPYBT,XPrTF,YBTE,YMTE
WRITE(IO,22)
RFAD(IN,1) CHDYMT,XMTF,CPYMTF,XPMTE
WRITE(IO,7) CHDYMT,XMTF,CPYMTF,XPMTE
WRITE(IO,23)
RFAD(IN,1) CREF,CFLIB,CFLOB,CPMIB,CPMOB
WRITE(IO,8) CREF,CFLIB,CFLOB,CPMIB,CPMOB
WRITE(IO,24)
RFAD(IN,1) CPFLIR,CPFLOB,XIB,XOR,XPGCRD,XCG
WRITE(IO,7) CPFLIR,CPFLOB,XIB,XOR,XPGCRD,XCG
WRITE(IO,25)
RFAD(IN,1) CMOLFU,EPTIN,EPTEOB
WRITE(IO,9) CMOLFU,EPTIN,EPTEOB
WRITE(IO,26)
READ(IN,33) THQM,TLQM,NWINGH,(WHQM(I),I=1,NWINGH)
WRITE(IO,34) THQM,TLQM,NWINGH,(WHQM(I),I=1,NWINGH)
WRITE(IO,28)
RFAD(IN,1) STAIL,EP50,DEPDAL,DCPDMN,DCDDCL
WRITE(IO,9) STAIL,EP50,DEPDAL,DCPDMN,DCDDCL
WRITE(IO,43)
43 FORMAT( 77H0 RAM DRAG SIGMA ENG X NACELLE X NUZZLE Z NOZ
1ZLF X INLET Z INLET )
READ(IN,1) CDRAM,ENGVEC,XNACEL,XNOZLE,ZNOZLE,XINLET,ZINLET
WRITE(IO,8) CDRAM,ENGVEC,XNACEL,XNOZLE,ZNOZLE,XINLET,ZINLET
WRITE(IO,101)
101 FORMAT( 63H0NO. OF CJ CJ(1) CJ(2) CJ(3) CJ(4)

```

```

1 CJ(5) )
  READ(IN,160)NCJ,(ACJ(I),I=1,NCJ)
160 FORMAT(I7,5F7.0)
  WRITE (IO,102)NCJ,(ACJ(I),I=1,NCJ)
102 FORMAT(5X,I1,5X,5(F7.2,4X))
C SET CARD READER FLAG TO RESTORE TABLES
  ICR = 0
C * *
C * CONVERT ALL ANGLES TO RADIANS AND STORE IN SAME LOCATIONS
C * CONVERT FEET TO INCHES (AS READ) AND STORE IN SAME LOCS.
C * *
  AGCORD = AGCORD/RAD
  AHCORD = AHCORD/RAD
  AOLFU = AOLFU /RAD
  ALPHA1 = ALPHA1/RAD
  DALPHA = DALPHA/RAD
  APOCHD = APOCHD/RAD
  EPSO = EPSO /RAD
  DEPDAL = DEPDAL/RAD
  AHLAFT=AHLAFT/RAD
  IF (IFLAP.GT.2) AHLFWD=AHLFWD/RAD
  DLEDGE=DLEDGE/RAD
  ENGVEC=ENGVEC/RAD
  WSPAN =12.*WSPAN
  WPERMT =12.*WPERMT
  CPRIME =12.*CPRIME
  CFLAP =12.*CFLAP
  CPFLAP =12.*CPFLAP
  CAFT =12.*CAFT
  CLFDGF =12.*CLFDGF
  CHORD =12.*CHORD
  CHRDLE =12.*CHRDLE
  CLFNLF =12.*CLFNLF
  CRDNLE =12.*CRDNLE
  CRDDPM =12.*CRDDPM
  XAC =12.*XAC
  CHDYB =12.*CHDYB
  XR =12.*XR
  CHDPYB =12.*CHDPYB
  XPR =12.*XPR
  YR =12.*YR

```

```

YM          =12.*YM
CHDYM      =12.*CHDYM
XM         =12.*XM
CHDPYM     =12.*CHDPYM
XPM       =12.*XPM
CHDYRT    =12.*CHDYRT
XRTE      =12.*XRTE
CDPYRT    =12.*CDPYRT
XPRTF     =12.*XPRTF
YBTE      =12.*YBTE
YMTF      =12.*YMTF
CHDYMT    =12.*CHDYMT
XMTF      =12.*XMTF
CPYMTF    =12.*CPYMTF
XPMTF     =12.*XPMTF
CRFF      =12.*CRFF
CFLIR     =12.*CFLIR
CFLOB     =12.*CFLOB
CPMIR     =12.*CPMIR
CPMOR     =12.*CPMOR
CPFLIR    =12.*CPFLIR
CPFLOR    =12.*CPFLOR
XIR       =12.*XIR
XOR       =12.*XOR
YPCQRD    =12.*YPCQRD
XCG       =12.*XCG
THQM=12.*THQM
TLQM      =12.*TLQM
DO 200 II=1, NWINGH
WHQM(II) = 12.*WHQM(II)
XNOZLE =12.* XNOZLE
ZNOZLE =12.* ZNOZLE
XINLFT =12.* XINLFT
ZINLFT =12.* ZINLFT
IF(IFLAG.EQ.0) RETURN
WRITE(10,42)
IPAGE=IPAGE+1
GO TO 45
END

```

C RDEFTR REDEFINES NT TABLES IN THE COMMON BLOCK.

```

THE REPLACED TABLES ARE READ FROM THE CARD READER.
IFF - ERROR FLAG = 0 SUCCESSFUL READ.      = 1 UNSUCCESSFUL, SO DO NOT
UPDATE THE PERMANENT FILE TABLE.

REAL KFAP12,KFIFO2,LAMETA
COMMON
  ACRES2(77),ACKFD2(77),ADCKA2(77),LAMETA(30),
  1ADLCR (30),DCLACC(30),DCLACS(30),DCLRCR(30),DCLACM(30),
  2DCDTFD(30),DCDTFI(30),DRCR(30),KEAPI2(77),KFIFO2(77),DCDCLR(30),
  3KXSR(30),XCPAR2(77),FCPEI2(77),DCABT(30),ANKYCY(30),BNCLE2(77),
  4CLIAS2(77),DCLI3(182),CUI3(231),CMI3(231),DEPS3(182),DCLI32(77),
  5DCMIG2(77),DCDIG2(77)
INTEGER TNAME
FOR ADDITION OF NEW TABLES, UPDATE LENGTH OF TNAME, DATA ENTRIES AND DO IO
3 LATER - CHANGE FIRST DIMENSION OF TNAME AS TABLES ARE ADDED. ***
DIMENSION DUM(128),TRLS(3000),TNAME(29,2)
EQUIVALENCE (ACRES2,TRLS)
COMMON /INTARC/IU,IN,IO,ICR,NPTRL,IP
DATA TNAME
  16HDCLACC,6HDCLACS,6HDCLRCR,6HDCLACM,6HDCLTFD,6HDCLTFI,6HFDRCR,
  26HKEAPI2,6HKEIFE02,6HCDCLR,6HMSBR,6HXCPAR2,6HECPEI2,6HDCABT,
  36HAKRYCY,6HBKCLE2,6HCLIAS2,6HDCLI3,4HCDI3,6HDEPS3,6HDCLI32,
  45HDCMIG2,6HDCDIG2,
  51,78,155,232,262,292,322,382,412,442,472,502,579,656,686,716,
  6793,870,900,930,1007,1084,1266,1497,1728,1910,1937,2064,2141 /
ITMP = IU
IU = IN
FORMAT(10A7)
FORMAT(41H)NO MATCH FOUND FOR PERMANENT TABLE NAME , A12,
1 55H)THE TABLE FOLLOWS, BUT IS NOT BEING USED FOR THIS RUN. )
FORMAT(34H)TABULAR DATA FOR PERMANENT TABLE , A12/,71H IS IN ERRO
1R. OLD BACKUP FILE OF TABLE WILL BE USED. CORRECT INPUT. /
228H FIRST CARD OF TABLE FOLLOWS )
DO 100 K = 1,NT
READ(IN,1) NAME
DO 10 I=1,29
  II=I
  IF(NAME.EQ.TNAME(I,1))GO TO 20
10 CONTINUE
C NO MATCH FOUND.
WRITE(10,2)NAME
N =INTAR(DUM)

```

```

FR = OUTTAB(0,NUM)
GO TO 100
C TABLE NAME FOUND
20 INAM = TNAME(II,2)
N = INTAB(TPLS(INAM))
IF(N.GT.0)GO TO 30
C ERROR ON PERMANENT UPDATE READ. PERM FILE CANNOT BE UPDATED. SET FLAG
IEF = 1
WRITE(IO,3) NAME, N
ER = OUTTAB(0,TRLS(INAM))
GO TO 100
30 ER = OUTTAB(0,TRLS(INAM))
100 CONTINUE
IU = ITEMP
RETURN
END
SUBROUTINE CASOUT(IMODE,WINGH)
C THIS ROUTINE PRINTS OUT THE RESULTS FOR EACH CASE AFTER IT IS
C COMPUTED.
C
C IMODE 1 - FIRST ENTRY BASIC DATA, FREE AIR, GROUND EFFECT WINGH(1)
        = 2 - GROUND EFFECT WINGH(2),ETC.
C WINGH WHQM(I), J=1 FOR IMODE(1), ETC.
C
C CLAFU LIFT CURVE SLOPE FLAPS UP
C CLAFD LIFT CURVE SLOPE FLAPS DOWN
C CLTO COEF LIFT TAIL OFF FREE AIR
C AOLFU ANGLE OF ATTACK FOR ZERO LIFT - FLAPS UP
C LFD ANGLE OF ATTACK FOR ZERO LIFT - LE DOWN
C TFD ANGLE OF ATTACK FOR ZERO LIFT - TE DOWN
C FDFD ANGLE OF ATTACK FOR ZERO LIFT - BOTH DOWN
C DCLBFD FLAP LIFT INCREMENT BOTH FLAPS DOWN
C CLMAXU MAX LIFT FLAPS UP
C CLMAXD MAX LIFT FLAPS DOWN
C CDPMEU MINIMUM DRAG FLAPS UP
C DCOTE MINIMUM DRAG INCREMENT TE FLAPS
C DCOLE MINIMUM DRAG INCREMENT LE FLAPS
C CMOLFU ZERO LIFT PITCHING MOMENT INCREMENT TE
C DCMOTE ZERO LIFT PITCHING MOMENT INCREMENT LE
C DCMOLF ZERO LIFT PITCHING MOMENT BOTH FLAPS DOWN

```

```

C CLMAXG MAX LIFT IN GROUND EFFECT - ARRAY FOR SEVERAL WING HEIGHTS
C ALPHA INITIAL ANGLE OF ATTACK FOR LIFT,DRAG, MOMENT COEFFICIENTS
C DALPHA INCREMENT TO ALPHA
C NALPHA NUMBER OF INCREMENTS TO ALPHA
C
C CLTOG COEF LIFT TAIL OFF GROUND EFFECT
C CLTRG COEF LIFT TRIMMED GROUND EFFECT
C CLTRG COEF LIFT TAIL OFF FREE AIR
C CDTO COEF DRAG TAIL OFF FREE AIR
C CDTOG COEF DRAG TAIL OFF GROUND EFFECT
C CDTRG COEF DRAG TRIMMED GROUND EFFECT
C CDTR COEF DRAG TRIMMED FREE AIR
C
C CMTO COEF PITCHING MOMENT TAIL OFF FREE AIR
C CMTOG COEF PITCHING MOMENT TAIL OFF GROUND EFFECT
C CMTRG COEF PITCHING MOMENT TRIMMED GROUND EFFECT
C CMTR COEF PITCHING MOMENT TRIMMED FREE AIR
C
COMMON /INTARC/1U,IN,IO,ICR,NPTBL,IP
COMMON /IPAGE/ IPAGE,ICASE
COMMON /CJ/NCJ,ACJ(5)
COMMON /CASEIN/ TITLE(18),IFLAP,WGRUSS,WKEF,WPERKI,NDFLAP,
ACPRIME,CFLAP,DFLAP(4),CFWD,CPFLAP,CAFT,DFEWD,DFEFT,ACURD,ATCURD,
1AHLFWD,AHLAFT,FEIN,FEOUT,CEDGE,CHUKD,DLEGGF,ELEIN,ELEOUT,CLAFU,
2AOLFU,CLENLE,CRDNLE,WGRUS,DWTE,DWLE,CLMAXU,ALPHA1,CULLE,DALPHA,
3WGLFAP,SPANLE,CHKDLF,XCP1,XCPLE,XCP2,XCP2TE,XAC,S2,DSLLE,S3,CPMUB
4,XCG,CREF,CFLIR,CFLOR,CPMIB,CPFLIR,CPFLUB,XIB,XUB,EPTEIN,XPCCKD,
5CMOLFU,WHQM(3),NWINGH,THUM,WSPAN,TLOW,STAIL,EPSPU,DCPDMM,DCDDCL
6,CHDYR,CHDPYR,CMU,AP,UCHD,XPB,XB,YR,YM,CHDYMT,XM,CHDPYM,XPM,IEDGF
7,CHDYRT,XBTE,COPYRT,XPBT,YBTE,YMTF,CHDYMT,XMTE,CPYMT,XPMTE
8,DFLAP,DFEW(4),DFAF(4),CRDDPM,CDPMFU,EPTEOB,EPSO,DFPDAL
9,CJ,ENGVEC,XNACFL,XNOZLE,ZNOZLE,XINLET,ZINLET,CDKAM,ILE,ITE
COMMON /OUTPUT/ NALPHA,CLAFD,AULLFD,AULTFD,AULBFD
1,DCLBFD,CLMAXD, DCOTE,DCULE,DCMOTE,DCMOLE,CDFATR(20),
2CMOBFD,CLMAXG(3)
COMMON /OUTPUT/ ALPHA(20),CLTU(20),CDTU(20),CMTU(20),CLTK(20),
1CDTR(20),ALPHAG(20),CLTOG(20),CLTOG(20),CMTUG(20),CLTRG(20)
1,CDTRG(20),CLPOFA(20),CLINT(20),CDPOFA(20),CMPOFA(20),DLPOFA(20),
5CLPOGE(20),CDPOGE(20),CMPOGE(20),CLUEIR(20),CDUEIR(20),CLFATR(20)
DATA DFG /57,295779/
FORMAT(1H), 115X, 5HPAGE ,I2)
2 FORMAT(/// 40X,28ANGLES OF ATTACK - ZERO LIFT / 49X,28(IH-))//

```


PRINT BASIC DATA WHICH REMAINS CONSTANT FOR THIS CASE.

```

IPAGE = IPAGE+1
WRITE (IO,1) IPAGE
WRITE (IO,15) TITLE
WRITE (IO,2)
WRITE (IO,3) AOLEF,AOLLEF,AULTED,AOLMED
WRITE (IO,7)
ZZ=CLAFD/DEG
WRITE (IO,4) CLAFU,ZZ ,DCLBFD,CLMAXU,CLMAXD
WRITE (IO,8)
WRITE (IO,5) CORMEU,DCOTE,DCDLE
WRITE (IO,9)
WRITE (IO,14) CMOLFU,DCMOTE,DCMOLE
    
```

FREE AIR TABLE ALPHA VS COEFFICIENTS

```

IPAGE=IPAGE+1
WRITE (IO,1) IPAGE
WRITE (IO,15) TITLE
WRITE (IO,101)
WRITE (IO,10)
WRITE (IO,11)
IF (IFLAP.LE.2) WRITE (IO,16) ZERU, DS, ZERU
IF (IFLAP.GT.2) WRITE (IO,17) FERU, DF, DA, ZERU
WRITE (IO,13)
DO 50 I=1,NALPHA
50 WRITE (IO,104) ALPHA(I),CLTU(I),CRTU(I),CMTU(I),CLTR(I),CTR(I)
    
```

```

IPAGE=IPAGE+1
WRITE (IO,1) IPAGE
WRITE (IO,15) TITLE
WRITE (IO,102)
WRITE (IO,10)
WRITE (IO,11)
IF (IFLAP.LE.2) WRITE (IO,16) CJ,DS,ZERU
IF (IFLAP.GT.2) WRITE (IO,17) CJ,DF,DA,ZERU
WRITE (IO,13)
DO 51 I=1,NALPHA
WRITE (IO,104) ALPHA(I),CLPUFA(I),CMPUFA(I),CLFATR(I),
1 CFEATR(I)
51 CONTINUE
    
```

```

C GROUND EFFECT TABLE ALPHA VS COEFFICIENTS
C TMODE - SUBSCRIPT OF WING HEIGHT
C
200 IPAGE = IPAGE + 1
   WRITE(IO,1) IPAGE
   WRITE (IO,15)TITLE
   WRITE (IO,101)
   WRITE (IO,12)
   WRITE (IO,11)
   IF (IFLAP.LE.2) WRITE (IO,16)ZERO, DS, WOB
   IF (IFLAP.GT.2) WRITE (IO,17)ZFKO, DF, DA, WOB
   WRITE (IO,13)
C
DO 210 I=1,NALPHA
210 WRITE (IO,104)ALPHAG(I),CLTUG(I),CDTUG(I),CDTUG(I),CLTRG(I),
      1 CDTRG(I)
C
   IPAGE=IPAGE+1
   WRITE (IO,1)IPAGE
   WRITE (IO,15)TITLE
   WRITE (IO,102)
   WRITE (IO,12)
   WRITE (IO,11)
   IF (IFLAP.LE.2) WRITE (IO,16)CJ,DS,WOB
   IF (IFLAP.GT.2) WRITE (IO,17)CJ,DF,DA,WOB
   WRITE (IO,13)
DO 300 I=1,NALPHA
300 WRITE (IO,104)ALPHAG(I),CLPUGE(I),CDPUGE(I),CDPUGE(I),CLGETK(I),
      1 CDGETR(I)
C
C CONVERT DEGREES BACK TO RADIANS FOR NEXT GROUND HEIGHT.
DO 220 I=1,NALPHA
220 ALPHA(I) = ALPHA(I)/DEG
   ALPHA(I) = ALPHA(I)/DEG
   AOLF(I) = AOLF(I)/DEG
   RETURN
END
SUBROUTINE LIFT(IFERROR)
COMMON /INTABC/II,IN,IO,ICK,NPTBL,IP

```

```

REAL KEAPI2,KEIF02,LAMFTA
COMMON
  ACRFS2(77),ACRFD2(77),ADCRA2(77),LAMETA(30),
  1ADLECR(30),DCLACC(30),DCLCK(30),DCLCKM(30),
  2DCDTR(30),DCDTR2(30),FDKCK(30),NEAPI2(77),NETEV2(77),DCDCLK(30),
  3AMSBR(30),XCPAR2(77),ECP12(77),DCABT(30),AKRYC(30),SKCLE2(77),
  4CLIAS2(77),DCLI3(182),CMI3(231),DEPS2(182),DCLIG2(77),
  5DCMIG2(77),DCDIG2(77)
COMMON/BASIC/ARATIO,PI,RAD,AREF
COMMON/INTER/DCLTE,FIATE,DCLLE,DEPST,DCLB
COMMON/CASEIN/TITLE(18),IFLAP,WGROSS,WKEF,WPERMT,INDFLAP,
ACPRIME,CFLAP,DFLP(4),CFWD,CPLAP,CAFT,DFWU,DFAPT,AUCURU,AMCURU,
1AHLFWD,AHLAFT,FTFIN,STEVUT,CLEDGE,CHUNK,DLEDGE,ELEIN,ELEVUT,CLAFU,
2AULFU,CLENLE,CRDNLE,WPGROSS,DWTE,DWLE,CLMAXU,ALPHA1,CULE,DALPHA,
3WGFLAP,SPANLE,CHRDLE,XCP1,XCPLE,XCP2,XCP2TE,XAC,DS2,DSLE,S3,CPMUB
4,XCG,CREF,CFLIR,CFLOR,CPMIB,CPFLIR,CPFLUB,XIB,XUB,EPTIEN,XPWCARD,
5CMOLFU,WGM(3),NWRNGH,THUM,WSPAN,TLWM,STAIL,EPFUF,DCPDMIN,DCDDCL
6,CHDYR,CHDPYR,CMO,APWCHD,XPB,XB,YR,YM,CHDYM,XM,CHDPYM,XPW,IEDGF
7,CHDYPT,XRTE,COPYRT,XPRT,YRTE,YMTE,CHDYMT,XMTE,CPYMT,XPMT
8,DElap,DEFW(4),DEAF(4),CRDDPM,CDPMFU,EPTEOB,EPSO,DEPDAL
9,CJ,ENGVEC,XNACEL,XNOZLE,ZNOZLE,XINLET,ZINLET,CDXAM,ILE,ITE
COMMON/OUTPUT/ NALPHA,CLAFD,AULLED,AULTFD,AULBFD
1,DCLBFD,CLMAXU, DCUTE,DCLLE,DCMTE,DCMOLLE,CUFATR(20),
2CMORFD,CLMAXG(3),ALPHA(20),CLTY(20),CDTU(20),CMTU(20),CLTK(20),
1CDTR(20),ALPHAG(20),CLTUG(20),CDTUG(20),CMTUG(20),CLTRG(20)
1,CDTRG(20),CLPOFA(20),CLINT(20),CDPOFA(20),CMPUFA(20),DEPUFA(20),
5CLPOGF(20),CDPOGE(20),CMPUGE(20),CLGETK(20),CDGETK(20),CLFATK(20)
DIMENSION V(3), DI(3)
DATA DI/3*1./
**
**
**
IFERROR=0
ARATIO=WSPAN**2/(144.*WGROSS)
AREF=WSPAN**2/(WREF*144.)
**
** FLAPS DOWN LIFT CURVE SLOPE
**
**
X=2.*PI*ARATIO/((WPERMT/WSPAN)*ARATIO+2.)
CLAFD=X*(WGROSS/WREF)

```

```

C
C
C
C
C
C
C
C
C
C

```

```

*****
**      SHIFT IN ANGLE OF ATTACK FOR ZERO LIFT WITH T.E. FLAP DOWN
**
*****
IF (IFLAP.LE.0.OR.IFLAP.GT.4) GO TO 9100
V(1)=ETFIN
ZIN=TRL(LAVETA,V,DI,IE)
V(1)=FTFCUT
ZOUT=TRL(LAMETA,V,DI,IE)
IF (IF.NE.0) GO TO 9100

STATE=ZOUT-ZIN
IF (IFLAP.GT.2) GO TO 10

**      SINGLE AND DOUBLE SLOTTED-SINGLE HINGED FLAPS (TYPES 1-2)
**
ZZA=TAN(DFLAP)*COS(AHCORJ-AHLAFT)
DEF1=ATAN(ZZA)
V(1)=CFLAP/CPRIME
V(2)=DFLAP
IF (IFLAP.EQ.1) X=TRL(ACRF2,V,DI,IE)
IF (IFLAP.EQ.2) X=TRL(ACRF2,V,DI,IE)
IF (IF.NE.0) GO TO 9100

V(1)=CFLAP/CPRIME
V(2)=1./ARATIO
Y=TRL(ADCRA2,V,DI,IF)
IF (IE.NE.0) GO TO 9100

DAOL=X*DEF1*Y*ETATF*((COS(AHCORJ)**2/COS(AWCORJ))
GO TO 200

100 CONTINUE
**
**      DOUBLE AND TRIPLE SLOTTED-DOUBLE HINGED FLAPS (TYPES 3-4)
**
ZZA=TAN(DFEWD)*COS(AHCORJ-AHLEWD)
DEF1=ATAN(ZZA)
ZZA=TAN(DFEWD)*COS(AHCORJ-AHLAFT)

```

```

DE2=ATAN(ZZA)
V(1)=CPFLAP/CPRIME
V(2)=DFFWD
IF (IFLAP.NE.4) X1=TRL(ACRFS2,V,DI,IE)
IF (IFLAP.EQ.4) X1=TRL(ACRFS2,V,DI,IE)
IF (IF.NE.0) GO TO 9100

V(1)=CAFT/CPRIME
V(2)=DEAFT
X2=TRL(ACRFS2,V,DI,IE)
IF (IF.NE.0) GO TO 9100

V(1)=CPFLAP/CPRIME
V(2)=1./ARATIO
Y=TRL(ACRA2,V,DI,IE)
IF (IF.NE.0) GO TO 9100

DAOL=(X1*DE1+X2*DE2)*Y*FTATE*(COS(APCGRD))*R2/COS(ANGCGRD))

200 CONTINUE
IF (IP.NE.2) GO TO 7000
WRITE (IO,8000)DE1,DE2,ZIN,ZOUT,DAOL,X1,X2
8000 FORMAT(IH1,27HSE1,DE2,ZIN,ZOUT,DAOL,X1,X2/ 7(IX,F10.4))
7000 CONTINUE
**
** T.F. FLAP INCREMENT AT THE ANGLE FOR ZERO LIFT WITH
** FLAPS RETRACTED
**
DCLTF=CLAFD*(-DAOL)
**
** BODY CARRY OVER LIFT INCREMENT
**
V(1)=DCLTF
V(2)=FTFIN
X=TBL(BKCLE2,V,DI,IE)
IF (IF.NE.0) GO TO 9100

DCLR=DCLTF*X*(ZIN/FTATE)
**

```

```

** SHIFT IN ANGLE OF ATTACK FOR ZERO LIFT WITH L.F. FLAPS DOWN **
**
V(1)=CEEDGE/CHORD
X=TBL(ADLECR,V,DI,IF)
IF (IF.NF.0) GO TO 9100

V(1)=ELEIN
ZIN=TRL(LAMETA,V,DI,IE)
V(1)=FLFOUT
ZOUT=TRL(LAMETA,V,DI,IF)
IF (IF.NF.0) GO TO 9100

ETALE=ZOUT-ZIN
DAOLLE=X#DLEFGE*(COS(AGCORD))*ETALE

** L.F. LIFT INCREMENT AT ANGLE FOR ZERO LIFT FLAPS RETRACTED **
**
DCLLE=CLAFD*(-DAOLLE)

** L.F. AND T.F. FLAP LIFT INCREMENT AT ANGLE FOR ZERO LIFT **
** WITH FLAPS DOWN **
DCLRFD=DCLLE+DCLTF+DCLB

** ANGLE OF ATTACK FOR ZERO LIFT L.F. FLAPS DOWN **
AOLLEF=AOLFU+DAOLLE

**

```

```

** ANGLE OF ATTACK FOR ZERO LIFT T.E. FLAPS DOWN
**
AOLTFD=AOLFU+DAOL-(DCLB/CLAFD)

**
** ANGLE FOR ZERO LIFT L.E. AND T.E. FLAPS DOWN
**
**
AOLRFD=AOLFU+DAOL+DAOLLE-(DCLB/CLAFD)
IF (IP.NF.2) GO TO 7001
WRITE (10,8001)DCLTE,DCLR,DAJLLE,DCLLE,DCLBFD,AULLFD
FORMAT(1H0,37HDCLTE,DCLB,DAOLLE,DCLLE,DCLBFD,AULLFD/ 6(1X,F10.4))
7001 CONTINUE
GO TO 9200

9100 CONTINUE
IFERROR=1

9200 CONTINUE
RETURN
END
SUBROUTINE MXLIFT(IFERROR)
COMMON /INTARC/IU,IN,IO,ICR,NPTBL,IP
REAL KEAPI2,KEF02,LAMETA
COMMON ACRFS2(77),ACRFD2(77),ADCRA2(77),LAMETA(30),
1ADLECR(30),DCLACC(30),DCLACS(30),DCLRCR(30),DCLACM(30),
2DCDTFD(30),DCDTFT(30),FDRCK(30),KEAPI2(77),NEIEV2(77),DCDCLK(30),
3AMSBR(30),XCPAR2(77),ECEPI2(77),DCAUT(30),AKRYCY(30),BKCLE2(77),
4CLIAS2(77),DCLI3(182),CDI3(231),CMI3(231),DEPS3(182),DCLIG2(77),
5DCMIG2(77),DCDIG2(77)
COMMON/INTER/DCLTE,ETATE,DCLLE,DEPSF,DCLB
COMMON/RASIC/ARATIO,PI,RAD,AKEF
COMMON /CASFIN/ TITLE(18),IFLAP,WGROSS,WKEF,WPERMT,NDFLAP,
ACPRIME,CFLAP,DFLP(4),CFWD,CPFLAP,CAFT,DFWFD, DFAFT,AJCURD,AHCURD,
1AHLFWD,AHLAFT,FTEIN,FTEOUT,CLEDGE,CHORD,DLEDGE,ELEIN,ELEOUT,CLAFU,
2AULFU,CLFNLF,CRNLF,WPGKUS,DWTE,DWLE,CLMAXU,ALPHA1,CULE,DALPHA,
3WGLFAP,SPANLF,CHRDLE, XCP1,XCPLE,XCP2,XCP2TE,XAC,S2,JSLE,S3,CPM00
4,XCG,CREF,CFLB,CFLOB,CPMIB,CPFLB,CPFLVB,XIB,XUB,EPTFIN,XPUCKD,
5CMOLFU,WHM(3),NWMINGH,THWM,WSPAN,TLWM,STAIL,EPSFU,DCPD,DCDDCL
6,CHDYR,CHDPYB,CMO,APUCHD,XPB,XB,YR,YM,CHDYM,XM,CHDPYM,XPYI,IEDGE
7,CHDYRT,XBTE,COPYRT,XPRTE,YBTE,YMTE,CHDYMT,XMTE,CPYITE,XPYTE
8,DFLAP,DFFW(4),DFAF(4),CRDUPM,CDPMPFU,EPTLUB,EP50,DEPDAL

```



```

IF (IF,NF,0) GO TO 9100
SLOPE=Y1/X1
IF (IP,NF,2) GO TO 7001
WRITE (IO,8001)X,Y,DCLCAM,X1,Y1,SLOPE
8001 FORMAT(1H3,28HX,Y,DCLCAM,X1,Y1,SLOPE / (10(1X,F10.4)))
7001 CONTINUE
X=(CLMAXU+DCLMLF)*(DATE/(WPGROS+DWLE))
Y=SLOPE*(COS(ACCORD))**2
Z=(CLEDFG/CHORN-CLEDFG/CHKDLE)*(WPGROS+DWTE)/WKEF
DCLFOW=(X-Y*Z)*ETATE
DCLMTE=DCLCAM+DCLFOW
IF (IP,NF,2) GO TO 7002
WRITE (IO,8002)X,Y,Z,DCLFOW,ETATE,DCLMTE
8002 FORMAT(1H0,25HX,Y,Z,DCLFOW,ETATE,DCLMTE / (10(1X,F10.4)))
7002 CONTINUE
**
** LIFT INCREMENT FROM LEADING EDGE BLC
**
V(1)=CUILE
X=TRL(DCLACM,V,DI,IF)
DCLBLC=X*(COS(ACCORD))**2
**
** MAX LIFT FLAPS DOWN
**
CLMAXD=CLMAXU+DCLMLF+DCLMTE+DCLBLC
**
** GFNERATE ANGLES OF ATTACK AND CORRESPONDING LIFT CUFF.
**
XEWANG=ALPHA1
DO 300 I=1,20
IF ((CLAFD*(XEWANG-AOLPFD)).GT.CLMAXD) GO TO 920
NALPHA=I
ALPHA(I)=XEWANG
CLTO(I)=CLAFD*(XEWANG-AOLBFD)
XEWANG=XEWANG+DALPHA
300 CONTINUE
GO TO 9200

```

**
**
**

**
**
**

**
**
**

**
**
**

```

C C C
C ** TRAILING EDGE FLAPS PARASITE DRAG
C **
C ** IF (IFLAP .LT. 3) GO TO 1
C ** V(1)=CPFLAP/CPRIME
C ** V(2)=DFFWD
C ** IF (IFLAP.EQ.3) ALF1=TRL(ACRFS2,V,DI,IE)
C ** IF (IFLAP.EQ.4) ALF1=TRL(ACRFD2,V,DI,IE)
C ** IF (IF.NE.0) GO TO 9100
C
C V(1)=CAFT/CPRIME
C V(2)=DFAFT
C ALF2=TRL(ACRFS2,V,DI,IE)
C IF (IF.NE.0) GO TO 9100
C
C 10 CONTINUE
C IF (IFLAP.LE.2) FFQ=DFLAP
C IF (IFLAP.GE.3) FFQ=DFFWD+(ALF2/ALF1)*DFAFT
C V(1)=FFQ
C IF (IFLAP.EQ.4) X=TRL(DCDTFT,V,DI,IE)
C IF (IFLAP.NE.4) X=TRL(DCDTFD,V,DI,IE)
C IF (IF.NE.0) GO TO 9100
C
C IF (IFLAP.LE.2) V(1)=CFLAP/CRDDPM
C IF (IFLAP.GE.3) V(1)=CPFLAP/CRDDPM
C Y=TRL(FDRCR,V,DI,IE)
C IF (IE.NE.0) GO TO 9100
C
C DCDTE=X*(WGFLAP/WREF)*Y
C
C ** LEADING EDGE FLAP PARASITE DRAG
C **
C ** DCDLF=.154*(SPANLE/WREF)
C
C ** FLAP INDUCED DRAG
C **
C ** V(1)=ETFIN
C ** V(2)=.5*ARATIO/PI
C ** CA=TRL(KEAPI2,V,DI,IE)

```

**
**
**

**
**
**

```

IF (IF.NF.0) GO TO 9100
V(1)=FTFOUT
V(2)=FTFIN
CF=TRL(KFIEO2,V,DI,IE)
IF (IF.NF.0) GO TO 9100
C=CA*CF
DCDI=C*(DCLTE)**2/(PI*AREF)
**
** RLC DRAG DELTA
**
DCDRLC=-.5*CULF
**
** CALCULATE DRAG VALUES FOR OUTPUT
**
DO 300 I=1,NALPHA
V(1)=CLTO(I)/CLMAXD
DCDP=TRL(DCDCLR,V,DI,IE)
IF (IF.NE.0) GO TO 9100
CDI=CLTO(I)**2/(PI*AREF)
CDTO(I)=CDPMFU+DCULE+DCDTL+DCDI+DCDP+CDI+DCDBLC
300 CONTINUE
GO TO 9200
9100 CONTINUE
IFERROR=1
9200 CONTINUE
RETURN
END
SUBROUTINE PITCH(IEFFOR)
REAL KEAPI2,KFIEO2,LAMETA
COMMON
ACRES2(77),ACKFD2(77),ADCKA2(77),LAMETA(30),
1ADLECR(30),DCLACC(30),DCLACS(30),DCLKCK(30),DCLACM(30),
2DCDTEF(30),DCDTFT(30),FDRCR(30),KEAPI2(77),KEIEO2(77),DCDCLR(30),
3AMSPR(30),XCPAR2(77),FCPEI2(77),DCABT(30),AKKYCY(30),BKCLF2(77),
4CLIAS2(77),DCLIA2(182),CDI3(231),CMI3(231),DEPS3(182),DCLIG2(77),

```

**
**
**

**
**
**

```

50CMIG2(77),DCDIG2(77)
COMMON /INTARC/ IU, IN, IO, ICR, NPTBL, IP
COMMON /INTER/DCLTE, ETATE, DCLLE, DEPSF, DCLD
COMMON /BASIC/ARATIO, PI, RAD, AREF
COMMON /CASEIN/ I1LE(18), IFLAP, WGRGSS, WKEF, WPERKI, INDFLAP,
ACPRIME, CFLAP, DFLP(4), CFWD, CPFLAP, CAFI, DFFWD, DFLAT, AGCORU, ANCORU,
1AHLFWD, AHLAFT, ETEIN, TEOUT, CEEDGE, CHOND, DLEDGE, ELEIN, ELEOUT, CLAFU,
2AOLFU, CLFNLF, CRNLF, WGRGSS, DWTE, DWLE, CLMAXU, ALPHAI, CULU, DALPHA,
3WGLAP, SPANLE, CHRDLF, XCP1, XCPLE, XCP2, XCP2LE, XAC, S2, DSLE, S3, CPMOB
4, XCG, CREF, CFLIR, CFLOR, CPMID, CPULIR, CPFLUB, XID, XUB, ETEIN, XFWCKD,
5CMOLFU, WHQM(3), NWINGH, THGM, WSPAN, TLEM, STAIL, EPSFU, DCPOMW, DCDCL
6, CHDYR, CHDPYR, CMU, AP, CHD, XPR, XBY, YR, YM, CHDYM, XM, CHDPYM, XPM, IEDGF
7, CHDYRT, XRTE, CDPYRT, XPBTE, YBTE, YMTE, CHDYMI, XMTE, CPMYTE, XPMTE
8, DFLAP, DFFW(4), DFAF(4), CRDPPM, CDPYFU, CPTEDD, EP50, DEPVAL
9, CJ, FNGVEC, XNACFL, XNOZLE, ZINLEI, ZINLET, CDKAM, ILE, IIF
COMMON /OUTPUT/ NALPHA, CLAFD, AULFD, AULFD, AULBFD
1, DCLBFD, CLMAXD, DCBTE, DCDLE, DCMUTE, DCMULE, CLFATK(20),
2CMOBFD, CLMAXG(3), ALPHA(20), CLTU(20), CPTU(20), CMTU(20), CLTK(20),
3CTR(20), ALPHAG(20), CLTUG(20), CDTUG(20), CMTUG(20), CLTKG(20)
1, CTRG(20), CLPOFA(20), CLINT(20), CDPUEA(20), CDPUEA(20), DEPUEA(20),
5CLPUG(20), CDPUG(20), CDPUG(20), CLGETK(20), CGETK(20), CLFATK(20)
DIMENSION V(2), D1(3), D2(3), D3(3)
DATA D1/3*1./, D2/3*2./, D3/1., 2., 0./
**
*****
**
ERROR=0
**
** AERO CENTER SHIFT DUE TO L.E. DVICL (FOWLER ACTION)
**
V(1)=YR/CHDYR
XK=TBL(AKRYCY,V,D2,IE)
IF (IF.NE.0) GO TO 9100
Y1=XP+CHDYR*(.25+AGCORD*XK)
V(1)=YR/CHDPYR
YK=TBL(AKRYCY,V,D2,IE)
X1P=XP+CHDPYR*(.25+APQCHD*XK)
IF (IF.NE.0) GO TO 9100

```

```

V(1)=YM/CHDYM
XK=TRL(AKRYCY,V,D2,IF)
IF (V(1).GT.1.) XK=0.
Y2=XM+CHDYM*(.25+AGCORD*XK)
IF (IF.NE.0) GO TO 9100

V(1)=YM/CHDPYM
XK=TRL(AKRYCY,V,D2,IF)
IF (V(1).GT.1.) XK=0.
X2P=XPM+CHDPYM*(.25+APGCHD*XK)
IF (IF.NE.0) GO TO 9100

V(1)=ELEFOUT-ELEFIN
XMU=TRL(AMSPR,V,D2,IF)
IF (IF.NE.0) GO TO 9100

V(1)=ELEFIN
XJN=TRL(LAMETA,V,D1,IF)
IF (IF.NE.0) GO TO 9100

V(1)=ELEFOUT
XAT=TRL(LAMETA,V,D1,IF)
IF (IF.NE.0) GO TO 9100
XOT=XAT-XIN

A=(1.+XMU*DSLE/S2)*X2P-X2
R=1.+(XMU*DSLE/S2)*XOT
DXLESB=((XIN*(X1P-X1)+XOT*A+XAC)/R)-XAC
DXLFOR=((A*XOT+XAC)/R)-YAC
IF (IP.NE.2) GO TO 7000
WRITE (10,8000)X1,X1P,X2,X2P,XMU,XIN,XOT,A,B,DXLESB,DXLFORB
8000 FORMAT(1H0, 43H X1,X1P,X2,X2P,XMU,XIN,XOT,A,B,DXLESB,DXLEUB
1 (10(1X,F10.4)))
7000 CONTINUE

**
** AFRO CENTER SHIFT DUE TO T.E. FLAPS (FOWLER ACTION)
**
V(1)=YRTE/CHDYRT
XK=TRL(AKRYCY,V,D2,IF)
X1=XRTE+CHDYRT*(.25+AGCORD*XK)

```

**
**
**

```

IF (IF.NE.0) GO TO 9100
V(1)=YBTE/CDPYBT
XK=TRL(AKRYCY,V,D2,IE)
X1P=XPBTE+CDPYBT*(.25+APQCHD*XK)
IF (IF.NE.0) GO TO 9100

```

```

V(1)=YMTE/CHDYMT
XK=TRL(AKRYCY,V,D2,IE)
IF (V(1).GT.1.) XK=0.
X2=XMTE+CHDYMT*(.25+AQCORD*XK)
IF (IF.NE.0) GO TO 9100

```

```

V(1)=YMTF/CPYMTF
XK=TRL(AKRYCY,V,D2,IE)
IF (V(1).GT.1.) XK=0.
X2P=XPMTF+CPYMTF*(.25+APQCHD*XK)
IF (IF.NE.0) GO TO 9100

```

```

V(1)=ETFIN
XIN=TRL(LAMFTA,V,D1,IE)
IF (IF.NE.0) GO TO 9100

```

```

V(1)=ETFOUT
XAT=TRL(LAMFTA,V,D1,IE)
IF (IF.NE.0) GO TO 9100
XOT=XAT-XIN

```

```

V(1)=ETEQUT-ETFIN
XMU=TRL(AMSTR,V,D2,IE)
IF (IF.NE.0) GO TO 9100

```

```

A=(1.+XMU*DWTF/S3)*X2P-X2
R=1.+(XMU*DWTF/S3)*XOT
DYTESD=((XIN*(Y1P-X1)+XOT*A+XAC)/B)-XAC
DXTEOB=((A*XOT+XAC)/B)-XAC

```

```

**
** PITCHING MOMENT AT ZERO LIFT DUE TO T.E. FLAPS
**
YCON=ARATIO/(WPERMT/WSPAN)*ARATIO+2.)

```

```

**
**
**

```

```

IF (IP,NF.2) GO TO 7001
WRITE (IO,8001)X1,X2,X1P,X2P,XIN,XOT,XMU,A,B,DXTESD,DXTEUB,YCUN
8001 FORMAT(1H0, 48HX1,X2,X1P,X2P,XIN,XO1,XMU,A,B,DXTESD,DXTEUB,YCUN /
1 (10(1X,F10.4)))
7001 CONTINUE
XACFX=XAC+DXTFSD
IF (ITE,EQ.2) XACFX=XAC+DXTFOR
V(1)=FTFIN
V(2)=FTFOUT-FTFIN
ETACP=TRL(CEPEI2,V,D2,IE)
IF (IF,NE.0) GO TO 9100

V(1)=YCON
V(2)=CFLIB/CPMTR
IF (IFLAP,GT.2) V(2)=CPFLIB/CPMIB
CCPIP=TRL(XCPAR2,V,D3,IF)*CPMIB
IF (IF,NE.0) GO TO 9100

V(1)=YCON
V(2)=CFLOB/CPMOR
IF (IFLAP,GT.2) V(2)=CPFLOB/CPMOB
CCPOR=TRL(XCPAR2,V,D3,IF)*CPMOB
IF (IF,NE.0) GO TO 9100

**
** DETERMINE INBOARD FLAP LOAD POINT
**
DCP=CCPIR-.5*CPMIR
XIRLD=DCP*COS(AHCORR)+XIB
IF (IP,NF.2) GO TO 7002
WRITE (IO,8002)XACFX,ETACP,CCPIB,CCPOB,DCP,XIRLD
8002 FORMAT(1H0, 39HXACFX,ETACP,CCPIB,CCPOB,DCP,XIRLD /
1 (10(1X,F10.4)))
7002 CONTINUE

**
** DETERMINE OUTBOARD FLAP LOAD POINT
**
DCP=CCPOR-.5*CPMOP
XORLD=DCP*COS(AHCORR)+XOB
XX=XORLD-XIRLD

```

**
**
**

**
**
**

```

YY=1./(FTFOUT-FTFIN)
Z7=ETACP-FTFIN
XCPIE=XX*YY*ZZ+XI*RD
DCNOTE=((DCLB+DCLTF)*(XCPIE-XACEX)/CREF
**
**
**
**
** PITCHING MOMENT AT ZERO DUE TO L.E. DEVICES
**
XACLE=XAC+DXLE*F
IF (IP,NE,2) GO TO 7003
WRITE (10,8003)DCP,XOBLD,
      XCPIS,DCMOTE,XACLE /
      XCPTE,DCMOTE,XACLE /
      FORMAT(1H0, 28HDCP,XOBLD,
            10(1X,F10.4))
7003 CONTINUE
IF (ILE,EO,2) XACLE=XAC+DXLE*F
DCMOLF=DCLLE*(XPGCRB-XACLE)/CREF
**
** CALCULATE PITCHING MOMENT FOR OUTPUT
**
YX=DXTE*F
IF (ITE,EQ,2) YX=DXTE*F
YY=DXLE*F
IF (ILE,EO,2) YY=DXLE*F
TXAC=XAC+XX+YY
CON=XCG/CREF-(TXAC/CREF)
DO 300 I=1,NALPHA
CMT0(I)=CMOLF+DCMOTE+DCMOLF+CON*CLT0(I)
300 CONTINUE
**
** CHANGE IN DOWNWASH AT THE TAIL DUE TO L.E. AND T.F. FLAPS
**
CALL DELTAF(TE)
IF (IP,NE,2) GO TO 7004
WRITE (10,8004)DCMOLF,XX,YY,TXAC,CON,DEPSF
      XCPIS,DCMOTE,XX,YY,TXAC,CON,DEPSF /
      FORMAT(1H0, 28HDCMOLF,XX,YY,TXAC,CON,DEPSF /
            10(1X,F10.4))
7004 CONTINUE
IF (IE,NE,0) GO TO 9100

```

**
**
**

CALCULATE TRIM CL AND CD FOR POWER OFF IN FREE AIR

MODE=1
CALL TRIM(MODE,DUMMY)
GO TO 0200

0100 CONTINUE
IFERROR=1

0200 CONTINUE
RETURN
END

SUBROUTINE DELTAF(LF)
REAL KEAIP12,KEFEO2,LAMETA
COMMON

ACFES2(77),ACREF2(77),AUCRA2(77),LAMEIA(30),
LADLECR(20),DCLACC(30),DCLACK(30),DCLACK(30),DCLACK(30),
DCCATER(20),DCPTET(20),DCKCK(30),KFAFT2(77),SEFEO2(77),DCCLEA(30),
RAMARR(30),XCPAR2(77),SCPLI2(77),DCAUT(30),ANNVXY(30),SCLE2(77),
4CLIAS2(77),DCLIR(180),CHI3(23),ALP33(180),DCLIG2(77),
3DCMIG2(77),DCPIG2(77)
COMMON/INTER/DCLTS,PCATL,CLLE,DEPTE,DCEB
COMMON/BASIC/ABATIN,PI,RA,AREF
COMMON/CASIN/ITL(18),IFLAP,WRGRO,ANKEF,PEKX,VOLEAP,
ACBIM,CEFLAP,DELPAI,DEFWD,CEFLAP,CAF,DEFWD,SPAT,ANVCK,AMCOW,
1AULFD,AHLAEI,ETEIN,ITOUT,CLPGE,CHJND,DEBDF,DEFIN,DEFOUT,CELEO,
2ALFN,CLENGE,CPOME,PRKUS,DAI,DWL,CLAA,AFPAI,CLLE,ALVET,
3CEFLAP,SPANLE,CHROLL,XPPI,XPPL,XPPI,XPPI,XAC,XP,XP,XP,XP,XP,
4,XCG,CREF,CLLE,CELEO,CPPI,CPPI,CPPI,CPPI,CPPI,CPPI,CPPI,CPPI,
5CMLEFI,MPX(2),MTRNH,IND,MPAN,TL,CLLE,EPSE,DEK,XP,XP,
6,CHRYR,CHRYR,CHD,AR,CHD,XP,XP,XP,XP,XP,XP,XP,XP,XP,XP,
7,CHRYR,XPTE,CPYR,CPYR,XP,XP,XP,XP,XP,XP,XP,XP,XP,XP,
8,FLAP,DEFY(4),DEFY(14),KPI,CPBME,PI,FB,FB,FB,FB,
9,CJ,FCGV,XYNCEL,XYNCEL,XYNCEL,XYNCEL,XYNCEL,XYNCEL,XYNCEL,XYNCEL,
COMMON/OUTPUT/VALPWA,CLAP,AVLLEO,AVLFD,AVLFD,
1,DCLBIO,CLMAXI,
2,CPBES,CLMAX(2),ALPHA(20),ITL(20),CPIT(20),CPIT(20),CLTK(20),
1,CPTR(20),ALPHAC(20),CLTC(20),CPIT(20),CPIT(20),CLTK(20),
1,CPTR(20),CLPWA(20),CLM(20),CPBFA(20),CPBFA(20),CPBFA(20),
1,CPBCE(20),CPBCE(20),CPBCE(20),CLGFK(20),CPBFA(20),CLPWA(20)

```

DIMENSION V(3), DI(3)
DATA DI/3*1./
**
** *****
**
**
IF=0
DEPSF =0.
**
** ** CHANGE IN DOWNWASH AT THE TAIL DUE TO L.E. AND T.E. FLAPS
**
**
V(1)=2.*THQM/WSPAN
X=TRL(DCART,V,DI,IF)
IF (IE.NF.0) GO TO 9100
Y=X*(DCLREFD-DCLLE)
DEPSF=Y/(AKEF*(FTEOUT-EETEIN))
GO TO 9200

9100 CONTINUE
IF=1

9200 CONTINUE
RETURN
END
SURROUTINE GRNDF(IWING)
GEHIGH WHQM(I), WING HEIGHT OF THIS ITERATION

SECTION 6 GROUND EFFECT

ALPHA ARRAY PITCH FOR GROUND EFFECT.
CLTOG ARRAY CL TAIL OFF GROUND EFFECT FOR ALPHA(I) - OUTPUT
CLTO ARRAY CL TAIL OFF FOR CL(ALPHA(I) TO CLMAXD. - INPUT
ALPHA ARRAY PITCA ANGLE

CNTG ARRAY CD TAIL OFF - INPUT
CNTOG ARRAY CD TAIL OFF GROUND EFFECT - OUTPUT
CMTG ARRAY CM TAIL OFF - INPUT
CMTOG ARRAY CM TAIL OFF GROUND EFFECT - OUTPUT
REAL KEAPI2,KEI502,LAMETA
COMMON ACRI52(77),ACRFU2(77),ADCR42(77),LAMETA(30),
JANLECR (30),DCLACC(30),DCLACS(30),DCLCKR(30),DCLACM(30),

```

```

20 CDTEO(30),CDTFT(20),EDRCK(30),KEAP12(77),KEIEU2(77),DCDCLK(30),
30 WSR(30),XCPAR2(77),FCPE12(77),DCAPT(30),AKKYCY(30),BNCLE2(77),
40 CLIAS2(77),DCLI3(182),CMI3(231),DEFS3(182),DCLIG2(77),
50 CMIG2(77),DCDIG2(77)
COMMON /CASEIN/ TITLE(18),IFLAP,WGROSS,WKEF,*PENMT,NDFLAP,
ACPRIME,CFLAP,DFLP(4),CFWD,CPFLAP,CAFT,DFFWD,DFAPT,AGCURD,ANCURD,
1 AHLEWD,AHLAFT,ETEIN,ETEOUT,CLEDGE,CHORD,DLEDDG,ELIN,ELUUT,CLAFU,
2 AOLEU,CLENL,CRDNL,MPGKUS,DWTE,DWLE,CLMAXU,ALPHA1,CULE,DALPHA,
3 WGLFAP,SPANLE,CHRIDE,XCPI,XCPLE,XCP2,XCP2TE,XAC,S2,USLL,S3,CPMOD
4,XCG,CREF,CFLIR,CFLUR,CPMIB,CPFLIR,CPFLUB,XIB,XUB,EPTEin,XPWCKD,
5 MOLEU,WHM(3),GWMING,THM,SPAN,TLW,STAIL,EPSEU,DCPDMM,DCDDCL
6,CHDYP,CHDYPB,CLO,APUCHD,XPB,XB,YR,YM,CHDYM,XH,CHDPM,XPM,IEDGE
7,CHDVT,XPTE,CPYRT,XPRTF,YRTE,YMTE,CHDYM,XPTE,CPYMT,XPMTE
8,DFLAP,DEFW(4),DEAF(4),CRDPR,CPMFEU,EPTLUB,EP50,DFPDAL
9,CJ,ENGVEF,XMACFL,XNOZLF,ZNOZLF,XINLET,ZINLET,CRKAM,ILE,ITE
COMMON /OUTPUT/ NALPHA,CLAFD,AULLEF,AULTFD,AULBEF
10,CLBEF,CLMAXD,RCOTE,DCOLE,DCMUTE,DCMULE,COFATR(20),
20 WREF,CLMAXG(3)
COMMON /OUTPUT/ ALPHA(20),CLTO(20),COTU(20),CMTU(20),CLTK(20),
10CTR(20),ALPHAG(20),CLTOG(20),COTOG(20),CMTOG(20),CLTKG(20)
1,COTRG(20),CLPOEA(20),CLINT(20),COPCEA(20),CMPCEA(20),DEPUFA(20),
5 CLPOGE(20),CDPOGE(20),CMPUG5(20),CLGETK(20),CONETK(20),CLFATR(20)
COMMON/BASIC/RATIO,PI,RAD,AKEF
DATA PI/3.1415926535897932384626433832795
C CALCULATE CONSTANTS FOR FORMULAE OUTSIDE LOOP
GEHIGH=WHQM(TWING)
C1=(SQRT(PI*WSPAN/(R*GEHIGH))**2+1.)-1.)/(PI*WSPAN*AKEF)
C2=ALOG(1.+(WSPAN*PI/(R*GEHIGH))**2)/((PI*WSPAN*AKEF)**2)
C3=2./((PI*WSPAN*AKEF)**2)*ALOG(1.+(WSPAN*PI/(R*GEHIGH))**2)
20 50 I=1,NALPHA
CLTOG(I)=CLTO(I)*(1./ (1.+2.*CLTO(I)*C1))**2
ALPHAG(I)=ALPHA(I)-(2.*CLTO(I)*C2)
IF (CLTO(I).EQ.0.) GO TO 100
CMTOG(I)=CMTO(I)/CLTO(I)*CLTOG(I)
COTOG(I)=COTO(I)*(1.-CLTO(I)**2/COTU(I)*C3)*CLTO5(I)/CLTO(I)
CLMAXG(TWING)=CLTOG(I)
50 TO 50
100 CONTINUE
CMTOG(I)=CMTO(I)
COTOG(I)=COTO(I)
50 CONTINUE

```



```

*****
**
PJSQ=PI*PI
IF (MODE.LT.1.OR.MODE.GT.4) GO TO 910
GO TO (100,200,300,400),MODE

100 CONTINUE
**
** CALCULATE TRIM CL AND CD FOR POWER OFF IN FREE AIR
**
DO 110 I=1,NALPHA
ERASIC=EPS0+DEPDAL*ALPHA(I)
FTAIL=ERASIC+DEPSE
DCLTR=CMTO(I)/TLQM*GREF
CLPTO=WREF/STAIL*DCLTR
DCDTR=DCDCLTR*FTAIL+(DCPDMIN+DCDDCL*CLPTO**2)*STAIL/WREF
CLTR(I)=CLTO(I)+DCLTR
CDTR(I)=CDTO(I)+DCDTR
110 CONTINUE
GO TO 9100

200 CONTINUE
**
** CALCULATE TRIM CL AND CD FOR POWER OFF IN GROUND EFFECT
**
C1 = TLQM*TLQM +(2.*GEHIGH-THQM)*(2.*GEHIGH-THQM)
C2 =(2.*GEHIGH-THQM)*(2.*GEHIGH-THQM) + PJSQ*WSPAN*WSPAN/64.
C3 = THQM*THQM + C3
SORC2= SORT(C2)

```

CARD COUNT 644

```

EGEHT=WREF/(8.*PI)*(TL00/C1/5WK2+(1.+TL00/5WK2)/C3)
DO 210 I=1,NALPHA
EBASIC=EPS0+DEPDAL*ALPHA(I)
EGE=C10(I)*EGEHT
FTAIL=EBASIC+DEPSF+5KE
DCLTRG=CMTOG(I)/TL00*CRFF
CLPT05=WREF/STAIL*DCLTRG
DCDTRG=DCLTRG*FTAIL+(DCPDMM+DCDDCL*CLPT05**2)*5TAIL/WREF
CLTRG(I)=CLT0G(I)+DCLTRG
CDTRG(I)=CDT0G(I)+DCDTRG
210 CONTINUE
GO TO 9100

300 CONTINUE
**
** CALCULATE TRIM CL AND CD WITH POWER ON IN FREE AIR
**
DEVT=GEHIGH
EBASIC=EPS0+DEPDAL*ALPHA(K)
FTAIL=EBASIC+DEPSF+DEVT
DCLTR=CMPOFA(K)/TL00*CRFF
CLPT0=WREF/STAIL*DCLTR
DCDTR=DCLTR*FTAIL+(DCPDMM+DCDDCL*CLPT0**2)*5TAIL/WREF
CLFATR(K)=CLPOFA(K)+DCLTR
CDFATR(K)=CDPOFA(K)+DCDTR
30 CONTINUE

400 CONTINUE
**
** CALCULATE TRIM CL AND CD WITH POWER ON IN INCOMING EFFECT
**
C1=TL00**2+(2.*GEHIGH-TH00)*(2.*GEHIGH+TH00)
C2=(2.*GEHIGH-TH00)*(2.*GEHIGH-TH00)+PI50**2**2/54.
C3=TH00**2+C2
C4=SQRT(C2)
EGEHT=WREF/(8.*PI)*(TL00/C1/C4+(1.+TL00/C4)/C3)
EGE=CLPOGE(K)*EGEHT
EBASIC=EPS0+DEPDAL*ALPHA(K)
FTAIL=EBASIC+DEPSF+5KE
DCLTRG=CMPOGE(K)/TL00*CRFF

```

**
**
**

**
**
**

```

CLPTOG=WREF/STAIL*DCLTRG
DCNTRG=DCLTRG*ETA1+(DCPDMN+DCDDCL*CLPTOG**2)*STAIL/WREF
CLGETR(K)=CLPOGE(K)+DCLTRG
CGGETR(K)=CDPOGE(K)+DCDTRG

0100 CONTINUE
RETURN
END
SUBROUTINE VTRFF( IERROR )
REAL KEAPT2, KTEF02, LAMETA
COMMON ACRES2(77), ACRFD2(77), ADCRA2(77), LAMETA(30),
1APLECR(30), DCLACC(30), DCLRCR(30), DCLACM(30),
2DCOTED(30), DCOTET(30), EDRCR(30), KEAPT2(77), KTEF02(77), DCDCR(30),
3AM5BR(30), XCPAR2(77), ECPE12(77), DCABT(30), AKRYCY(30), BKCLE2(77),
4CLJAS2(77), DCLT3(182), CDT3(231), CMT3(231), DEPS5(182), DCLIG2(77),
5DCMIG2(77), DCDIG2(77)
COMMON /INTABC/IU, IN, IO, ICR, NPTBL, IP
COMMON /INTER/DCLTE, ETATE, DCLLE, DEPSF, DCLD
COMMON /BASIC/RATIO, PI, KAD, AREF
COMMON /CASFIN/ TITLE(18), IFLAP, WGRUSS, WKEF, WPERMT, WDFLAP,
ACPRIME, CFLAP, DELP(4), CFWD, CPFLAP, CAFT, DFFWD, DFAFT, ACCORD, AHCRD,
1AHLFWD, AHLAFT, FTEIN, ETEOUT, CLEUSE, CUCKO, DLEUGE, ELLIN, CLEOUT, CLAFU,
2ACLFU, CLENLE, CRDNLE, APGROS, DWT, DWL, CLMAXU, ALPHAI, CULLE, DALPHA,
3WGEFLAP, SPANLE, CHRDLF, XCP1, XCPLE, XCP2, XCP2TF, XAC, S2, DSLE, S3, CPMUB
4, XCG, CREF, CFLIR, CFLOW, CPMIB, CPFLIR, CPFLUB, XIB, XUB, EPTIN, XPUCRD,
5CMOLFU, WHOM(3), NWRINGH, THOM, WSPAN, TLOW, STAIL, EPSFU, DCPDMN, DCDDCL
6, CHDYR, CHDPYR, CMO, AP, CHD, XPR, XB, YR, YM, CHDYM, XM, CHDPYM, XPM, IEDGE
7, CHDYRT, XBTE, COPYRT, XPBTE, YBTE, YMTE, CHDYMT, XMTE, CPMTE, XPMTE
8, DELAP, DFFW(4), DFAF(4), CKDDPM, CDPMEU, EPTEB, EPSO, DEPDAL
9, CJ, ENGVFC, XNACFL, XNUZLE, ZNUZLE, XINLET, ZINLET, CDKAM, ILE, ITE
COMMON /OUTPUT/ NALPHA, CLAFD, AULLFD, AULTFD, AULBFD
1, DCLREF, CLMAXD, DCDTE, DCDLE, DCMUTE, DCMULE, CDFATR(20),
2CMORFD, CLMAXG(3), ALPHA(20), CLTU(20), CDTU(20), CMTU(20), CLTK(20),
1CCTR(20), ALPHAG(20), CLTOG(20), CDTOG(20), CMTOG(20), CLTRG(20)
1, CDRG(20), CLPOFA(20), CLINT(20), CDPPOFA(20), CDPPOFA(20), DEPOFA(20),
5CLPOGE(20), CDPOGE(20), CPMOGE(20), CLGETR(20), CGGETR(20), CLFATR(20)
DIMENSION V(3), D1(3), D2(3)
DATA D1/3*1./
DATA D2/3*2./
**
*****

```



```

REAL KEAPI2,KEIE02,IAVFTA
COMMON
  ACRFS2(77),ACRFD2(77),ACRKA2(77),LAMEIA(30),
  1ADLECR(30),DCLACC(30),DCLACS(30),DCLKCN(30),DCLACK(30),
  2DCOTFD(30),DCOTFT(30),FBRCK(30),KEAPI2(77),KEIE02(77),DCOCLK(30),
  3AVMSR(30),XCPAR2(77),ECPEI2(77),DCABT(30),ANKYCY(30),RKCCLF2(77),
  4CLIAS2(77),DCLIR(182),CDIR(231),CMIR(231),DFPS3(182),DCLIG2(77),
  5DCMIG2(77),DCDIG2(77)
COMMON /INTARC/ IU,IN,IO,ICR,NPIRL,IP
COMMON /INTER/DCLTF,FTAF,DCLE,DEPCF,DCLB
COMMON /BASIC/ARATIO,PI,RAD,AREF
COMMON /CASEIN/ TITLE(18),IFLAP,WGRUSS,WREF,APKMI,INFLAP,
ACPRIME,CFLAP,DELP(4),CFWD,CFFLAP,CAFT,DFWD,DFAIT,ACCKU,AHCKU,
1AHLEWD,AHLAIT,PTHIN,LEOUT,CLEGE,CHOKD,CLEGE,LEIN,LEVOU,CLAFU,
2AOLFU,CLENLF,CRDNLF,WGRUSS,DWTE,DWLE,CUMAXU,ALPHA1,CULE,DALPHA,
3WGFAP,SPANLE,CHRDLE,XCP1,XCPLE,XCP2,XCP2IE,XAC,02,DSLE,S3,CPM00
4,XCG,CREF,CFLIR,CFLOB,CPMIB,CFLIR,CPFLUB,XIB,XUB,EPFIN,XPCKD,
5CMOLEU,WHM(2),NWHGH,THUM,WCPAN,TLW,STAIL,EPFBU,DCPDIM,DCDDCL
6,CHDYB,CHDPYR,CMO,AP,CHD,XPB,XB,YR,YM,CHDYM,XM,CHDYM,XM,CPYME,XPMTE
7,CHDYRT,XBTE,CPPYRT,XPTE,YSTE,YMTE,CHDYMT,XMTE,CPYME,XPMTE
8,DELP,DEFW(4),DFAF(4),CRDDPA,CDPMEU,EPTEUB,EP50,DEPDAL
9,CJ,ENGVFC,XNACEL,XNUZLE,ZNUZLE,XINLET,ZINLET,CKAM,ILE,ITE
COMMON /OUTPUT/ NALPHA,CLAFD,AULFD,AULTFD,AULBFD
1,DCLBFD,CLMAXP,DCDTE,DCLE,DCMUTE,DCMULE,CPATA(20),
2CMOBFD,CLMAXG(2),ALPHA(20),CLT(20),CLT0(20),CM10(20),CLTR(20),
1CCTR(20),ALPHAG(20),CLTG(20),COTJG(20),CHTWG(20),CLTRG(20)
1,CTRIG(20),CLPOFA(20),CLINT(20),CPOFA(20),CPOFA(20),CPOFA(20),
5CLPOGE(20),CPOGE(20),CPOGE(20),CLTR(20),CDETR(20),CLFAIR(20)
DIMENSION V(2),D1(2),D2(2)
DATA D1/2*1./
DATA D2/2*2./
**
*****
**
ERROR=0
IF (NALPHA.LE.0) GO TO 9100
WINGHT=WH3W(IWING)
DXC=XNACEL-.35
XANG=ENGVEF
YX=30./RAD
IF (ENGVFC.LE.XX) XANG=XX
YY=60./RAD

```

```

IF (FNGVFC.GF.VY) XANG=YY
YTFRM=CJ*(XNOZLF/CREP*SIN(ENGVEC)+ZNOZLE/CREP*COS(ENGVEC))

DO 100 I=1,NALPHA
XTFRM=CDRAM*(XINLET/CREP*SIN(ALPHAG(I))-ZINLET/CREP*
1COS(ALPHAG(I)))
C
C
C
C
**
** CALCULATE LIFT IN GROUND EFFECT FOR POWER ON
**
V(1)=XANG
V(2)=WINGHT/WSPAN
DCLTGE=TBL(DCLIG2,V,D1,IE)
IF (IF.NE.0) GO TO 9100

V(1)=ALPHAG(I)
V(2)=FNGVEC
XCL=TBL(CLIAS2,V,D2,IE)
IF (IE.NE.0) GO TO 9100

V(1)=ALPHAG(I)
V(2)=FNGVFC
V(3)=DXC
XDCL=TBL(DCLI3,V,D2,IE)
IF (IF.NE.0) GO TO 9100

CLFAGE=(XCL+XDCL)*SQRT(.5*CJ)
IF (IP.NE.2) GO TO 7000
WRITE (IO,8000)XANG,WINGHT,WSPAN,DCLTGE,XCL,DXC,XDCL,CLFAGE
8000 FORMAT(1H0, 44HXANG,WINGHT,WSPAN,DCLTGE,XCL,DXC,XDCL,CLFAGE
1 10(1X,F10.4))
7000 CONTINUE
CLPOGE(I)=CLTGE(I)+CLFAGE+DCLTGE+CJ*SIN(ALPHAG(I))+ENGVEC)
C
C
**
** CALCULATE DRAG IN GROUND EFFECT FOR POWER ON
**
V(1)=XNACEL
V(2)=FNGVFC
V(3)=CLFAGE
CDFAGE=TBL(CDI3,V,D2,IE)

```

```

C
IF (IF.NE.0) GO TO 9100
V(1)=XANG
V(2)=WINGHT/WSPAN
DCDGE=TRL(DCNIG2,V,D1,IF)
IF (IF.NE.0) GO TO 9100
C
CDPOGE(I)=CDTQG(I)+CDFAGE+DCDGE-CJ*COS(ALPHA(I)+ENGVEC)+CDRAM
C
**
**
**
C
CALCULATE PITCHING MOMENT IN GROUND EFFECT FOR POWER ON
**
**
IF (IP.NE.2) GO TO 7001
WRITE (10,8001)CLPQGE(I),CDFAGE,DCDGE,DCDGE,CDPOGE(I),YTERM,XTERM
8001 FORMAT(1H0,44HCLPQGE(I),CDEFAGE,DCDGE,DCDGE,CDPOGE(I),YTERM,XTERM /
10(1X,F10.4))
7001 CONTINUE
V(1)=XNACFL
V(2)=ENGVEC
V(3)=CLFAGE
CMFAGE=1BL(CM13,V,D1,IF)
IF (IF.NE.0) GO TO 9100
C
V(1)=XANG
V(2)=WINGHT/WSPAN
DCMGE=TRL(DCMIG2,V,D1,IF)
IF (IF.NE.0) GO TO 9100
C
CMPOGE(I)=(MTQG(I)+CMFAGE+DCMGE+YTERM+XTERM)
IF (IP.NE.2) GO TO 7002
WRITE (10,8002)CMFAGE,DCMGE,CMPOGE(I),CJ,ALPHA(I)
8002 FORMAT(1H0,45HCFAGE,DCMGE,CMPOGE(I),CJ,ALPHA(I) /
10(1X,F10.4))
7002 CONTINUE
C
**
**
**
CALCULATE TRI (L AND C) FOR POWER ON IN GROUND EFFECT
**
**
MODE=4
CALL TRIV(MODE,WINGHT,I)
100 CONTINUE

```

Contrails

CARD COUNT 295

GO TO 9200

9100 CONTINUE
TERROR=1

9200 CONTINUE
RETURN
END

217
(218 Blank)

Contrails

REFERENCES

1. Ellison, D. E. and Malthan, L. V., USAF Stability and Control Datcom, Revised July 1963.
2. Royal Aeronautical Society Aerodynamics Data Sheets.
3. Polhamus, E. C., A Simple Method of Estimating the Subsonic Lift and Damping in Roll of Sweptback Wings, NACA TN 1862, April 1949
4. Jones, R. T. and Cohen, D., High Speed Wing Theory, Princeton University Press, Princeton, N. J., 1960 (Unclassified).
5. Monk, J. R., et al, STOL Tactical Aircraft Investigation, Volume IV, Technical Report AFFDL-TR-73-19 Vol. IV.
6. Eldridge, A. H., Informal Communication (Unclassified).
7. Eldridge, A. H., Approximate Calculation Procedures for Aeroplane Aerodynamic Characteristics, D6A12022-p, The Boeing Company, July 1970.
8. Campbell, I. J., Aerodynamic Characteristics of Rectangular Wings of Small Aspect Ratio, Aeronautical Research Council R&M 3142, December 1956
9. Herbert, J., et al, Effects of High Lift Devices on V/STOL Aircraft Performance, USAAVLABS TR 70-33A, Vol. 1, June 1969
10. Young, A. D., Aerodynamic Characteristics of Flaps, Aeronautical Research Council R&M 2622, February 1947.
11. Neely, R. H., et al, Summary and Analysis of Horizontal Tail Contributions to Longitudinal Stability of Swept Wing Airplanes at Low Speeds, NACA TR R-49, 1959.
12. Carroll, R., et al, STOL Tactical Aircraft Investigation Configuration Definition: Medium STOL Transport with Vectored Thrust/Mechanical Flaps, AFFDL-TR-73-19, Vol. 1, May 1973.
13. Redig, P. J., STOL Tactical Aircraft Investigation, High Lift Programmers Manual, D180-14409-3, The Boeing Company, February 1973.

Contrails

Unclassified

Security Classification

DOCUMENT CONTROL DATA - R & D		
<i>(Security classification of title, body of abstract and indexing annotation must be entered when the overall report is classified)</i>		
1. ORIGINATING ACTIVITY (Corporate author) The Boeing Aerospace Company P.O. Box 3999 Seattle, Washington 98124		2a. REPORT SECURITY CLASSIFICATION Unclassified
		2b. GROUP ---
3. REPORT TITLE STOL Tactical Aircraft Investigation - Aerodynamic Technology: Design Compendium, Vectored Thrust/Mechanical Flaps		
4. DESCRIPTIVE NOTES (Type of report and inclusive dates) Final Technical Report 8 June 1971 to 8 December 1972		
5. AUTHOR(S) (First name, middle initial, last name) William J. Runciman Bernard F. Ray Gary R. Letsinger Fred W. May		
6. REPORT DATE May 1973	7a. TOTAL NO. OF PAGES 217	7b. NO. OF REFS 12
8a. CONTRACT OR GRANT NO. F33615-71-C-1757	9a. ORIGINATOR'S REPORT NUMBER(S) AFFDL-TR-73-19	
b. PROJECT NO. c. 643A d.	9b. OTHER REPORT NO(S) (Any other numbers that may be assigned this report) D-180-14409-1, Volume II, Part I	
10. DISTRIBUTION STATEMENT Approved for public release; distribution unlimited.		
11. SUPPLEMENTARY NOTES None	12. SPONSORING MILITARY ACTIVITY Air Force Flight Dynamics Laboratory Wright-Patterson AFB, Ohio 45433	
13. ABSTRACT This report presents methods for predicting the performance determining aerodynamic characteristics and the stability derivatives of transport-type configurations employing the vectored-thrust mechanical-flap high-lift concept. These methods are suitable for preliminary design. They have been automated in a FORTRAN IV computer program, for which a users' manual and listing are included in this document.		

DD FORM 1 NOV 65 1473

Unclassified
Security Classification

Unclassified
Security Classification

14. KEY WORDS	LINK A		LINK B		LINK C	
	ROLE	WT	ROLE	WT	ROLE	WT
Aerodynamic characteristics						
Vectored thrust						
High-lift systems						
Stability and control						
STOL						
Powered lift						